

IMMUNOLOGICAL INVESTIGATIONS IN THE WEST INDIAN MANATEE (*Trichechus manatus*) AND ASIAN ELEPHANT (*Elephas maximus*)

By

JENNIFER LYNN MCGEE

A DISSERTATION PRESENTED TO THE GRADUATE SCHOOL
OF THE UNIVERSITY OF FLORIDA IN PARTIAL FULFILLMENT
OF THE REQUIREMENTS FOR THE DEGREE OF
DOCTOR OF PHILOSOPHY

UNIVERSITY OF FLORIDA

2012

1

© 2012 Jennifer Lynn McGee

To the best parents a girl could ask for; for their endless support and encouragement
and for always fostering my curiosity in nature

ACKNOWLEDGMENTS

I would like to thank everyone who has helped me get where I am today. I am so grateful to my friends and family for all of their encouragement and support. I would especially like to thank my parents, Dennis and Gail McGee, for their unwavering support and for always encouraging me to pursue my passion. I could not have completed this without you! Additionally, I would like to thank Sr. Connie Marlowe, Drs. William Schutt and Maria Kretzmann, Kelli McGee, and Rob Yordi for always believing in me, for encouraging me to pursue my passion for aquatic animals, and for encouraging me to pursue graduate studies.

I also thank my advisor, Dr. Don Samuelson for his unwavering support and encouragement and most of all, for understanding that I am most comfortable in the field. He has helped me to further develop my laboratory skills while also encouraging me to take part in numerous conferences, workshops, and field research opportunities. I would like to thank my committee members, Drs. Ramiro Isaza, Peter McGuire, Thomas Brown, and Iske Larkin and my scientific advisors, Drs. Robert Bonde and Tracy Romano, for their expertise, guidance, advice, and patience

I would especially like to thank Dr. Robert Bonde without whom much of this work could not have been conducted. It was at Dr. Bonde's invitation in 2006 that I attended my first manatee health assessment captures in Crystal River, Florida. It was there that I first met the faculty, staff, and students of the University of Florida-College of Veterinary Medicine's Aquatic Animal Health Program and learned about the program's graduate opportunities. To this regard, I would like to thank Drs. Roger Reep, Ruth Francis-Floyd, and Charles Courtney who so graciously accepted me into the Aquatic Animal Health family. I would also like to thank Cathy Beck, Kelli McGee, Georgia Zern,

Keith Poster, Rob Yordi, and Alex Costidis for providing me with letters of recommendation for my graduate school application.

I am grateful to Patricia Lewis for her assistance and support throughout my dissertation, from laboratory support to conference travel and presentation planning. I appreciate all the time she spent training me in histotechniques as well as providing a shoulder to lean on. I am indebted to Linda Green, Diane Duke, and the staff of the University of Florida – Interdisciplinary Center for Biotechnology Research’s Hybridoma Core Laboratory for welcoming me into their lab, for providing copious technical support, and for taking time out of their busy schedules for the manatee and elephant projects. I am grateful for your expertise, time, enthusiasm, and patience. Additionally, I would like to thank Melanie Pate of the University of Florida-College of Veterinary Medicine, Diane Naydan of the University of California Davis-School of Veterinary Medicine, and Dr. Jeffrey Stott and Myra Blanchard of the University of California Davis, School of Veterinary Medicine, Department of Pathology, Microbiology and Immunology for their laboratory support and collaboration. For their technical assistance and advice, I would like to thank Michele Halvorson and Dan McElroy of FortéBio, Inc.

I greatly appreciate Drs. Robert Bonde and James ‘Buddy’ Powell for providing me with archived manatee samples, inviting me to participate in numerous manatee health assessment captures both nationally and internationally, and for sharing their vast knowledge of everything sirenian with me. I am very thankful to work alongside such experts in the field. I have learned so much from you both and am excited to continue collaborating on future sirenian research projects. This project would not have been possible without the assistance and collaboration of numerous agencies and

organizations, including Dr. Robert Bonde, Cathy Beck, and everyone at the U.S. Geological Survey Sirenia Project - Sirenia Project; Dr. Martine de Wit, Kane Rigney, Amber Howell, Andy Garrett, and Brandon Bassett of the Florida Fish and Wildlife Conservation Commission's Marine Mammal Pathobiology Laboratory and former employees and interns: Katie Brill, Vince Bacalan, Chris Torno, and Mark Flint. I would like to thank the veterinarians and staff at Lowry Park Zoo, Homosassa Springs Wildlife State Park, and South Florida Museum's Parker Manatee Aquarium. Thank you to Nicole Adimey of the U.S. Fish and Wildlife Service for facilitating sample collection. For the samples used in this study, I am grateful to the many collaborators that made this work possible. Again, I would like to thank Dr. Robert K. Bonde and the U.S. Geological Survey's Southeast Ecological Science Center -Sirenia Project, Dr. James 'Buddy' Powell and Nicole Auil and Sea to Shore Alliance, Drs. Chip Deutsch and Martine de Wit and the FWC, Fabia Luna and Dr. Fernanda Löffler Niemeyer Attademo and O Centro Nacional de Pesquisa e Conservação de Mamíferos Aquáticos/ Instituto Chico Mendes de Conservação da Biodiversidade-CMA/ICMBio, Drs. Chip Deutsch and Martine de Wit and the Florida Fish and Wildlife Conservation Commission (FWC), Dr. Antonio Mignucci and the Red Caribeña de Varamientos, and Dr. Janet Lanyon and the University of Queensland's Marine Vertebrate Ecology Research Group (MarVERG).

Research funding is provided through the University of Florida-College of Veterinary Medicine's (UF-CVM) Aquatic Animal Health Program, the Florida Fish and Wildlife Conservation Commission, the University of Florida Whitney Marine Laboratory for Marine Bioscience, and the UF-CVM Consolidated Faculty Research Development Grants 2009, 2011. This study was conducted under IACUC#200801803, #200802129,

and #201106011, Federal Fish and Wildlife Permit (USFWS) #MA067116-1 and #MA791721, and CITES Permit #11US808447.

TABLE OF CONTENTS

	<u>page</u>
ACKNOWLEDGMENTS.....	4
LIST OF TABLES.....	11
LIST OF FIGURES.....	12
LIST OF ABBREVIATIONS.....	17
ABSTRACT.....	25
CHAPTER	
1 INTRODUCTION.....	27
Sirenians.....	27
West Indian Manatee Biology.....	29
Florida Manatee Conservation Status.....	33
Antillean Manatee Conservation Status.....	34
Overview of the Immune System.....	35
Mucosal Immunology.....	37
Immunoglobulins.....	49
Manatee Health Assessments and Immunology.....	54
Paenungulata.....	57
Asian Elephant Biology and Conservation Status.....	61
Overview of Elephant Immunology and Reproduction.....	62
Research Significance and Objectives.....	65
2 CELLULAR AND ANATOMICAL CHARACTERIZATION OF VARIOUS MUCOUS ASSOCIATED LYMPHOID TISSUES IN THE FLORIDA MANATEE	69
Introduction.....	69
Material and Methods.....	70
Study Samples.....	70
Histology.....	71
Flow Cytometry.....	71
Immunohistochemistry.....	72
Transmission Electron Microscopy.....	74
Results.....	74
Mucous Associated Lymphoid Tissue.....	74
Conjunctival Associated Lymphoid Tissue.....	75
Gut Associated Lymphoid Tissue.....	79
Histology and Immunohistochemistry of Select Lymphoid Tissues.....	81
Discussion.....	81

3	USE OF BIOLAYER INTERFEROMETRY TO DEFINE BASELINE CIRCULATING AND SECRETED IMMUNOGLOBULIN G IN WEST INDIAN MANATEE POPULATIONS	127
	Introduction	127
	Materials and Methods.....	128
	Study Animals	128
	Sample Collection and Complete Blood Counts.....	128
	Florida Sub-Species Populations	130
	Antillean Sub-Species Populations	132
	Quantitative Assay Development and Optimization.....	133
	Data Analysis and IgG Levels	137
	Results.....	138
	Circulating IgG Levels	138
	Secreted IgG Levels in Tear Film	140
	Reference Ranges	140
	Predictors of Total IgG Levels	141
	Discussion	141
	Sub-Species and Population Variability.....	141
	Secreted and Circulating IgG Correlations	144
	Outliers	145
	Passive Transfer	147
	Conclusion and Future Studies	148
4	UTILIZATION OF A MONOCLONAL ANTIBODY FOR THE DETECTION OF IMMUNOGLOBULIN G IN THE ASIAN ELEPHANT.....	164
	Introduction	164
	Material and Methods	167
	Study Animals	167
	Tuberculosis, Rabies, and Tetanus Assay	168
	cELISA Development and Validation for Elephant IgG Quantification.....	170
	Data Analysis	178
	Reference Ranges	179
	Results.....	179
	cELISA and Population Levels	179
	Vaccine Response	181
	Passive Transfer of Immunoglobulins	181
	Discussion	182
5	CONCLUSIONS AND FUTURE DIRECTIONS	201
	APPENDIX	
A	TISSUE PROCESSING AND STAINING PROTOCOLS	224
B	WEST INDIAN MANATEE CIRCULATING IMMUNOGLOBULIN G	227

C	WEST INDIAN MANATEE BLOOD AND TEAR IGG VALUES.....	231
D	MANATEE IGG LEVELS AND COMPLETE BLOOD COUNTS.....	233
E	ELEPHANT IGG LEVELS-PASSIVE TRANSFER OF IMMUNOGLOBULINS.....	251
	LIST OF REFERENCES	253
	BIOGRAPHICAL SKETCH.....	265

LIST OF TABLES

<u>Table</u>		<u>page</u>
4-1	A comparison of total serum IgG (mg/mL) values for pre-suckling Asian elephant calves and IgG range for a captive Asian elephant population using two quantitative assay formats.	200
5-1	Mean concentration (mg/mL) and range IgG in mammalian species.....	223

LIST OF FIGURES

<u>Figure</u>	<u>page</u>
1-1 Global distribution of sirenian species	67
1-2 Overview of Mucosal Associated Lymphoid Tissues	68
1-3 The re-invented nasolacrimal system in Paenungulata	68
2-1 Antibodies tested for cross-reactivity with Florida manatee tissues.....	89
2-2 Mucosal-associated lymphoid tissue (MALT) identification legend.....	90
2-3 Conjunctiva-associated lymphoid tissue (CALT) in the manatee.....	91
2-4 Third eyelid (nictitating lens) of the manatee	91
2-5 Cross section of the conjunctival associated lymphoid tissue in the manatee showing glands and lymphoid nodules in the upper and third eyelid.	92
2-6 Conjunctival-associated lymphoid tissue in the manatee	92
2-7 Lymphoid nodules of the conjunctiva exhibiting prominent germinal centers, corona/mantle zones, subepithelial domes, and interfollicular regions in close association with the accessory gland and ducts	93
2-8 CALT epithelium.....	94
2-9 Ducts and duct-associated lymphoid tissue (DALT) of the upper eyelid.....	95
2-10 Ducts and glands of the upper and third eyelid.....	96
2-11 Lymphoid tissue of the third eyelid.	97
2-12 Lymphoid tissue from manatees whose cause of death (COD) was acute watercraft related.....	98
2-13 Diffuse CALT and accessory glands of a manatee whose COD was cold stress related.....	99
2-14 CALT with lymphoid nodules and hemorrhaging in the upper eyelid of a manatee whose COD was red tide related	99
2-15 Lymphoid nodules	100
2-16 Numerous M-cells at the apical surface of a lymphoid nodule in the upper eyelid.	101

2-17	Immunohistochemical localization of immunoglobulin G (IgG) in the CALT using the mouse anti-manatee IgG mAb in a red tide COD manatee.....	102
2-18	Immunohistochemical localization of IgG in manatees with various CODs	103
2-19	Immunohistochemical localization of plasma cells within the CALT using the Mum-1 mAb.....	104
2-20	Immunohistochemical localization of plasma cells (via Mum-1 mAb) in the third eyelid	105
2-21	Immunohistochemical localization of plasma cells in diffuse lymphoid tissue...	106
2-22	Immunohistochemical localization of plasma cells in the accessory glands and ducts	107
2-23	Immunohistochemical localization of T cells (via CD3) in the CALT	108
2-24	Immunohistochemical localization in of T cells (via CD3) in the CALT	109
2-25	Immunohistochemical localization of T-cells (via CD3) associated with the goblet like cells and ducts of the upper eyelid	109
2-26	Immunohistochemical localization of B cells (via CD20) in the CALT	110
2-27	Immunohistochemical localization of B cells (via CD20) in the third eyelid.....	111
2-28	Immunohistochemical localization of B cells (via CD20) associated with the accessory gland and ducts of the upper eyelid.....	111
2-29	Immunohistochemical localization of B cells (via CD20) associated with the ducts of the upper eyelid	112
2-30	Immunohistochemical localization of B cells (via CD20) in diffuse lymphoid tissue.....	113
2-31	Summary of immunohistochemical localization in the CALT	113
2-32	CALT within the lower eyelid of an adult male	114
2-33	TEM of epithelial lining and apparent M cells with endocytotic vesicles	114
2-34	Large ducts emptying nearby accessory glands are lined by simple columnar epithelia	114
2-35	CALT associated with the nictitating membrane and gland	115
2-36	Gut-associated lymphoid tissue (GALT)	116

2-37	Cross section of the small intestine with an aggregations of lymphoid nodules in the lamina propria and submucosa (Peyer's patch).....	117
2-38	Peyer's patch lymphoid nodules	117
2-39	Follicle associated epithelium which may be associated with M cells in this region	118
2-40	Potential lymphoglandular complexes and cryptopatch (square) in the colon. Small lymphoid nodules associated with goblet cells	118
2-41	Immunohistochemical localization of plasma cells (via Mum-1 mAb) in the Peyer's patch.....	119
2-42	Immunohistochemical localization of T cells (via CD3 mAb and pAb) in the Peyer's patch.....	120
2-43	Immunohistochemical localization of B cells (via CD20 mAb) in the Peyer's patch.....	121
2-44	Immunohistochemical localization of membrane-bound immunoglobulin in B cells (via CD79 α)	122
2-45	The mammary gland of the Florida manatee	123
2-46	The teat of the lactating Florida manatee	124
2-47	The progression of lactiferous duct morphology in the teat of a lactating Florida manatee.....	124
2-48	Transmission electron microscopy of the mammary gland and teat in a lactating Florida manatee	125
2-49	The thymus, spleen, and mandibular lymph node of the Florida manatee	126
3-1	Florida manatee populations and blood sample numbers	150
3-2	Biosensor tip with immobilized protein and the change in biolayer thickness and resulting wavelength shift.	151
3-3	Biolayer Interferometry assay duplicate standard curve for quantitative analysis of immunoglobulin G (IgG) in manatee sera	152
3-4	Biolayer Interferometry assay duplicate standard curve for quantitative analysis of immunoglobulin G (IgG) in manatee tear film	153
3-5	Basic Kinetics Assay Steps	154

3-6	Species, sub-species, and population mean, minimum, and maximum total circulating IgG.....	155
3-7	Mean circulating IgG versus median circulating IgG in the West Indian manatee.	156
3-8	Total circulating IgG in males versus females in the Crystal River Florida manatee population	157
3-9	Total circulating IgG reference ranges by species, sub-species, and populations.	158
3-10	Total circulating IgG for the Puerto Rico Antillean manatee population.....	159
3-11	Mean circulating total IgG for the Belize Antillean manatee populations	160
3-12	Mean total IgG in manatee tear film, right eye samples versus left eye samples.	161
3-13	Mean total circulating IgG (blood) versus mean total secreted IgG (tear film) ..	162
3-14	Mean circulating total IgG for the Crystal River Florida manatee population across 5 years	163
3-15	Mean circulating total IgG for the Everglades Florida manatee population across years.	163
4-1	Standard curve of the competitive ELISA for quantification of elephant IgG in serum	191
4-2	Biosensor tip with immobilized protein and the change in biolayer thickness and resulting wavelength shift	192
4-3	Basic Kinetics Assay Steps	193
4-4	Duplicate standard curve for the Octet QKe quantitative elephant biolayer interferometry assay	194
4-5	OD results (405nm) for quantitative elephant IgG cELISA	195
4-6	Total IgG values for captive manage population of Asian elephantS.....	195
4-7	Distribution of total IgG values for 82 serum samples	196
4-8	Rabies titers for 8 Asian elephants	197
4-9	Tetanus titers for 8 Asian elephants	198

4-10	Total serum IgG levels for 8 Asian elephants vaccinated concurrently against rabies and tetanus	199
4-11	Total serum IgG levels for 5 Asian elephants vaccinated against tetanus only.	200
5-1	Simple Blue stained gel of milk proteins	219
5-2	Simple Blue stained gel for J-chain	220
5-3	Protein identification in manatee milk	221
5-4	Protein identification in manatee milk	222

LIST OF ABBREVIATIONS

Organizations

AAH	Aquatic Animal Health Program
CITES	Convention for the International Trade of Endangered Species of Flora and Fauna
CMA/ICMBio	O Centro Nacional de Pesquisa e Conservação de Mamíferos Aquáticos/ Instituto Chico Mendes de Conservação da Biodiversidade
FWC	Florida Fish and Wildlife Conservation Commission
FWRI	Fish and Wildlife Research Institute
IACUC	Institutional Animal Care and Use Committee
IBAMA	Instituto Brasileiro do Meio Ambiente e dos Recursos Naturais Renováveis
ICBR	Interdisciplinary Center for Biotechnology Research
IUCN	International Union for the Conservation of Nature
LPZ	Lowry Park Zoo
MMPL	Marine Mammal Pathobiology Laboratory
UC	University of California
UF	University of Florida
UF-CVM	University of Florida - College of Veterinary Medicine
UF-ICBR	University of Florida - Interdisciplinary Center for Biotechnology Research
USFWS	United States Fish and Wildlife Service
USGS	United States Geological Survey
VMTH	Veterinary Medical Teaching Hospital

VMRD VMRD, Inc. (Veterinary Medical Research & Development)

General Abbreviations

COD Cause of death

CR Crystal River, Florida

EEHV Elephant endotheliotropic herpesvirus

E.m. *Elephas maximus*, Asian elephant

ESA Endangered Species Act

LB Lemon Bay, Florida

MIPS Manatee individual photo-identification system

MMPA Marine Mammal Protection Act

Mya Million years ago

PIT Passive integrated transponder

PR Puerto Rico

SSP Specie survival plan

TB Tuberculosis

T.m. *Trichechus manatus*, West Indian manatee

T.m.l. *Trichechus manatus latirostris*, Florida manatee

T.m.m. *Trichechus manatus manatus*, Antillean manatee

UME Unusual mortality event

Immunology

APC Antigen presenting cell

BALT Bronchi-associated lymphoid tissue

CALT Conjunctiva-associated lymphoid tissue

CCR	C-C Chemokine receptor
CCL	C-C Chemokine ligand
CD	Cluster of differentiation
CMIS	Common mucosal immune system
DC	Dendritic cell
EALT	Eye-associated lymphoid tissue
FAE	Follicle associated epithelium
Fc	Fragment, crystallizable region
FDC	Follicular dendritic cell
FPT	Failure of passive transfer of immunoglobulins
GALT	Gut-associated lymphoid tissue
GC	Germinal center
HEV	High endothelial venule
IEL	Intraepithelial lymphocytes
IFR	Interfollicular region
Ig	Immunoglobulin
IgA	Immunoglobulin A
IgD	Immunoglobulin D
IgE	Immunoglobulin E
IgG	Immunoglobulin G
IgM	Immunoglobulin M
IHC	Immunohistochemistry
IHC-P	Immunohistochemistry-paraffin embedded tissues

IL	Interleukin
LALT	Larynx-associated lymphoid tissue
LN	Lymph node
mAb	Monoclonal antibody
MALT	Mucosa-associated lymphoid tissue
MatAb	Maternal antibodies
MEC	Mucosa-associated epithelial chemokine
MHC	Major histocompatibility complex
MLN	Mesenteric lymph node
NK	Natural killer cell
PC	Plasma cell
PP	Peyer's patch
SAA	Serum amyloid-A
SC	Secretory component
SED	Sub epithelial dome
S-IgA	Secretory immunoglobulin A
SIgAD	Selective IgA deficiency
TECK	Thymus-expressed chemokine
T _H	Helper T cells
T _{Reg}	Regulatory T cells
pAb	Polyclonal antibody
pIgR	Polymeric immunoglobulin receptor

Laboratory and Analyses

ACD	Acid citrate dextrose
AEC	Substrate for colorimetric reaction, 3-amino-9-ethylcarbazole
BLI	Biolayer interferometry
BSA	Bovine serum albumin
°C	Degrees celsius
CBC	Complete blood count
cELISA	Competitive ELISA
COMP	Competition Plate, 96-well polypropylene, round bottom, micro plate
CO ₂	Carbon dioxide
cP	Centipoise
CV	Coefficient of variation
DAB	Substrate for colorimetric reaction, 3,3'-diaminobenzidine
dL	Deciliter
DNA	Deoxyribonucleic acid
EDTA	Ethylenediaminetetraacetic Acid
ELISA	Enzyme-Linked Immunosorbent Assay
EM	Electron microscopy
EtOH	Ethyl alcohol
FC	Flow cytometry
fL	Femtoliter
g	Gram

x g	Gravitational
HCT	Hematocrit
H&E	Hematoxylin and eosin
HGB	Hemoglobin
H_2O_2	Hydrogen peroxide
HRP	Horse radish peroxidase
IHC	Immunohistochemistry
KB	Kinetics buffer
kDa	Kilodaltons
kg	Kilogram
kHz	Kilohertz
kPa	Kilo Pascal
L	Liter
LC-MS/MS	Liquid chromatography tandem mass spectrometry
LiHep	Lithium heparin plasma
M	Molar
m	Meter
MAPIA	Multiantigen print immunoassay
MCH	Mean corpuscular hemoglobin
MCHC	Mean corpuscular hemoglobin concentration
MCV	Mean corpuscular volume
mg	Milligram
min	Minute

mL	Milliliter
mM	Milimolar
mmol/L	Millimoles per liter
MW	Molecular weight
N	Number of samples
NaCl	Sodium chloride
NBF	Neutral buffered formalin
nm	Nanometer
NUNC	ELISA plate, 96-well Nunc Maxi Sorp, flat bottom micro plate
OD	Optical density
P	P-value; probability of incorrectly rejecting null hypothesis
PAS	Periodic acid schiff
PBS	Phosphate buffered saline
PCV	Packed cell volume
PCR	Polymerase chain reaction
pg	Picogram
P-NPP	P-nitrophenyl phosphate substrate
R	Correlation coefficient
RDW	Red cell distribution width
RBC	Red blood cell
rRNA	Ribosomal ribonucleic acid
SD	Standard deviation
SDS-PAGE	Sodium dodecyl sulfate-polyacrylamide gel electrophoresis

sflt-1	Soluble fms-like tyrosine kinase-1
TEM	Transmission electron microscopy
μg	Microgram
μL	Microliter
μm	Micrometer/microns
WBC	White blood cell
WBC, corr.	White blood cell, corrected

Abstract of Dissertation Presented to the Graduate School
of the University of Florida in Partial Fulfillment of the
Requirements for the Degree of Doctor of Philosophy

IMMUNOLOGICAL INVESTIGATIONS IN THE WEST INDIAN MANATEE (*Trichechus
manatus*) AND ASIAN ELEPHANT (*Elephas maximus*)

By

Jennifer Lynn McGee

May 2012

Chair: Don A. Samuelson

Major: Veterinary Medical Sciences

The West Indian manatee (*Trichechus manatus*) consists of two sub-species, the Florida manatee and the Antillean manatee. While the West Indian manatee has been hypothesized to possess a strong immune system, the true extent currently remains unknown. The manatee, which belongs to the order Sirenia, has been found to be closely related to members of the order Proboscidea (elephants) grouping the two orders together in the Paenungulata. Immunological data available for both manatees and elephants are currently insufficient. Because of the limited number of immune studies having been conducted in these species, even the most basic properties of the immune system are lacking such as baseline immunoglobulin reference ranges in circulation and secretions and characterization of various immune tissues.

In this study, various mucosal associated immune tissues (MALT) were cellularly and anatomically characterized in the Florida manatee. In the gut, Peyer's patches and isolated lymphoid follicles were identified, exhibiting characteristics comparable to those observed in other mammalian species. Conjunctiva associated lymphoid tissue (CALT) revealed the potential presence of overlapping mucosal inductive and effector sites unique in the MALT system as well as the presence of M cells in the upper, lower, and

third eyelids. These characteristics potentially reveal adaptations concomitant with the previously observed reinvention of the nasolacrimal system in paenungulata.

Serving as a tool for future immune studies, baseline immunoglobulin G (IgG) reference ranges for the Florida manatee and Asian elephant were also established in this study using newly developed quantitative assays for measuring total IgG. IgG levels were comparable between manatee sub-species and populations with the east coast Brevard population having the highest mean IgG and captive managed orphaned manatees in rehabilitation having the lowest. Employing both the competitive ELISA and biolayer interferometry assays developed, we were also able to provide preliminary evidence of passive transfer of immunoglobulins in manatees and confirm passive transfer of IgG across the placenta in the elephant. The information from this study provides invaluable foundation tools and data for future immunological research and diagnostics. Incorporation of these data would allow for more accurate assessments of health as well as mitigation of immune effectors.

CHAPTER 1 INTRODUCTION

Sirenians

The Order Sirenia is comprised of two families, Trichechidae (manatees) and Dugongidae (dugongs). Within the trichechids are three species of manatees: the Amazonian manatee (*Trichechus inunguis*), the West African manatee (*Trichechus senegalensis*), and the West Indian manatee (*Trichechus manatus*); of which the Antillean manatee (*Trichechus manatus manatus*) and the Florida manatee (*Trichechus manatus latirostris*) are sub-species. The dugong (*Dugong dugon*) and the recently extinct Stellar's sea cow (*Hydrodamalis gigas*) make up the Dugongidae family (Reep and Bonde, 2006). Having evolved from terrestrial quadrupeds nearly 40-50 million years ago (Mya), the modern Sirenians are fully aquatic/marine, long lived, obligate herbivores (Domning, 2005).

Once ranging from the waters of Northwest California to the waters of Northern Japan and throughout the Bering Strait, Stellar's sea cow was hunted to extinction less than three decades after its 'discovery' in 1768 by European settlers (Stejneger, 1887). In addition to using the meat and skins, hunters valued the subcutaneous fat of these slow moving marine mammals, which they used in lamps as a smokeless and odorless substitute for oil. Well suited for life in these subpolar regions, *Hydrodamalis* was the largest of all sirenians. Fueled by a diet of marine algae, these sirenians grew up to 8m in length and weighed more than 3,600 kg (according to fossil records) (Scheffer, 1972). The fully marine sirenian had a large dolphin-like fluke, similar to that of the dugong. Dugongs are also fully marine though, unlike the Stellar's sea cow, they inhabit the tropical and subtropical waters throughout the Indian Ocean and regions of the Pacific

Oceans (Figure 1-1). Due in part to their more equatorial distribution, dugongs are much smaller than the now extinct *Hydrodamalis*, measuring up to 3 m in length and weighing up to 600 kg (Lanyon, 2003).

The members of the family Trichechidae are also equatorially distributed and of comparable size to the dugong. Splitting from dugongids approximately 30 Mya, Trichechidae are more freshwater adapted, inhabiting river and estuary systems as well as coastal marine waters found within close proximity to fresh water sources (Domning, 1982). Commonly referred to as sea cows or Peixe-Boi (fish-ox), there are currently three species of Trichechidae: the Amazonian manatee, the West African manatee, and the West Indian manatee (Florida and Antillean sub-species) (Reep and Bonde, 2006). The Florida manatee inhabits rivers and coastal waters throughout the southeastern United States, extending west to Texas and north as far as New York in the warm summer months. The Antillean manatee is found throughout the Caribbean, extending to the rivers and coastal waterways along the northeast coast of Brazil at its southernmost range. Found exclusively in the Amazon and Orinoco River Basins, the Amazonian manatee, *T. inunguis*, is the only sirenian to inhabit freshwater systems exclusively. The West African manatee, *T. senegalensis*, inhabits coastal waters, rivers, and lakes along the west coast of Africa. Their range extends to Senegal in the north, Angola in the south, and east as far inland as Chad, some 1000 miles from the coast. All manatee species share a general morphology including a large torpedo shaped body with a paddle-like tail. West Indian manatees are the largest of the three species with an average weight of 200-600 kg and length of 2.7 - 3.5 m (Reep and Bonde, 2006). They are similar to the West African manatee in their grey-brown

coloration, while the Amazonian manatee is darker with white patches on its chest and abdomen; suitable countershading in a habitat surrounded by dense tropical rainforest. The Amazonian manatee also lacks the fingernails found on other sirenians hence the species name *inunguis* which literally translated means 'no nails'.

West Indian Manatee Biology

The West Indian manatee, comprised of the Florida and Antillean sub-species, is the largest of the Trichechids. Their sensory systems reflect adaptation to their aquatic environment. They have gray to brown skin which is covered in sparsely dispersed tactile hairs (vibrissae). Manatees often inhabit dark, murky waters. Vocal communication is rare, with the exception of cow/calf pairs, and their hearing is best between 10-18 kHz (Bullock et al., 1982; Gerstein, et al., 1999; Niezrecki et al., 2003). Sight is also not a predominant sensory system used. They have small eyes, averaging 18mm in diameter, surrounded by sphincter-like eyelids endowed with immune tissues termed conjunctiva associated lymphoid tissues (CALT). Having the thickest tear film of any mammal studied to date (78.5 - 81.0 cP), manatees have highly vascularized corneas, absent of any ocular pathology, that is hypothesized to oxygenate the very active anterior epithelium obscured by the highly viscous tear film (Brightman et al., 2003). Manatees have reduced vision and as a result, use their tactile hairs to identify vibrations and movements (Bachteler and Gehnhardt, 1999; Bauer et al., 2003; Griebel and Schmid, 1996; Reep et al., 2002). These hairs are concentrated around their prehensile muzzle which they employ for exploration and feeding (Marshall et al., 1998). While the hairs on the oral plate can be used to facilitate the movement of food into their mouths, they also use their flexible pectoral flippers to manipulate food. While their large paddle-like tail is primarily used for propulsion, the pectoral flippers can also be

employed for orienting movements within the water column and for maneuvering along the sea and river floors during feeding, a behavior often referred to as 'bottom-walking'. Males also use their long pectoral flippers to 'grip' females during copulation, and often possess rough epidermis on the medial side of their flippers hypothesized to facilitate this behavior. Olfaction and taste are presumed to be reduced in aquatic mammals, though recent data suggest that these senses are quite active in the manatee and correlate with reproductive state and behavior (Levin and Pfeiffer, 2002; Mackay-Sim et al., 1985; Bills et al., unpublished data).

Generally reaching sexual maturity between 2-5 years of age, these slow reproducing mammals are polygamous with mating behavior often comprised of one female with numerous males competing for copulation (aka mating herds) (Koelsch, 2001; Larkin, 2000; Rathbun et al., 1995; Reep and Bonde, 2006). Gestation lasts approximately 13 months, resulting in a single offspring weighing approximately 27 kg and measuring ~1.2 m in length (Reep and Bonde, 2006). Due to energetic constraints, twinning rarely occurs. Calves will remain dependent on the cow for generally 1-2 years, suckling from their axillary teats. While mature adult females tend to be slightly larger than mature adult males, and males with the aforementioned longer and rougher pectoral flippers, there is no obvious sexual dimorphism other than the location of the genital slits; females are more caudal while males are more medial. Similarly, the Florida sub-species tend to be slightly larger than the Antillean sub-species. West Indian manatees measure 2.7 - 3.5 m in length with an average weight of 200-600 kg (Reep and Bonde, 2006). While manatees are known to be long lived marine mammals, most estimates are based on carcass data with maximum estimates of greater than 50

years old (Reep and Bonde, 2006). One captive born, and still currently captive managed male manatee however, will turn 64 in July, 2012.

Manatees are generally solitary animals with the exception of congregations around sea grass beds and warm water sources and the fission-fusion formation of mating herds (Reynolds III and Odell, 1991). The main social unit for this species is the 1-2 year cow-calf pairing. Based on tagging and tracking studies as well as photo-identification (Manatee Individual Photo-Identification System-MIPS), seasonal migrations have been observed between warm water refuges in the winter (both natural and artificial) and summer feeding and calving areas (Beck and Reid, 1995; Deutsch et al., 2003; Reid et al., 1991). Florida manatees are at the northern most range of the West Indian manatee. In warm summer months, they have been observed to travel as far north as New York and as far west as Texas. They are constrained by water temperatures. Their diet of calorically low aquatic plants and consequent lack of true blubber (as observed in other marine mammals) limits their ability to maintain sufficient body heat, resulting in limited cold tolerance (Dawes and Lawrence, 1983; Reep and Bonde, 2006).

Manatees eat a wide variety of both saltwater and freshwater plants found throughout marine, estuarine, and riverine systems. They are documented to consume approximately 60 different plant species, examples include: manatee grass (*Syringodium filiforme*), turtle grass (*Thalassia testudinum*), parrot feather (*Myriophyllum aquaticum*), widgeongrass (*Ruppia maritime*), shoal grass (*Halodule wrightii*), american eelgrass (*Vallisneria Americana*), hornwort (*Ceratophyllum demersum*), hydrilla (*Hydrilla verticillata*), and smooth cord grass (*Spartina alterniflora*) (Baugh et al., 1989; Best,

1981; Dawes and Lawrence, 1980; Domning, 1981; Etheridge et al., 1985). Feeding from 4-8 hours per day, manatees can consume 5-10% of their body weight in one day. This diet of fibrous plant material, as well as the incidental consumption of epiphytes and substrate, erodes their 24-32 molars over time. Manatees have continuous tooth replacement (aka 'marching molars'), which have evolved to compensate for this continuous wear (Domning, 1983). Gut transit time for these animals is highly specialized, averaging around 7 days with hindgut fermentation similar to, though longer than horses which average 1-2 days (Larkin et al., 2007).

The degree of rostral deflection in sirenian species reflects their feeding strategies. The West Indian manatee has the moderate degree of rostral deflection, feeding on both submerged and floating vegetation (Domning and Hayek, 1986). Manatees generally maintain a horizontal body position within the water column. The majority of their body weight is located in their mid section to maximize maneuverability. While their dense, pachyosteosclerotic bones, specifically their rib bones (comprising 60% of total skeletal weight in adults), make them less buoyant, their often gas filled intestines (~50m) and horizontally positioned and elongated lungs serve as a counterbalance (Rommel and Reynolds III, 2000; Reep and Bonde, 2006). Their bones also differ from classic mammalian bones in that the majority does not contain bone marrow. In the manatee, bone marrow is restricted to the tips on the rib bones, the skull, sternum, and vertebrae (Clifton et al., 2008). Their bone composition also makes them particularly susceptible to boat collision related mortality as their bones most often shatter and splinter upon impact, penetrating and potentially compromising vital organs.

Florida Manatee Conservation Status

Florida manatees inhabit shallow waters in and around the coast of Florida, extending north and west along the US coast in the warm summer months. Their close proximity to developed areas and overlapping habitat with many human recreational water activities makes them susceptible to a myriad of both anthropogenic and anthropogenically-induced threats (Ackerman et al., 1995). From 1974-2004, 23% of all manatee mortalities were categorized as due to 'watercraft', with 3% 'other human', and 4% 'floodgate' (Reep and Bonde, 2006). Twenty percent were categorized as due to 'other natural' and 21% 'perinatal' with a remaining 32% 'undetermined'. Most recently, severe weather events have also severely impacted manatee health and mortality resulting in the 2009-2010 winter season being classified as an 'Unusual Mortality Event' (UME) (FWC-FWRI, 2012a). During this event, January-April 2010, 503 manatee carcasses were recovered, surpassing the previous annual record in 2009 of 429. Of the 503 animals that died in the first third of 2010, 244 have been confirmed cold stress related with the majority of the remaining 'undetermined' animals, cold stress suspected cause of death (FWC-FWRI, 2012a). UME's do not just apply to mortalities as a result of severe cold weather events. The harmful algal bloom (HAB) known as red tide, caused by the *Karenia brevis* organism, has also resulted in mass manatee mortalities. Manatees are also susceptible to threats such as entanglement and habitat degradation (i.e., oil spills) (O'Shea et al., 1985).

To assess population size, synoptic surveys are conducted annually during the winter months when manatees congregate in warm water refuges, thus making them easier to count during these aerial surveys. Over 2,500 individual manatees have been identified by photo-identification in the MIPS database by aerial surveys over the past

several years, estimating a population around 3,700 individuals (Beck and Reid, 1995; Beck and Langtrimm 2002; Cathy Beck, personal communication). However, during the 2009-2010 extreme cold weather event, these surveys counted more than 5,000 individuals (FWC-FWRI, 2012b). Due in part to the anthropogenic and naturally occurring threats mentioned above, the Florida manatee is listed as Endangered (C1) by the IUCN (Deutsch et al., 2008). Reclassification of the Florida manatee status to Threatened has been proposed, but thus far has been rejected. The recent UME has also re-emphasized the importance of conserving natural warm water manatee refuges as well as further understanding the implications of reduced artificial warm water sources due to electric power plant closures.

Antillean Manatee Conservation Status

Antillean manatees are also listed as Endangered (C1) by the IUCN (Deutsch et al., 2008). Their true population size throughout their expansive range is unknown but estimated at less than 2,500 individuals. This subspecies faces some of the same threats as the Florida manatee, such as entanglement/fisheries interactions, boat strikes, and pollution/habitat degradation. However, circumstances such as cold weather and floodgates pose minimal to no threat. Antillean manatees however, are still hunted throughout much of their range, a threat no longer encountered in the Florida subspecies (Best, 1984; IBAMA, 2001; Lima, 1997; Luna, 2001; Powell, 2002). Manatees are hunted for both meat and various medicinal properties they are believed to possess. Accurate population estimates are limited, in part by researcher access to remote manatee habitat, dark turbid waters, and the financial and logistical resources available to conduct surveys throughout the Antillean manatees range. For example, in Florida, annual population surveys are conducted via aerial surveys, an option not

available in some Central American and Caribbean countries. Furthermore, due to the number of countries which the Antillean manatee population spans and their various political stances, lack of agreement on responsibilities for managing and assessing natural resources further hinders an accurate assessment of the Antillean manatee population and an assessment of West Indian manatees as a whole.

Overview of the Immune System

The immune system defends the body against potential pathogens via various biological structures and functions within an individual organism. Immunological recognition, immune effector functions, immune regulation, and immunological memory are essential tasks for an effective immune response (Murphy et al., 2008).

The immune system can be divided into the innate and adaptive immune responses. If physical and chemical barriers are breached by a pathogenic organism, the cells of the innate system provide immediate response by detecting the first presence of a potential pathogen in an organism. The innate immune response is a more immediate, generalistic approach to bodily defense against disease because it does not allow for the development of long term protective immunity. Many of the mucosal associated lymphoid tissues (MALT), along with their secretions, serve as physical and chemical barriers in the innate immune system. This system either removes the infectious or potentially infectious agent, recruits immune cells, activates the complement cascade, or activates the adaptive immune response (Murphy et al., 2008). The inflammatory response also serves as a physical barrier against the spread of infection, while also promoting healing and pathogen clearance. Immune cells already present in all tissues, such as dendritic cells and macrophages, are involved in this process, as well as the cytokines they produce. Macrophages, neutrophils, and

dendritic cells engulf potential pathogens to facilitate clearance. Other white blood cells involved in the innate immune response, though not necessarily in the inflammatory response, include natural killer cells, mast cells, eosinophils, and basophils (Murphy et al., 2008). Mast cells are most often associated with allergic response, but are also involved in wound healing, while both basophils and eosinophils also play a role in allergic response (Murphy et al., 2008). Eosinophils are effective in defense against bacteria and parasites while basophils are more specialized for parasites. Natural killer cells, as the name would imply, attack and kill compromised host cells rather than the potential pathogen itself.

In addition to providing the first immune response, the innate immune system can also lead to activation of the adaptive immune system. The adaptive immune response involves the response generated to a particular pathogen and is developed over an organism's lifetime. This type of response often leads to the formation of immunological memory, thus providing long term protective immunity. Adaptive immunity involves both cellular immune response and humoral (antibody) immune response as further discussed below.

The immune system can also be divided anatomically, with special adaptations specific to the tissues in these distinct immunological compartments. The peripheral lymph nodes and spleen are responsible for primarily generating the adaptive immunity in response to pathogens in tissues and blood and are the most studied response by immunologists. The MALT, though less well studied, is a second compartment of the adaptive immune system, and is quite a bit larger in size. Data supports differential immune response mucosally and systemically however, an immune response initiated

at a mucosal surface is capable of inducing a systemic immune response (Burns et al., 1982; German et al., 1998; Gupta and Sarin, 1983; Kurimoto et al., 1982).

Mucosal Immunology

The mucosal surfaces of the body are exposed to a greater number of potential pathogens when compared to the rest of the immune system due to the exposure of their epithelial surfaces to the external environment (Brandtzaeg, 2009; Cesta, 2006; Ogra et al., 1999). The immune components associated with mucosal surfaces are termed mucosal associated lymphoid tissues or MALT (Figure 1-2). These tissues include the oral/respiratory, urogenital, and gastrointestinal tracts as well as the ocular system. Upon further investigation, these systems have been divided into subcategories under the MALT system. BALT is the bronchus-associated lymphoid tissues, GALT is the gastrointestinal- or gut-associated lymphoid tissues, NALT is the nasal-associated lymphoid tissues, and CALT is the conjunctiva-associated lymphoid tissues. In recent literature, the CALT has become incorporated into an EALT or eye-associated lymphoid tissue system with a LDALT or lacrimal drainage-associated lymphoid tissue subdivision (Brandtzaeg et al., 2008; Ogra et al., 1999). GALT contains a DALT or duct-associated tissue (which may also be shared with the CALT system) subdivision and with the BALT, a LALT or larynx-associated lymphoid system. The common mucosal immune system (CMIS) links the inductive sites and effector sites of the mucosal immune system thereby linking several mucous membrane sites. Inductive sites are the sites of initial antigen exposure and include such systems as GALT, BALT, NALT, and CALT. Once the antigen has induced an immune response, mucosal lymphocytes home to effector sites via the CMIS. Effector sites include tissues such as

the lamina propria of the gastrointestinal tract, respiratory tract, and possibly the genitourinary tract as well as the mammary, salivary and lacrimal glands.

At these mucosal surfaces, a number of mechanisms exist to protect the body from potential pathogens. The innate immune system involves a combination of mechanical, chemical, and microbiological attributes. Examples of mechanical protective mechanisms include tight junctions at the epithelial surfaces, peristalsis, movement of mucus by cilia, and tears. Enzymes such as lysozyme in tears and low pH and digestive enzymes in the gut provide chemical defense. The normal commensal flora of the gut is an example of a microbiological attribute. Due to their physiological functions (i.e., gas exchange (lungs), food absorption (gut), and reproduction (uterus and vagina) and sensory activities (eyes, nose, mouth, throat) it is natural that these thin, permeable membranes would contain suitable compensatory defense mechanisms against infiltration by potential pathogens.

The mucosal immune system is often considered a minor subcomponent of the immune system in traditional immunology (Brandtzaeg, 2009; Cesta, 2006). The mucosal immune system, however, forms the largest part of the body's immune tissues (approximately 400 m² of surface area in adult humans), containing approximately three-quarters of all lymphocytes and producing the majority of immunoglobulin in healthy individuals (Murphy et al., 2008). This system contains some distinctive anatomical features, effector mechanisms, and immunoregulatory environments involved in the adaptive immune response and which are complementary to those mentioned in the innate immune response above.

Even in the absence of infection, activated/memory T cells predominate as do nonspecifically-activated natural effector/regulatory T cells demonstrating some of the unique effector mechanisms associated with mucosal tissues. The mucosal immune system is capable of active down regulation of immune responses such as that to food or other innocuous antigens (Ogra et al., 1999). Inhibitory macrophages and tolerance inducing dendritic cells also play a role in the immunoregulatory environment (Ogra et al., 1999). Distinctive anatomical characteristics of this system include the close interactions between lymphoid tissue and epithelium found at mucosal surfaces as will be described later in more detail. This system is divided into discrete subcompartments of diffuse lymphoid tissue as well as tissues such as the tonsils, Peyer's patches, and isolated lymphoid follicles that exhibit more organization within the system. At these sites, a specialized antigen-uptake mechanism exists. M-cells function as portals and allow antigen to pass through the epithelial surface where it is then recognized by professional antigen presenting cells (APCs) in the tissues below (Brandtzaeg, 2009; Cesta, 2006; Giuliano et al., 2002; Hanson et al., 1983; Knop and Knop, 2005a). The M-cells do not possess any antigen-presenting properties.

The GALT system is thus far the most well studied and therefore best described compartment of the mucosal immune system and is often used for comparison when studying other associated lymphoid systems (Cesta, 2006; Hanson et al., 1983; Ogra et al., 1999). GALT can be divided into inductive and effector sites, neither of which is entirely absolute. Peyer's patches (PPs) serve as the primary inductive sites and are typically large enough to be seen by the naked eye upon gross examination of the intestinal walls. All mammals studied thus far have been found to possess these

organized structures with most features being conserved across species. PPs are primarily identified histologically by the presence of a follicle-associated epithelium (FAE), a subepithelial dome (SED) that covers the B-cell follicles containing germinal centers (GCs), and interfollicular regions (IFR) containing high endothelial venules (HEV) and efferent lymphatics (Cesta, 2006). The PPs contain no afferent lymphatics as would normally be seen in other peripheral lymphoid tissues. All cell trafficking to this “lymphoepithelium” is via migration from the bloodstream across the Peyer’s patch HEVs (Cesta, 2006). Additional lymphoid aggregates are found throughout the gastrointestinal tract, however these are more widely distributed and often detected microscopically (Cesta, 2006; Ogra et al., 1999).

The main effector sites of the GALT system are the intestinal lamina propria and the intestinal epithelium. In the lamina propria mature T and B cells are found that have migrated following induction in the Peyer’s patch. The intestinal epithelium contains a unique population of T-cells that develop independent of the Peyer’s patches. These cells are called intraepithelial lymphocytes (IELs). In addition to lymphocytes, the lamina propria contains additional cell populations of low numbers that include macrophages and dendritic cells, neutrophils, other granulocytes, and mast cells (Ogra et al., 1999).

In the intestine, antigen processing occurs in two primary ways. If the antigen is able to cross the mucosal epithelium and come in contact with APCs, the antigen will be processed as a whole. Alternatively, epithelial transport could disrupt the antigenic structure, resulting in peptide fragments, which are then processed in the mucosal immune system. In both scenarios, antigen uptake by the epithelium is essential.

Transport of macromolecules can occur via receptor bound transport (as is the case of IgG in neonates), through specialized cells (M cells), or through direct sampling by dendritic cells.

As mentioned previously, M cells are a distinctive feature of the mucosal immune system. They allow antigen to pass through the mucosal epithelium, however, they do not play the role of APC (Brandtzaeg, 2009; Giuliano et al., 2002). M-cells are somewhat difficult for researchers to study as there is currently no antibody specific for M cell detection; they are often detected via transmission electron microscopy (Giuliano et al., 2002; Ogra et al., 1999). Following transport from the intestinal lumen, through the FAE, the antigen enters the SED region of the Peyer's patch. It is at this site that the antigen encounters dendritic cells, macrophages, CD4+ T cells, and B cells. CD 4+ T cells can differentiate into T_{H1} and T_{H2} helper cells or T_{Reg} cells. A function of the T_{H2} helper cells is to stimulate B cells for antibody production. If the antigen is thymic dependent, then T cells are required for antibody production. If the antigen is thymus independent, it is capable of eliciting antibody production in B cells in the absence of T cells via intrinsic B-cell activating activity or having multiple identical epitopes that cross link the B cell receptor.

Typically, the antigen is recognized and bound by a dendritic cell (DC). The immature DC takes up the transported material and processes it for presentation to T lymphocytes. At this stage DCs can migrate and take two potential antigen processing pathways (Ogra et al., 1999). 1) After the DC has acquired an antigen, it begins to differentiate as it travels to the IFR. The antigen is processed resulting in peptides that are expressed on the DC surface associated with major histocompatibility complex

(MHC) class I or II antigens. Adhesion molecules and co-stimulatory molecules are also upregulated at this time. Within the IFR there are CD4+ and CD8+ cells that through IFR HEVs, have gained access to the PPs. These DCs may also migrate to the draining lymphatics directly and travel to the mesenteric lymph nodes (MLN). 2) It is also possible that after having been processed by SED DCs, antigens are presented to CD4+ cells at this site or after follicular migration. This results in T cell induction and positions the T cells in an ideal location to provide help for B cells to undergo isotype switching to IgA producing cells in the germinal centers. Before this can happen, B cells must first undergo clonal expansion in the outer layer of the GC and then migrate to the inner layer. Here B cells undergo the processes of somatic mutation, positive and negative selection, isotype switching, and final differentiation into memory B cells.

The GC of the PP also contains follicular dendritic cells (FDC) whose apparent main function involves displaying the antigen bound to long filamentous arms and thus providing a continuous stimulatory effect on B cells in the GC (Ogra et al., 1999). With this pathway, T cells and FDCs may doubly stimulate B cells. The B cell process in the PPs differs from that of other GCs in two important ways. Firstly, isotype switch differentiation is highly skewed to IgA. Secondly, instead of undergoing terminal differentiation into plasma cells and migrating to the peripheral lymph nodes, mature B cells in the PP either remain in the SED region of the PP or migrate to draining lymph nodes or even distal mucosal effector sites before they begin terminal differentiation (Ogra et al., 1999). Typically, once the B cells undergo IgA isotype switching and consequent affinity maturation, they migrate, via the efferent lymphatics, from the PP,

through the MLN, and into the lamina propria. It is here that they then undergo terminal differentiation into plasma cells.

The lamina propria contains an abundance of subepithelial immune cells. These include a predominance of CD4⁺ T cells, CD8⁺ cells, macrophages, plasma cells, Natural Killer cells (NK), and non-follicular DCs. In the lamina propria, T cells that have been stimulated by DCs and macrophages secrete cytokines. These cytokines are essential for B cell differentiation. Until this time, T cells lie dormant as resting memory cells. As previously mentioned, intraepithelial lymphocytes are also present in this region. These cells likely contain cytotoxic mechanisms capable of eliminating infected epithelial cells, however the function of IEL is not fully known (Cesta, 2006). Although the lamina propria is predominantly an effector site, non-follicular DCs are capable of extending processes across the epithelial layer and directly sampling antigen from the luminal surface (Cesta, 2006). Another exception to this rule is the activity of IEL and the potential for polymeric IgA in the process of transcytosis to encounter epithelial invading pathogens. The plasma cells in the lamina propria are predominantly of the IgA isotype. These cells secrete dimeric IgA which is comprised of two monomers of IgA joined together by a J-chain. The dimeric IgA binds to the polymeric Ig receptor (pIgR) that is secreted on the basolateral side of epithelial cells in the lamina propria. This binding causes the pIgR dimeric IgA complex to undergo endocytosis. The complex then undergoes transcytosis to the apical face of the epithelial cell. It is during this process that the complex is capable of encountering and acting on invading epithelial pathogens. Once the complex reaches the apical surface, a small portion of the pIgR is cleaved resulting in a dimeric IgA molecule bound to a now termed secretory

component (SC). At this stage, IgA becomes secretory IgA (S-IgA). Within secretions, immunoglobulins can identify and bind directly to antigens, thereby preventing them from adhering to the mucosal epithelium or compete with binding resulting in antigen neutralization or opsonization. S-IgA is the predominant immunoglobulin found in mucosal secretions such as saliva, intestinal, nasal, and urogenital secretions, milk, and tears (Carbonare et al., 2005; Murphy et al., 2006; Ogra et al., 1999).

Secretions such as tears are part of the innate defense mechanisms, in this case defense against potential pathogens at the ocular surface (Akpek and Gottsch, 2003). Tears have been found to vary greatly in viscosity ranging from 0.44cP in humans to 81.0cP in manatees (thus far, the most viscous known) (Brightman et al., 2003). Though tear film analysis is a relatively new field, there is strong evidence of its benefits in immune monitoring and diagnostic studies in humans and several other species (Giuliano et al., 2002; Gudmundsson et al., 1985; Kageyama et al., 2006; Knop and Knop, 2000, 2005a; Knop et al., 2008; Sakimoto et al., 2002; Zierhut and Forrester, 2000). Conjunctiva associated lymphoid tissue (CALT) is closely associated with tears and their formation and provides part of the first line of defense to protect the eye as part of the greater lymphatic system. The primary tissues involved in immunological protection at the ocular surface are the conjunctiva and lacrimal gland (Knop and Knop, 2000, 2005a, b; Knop et al., 2008; Zierhut and Forrester, 2000)

The lacrimal gland is the primary effector mechanism in the CALT system as it is the predominant source of S-IgA that is contributed to the tear film. In many species, this gland possesses a wide array of lymphocytes with IgA secreting plasma cells that bind both J-chain and pIgR which is the predominant cell in the human lacrimal gland

(Knop et al., 2008). Plasma cells secreting additional antibody types are also found here, however they represent a minor population. The second largest cell population is T cells which are found distributed throughout and around the lacrimal gland. Within the periductular lymphocyte foci of humans, infrequent populations of B cells, dendritic cells, macrophages and activated B cells can be found. Interestingly, while common features in humans, these aggregates are not often found in other species except under pathological conditions (Knop et al., 2008).

Currently, the primary source of IgA containing lymphocytes and T cells in the lacrimal tissue is variably confirmed (Knop et al., 2008). In the GALT system, these lymphocytes migrate, via the efferent lymphatics, from the PP through the MLN, to the lamina propria where they undergo terminal differentiation into plasma cells. In the CALT system, they are hypothesized to originate from the nasal, local cervical, distant peripheral lymph nodes, and GALT as well as potentially the thoracic duct, spleen and mammary gland (Knop et al., 2008). While lymphocyte migration into the lacrimal gland appears random, retention and distribution are not (Knop et al., 2008). Cytokines, adhesion molecules, and receptors can also be found in the lacrimal gland acting not only on the local tissue but also being contributed to the tears and therefore the ocular surface. As previously mentioned, S-IgA is also contributed to the tears. The acinar and ductal epithelium of the lacrimal gland provides the pIgR and subsequent SC that is released into the tears. The synthesis and secretion of the pIgR glycoprotein has been found to be influenced by a number of factors including cytokines, glandular factors, and endocrine factors to name a few while the production of IgA itself may be regulated by hormonal, neural, and immune factors.

The counterpart to the lacrimal gland is the conjunctiva, which is thought to serve as both an effector and inductive site for mucosal immune response at the ocular surface. Some species investigated have been found to have high numbers of IgA secreting plasma cells here as well as distinct populations of B and T cells aggregated into lymphocytic follicles. Conjunctiva has also been found to possess SC in the epithelial cells as well as lymphoid aggregates, lymphocyte subpopulations, lymphatic channels and cytokines, chemokines, and adhesion molecules similar to those found in the lacrimal gland according to several studies. Collectively, this information supports the notion that the conjunctiva might play a role in antigen processing as well as lymphocyte migration and immune defense at the ocular surface.

While the role of the conjunctiva is hypothesized, currently it remains somewhat controversial (Knop and Knop, 2005a). Mucosal immunology at the ocular surface is still a relatively new field with a limited number of species having been investigated (Giuliano et al., 2002; Gudmundsson et al., 1985; Kageyama et al., 2006; Knop and Knop, 2000, 2005a; Knop et al., 2008; Sakimoto et al., 2002; Zierhut and Forrester, 2000). Current investigations have led to some variability in not only investigational techniques but also in the species themselves that have been investigated. Variables such as disease state, ocular health history, host age, and gender have been even further limited in the depth of detailed analysis. Some examples of the variability in current knowledge are discussed below.

While plasma cells have been described in human conjunctival tissue, the various techniques used have produced variable results. Using light microscopy, plasma cells were identified morphologically in the investigated tissue (Kageyama et al.,

2006). However, localization staining of these cells produced no results in one study and showed high cross reactivity with T cells in another (Kageyama et al., 2006; Knop et al., 2008). Still further studies have found a near complete lack of plasma cells in humans as well as in an array of species including mice, rats, guinea pigs, rabbits, cats, dogs, sheep, cows, owl monkeys, and baboons (Giuliano et al., 2002; Gudmundsson et al., 1985; Kageyama et al., 2006; Knop and Knop, 2000, 2005a; Sakimoto et al., 2002; Zierhut and Forrester, 2000). More recent studies have optimized techniques and have demonstrated the presence of IgA+ plasma cells within the conjunctiva and lacrimal drainage system (Knop et al., 2008). With regard to T cells, GALT tissue shows high levels of CD4+ helper T cells with few CD8+ suppressor or cytotoxic T cells. In the CALT, most T cells identified thus far have shown a preponderance of CD8+ cells. Furthermore, activated T cells and B cells have rarely been found in “normal” human conjunctiva in the majority of studies (Knop et al., 2008).

Secretory component was found to exist in rabbit and human epithelial tissue of the conjunctiva. None has been found to be expressed in rat studies, and other species remain to be investigated (Gudmundsson et al., 1985; Knop and Knop, 2005b). The conjunctival epithelium has also been found to lack M cells for antigenic passage into the immune tissue in a wide array of species further complicating the notion of the role of the conjunctiva as an inductive site (PP serve as the inductive site in GALT) (Akpek and Gottsch, 2003). Two theories have been presented in the absence of M cells though both have yet to be explored and could potentially occur even in the presence of M cells. The first theory of antigenic sampling involves the extension of dendritic cell processes across the epithelium as has been seen in the lamina propria. The second

theory suggests the involvement of lymphatic sinusoids adjacent to the conjunctival lymphoid aggregates. Should CALT be found to not play a significant role in antigenic processing, it would still provide protection at the ocular surface via the innate tear film mechanism as well as cell-mediated immunity.

More recent human studies, however have identified lymphoid follicles in nearly all samples of conjunctiva with larger aggregates in the lacrimal drainage system, a feature previously described only in the guinea pig (Knop and Knop, 2000, 2005a). Follicles also appeared to show an increase with age. These follicles showed typical characteristics to FAE as demonstrated in the GALT system as well as GCs and structures resembling M cells. FAE, GC, and M cells have also been demonstrated in dogs, rabbits, and Japanese monkeys (which also showed the presence of IEL) (Giuliano et al., 2002; Kageyama et al., 2006; Knop and Knop, 2005b). This study supported the high presence of T cell (cells positive for CD3 though no differentiation among CD4+ and CD8+ cells) as well as B cell presence which was mostly restricted to follicle aggregates. Diffuse lymphoid tissue was also noted to extend from the lacrimal gland across the entire surface of the conjunctiva. The conjunctiva and lacrimal drainage system also showed specialized HEV, a feature not previously described in the literature. Follicles and other components of the EALT, CALT, and LDALT systems may be preferentially distributed based on the affinity for foreign matter accumulation across the ocular surface. Ocular immune response and the retention of Ig+ lymphocytes in the lacrimal gland may be induced by local antigenic stimulation or by antigenic stimulation at sites such as intranasal, oral, intrabronchial, gastric, intravenous, or subcutaneous regions.

Currently, the data to implicate conjunctival tissue in the effective processing and presentation of antigen are limited though progressing swiftly. Current studies have provided multiple breakthrough discoveries with regard to the CALT system. The suggestion that the secretory immune response may require antigenic clearance through the nasolacrimal duct and stimulation of the NALT and GALT has been in part supported by current research though more research is needed.

Immunoglobulins

Plasma cells are the only cells capable of secreting immunoglobulins (aka antibodies). Bone marrow is the major site of B cell production in adults. B cell development begins with cells known as pro-B cells which do not express any immunoglobulin. In the second stage of B-cell development, pre-B cells express the heavy chain of IgM, however, this expression is confined to the cytoplasm therefore this type of B cell is not capable of recognizing antigen. Once the heavy chain is formed, the B cell forms the light chain assembling an IgM molecule on the cell surface that has distinct antigen specificity. It is at this stage that the B cell also begins to co-express IgD. This immunoglobulin bearing B cell leaves the bone marrow and migrates to peripheral lymph tissues and begins circulation throughout the lymph and blood. B cells become activated when they encounter an antigen and cross linking ensues. B cells recognize glycoproteins, foreign proteins, polysaccharides, and lipids. If an antigen is “thymus-independent”, T cells are not required to “assist” B cells (Murphy et al., 2006). “Thymus-dependent antigens” rely on T cell help for further activation, proliferation, and eventual antibody secretion in the B cell. When an antigen is encountered, it is internalized, processed, and presented on the B cell surface along with MHC class II which enables the cell to be recognized by T cells. As mentioned above, the T cells

subset capable of co-stimulating B cells is referred to as helper T cells (T_H1 and T_H2). It is the T_H2 cells specifically that co-stimulate B cells. Now that the B cell is presenting the antigen on its cell surface for T cell recognition, the B cell now serves the function of antigen presenting cell (APC). IL-4 and IL-5, produced by T_H2 cells, activate B cells. Cytokines IL-1, IL-6, and IL-10 are also involved in B cell development and activation. IL-4 is made when the T cells recognize their specific ligand on the B cell surface.

B cells most often encounter T cells as naïve B cells migrate via HEVs into peripheral lymphoid tissue. As they pass through the HEV, they also pass through the T cell zone of the lymphoid tissue where they become trapped. Antigen stimulated B cells that fail to interact with T cells that recognize the same antigen die within 24 hours. Activation leads to isotype switching whereby the heavy chain changes while the antigen specificity of the B cell remains constant (Ogra et al., 1999). The heavy chain determines the effector function of the B cell. The B cells then continue toward proliferation which they undergo for several days. These cells termed plasmablasts, have begun to secrete antibody but still possess many characteristics of the activated B cell. Once division is complete, the cell, now termed plasma cell, is capable of producing large amount of antibody.

IgG is found to be the predominant antibody in serum, while secretory IgA (S-IgA) is the one most commonly found in mucosal secretions such as tears, milk, and saliva. Immunoglobulin A (IgA) and immunoglobulin M (IgM) are also found in circulation, however levels are generally quite low, with high levels indicative of a disease state (Murphy et al., 2006; Ogra et al., 1999). Immunoglobulin D (IgD) and immunoglobulin E (IgE) are also present but at significantly lower levels. IgE is often

associated to function in allergic response whereas the exact function of IgD remains unknown. It is known however, that IgD is co-expressed with IgM.

Immunoglobulin G (IgG) is an immune protein found in all body fluids and the predominant antibody found in blood and extracellular fluid. This large antibody (150 kDa) is made up of 2 heavy chains (50 kDa each) and 2 light chains (25 kDa each) with Fc regions bearing N-glycosylation sites which are highly conserved. Primarily involved in secondary immune response, IgG protects the body by binding to an array of pathogens, thus providing protection from viral and bacterial infections. The presence of IgG in serum corresponds to a 'progressed' humoral immune response as IgM is the first antibody produced in response to antigenic challenge (Murphy et al., 2006). As discussed further in Chapter 4, IgG is the only immunoglobulin capable of crossing the placenta, though it is also transferred, along with IgA and IgM, in milk and colostrum. Maternal IgG provides the offspring with humoral immune protection until the neonatal immune system is capable of producing its own immunoglobulins in some species. IgG induces protection via agglutination, toxin neutralization, complement activation, and opsonization (Murphy et al., 2006).

Thus far, two antibodies specific for the detection of manatee immunoglobulin G have been developed at the University of Florida (manuscript in preparation). Rabbit anti-manatee polyclonal antibody (pAb) and a mouse anti-manatee monoclonal antibody (mAb) were a gift from the Hybridoma Core Laboratory at the University of Florida Interdisciplinary Center for Biotechnology Research (ICBR). Polyclonal antibodies are capable of binding to multiple sites or epitopes due to the mixture of different immunoglobulin types encompassing a large range of epitope affinities. A benefit of this

approach is the ability of this one antibody to target an antigen containing multiple epitopes. PAbs are capable of targeting many of these binding sites thereby increasing detection sensitivity. In contrast to pAbs, mAbs are highly selective in their affinity and unlimited amounts of equal quality can be produced. These antibodies produce the exact same binding characteristics each time and are therefore considered to be extremely useful in research, diagnostic, and therapeutic conditions, even functioning as standard chemical reagents. Due to the fact that they are specific for one epitope on a specific antigen, they will likely produce less background staining than would a pAb. Previous studies of elephant immunoglobulins are limited. While the presence of IgG has been investigated, as well as potential subclasses, no evidence of IgA or IgM has been noted (Guo et al., 2011; Kelly et al., 1998). Also through the UF-ICBR, elephant IgG has been purified and a monoclonal antibody for its detection has been developed similar to the methods described in Nollens et al. (2007) (manuscript in preparation). The monoclonal antibodies for both the manatee and elephant were used for this study.

Through the covalent linkage via disulfide bonds, multiple immunoglobulins are joined to form large pentameric Immunoglobulin M (IgM). With a pentameric mass of 900 kDa, it is limited in its distribution within the body due to its limited diffusion abilities. IgM is primarily found in serum in addition to IgG and dimeric IgA. It is also found within secretions of IgA deficient humans. Secretory IgM (S-IgM) is comprised of a pentameric molecule with an attached secretory component (SC) and J-chains, similar to those of S-IgA. It is particularly effective at complement activation (Murphy et al., 2006). IgM is detectable upon initial antibody response before isotype switching, somatic hypermutation, and affinity maturation result in a switch to IgG and/or IgA (or

even IgD and IgE), making the identification of IgM particularly useful in detecting recent infections. In situations of selective IgA deficiency (SIgAD), S-IgM may play a compensatory role (Ogra et al., 1999). In species where passive transfer of immunoglobulins across the placenta does occur, IgG should be the only immunoglobulin present in fetal serum, with IgM presence being indicative of intrauterine infection.

Concomitant with the development of the anti-manatee IgG mAb discussed above, a rabbit anti-manatee polyclonal antibody for the detection of manatee IgM was also developed. Since neither Protein A or G has a high binding specificity for IgM, IgG depleted serum fractions were used for immunization. Polyclonal serum was tested for antibody specificity. In 1998, Kelly et al. concluded that they were not able to detect IgM or IgA in the serum of African elephants. The authors recognize that these antibodies exist in relatively low quantities in serum and suggest the use of colostrum for future immunoglobulin identification. Guo et al. (2011) investigated the immunoglobulin gene repertoire of the African elephant and found it to be highly diverse and complex. The authors found evidence for IgG, IgD, and IgM. Additionally, preliminary investigations of the African elephant genome by UF researchers have also revealed evidence of IgM in the elephant. A BLAST search using IgM, pIgR, SC, J-chain, IgA, and S-IgA mammalian sequences revealed data supporting the presence of IgM, pIgR, SC, and J-chain within the African elephant genome, but no evidence of IgA or S-IgA.

IgA is found in two main forms, the monomeric form (IgA) found in serum and the dimeric secretory form (S-IgA) found on mucosal surfaces. IgA levels have been measured in both serum and plasma in a wide array of species. In “normal healthy”

conditions IgA is found at low levels in circulation with IgG dominating. It is also possible to be entirely IgA deficient. In these situations, elevated IgM levels were noted, acting to compensate for lack of IgA (Ogra et al., 1999). In MALT, plasma cells, which are predominantly IgA specific, produce polymeric IgA (two monomers joined by a 15 kDa J-chain) which are then bound as transported as previously discussed. S-IgA will be further discussed in the Chapter 5.

Manatee Health Assessments and Immunology

Manatee health and risk assessment captures are extensive studies that are currently being conducted in Florida, Belize, Cuba, and Brazil and have been conducted in Mexico and Puerto Rico as well. These captures are conducted at various times throughout the year and are the result of collaborations among numerous agencies and organizations. Health assessment teams are made up of federal, state, and local biologists, students, veterinarians, and volunteers. These extensive studies allow us to further understand both individual and population health by incorporating various diagnostic tools, research methodologies, and technologies. Currently, upon capture, an animal is first identified by gender and age class. Temperature, heart rate, and respirations are monitored and team members then check for fecal samples and place a Frisbee under the urogenital opening to collect urine. Morphometrics and ultrasounds are conducted as the team prepares sample collection sites. Each manatee receives two passive integrated transponder (PIT) tags with some also having a satellite tag attached. The animal is examined for external scars, parasites, and/or lesions. Samples collected include feces, urine, tear film, blood, genetic and lesion biopsy, parasites, nasal, oral, and urogenital swabs, and milk when present. Routine sample analyses include hematological and serum chemistry profiles with additional laboratory

tests for immunological, reproductive, and toxicology studies conducted when necessary. As a result of these health assessment captures, a large sample set of tissues has been archived for use in future studies.

The endangered West Indian manatee has no natural predators, however events such as collisions with boats, red tide blooms, and cold weather have detrimental effects on manatee health as previously discussed (Bossart et al., 1998, 2001, 2002; Bossart, 2006; Flewelling et al., 2005). While the West Indian manatee has been hypothesized to possess a strong or even superior immune system, 'the true extent currently remains unknown (Bossart, 2001). Their wound healing abilities, as demonstrated by the over 2,500 boat and entanglement scarred manatees in the MIPS database, in addition to their apparent disease resistance, particularly when compared to other marine mammals, warrants a further understanding of their immunological adaptations to the sometimes harsh and polluted marine and freshwater environment (i.e., Deepwater Horizon Oil Spill) (Bonde et al., 2004; Bossart et al., 2002; Buergelt and Bonde, 1983; White and Francis-Floyd, 1990).

Immune studies in the manatee have thus far been limited, focusing predominantly on correlations with cold stress syndrome and red tide exposure (Bossart et al., 1998, 2002; Walsh et al., 2004). Generalized hematological studies indicate that when compared to domestic species, manatees have low WBCs and possess heterophils versus typical neutrophils, a characteristic shared among paenungulata discussed below. Though the distribution of lymph nodes has been mapped and some investigations have examined cross reactive antibodies, studies are limited (Rommel et al., 2002; Sweat et al., 2005). More recently, it was discovered that the manatee had a

reinvented nasolacrimal system, a component of the CALT and EALT (Samuelson et al., manuscript in preparation) (Figure 1-3). This discovery, along with the fact that it was also documented in other members of paenungulata has led to the current tear film and mucosal immune studies.

Immunological investigations have also focused on the effects of cold stress and red tide on immune function via lymphocyte proliferation tests and hematological analysis. While red tide exposure resulted in a severe and often acute inflammatory response, cold stress resulted in suspected 'immunosuppression' evidenced by decreased cell counts and lymphocyte proliferation and lymphoid depletion (Bossart et al., 1998, 2002; Walsh et al., 2004). Manatees can endure cold temperatures of short durations, however, prolonged exposure to water lower than 20°C can result in 'cold stress syndrome', which suppresses the animal's immune function leaving it more susceptible to disease-causing pathogens (Bossart et al., 2002).

Living in the northernmost range for sirenians, the Florida manatee seeks refuge from winter cold water temperatures in naturally and artificially warm water sites. There are few natural warm waters springs in Florida, and both water quality as well as flow rates are of great concern (Reep and Bonde, 2006). Additionally, the projected closure of artificial warm water sources could have detrimental effects on manatees in the cold winter months, forcing changes in seasonally learned migrations and a marked increase in individuals competing for access to the natural springs. Global climate change will also likely present further threats to manatee health and survival. Extreme weather events such as extreme warm or cold and increases in hurricane frequency and

intensity are likely to affect manatee health, habitat, and, potentially, distribution patterns.

Paenungulata

The manatee, which belongs to the order Sirenia, has been found to be closely related to members of the order Hyracoidea (hyrax) and Proboscidea (elephants), combining the three orders into the group referred to as Paenungulata (“near-ungulate”). The three orders that the present species represent have been ancestrally linked through both morphological and molecular evidence. To date, the evidence for the close phylogenetic relationship of the Sirenia, Proboscidea and Hyracoidea consists of a combination of similarities across a wide range of characteristics, such as chromosomal painting, mitochondrial rRNA sequences, as well as dental, taxepodial and other anatomical features (Carter et al., 2004; Kellogg et al., 2007; Kleim Schmidt et al., 1986; Lavergne et al., 1996; Murata et al., 2003; Nishihara et al., 2005; Pardini et al., 2007; Rasmussen et al., 1990; Samuelson et al., 2007; Seiffert et al., 2007).

Afrotheria are a clade of placental mammals that represent one of the major superorders within Eutheria. Afrotheria can be traced back nearly 100 Mya and are comprised of golden moles, elephant shrews, tenrecs, armadillos, hyraxes, manatees, dugongs, and elephants, the last 4 of which are grouped into a taxon called Paenungulata. Sirenians (manatees and dugongs) and proboscideans (elephants) diverged approximately 50-60 Mya (Rainey et al., 1984). The earliest known ancestors to the modern day proboscideans were the *Moeritherium*, evolving approximately 50 Mya and living a semi-aquatic lifestyle. The most recent proboscidean ancestor is *Primelephas*. *Primelephas* appears to have divided into two branches, one evolving into the modern day African elephant and the other into the modern day Asian elephant

and extinct Mammoth. For sirenians, *Prorastomus* (48-37 Mya) is the most primitive sirenian known to date (Owen, 1855; Savage et al., 1994). Modern sirenians still exhibit adaptations observed in *Prorastomus*, such as dense rib bones. *Protosiren* (37-33 Mya) is the most recent common sirenian ancestor (Domning, 2005).

For a wide range of species, amino acid differences among hemoglobin sequences were investigated, suggesting grouping of the manatee, Indian and African elephant, and rock hyrax into a monophyletic clade known as Paenungulata (Kleimschmidt et al., 1986). This study focused on the use of the α and β -hemoglobin sequence data available on eutherians and other vertebrates to test the cladistic validity of Paenungulata. In particular, amino acid replacements at positions α 19, α 110, α 111, β 23, β 44, and β 56 provide evidence supporting the grouping of Sirenia, Hyracoidea, and Proboscidea. It has often been implied that Hyracoidea may belong to Perissodactyla. The similarities in hemoglobin sequences provided evidence that the Hyrax was closely related to manatees, dugongs, and elephant. Additionally, various hematological characteristics discussed previously in the manatee, such as the presence of heterophils, are also observed in the elephant and rock hyrax (Kleimschmidt et al., 1986)

Further evidence to support Paenungulata comes from the osteological evidence. It has been confirmed that they share a 'taxeopode arrangement of tarsal and carpal bones' showing minimal interlocking between adjacent elements (Rasmussen et al., 1990). It was thought that the taxeopody in hyraxes was the result of an independent adaptation to climbing rather than indicative of a close phyletic link as it is usually attributed. This idea was disregarded as there is considerable body size and

consequently locomotor specialization in both modern day specimens and fossil records.

The relationship between sirenians and proboscideans is also supported by the characterization of an endogenous retrovirus class among Paenungulata, retroposon analysis, and the expression of *sflt-1* in elephants and dugongs but not manatees with regard to corneal avascularity (Nishihara et al., 2005). Similarly, the recent discovery of 6 novel gamma herpes viruses from elephants, rock hyraxes, and manatees, that were able to be categorized into two separate groups based on analysis of DNA polymerase genes, suggests that the viruses may have codiverged with Afrotheria (Wellehan et al., 2007). Further genomic evidence (i.e. chromosome painting) also supports the relationship of manatees as part of both Paenungulata and Afrotheria while separating the sirenians, proboscideans, and hyracoidean from Tethytheria (Kellogg et al., 2007). Tethytheria combines Sirenia, Proboscidea, Desmostylia (extinct) and Embrithopoda (extinct), forming the clade Paenungulata when Hyracoidea are added.

Anatomical characteristics of the evolutionary relationship between manatees and elephants are reflected in part by tooth morphology, skeletal characteristics, toenails, skin, hair, and prehensile oral disc and trunk in the manatee and elephant respectively (Domning, 2005; Reep and Bonde, 2006). The nasolacrimal system of the manatee, elephant, and hyrax have also been investigated and found to be reinvented in all three species (Samuelson et al., manuscript in preparation) (Figure 1-3). The members of Paenungulata have been found to lack lacrimal glands, drainage punctae, nasolacrimal ducts, and the tarsal glands. This reinvention is unique within not only mammals, but also vertebrates in general. In humans, the loss of lacrimal gland is tied to the lack of

salivary glands. The formation of accessory glands and glandular tissue associated with the nictitating membrane appears to have adequately compensated for the loss or reinvention of the lacrimal gland in these species.

Another common anatomical feature between elephants and manatees is their similar placenta type: zonary and endotheliochorial (Allen, 2003; Allen et al., 2006; Carter et al., 2004, 2008; Cooper et al., 1964; Enders and Carter, 2004; Wooding et al., 2005). Currently, the degree of passive transfer of immunoglobulins, if any, for these species is unknown. It is presumed that the calf acquires maternal immune protection entirely after birth via consumption of colostrum and milk however, this remains to be confirmed (Araújo et al., 2001; Langer et al., 2009). IgG is the only immunoglobulin capable of transplacental transfer and therefore milk and colostrum are the sole sources of S-IgA for the neonate (Ogra et al., 1999; Van de Perre et al., 2003; Wheeler et al., 2007). S-IgA is one of the most important immunoglobulins serving to protect neonates as their innate immune systems develop (Ogra et al., 1999; Wheeler et al., 2007, Wooding et al., 2005). The placenta type implies the potential for some degree of passive transfer. This would be of particular importance in evaluating immune development in calves, further aiding in resources available for successful neonatal care including hand rearing of orphaned or rejected calves and mitigation of maternal disease transfer to calves (Carbonare et al., 2005; Emanuelson and Kinzley, 2002; Gage, 2003; King et al., 2006; Van Elk et al., 2007).

While the evidence for the close phylogenetic relationship of the Sirenia and Proboscidea consists of a combination of similarities across a wide range of characteristics, such as chromosomal painting and mitochondrial rRNA sequences, as

well as dental, taxepodial and other skeletal features, no such evidence exists between manatees and dolphins. Manatees and dugongs are not evolutionarily related to any other extant marine mammal.

Asian Elephant Biology and Conservation Status

Within the genus *Elephas*, the Asian elephant (*Elephas maximus*) is the only living species. This species is distributed throughout Southeast Asia, with three recognized sub-species. *Elephas maximus indicus* inhabits mainland Asia and is commonly referred to as the Indian elephant, while *Elephas maximus maximus* and *Elephas maximus sumatranus*, inhabit Sri Lanka and the island of Sumatra, respectively (Shoshani, 2006). Listed as endangered (C1) by the IUCN, this genus is susceptible to population decline primarily as a result of habitat loss and degradation (Choudhury et al., 2008; Hedges, 2006).

Though both are long-lived large land mammals, Asian elephants are smaller in size than African elephants (*Loxodonta africana*). They weigh between 2000-5500 kg and measure 2-3.5 m in shoulder height (Shoshani, 2006). In African elephants, the top of the shoulder is the highest point of the elephant, in Asian elephants, it's the top of the head (Shoshani, 2006). Asian elephants also have smaller ears and a dished forehead with dorsal bulges. This genus feeds primarily by grazing, with teeth resembling narrow compressed loops, and tusks present in males only (Shoshani, 2006). Another distinctive physical characteristic of the Asian elephants is the one 'finger' on the tip of their prehensile trunk; African elephants have two 'fingers'.

Asian elephants have a long history of interactions with humans. Evidence of captive elephants 'likely predates archaeological evidence by some time' (Hedges, 2006). They were/are widely domesticated and have been used during wars,

ceremonial practices, and as aids in farming, agricultural, and construction activities (Shoshani, 2006). Across their range, Asian elephants inhabit a variety of systems, including deciduous forests, tropical evergreen forests, grasslands, and scrublands (Shoshani, 2006). Habitat loss and degradation have resulted in increased conflicts between humans and wild elephants as they compete for space and resources.

Overview of Elephant Immunology and Reproduction

“There is a paucity of literature on the anatomic and functional aspects of the elephant immune system. Much research is needed” (Lowenstine, 2006). While there is little known about the immune system in the historically related manatee, there is even less known about elephant immunology. Investigations have been brief and limited to gross and histological examination of the thymus, lymph nodes, tonsils, bone marrow, and MALT and serologic testing to a limited extent (Lowenstine, 2006).

Reproduction has been more thoroughly investigated due to the long history of elephants in captivity. Compared to other captive megavertebrates however, the survival rate for elephant calves, particularly Asian elephants, is very low (Emanuelson and Kinzley, 2002). At times, human intervention is required and hand-rearing is considered a difficult task. The Species Survival Plan (SSP) stated that it “strongly recommends that calves *not* be hand-reared, but rather encourages managers to reintroduce the calves to the dams if at all possible” (Emanuelson and Kinzley, 2002).

IgG is the only immunoglobulin that is prenatally transferred in mammals, such as humans, as it is the only one that can cross the placenta (Murphy et al., 2006). As mentioned above, for manatees and elephants, histological investigations of the placenta have led us to suspect that some degree of transfer is possible before birth (Carter et al., 2004, 2008; Allen et al., 2003). Manatee and elephant placentas have

both been found to be zonary and endotheliochorial. Placentation in the African elephant has been well studied (Allen et al., 2002, 2003, 2005; Allen, 2006). Common features found in the placenta and fetal membranes of both manatees and elephants are discussed. The placenta is circumferential, forming a broad equatorial band creating a zonary shape as opposed to discoid as seen in humans. Attachment to the uterus occurs via a narrow hilus. The interhemal area is endotheliochorial and maternal blood vessels are ensheathed by cellular trophoblasts (Allen et al., 2003). Trophoblast cells extend narrow processes through the basement membrane of the thickened maternal epithelial cells (Allen et al., 2003). Reducing the diffusion distance between maternal and fetal blood, the fetal side is comprised of deeply indented fetal capillaries (Allen et al., 2003). These prominent hemophagous regions lining the placental margins provide iron for the fetus via erythrocyte ingestion.

Endotheliochorial placenta types, as seen in manatees and elephants, retain only one maternal layer, the uterine epithelium, for separation between the fetus and maternal blood (Tizard, 2000). This holds the potential for some maternal transfer of antibodies across the placenta to occur. IgG is the only antibody capable of transplacental transfer and is seen in hemochorial placenta. All species, regardless of placenta type are dependent on colostrum and milk as the primary source of IgA and IgM in the neonate.

Despite the potential for immunoglobulin transfer, elephants (and manatees) are believed to acquire maternal immune protection entirely postnatally via colostrum and milk and as such, orphaned calves are presumed to experience failure of passive transfer (FPT) of immunoglobulins, though this has yet to be confirmed. FPT can

contribute to the mortality of hand-reared calves by potentially increasing susceptibility to pathogens such as Elephant Endotheliotropic Herpesvirus (EEHV). Similarly, actively shedding dams, could transfer the virus to the calves or alternately provide passive immunization if not actively shedding. While FPT is presumed, it has not been confirmed (Emanuelson and Kinzley, 2002).

Protocols for hand rearing orphaned or rejected manatees remain highly subjective as there is little known about manatee reproduction, due largely in part to the fact that there is no breeding allowed in captive managed manatees within the United States. When caring for elephant calves, much is modeled after the methods of care for foals in which FPT has been confirmed (Emanuelson and Kinzley, 2002; Lowenstine, 2006). If a hand-reared elephant calf does not receive colostrum, plasma is administered to provide essential immunoglobulins (Emanuelson and Kinzley, 2002). Quantitative data for circulating immunoglobulins could be used to more accurately administer therapeutic IgG to calves as opposed to the crude estimates currently used by veterinarians and managers. Similarly, defining immunoglobulin reference ranges throughout neonatal development would allow for the most accurate decisions about IgG quantities to be administered as well as provide a method to evaluate the effectiveness of such administrations.

In the neonate, maternal IgG, transferred either prenatally or postnally is taken up into circulation until the calf's immune system begins to produce its own immunoglobulins at about 30 days after birth (Tizard, 2000). While IgG provides maternally transferred immunity in circulation, secretory immunoglobulin A (S-IgA) transferred in colostrum and milk provides immunological protection throughout the

gastrointestinal system (Ogra et al., 1999). S-IgA is the predominant immunoglobulin expressed in secretions such as milk and tears (Murphy et al., 2006; Ogra et al., 1999). Combining IgG and sIgA analysis would be of particular importance in evaluating the immune development in calves, further aiding in resources available for successful neonatal care and hand rearing in these species.

Once the degree of passive transfer of immunoglobulins is established, we can begin to investigate further the effects of maternal antibodies in the development of the neonatal immune system. In elephants, of particular concern is the transmission of diseases such as the highly fatal EEHV. How the virus is transmitted from dam to calf whether by prenatal transfer of blood, postnatal transfer of milk, or via contact during early development when calves are most vulnerable (i.e. when maternal antibodies begin to be catabolized and the neonatal immune system is still not yet fully capable of producing its own antibodies) remains unknown. By measuring immunoglobulins in calves and cows/dams we can better assess the correlation between maternally transferred antibodies and those produced by the calves, allowing for a more accurate assessment of any potential maternally transferred diseases and/or passive immunization.

Research Significance and Objectives

Immunological data available for manatees and elephants are currently insufficient. For research, diagnostics, and health monitoring in these species, incorporation of these data would allow for more accurate assessments of health as well as mitigation of immune effectors. Because of the limited number of immune studies having been conducted in manatees and elephants, even the most basic properties of the immune system are lacking such as baseline immunoglobulin reference ranges in

circulation and in secretions and characterization of various immune tissues. This information will provide invaluable foundation tools for future immunological research and diagnostics.

Objective 1: Cellularly and anatomically characterize various mucous associated lymphoid tissues in the Florida manatee. Mucous associated lymphoid tissues associated with tear production (CALT), milk production, and gastrointestinal secretions (GALT) were investigated. The tissues were examined histologically, immunohistochemically, and electron microscopically. The overall goal was to characterize mucosal immune tissues in the manatee and investigate changes correlating to cause of death, gender, and age class.

Objective 2: Develop a quantitative assay to define baseline reference ranges for circulating (blood) and secreted (tears) immunoglobulin G in manatees. Using the mouse anti-manatee IgG mAb, a quantitative assay using the Octet QKe system was developed. The overall goal was to define baseline IgG reference ranges in West Indian manatees across population, sex, and sub-species with preliminary investigations of passive transfer of immunoglobulins.

Objective 3: Define baseline reference ranges for circulating (blood) immunoglobulin G in elephants. Using the mouse anti-elephant IgG mAb, an assay for quantitative analysis of IgG in elephant blood was developed. The overall goal was to define the baseline IgG reference range for a population of Asian elephants. Using this quantitative assay, the presence of passively transferred immunoglobulins in pre-suckling calves was established.

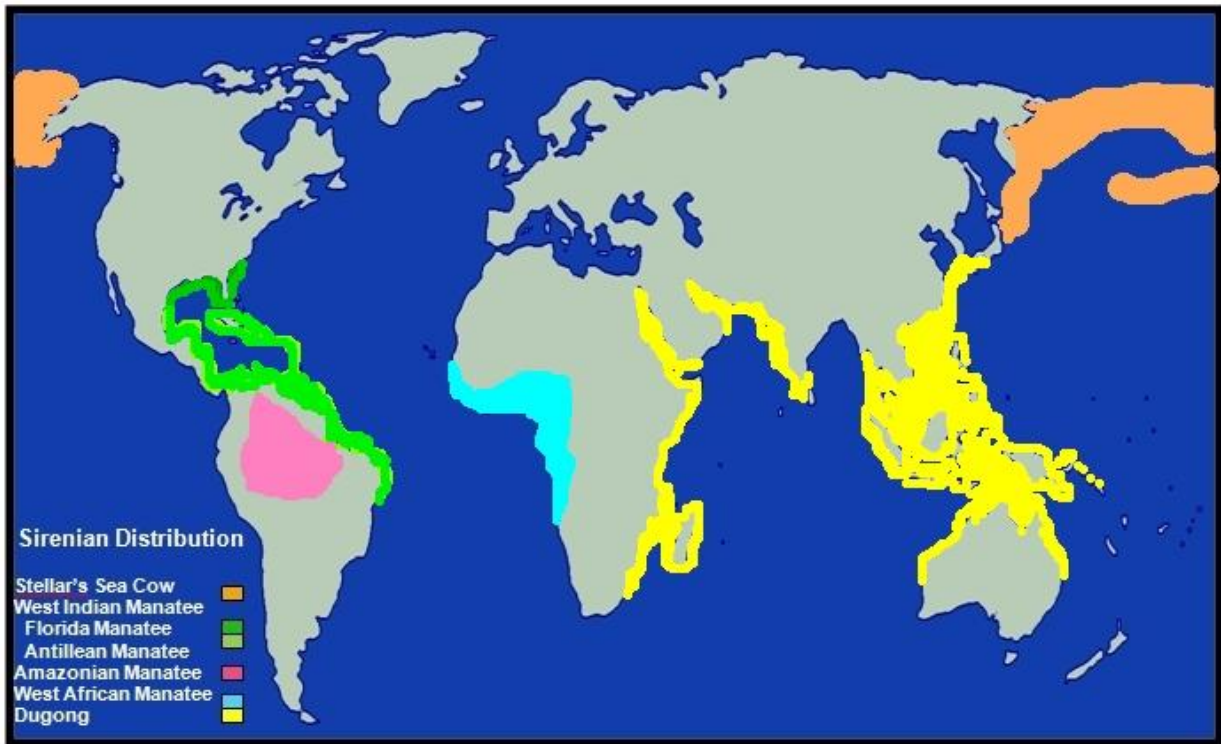


Figure 1-1. Global distribution of sirenian species. Orange-extinct Stellar's sea cow, Green-West Indian manatee (Florida and Antillean Sub-species), Pink-Amazonian manatee, Light Blue-West African manatee, and Yellow-Dugong.

Gastrointestinal Tract			Respiratory Tract		
Mouth	-salivary Glands	DALT	Nose	-paranasal sinuses	
Pharynx		Tonsils	Pharynx	-eustachian tube, middle ear	Tonsils
Esophagus			Larynx		LALT
Stomach			Trachea		
Small Intestine	-duodenum -biliary tract -liver -pancreas -jejunum	GALT	Bronchi		BALT
	-ileum	GALT	Alveoli		
	-caecum	GALT			
Large Intestine	-appendix vermiformis -colon -rectum		Ocular System		
			Conjunctiva		CALT/EALT
			Lacrimal Apparatus	-lacrimal gland -nasolacrimal duct	LDALT/EALT
Urogenital Tract					
<i>Urinary</i>			<i>Genital</i>		
Renal Pelvis			Uterine Tube		
Ureter			Uterus	-corpus -cervix	
Urinary Bladder			Vagina		
Urethra	-periurethral glands		Epididymis		
			Vas Deferens		
			Seminal Gland		
			Prostate		

Figure 1-2. Overview of Mucosal Associated Lymphoid Tissues. (Adapted from Brandtzaeg et al., 2008.)

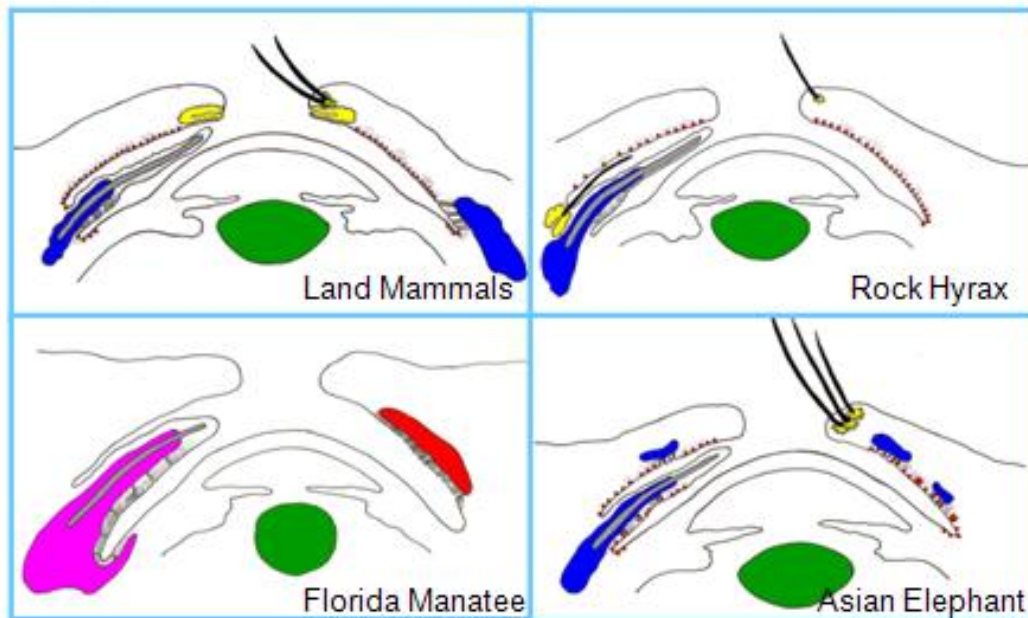


Figure 1-3. The re-invented nasolacrimal system in Paenungulata. Blue-Serous gland, Yellow-Sebaceous gland, Pink-Seromucous gland, Red-Mucous Gland. (Samuelson et al., manuscript in preparation)

CHAPTER 2 CELLULAR AND ANATOMICAL CHARACTERIZATION OF VARIOUS MUCOUS ASSOCIATED LYMPHOID TISSUES IN THE FLORIDA MANATEE

Introduction

The immune system of marine mammals is still largely in its nascent stage of understanding, having been limited to select species for which antibody probes have been developed for research and diagnostics. To date, several antibodies have been identified or developed for immunologic evaluation of manatee tissues. These include anti-manatee immunoglobulin G (IgG) monoclonal (mAb) and polyclonal (pAb) antibodies and anti-manatee IgM pAb (manuscript in preparation), a cross-reactive monoclonal with specificities for a pan T-cell marker (feline) and a pAb specific for interleukin-2 (human) (Sweat et al., 2005) and a monoclonal with specificities for macrophages (human Am3- K), (Komohara et al., 2006). Typically, when species specific antibodies are not available, antibodies from closely related species can sometimes serve as a substitute. Molecular and anatomical studies have revealed that the manatee is evolutionarily related to the elephant (Carter et al., 2004; Kellogg et al., 2007; Kleimschmidt et al., 1986; Lavergne et al., 1996; Murata et al., 2003; Nishihara et al., 2005; Pardini et al., 2007; Rasmussen et al., 1990; Samuelson et al., 2007; Seiffert et al., 2007). However, while little is known about the manatee immune system, even less is known about this system in elephants (Lowenstine, 2006). Limited in number, elephant-specific reagents have thus far shown no cross reactivity with manatee tissues (unpublished data). The aim of this study was to identify additional antibodies that could be incorporated into investigations that further define the manatee immune system and to provide an overview of immune tissue morphology in the Florida manatee with an emphasis on mucosal-associated lymphoid tissue. Definition of these structures would

allow us to better understand and evaluate their immunological role. For endangered animals such as the Florida manatee, overall health and management to ensure survival are of the utmost concern for the species.

Material and Methods

Study Samples

For this study, samples from 65 Florida manatees necropsied at the Florida Fish and Wildlife Conservation Commission's Marine Mammal Pathobiology Laboratory (MMPL) in St. Petersburg, Florida were included. Samples were collected from fresh or moderately fresh manatee carcasses. The manatees originated from various locations around Florida and represented both males and females of various age classes, causes of death, and reproductive statuses. The following tissues were collected: lymph nodes (any/all), eye and eye orbit, mammary gland and teat (when applicable), small intestine (duodenum, jejunum, ileum), and large intestine (cecum and colon). For histological and immunohistochemical investigations, the majority of samples were fixed in 10% neutral buffered formalin (NBF) and switched to phosphate buffered saline (PBS) after 24 hrs and stored at 4°C. These samples were trimmed, embedded in paraffin, sectioned at 4-5 µm, and placed on Fisher superfrost slides (Appendix A). For histology, sections were stained using either hematoxylin and eosin (H&E) or periodic acid Schiffs (PAS) or Mason's Trichrome (Appendix A). For immunohistochemistry (IHC), samples were processed according to standard IHC protocols that were adapted for the specific antibody of interest; paraffin embedded, cut at 4-5 µm, and placed on Fisher positively charged superfrost slides (Appendix A). Ten samples were fixed in 2% glutaraldehyde 0.1M sodium cacodylate buffer and stored at 4°C until processed for transmission electron microscopy (TEM). These samples were trimmed to no more

than two mm in thickness, and up to one cm in length and width. Samples were embedded in plastic, and sectioned at 1 μm for transmission electron microscopy (Appendix A).

Histology

Paraffin embedded samples were cut between 4-5 μm (Appendix A). Cut tissues were placed on Fisher superfrost slides. Sections were stained using either hematoxylin and eosin (H&E), Masson's trichrome or periodic acid Schiffs (PAS). Hematoxylin stains the nuclei of cells blue while eosin colors eosinophilic structures, which generally contain intracellular or extracellular protein, a reddish pink. This stain provides us with basic microanatomical views of the mucous associated lymphoid tissues. Masson's trichrome is a three-color staining method to distinguish cells from surrounding connective tissue. Keratin and muscle fibers will stain red, bone and collagen a blue/green, cytoplasm a light pink, and nuclei black. A PAS stain is used to identify carbohydrate rich structures such as glycogen in tissues and allows us to better identify and examine mucous secreting structures. Once the samples were stained, coverslips were placed on the slides using a glycerol gelatin mounting media. The MALT tissues were examined to identify mucous secreting glands, duct pathways, and lymphatic follicles (including size, shape, and abundance).

Flow Cytometry

Flow cytometry was used to identify potentially cross-reactive antibodies to add to the repertoire of antibodies currently available for immunohistochemical studies in the manatee. For flow cytometry, blood samples were collected (in ACD vacutainers) from the medial venous plexus of the pectoral flippers in free ranging adult manatees as part of United States Geological Survey-Sirenia Project's annual health assessment studies.

In collaboration with the University of California-Davis's School of Veterinary Medicine's Department of Pathology, Microbiology, and Immunology, these samples were used, via flow cytometry, to identify potential cross-reactivity of 19 monoclonals with specificity for Tursiops, bovine, human, ovine, and equine cell surface leukocyte differentiation antigens with a focus on lymphocyte markers. Flow cytometry results were plotted to show the flow profiles with the side scatter (complexity) on the Y axis vs. fluorescent staining on the X axis. The flow profiles were examined for expected binding patterns and approximate % positive. Antibodies were selected based on lymphocyte subpopulation analysis and a past track record for cross-reactivity in a variety of species.

Immunohistochemistry

As mentioned above, several antibodies have been identified or developed for immunologic evaluation of manatee tissues including an anti-manatee IgG mAb and pAb, an anti-manatee IgM pAb, a cross-reactive monoclonal with specificities for a pan T-cell marker (feline), a pAb specific for interleukin-2 (human) and an Am-3K mAb recognizing a CD163 anti-inflammatory macrophage phenotype (Komohara et al., 2006; Sweat et al., 2005).

For this study, we were particularly interested in detection of T and B cells within the MALT tissues. In this regard, we tested tissue samples collected from the Florida Fish and Wildlife Conservation Commission's Marine Mammal Pathobiology Laboratory which included the MALT, GALT, spleen, thymus and several lymph nodes from fresh adult manatee carcasses. Paraffin embedded samples were cut between 4-5 μm (as described above). Briefly, immunohistochemical protocols (Appendix A) involve placement of tissue sections on Fisher superfrost positively charged slides and

incubation at 56°C overnight. The slides were then washed in a series of 3 xylene baths, dehydrated through a graded series of 100% alcohol (3 times, 2 minutes each) and 95% alcohol (2 times, 2 minutes each), followed by rehydration in tap water for 10 minutes. After preparation of tissue sections, slides were incubated for 20 minutes in 3% hydrogen peroxide and then washed twice in PBS for 5 minutes each. Sections were incubated in 1.5% blocking serum in PBS for one hour prior to incubation with primary antibody. The primary antibody was incubated for 30 minutes at room temperature or overnight at 4°C and then washed with three changes of PBS for 5 minutes. The biotinylated secondary antibody was incubated for 30 minutes followed by another wash in three changes of PBS for 5 minutes each. AB enzyme reagent (avidin and biotinylated HRP) was added to the tissues, incubated for 30 minutes, and tissues washed three times, 5 minutes each. Finally, substrate solution was added to slides until the desired level of staining occurred at which time the tissues were washed with several changes of deionized water. Once samples were stained with substrate, coverslips were placed on the slides using a glycerol gelatin mounting media and slides examined microscopically. Negative control slides contained replaced the primary antibody with PBS. For our positive control slides, we included immune tissues from various species depending on which had been most extensively studied with regard to the respective antibodies and/or in which the antibody had been developed.

In collaboration with the University of California-Davis's School of Veterinary Medicine's Veterinary Medical Teaching Hospital, antibodies with the following specificities were investigated:

- Goat anti-human CD24 (B lymphocytes) polyclonal antibody 1:400 dilution
- Mouse anti-rat CD2 (T lymphocytes) monoclonal antibody 1:400 dilution

- Rat anti-mouse CD3 (T lymphocytes) monoclonal antibody 1:10 dilution
- Rabbit anti-human CD3 (T lymphocytes) polyclonal antibody 1:40 dilution
- Rabbit anti-human CD20 (B lymphocytes) polyclonal antibody 1:300 dilution
- Mouse anti-human CD79 α (B lymphocytes) monoclonal antibody 1:40 dilution
- Mouse anti-human Mum-1 (Plasma cells) monoclonal antibody 1:200 dilution

Transmission Electron Microscopy

The glutaraldehyde-preserved samples were washed three times in fresh buffer (0.1M phosphate buffer), 15 minutes for each wash and post-fixed in 1% osmium tetroxide for one hour at 37°C, washed with buffer (three times, 15 minutes each), dehydrated through a graded series (at 25% increments initially attenuating to 5% before reaching 100%) of ethanol and then into a graded series of acetone and ethanol before being placed into 100% acetone and subsequently embedded in plastic (Epon-Araldite mixture) (Appendix A). Plastic embedded samples were cut on an ultramicrotome initially at 1 μ m thickness and stained with 1.0% toluidine blue; to identify specific areas of interest. Ultrathin sections (70-90 nm thick) were cut and stained with Reynold's lead citrate and uranyl acetate (fully saturated) and then examined under a transmission electron microscope (Hitachi H 7000 series) at the University of Florida's Core EM Facility at an accelerating voltage of 100 kV. Images were digitally captured.

Results

Mucous Associated Lymphoid Tissue

For flow cytometry, manatee samples displayed a high degree of background that was mostly able to be gated out for analysis. Several of the antibodies displayed variable expression patterns; consequently a negative result may not be definitive. While the majority of antibodies which were tested via flow cytometry did not cross

react, several exhibited some degree of cross-reactivity. These included antibodies to an uncharacterized pan-leukocyte marker (equine), gamma-delta T cells (bovine) and a major histocompatibility complex (MHC) class II antigen (bovine) (Figure 2-1). In paraffin embedded tissues, antibodies specific for CD3, CD20 and Mum-1 exhibited a high degree of cross-reactivity in the lymphoid tissues tested, the antibody specific for CD79 α exhibited variable reactivity, and the antibodies for CD2 and CD24 showed little to no reactivity and had a high degree of false positives.

Conjunctival Associated Lymphoid Tissue

Histology. (Figures 2-2 to 2-16) All specimens revealed a well-developed CALT within the upper eyelid that extended from the fornix to the margin of the gray line of the eyelid. The CALT of the Florida manatee is highly developed, consisting of a prominent lymphoid layer along the superficial conjunctiva of the upper and lower eyelid and bulbar conjunctiva of the nictitating membrane. The CALT consisted of both diffuse and nodular lymphatic tissue, which lay immediately beneath the epithelium, that for the most part was stratified squamous but at times became reduced to simple squamous with intermittent areas of pseudostratified columnar epithelium. These latter areas were confluent with the ducts of the adjacent accessory mucous glands. The ducts were most developed in the regions between adjacent nodules and were often serpentine. In the nictitating membrane, the CALT consisted of both diffuse and nodular forms as well. The diffuse form was closely associated with the glandular tissue, especially within the nictitating membrane. Within the nictitating membrane the nodular form appeared to be less associated with the ducts than that seen in the upper eyelid. The lower eyelid also consisted of diffuse CALT. Animals whose cause of death (COD) was determined to be

boat strike related were found to have diffuse CALT from an animal in the SW region, nodular CALT from an animal in the SE region, and nodular in an animal from the NW region. Although the COD for the animal in the NW region was determined to be boat strike, red tide was also suspected. The animal with a COD related to cold stress from the SW region showed diffuse CALT. Of the animals whose COD was red tide-related, two had nodular CALT (both from the SW region), and the other two had diffuse CALT (NW and SW regions).

The conjunctiva and CALT were found to be identical in both the upper and lower eyelids. Its epithelium was most pronounced in thickness towards the external margins of these eyelids being strongly stratified squamous (7-15 layers). Melanocytes infiltrated throughout much of the basal cell layer, extending into ducts and became fewer towards the conjunctival fornix. Sporadically, the epithelium thinned to a few layers at locations where lymphoid tissue protruded towards the external surface. At these places, cells were observed with paler cytoplasm than surrounding epithelial cells and had numerous endocytotic vesicles when viewed ultrastructurally (see Transmission Electron Microscopy). We believe these cells to be M cells, similar to those described in the rabbit and dog. The organization of lymphatic follicles was similar to that described in humans and rabbits.

With regard to the third eyelid, a protruding follicular region on the lateral side facing the conjunctiva was observed in one specimen. The specimen also provided evidence for the potential presence of M cells within the epithelial lining. As in the upper and lower eyelids, the epithelium became reduced to few layers having transitioned into pseudostratified to stratified columnar epithelium as it became

confluent with the principal ducts of the nictitating gland. The epithelium along these largest ducts and those of the accessory glands of the upper and lower eyelids had prominent intercellular spaces, which appeared similar to examples of terrestrial species that had associated inflammation with or without infection. While lymphoid tissue existed primarily in a diffuse manner, occasional clusters of lymphocytes were observed, having been positioned mostly next to secretory cells. Small lymph vessels were observed in these regions. Other solitary cells of defense, including macrophages, plasma cells, heterophils and eosinophils were encountered.

Immunohistochemistry. (Figures 2-17 to 2-31) Immunohistochemistry revealed the presence of B and T cell populations (CD3 and CD20, respectively) with the conjunctival tissue and third eyelid as well as the presence of plasma cells (Mum-1), and IgG (HL767). For localization of IgG, it was found that the 1:50 and 1:100 dilutions gave effective staining results. In animals with a red tide-related COD, moderate reactivity was observed in the follicles with moderate to strong reactivity in the ducts and mucous. Cold stress COD animals showed little to no reactivity and acute water craft COD animals showed variable reactivity.

Mum-1 revealed strong reactivity in manatee conjunctival tissue. Reactivity was shown to occur variably within the germinal centers and consistently in the sub-epithelial dome and interfollicular regions surrounding lymphatic nodules in both the conjunctiva on the upper and lower eyelid and that of the third eyelid. In areas where CALT was more diffuse, so was the distribution of reactivity. The Mum-1 antibody also identified plasma cells both sparsely distributed and clustered within the accessory glands of the

upper and lower eyelids and the nictitating gland of the third eyelid. There was also moderate reactivity in the epithelial lining of some but not all ducts.

CD3 exhibited strong reactivity in the CALT of all three eyelids. Reactivity was concentrated in cells surrounding the follicles: the sub-epithelial dome and interfollicular regions similar to that of Mum-1. However, while Mum-1 showed more clustered reactivity, if any, in the germinal center (GC) and little to no reactivity in the follicle or mantle, CD3 reactivity was more evenly distributed throughout the mantle and the follicle zones with little to no staining in the GC. The polyclonal CD3 also exhibited moderate reactivity in cells sparsely distributed throughout the secretory glands as well as within the goblet cells and epithelium of the ducts.

CD20 exhibited a very strong reaction throughout the follicular nodules. The strongest reaction was observed in the sub-epithelial dome and follicle-associated epithelium with diffuse staining in the interfollicular regions CD20 also showed moderate to strong staining in the goblet cells and moderate staining in the epithelial cells lining the conjunctival tissues and ducts. Staining was also observed in the diffuse lymphoid tissues of the conjunctiva and third eyelid, though much less concentrated.

The goat anti-human CD24 (B lymphocytes) polyclonal antibody and the mouse anti-rat CD2 (T lymphocytes) monoclonal antibody were used to investigate GALT only. These antibodies did not exhibit the expected level of binding compared to their positive controls however, they did exhibit moderate, though variable, reactivity. Re-testing of these antibodies in various other immune tissues, including others area of the GALT is warranted with possible use of antigen retrieval methods to enhance potential reactivity/staining.

Transmission Electron Microscopy. (Figures 2-32 to 2-35) In the CALT of the Florida manatee, TEM confirmed the presence of many of the cells identified immunohistochemically as well as revealed the presence of cells indicative of inductive sites with the mucosal immune system. At the edge of follicles that extended toward the conjunctival surface, numerous plasma cells were identified. At the apical surface of the follicular protrusion, the epithelium was reduced to 1-2 layers of cells revealing apparent M cells with endocytotic vesicles. The cytoplasm of these cells possessed numerous filaments. Numerous lymphatic vessels were also seen in this region. The large ducts emptying the nearby accessory glands are lined by simple columnar epithelium and are closely integrated with CALT. TEM revealed extensive cellular processes between adjacent cells with varying amounts of intercellular space occupied with other cells. The CALT is lined mainly by pseudo-stratified columnar epithelium. Plasma cells were found to be diffusely scattered among the glandular tissue while lymphocytes were found both diffuse and clustered.

Gut Associated Lymphoid Tissue

Histology. (Figures 2-36 to 2-40) Several types of lymphoid nodules were identified in the intestine, including Peyer's patches and isolated lymphoid follicles with possible cryptopatches and, in the large intestine, lymphoglandular complexes. Aggregations of lymphoid follicles, or Peyer's patches, were distributed throughout the mucosa and submucosa of the gastrointestinal tract but were of greatest density in the ileum. The Peyer's patch follicles observed in this study were comprised of round lymphoid follicles, similar to those described in CALT, and typically contained 6-10 germinal centers. The follicle associated epithelium at the apical surface of these lymphoid nodules was flattened, lacking intestinal villi and containing numerous M-cells

for antigen uptake. Intraepithelial lymphocytes were also observed in basolateral spaces between luminal epithelial cells. Isolated lymphoid follicles were also observed, located throughout the large and small intestine and cecum. Similar to Peyer's patches, they were smaller in size and typically associated with a single dome. Possible cryptopatches, comprised of lymphoid aggregates in the lamina propria, were observed in one specimen, however immunohistochemical staining for T-cell aggregate presence was not conducted in this study for confirmation. Additionally, potential cryptopatches were observed in several colon specimens, resembling small Peyer's patches. Lymphocytes were also observed diffusely distributed throughout the lamina propria.

Immunohistochemistry. (Figures 2-41 to 2-44) Mum-1 had little to no reactivity in the GALT tissue investigated. The little reactivity that did occur was observed beyond the mucosal and submucosal regions of the gastrointestinal tissues and appeared to be predominantly non-specific staining. CD3 exhibited strong reactivity in manatee GALT. Reactivity was concentrated in the sub-epithelial dome with scattered reactivity in the germinal center and corona/mantle zone. Both monoclonal and polyclonal CD3 exhibited similar patterns of staining within the GALT tissues. CD20 exhibited little to no staining within the germinal centers of the follicular nodules. Strong reactivity was observed throughout the corona/mantle zone, the sub epithelial dome, and the follicle associated epithelium with diffuse staining in the interfollicular regions. CD79 α exhibited strong reactivity in GALT tissues with the most concentrated reactivity in the lymphoid follicle germinal centers and sub-epithelial domes. Diffuse staining was also observed in the corona/mantle zone and follicle associated epithelium. Scattered

staining was also observed within the interfollicular regions but to a much less degree than found in the follicles.

Histology and Immunohistochemistry of Select Lymphoid Tissues (Figures 2-45 to 2-49)

Histologically, the teats of the Florida manatee contained numerous lactiferous canals with varying epithelium. Similar to other eutherians, the lumens of the ducts and acini were enlarged in both lactating manatees and elephants. Lymphocytic cells were found lining the ducts, within the epithelium, and between distended acini, with a decrease in lymphocytic cells observed in non-lactating animals. The teats contain several teat canals with varying epithelium. Similar to other eutherians, the lumens of the ducts and alveoli will be enlarged in lactating manatees.

In paraffin embedded tissues, antibodies specific for CD3 and CD20 exhibited a high degree of cross-reactivity in the spleen, lymph nodes, and thymus while the antibody specific for CD79 α exhibited variable reactivity. In the spleen, CD20 showed strong reactivity and clustered staining in the germinal centers and follicular zones while CD3 stained the mantle zones. In mandibular lymph nodes, CD20 also stained the germinal centers and follicle zones of the lymphoid follicles while CD3 stained the mantle zones. In the thymus, CD3 showed strong reactivity throughout the tissue but concentrated in germinal centers.

Discussion

Some of the antibodies tested via flow cytometry caused some degree of background staining by nature which made analysis somewhat more challenging. Furthermore, several of the antibodies displayed variable expression patterns, so a negative result may not definitively rule them out. We expected that the majority of

antibodies tested via flow cytometry would not cross react with the manatee due to the highly specific nature of several antibodies tested as well as the manatee's lacking a terrestrial relative for which antibodies have been developed. All of the antibodies tested via flow cytometry have been reported only to bind native proteins and therefore would likely not bind in formalin-fixed manatee tissue sections. Snap freezing tissues would preserve these native proteins allowing us to immunohistochemically characterize the cross reactive antibodies identified by flow cytometry. Therefore future studies will examine frozen manatee lymphoid tissue sections collected from the FWC-MMPL. Application of the above-mentioned antibodies will allow us to expand the phenotypic identification of leukocyte subpopulations in manatees. Thus far, all identified cross-reactive antibodies have shown patterns of binding consistent with those found in a variety of other species which include several marine mammals (Cesta, 2006; Kawashima et al., 2004). The antibodies identified in the current study exhibiting cross-reactivity with manatee tissues will undoubtedly further our understanding of this unique and fascinating species. Development of manatee specific antibodies would be most useful for future studies targeting specific leukocyte cell surface markers.

Using both histological and immunohistochemical techniques, several types of lymphoid nodules were identified in the intestine, including Peyer's patches and isolated lymphoid follicles with potential cryptopatches, and, in the large intestine, lymphoglandular complexes. Peyer's patches and lymphoglandular complexes are the primary inductive sites in the gut, but the functions of the isolated lymphoid follicles and cryptopatches are unclear (Cesta, 2006). Peyer's patches are characterized by the predominance of B cells in the follicles' GCs and T cells in the interfollicular regions

(IFR), a characteristic consistent with the CD20 and CD3 staining in this study. Additionally, the lack of reactivity in GALT to Mum-1 (plasma cell marker) observed in this study does not imply lack of cross-reactivity as Mum-1 staining was observed in CALT. Isotype- and antigen-committed B cells leave the Peyer's patches and migrate to the mesenteric lymph nodes where they reach maturation. Once matured, they enter circulation where they eventually lodge in the mucosal tissues and glands, such as GALT. It is here that they undergo terminal differentiation into IgA producing plasma cells (Ogra et al., 1999). Only tissue sections composed of Peyer's patches or other lymphoid follicles were included in this study. In CALT, however, Mum-1 staining revealed the presence of plasma cells in the subepithelial domes (SED) and GCs of the nodular lymphoid tissue with moderate presence in the IFRs and throughout the diffuse lymphoid tissue. This suggests a re-invented source/path of immunoglobulin secretion in CALT. In other mammalian species, the lacrimal gland serves as the primary source of sIgA secretion, specifically, the gland's interstitium (Knop et al., 2008). T cells are the second largest cell population in lacrimal tissues. Their location within the tissues is somewhat diffuse, being found between acinar and ductal epithelial cells, throughout glandular interstitial regions, and within small lymphoid aggregates, which was also observed in the manatee's accessory lacrimal glands. In the manatee, however T cells were also identified (via CD3) in the lymphoid nodules SED and IFR and diffusely throughout the mantle/corona.

While mucosal inductive sites are generally limited to the GALT, BALT and NALT, CALT has been identified as an additional inductive site in rat, mice, dogs, and non-human primates (Giuliano et al., 2002; Gudmundsson et al., 1985; Kageyama et al.,

2006; Knop and Knop, 2005b). For animals that have a reinvented nasolacrimal system such as marine mammals, particularly manatees and the historically related elephant and hyrax, the current characterizations (follicular inductive and effector sites) could suggest potential concomitant reinvention of CALT cellular characteristics (manuscript in preparation). CALT is closely associated with tears and their formation and provides part of the first line of defense to protect the eye as part of the greater lymphatic system (Knop and Knop, 2005b; Schlegal et al., 2003). Manatees are believed to have the thickest tear film of any sea mammal, and possibly of any animal (Brightman et al., 2003). We suspect that manatees' thick, mucous tear film likely contains proteins, including antibodies that would attempt to prevent bacteria and other pathogens from causing disease. The CALT of the Florida manatee appears to be the most developed of any mammal studied to date, having a lymphoid layer that is especially prominent along the superficial conjunctiva of the upper eyelid and bulbar conjunctiva of the nictitating membrane.

The CALT consisted of both diffuse and nodular lymphatic tissue, which lay immediately beneath the epithelium, that for the most part was stratified squamous but at times became reduced to simple squamous with intermittent areas of pseudostratified columnar epithelium. These latter areas were confluent with the ducts of the adjacent accessory mucous glands. The occurrence of numerous large nodules within the conjunctiva of the upper and lower eyelid is a feature previously described only in the guinea pig and both morphologically and cellularly, is comparable to the Peyer's patches of the gastrointestinal tract (Cesta, 2006; Ogra et al., 1999). Additionally, areas of lymphatic aggregates, similar to cryptopatches in the gastrointestinal tract, were

observed. The lymphatic tissue appears to have a close association with the ducts of the large mucous accessory glands of the upper eyelid as well as the secretory tissue of the nictitating gland. The ducts were most developed in the regions between adjacent nodules and were often serpentine. IHC localization of macrophages revealed their presence within these ducts and indicated that duct-associated lymphoid tissue (DALT) occurs in the upper eyelids of this species. In the nictitating membrane, the CALT consisted of both diffuse and nodular forms as well. The diffuse form was closely associated with the glandular tissue, whereas the nodular form appeared to be less associated with the ducts than seen in the eyelids.

Variations in the development of the CALT were seen and may be indicative of the health of the animal. Prior to this study, characteristics such as FAE, HEV, and M cells had not yet been explored in marine mammals. However, germinal centers had been described in the numerous follicles present within the conjunctiva. The preponderance of lymphatic CALT follicles could be the result of several factors or combinations of factors. 1) Marine mammals often inhabit murky waters likely high in potential pathogens. This constant exposure would result in chronic antigenic stimulation and a more highly developed CALT. 2) The preponderance of follicles could be a compensatory response to a reinvented nasolacrimal system. In other species investigated thus far, follicles and consequently antigenic processing extends into the lacrimal ducts, a feature that marine mammals, elephants, and hyrax lack. 3) Even distribution of follicles across the conjunctiva may be required in marine mammals which possess sphincter-like eye closure that results in a more even distribution of foreign matter vs. accumulation as seen in terrestrial species. These combined factors

could call for a highly effective CALT system comparable to that found in GALT systems. Another aspect to note is that many marine mammals possess no EALT or LDALT. LDALT is associated with lacrimal drainage ducts, a feature lacking in many marine mammals. EALT consists of the lacrimal gland, conjunctiva, and lacrimal ducts, a system functionally connected by tear flow. As the tear producing glands have been modified and lacrimal ducts are absent, this system as well would not exist in cetaceans and sirenians or the historically related elephant and hyrax.

Another characteristic of a reinvented nasolacrimal system is attributed to effector associated glands. These glands appear to have adapted in response to environmental influence. Marine mammals and aquatic animals in general have a more highly viscous tear film compared to that of terrestrial animals (Brightman et al., 2003). Mammals typically possess mucous, serous, and sebaceous producing glands or cells contributing to tear formation. However, manatees have a complete lack of sebaceous glands resulting in tears that are a mixture of mucous and seromucous secretions. All marine mammals also possess some degree of corneal vascularization independent of any sort of ocular pathology (Harper et al., 2005). The degree of vascularization appears to increase as tear viscosity increases. This could serve to oxygenate a highly active anterior epithelium or even potentially provide factors that would contribute to the innate protection of the tear film.

Mucosal associated lymphoid tissue is an intricate and specialized system that comprises a significant and constantly active form of defense within the immune system. While GALT is the most well defined compartment of the MALT system, BALT, DALT, and NALT have been gaining more attention in recent years, though much

research is still needed across a variety of species. Histologically and using transmission electron microscopy, the conjunctivae and CALT were found to be identical in both the upper and lower eyelids. The epithelium was most pronounced in thickness towards the external margins of these eyelids being strongly stratified squamous (7-15 layers). Melanocytes infiltrated throughout much of the basal cell layer, extending into ducts and became fewer towards the conjunctival fornix. Sporadically, the epithelium thinned to a few layers at locations where lymphoid tissue protruded towards the external surface. At these places, cells were observed with more electron-lucent cytoplasm than surrounding epithelial cells and had numerous endocytotic vesicles. We believe these cells to be M cells, similar to those described in the rabbit and dog. The organization of lymphatic follicles was similar to that described in humans and rabbits (Knop and Knop, 2000, 2005 a,b). The epithelium along the largest ducts and those of the accessory glands of the upper and lower eyelids had prominent intercellular spaces, which appeared similar to examples of terrestrial species that had associated inflammation with or without infection (Zierhut and Forrester, 2000). In the manatee, the intracellular spaces may be a normal condition reflecting an adaptation to their aquatic environment.

Currently, the majority of data to implicate conjunctival tissue in the effective processing and presentation of antigen are limited though progressing swiftly (Knop and Knop, 2000, 2005 a,b). Current studies have provided multiple breakthrough discoveries with regard to the CALT system. The suggestion that the secretory immune response may require antigenic clearance through the nasolacrimal duct and stimulation

of the NALT and GALT has been in part supported by current research though more research is needed.

Antibody Clone	Target Cell	Target Species	Specificity	Cross-Reactive?	Tested By	Availability
UC-F6B	Pan Leukocyte	Horse	Unknown	Yes	FC	Stott Lab
CC1	Pan Leukocyte	Bovine	CD45	No	FC	
ILA24	Myeloid Cells	Bovine	Unknown	No	FC	
UC-F21.D	Pan Leukocyte (largely)	Tursiops	Unknown	No	FC	
UC-171.D3	Monocytes (some species), B cells, Activated T cells	Bovine	MHCII	Yes	FC	Stott lab
UC-F21.K	Monocytes (some species), B cells, Activated T cells	Tursiops	MHCII	No?	FC	
UC-F21.B	B cells	Tursiops	CD19	No?	FC	
UC-F21.F	B cells	Tursiops	CD21	No	FC	
B-ly4	B cells	Human	CD21	No	FC	
UC-F21.C	T Cells	Tursiops	CD2	No	FC	
ILA42	T Cells	Bovine	CD2	No	FC	
86D	gamma-delta T cells	Ovine	TcR1-N7 cluster	Yes	FC	VMRD
MMCI	T Cells	Bovine	CD3	No	FC	
UC-F6G	T Cells	Equine	CD3	No	FC	
CC17	T Cells	Bovine	CD5	No	FC	
UC-F13C	T Cells	Equine	CD5	No	FC	
CC76	Leukocyte subset	Bovine	CD45R	No	FC	
UC-F21.H	Leukocyte subset	Tursiops	CD45R	No	FC	
CC63	T cytotoxic cell subset	Bovine	CD8	No?	FC	
	B cells	Rat	CD20	Yes	IHC-P	VMTH
	B cells	Rabbit	CD79 α	Yes	IHC-P	VMTH
	T Cells	Rat	CD3	Yes	IHC-P	VMHT
	T cells	Rabbit	CD3	Yes	IHC-P	VMTH

Figure 2-1. Antibodies tested for cross-reactivity with Florida manatee tissues. FC= Flow Cytometry, IHC-P= Immunohistochemistry-Paraffin Embedded Tissues, VMTH= Veterinary Medical Teaching Hospital- University of California Davis (UC Davis). VMRD= VMRD, Inc. (Veterinary Medical Research & Development). Stott Lab = Department of Pathology, Microbiology, and Immunology, School of Veterinary Medicine, UC Davis.

1. Lymphatic Nodule
2. Accessory Gland
3. Duct
4. Diffuse Lymphatic Tissue
5. Epithelium
6. Nictitating Gland
7. Stratified Columnar Epithelium
8. Simple Squamous Epithelium
9. Stratified Squamous Epithelium
10. Goblet and Goblet-like Cells
11. Cartilage
12. Germinal Center
13. Sub-Epithelial Dome
14. M-Cell
15. Interfollicular Region
16. Corona/Mantle
17. Follicle Associated Epithelium
18. Inter Epithelial Lymphocytes

Figure 2-2. Mucosal-associated lymphoid tissue (MALT) identification legend.

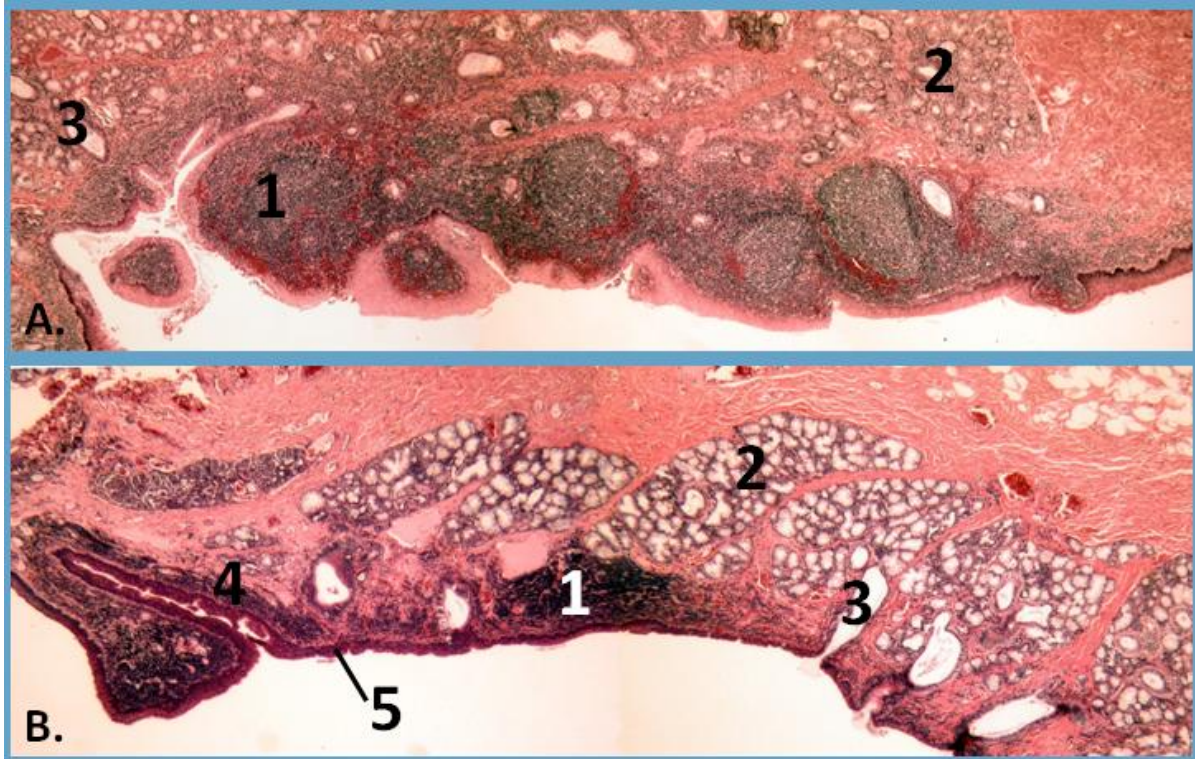


Figure 2-3. Conjunctiva-associated lymphoid tissue (CALT) in the manatee. A. Lymphoid nodules in the upper eyelid, H&E x10. B. Diffuse lymphoid tissue in the upper eyelid with associated glandular tissue, H&E x10.

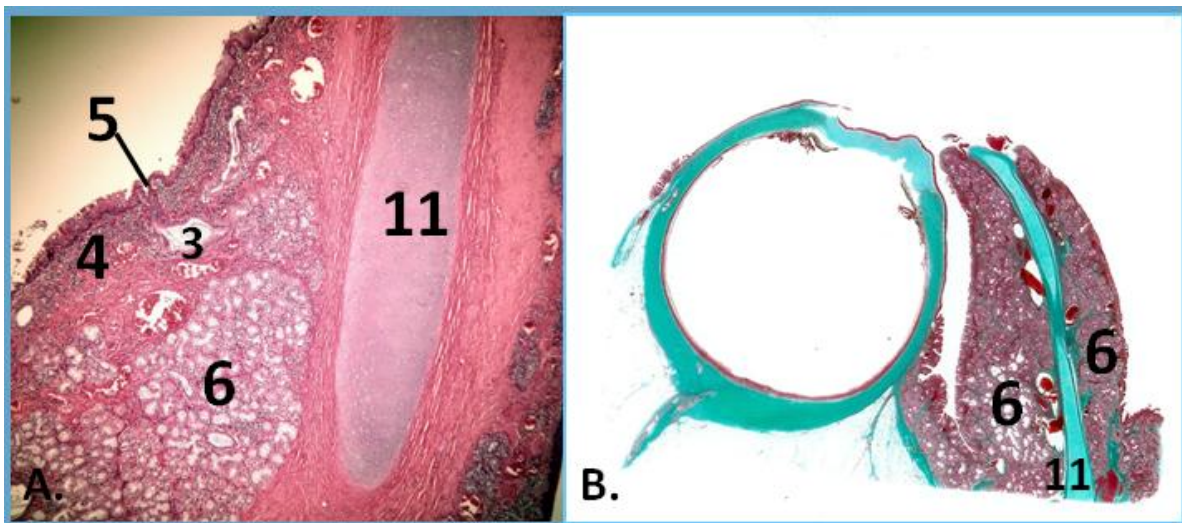


Figure 2-4. Third eyelid (nictitating lens) of the manatee. A. Nictitating gland and diffuse lymphoid tissue on the bulbar side of the third eyelid, H&E x2. B. Third eyelid and eye showing the cartilage of the third eyelid and nictitating glands on the bulbar and palpebral sides, Masson's Trichrome.

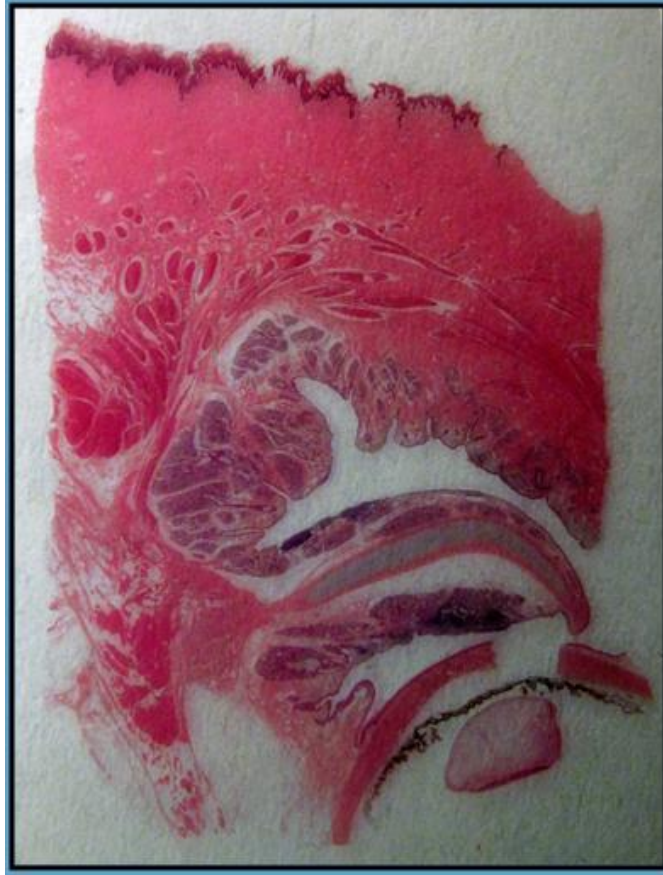


Figure 2-5. Cross section of the conjunctival associated lymphoid tissue in the manatee showing glands and lymphoid nodules in the upper and third eyelid.

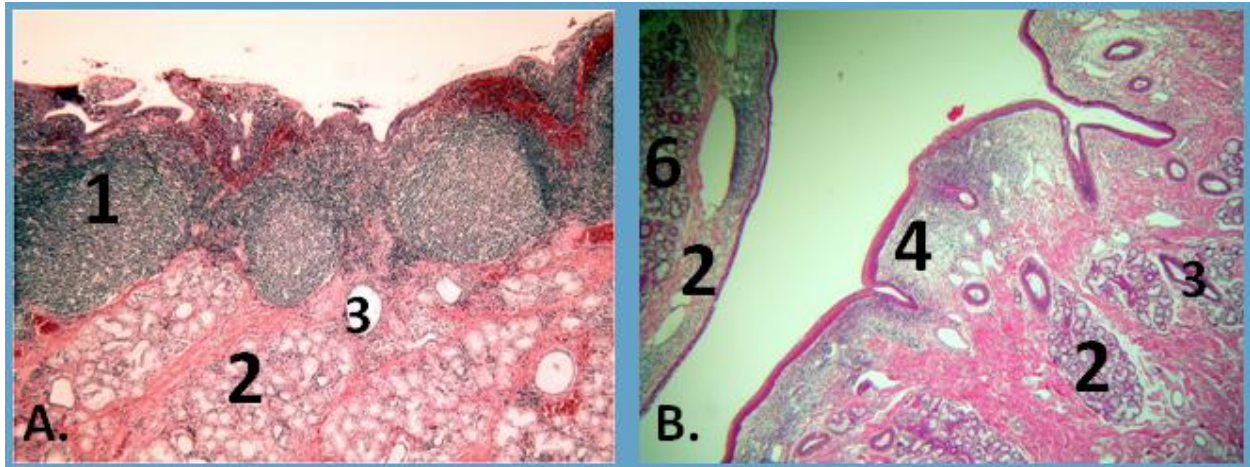


Figure 2-6. Conjunctival-associated lymphoid tissue in the manatee. A. Lymphoid nodules in the conjunctiva, H&E x10. B. Diffuse lymphoid tissue of the conjunctiva and third eyelid, PAS x2.

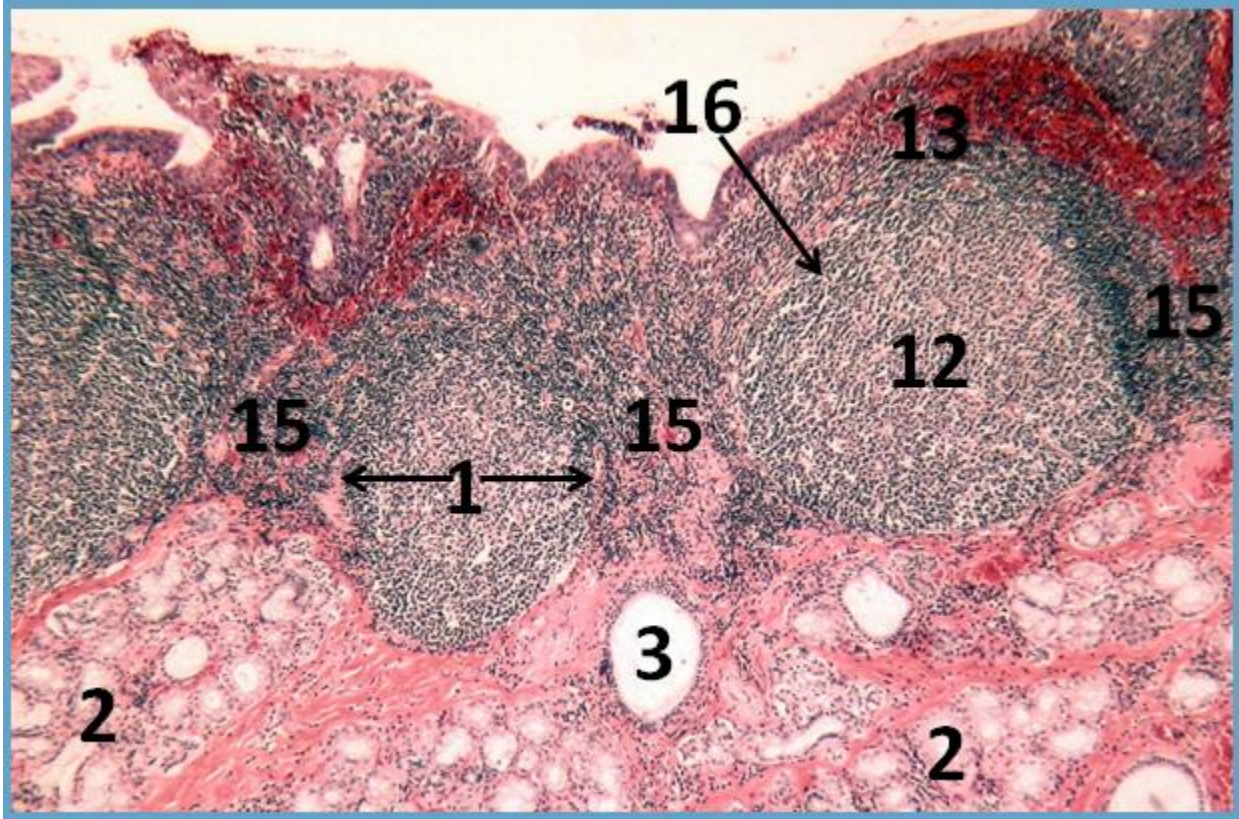


Figure 2-7. Lymphoid nodules of the conjunctiva exhibiting prominent germinal centers, corona/mantle zones, subepithelial domes, and interfollicular regions in close association with the accessory gland and ducts, H&E x10.

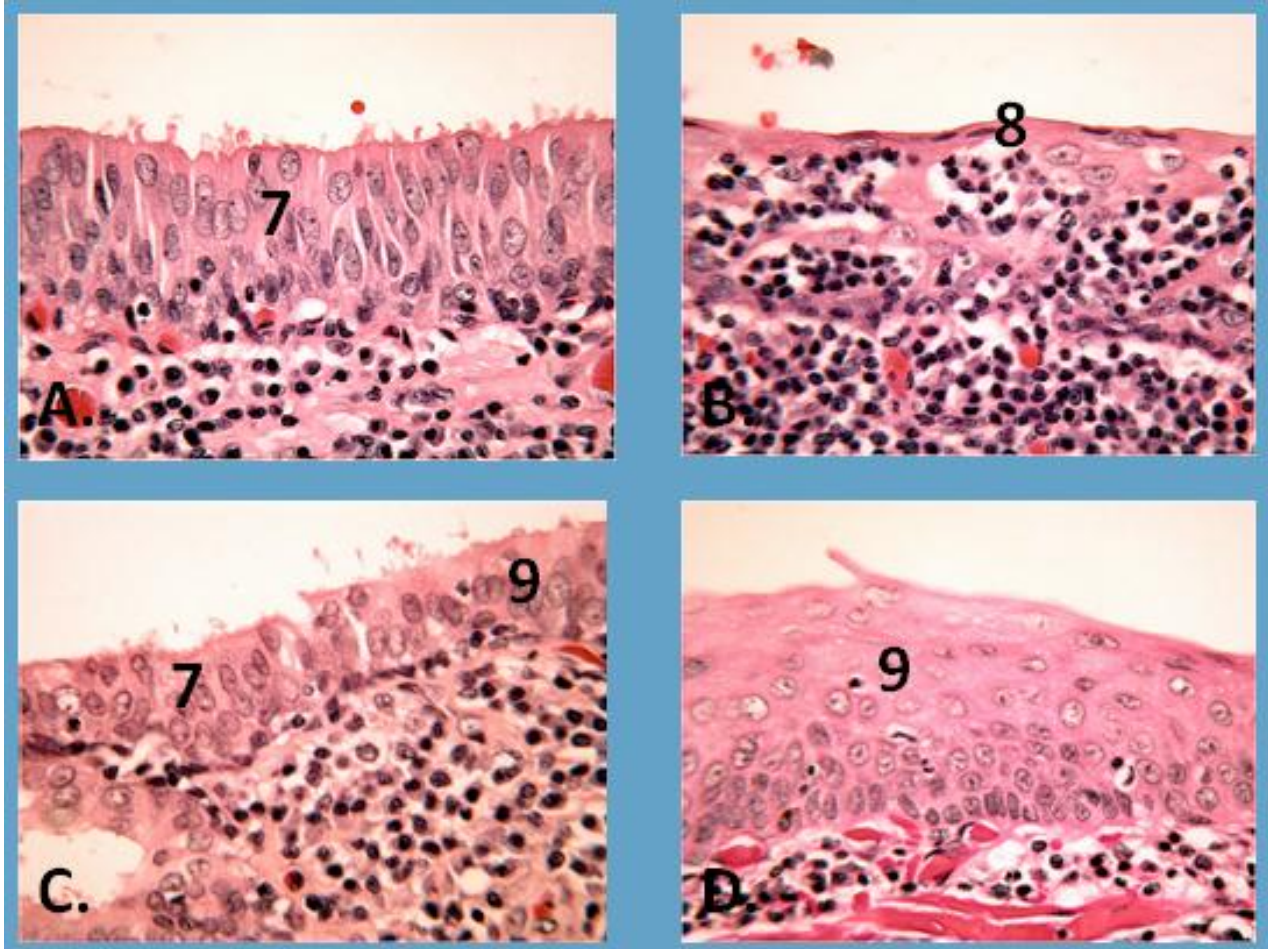


Figure 2-8. CALT epithelium. A. Stratified columnar epithelium mixed with pseudostratified epithelium, H&E x25. B. Simple squamous epithelium associated with lymphoid nodules and M-cells, H&E x25. C. Areas of pseudostratified epithelium becoming simple squamous epithelium, H&E x25. D. Stratified squamous epithelium, H&E x25.

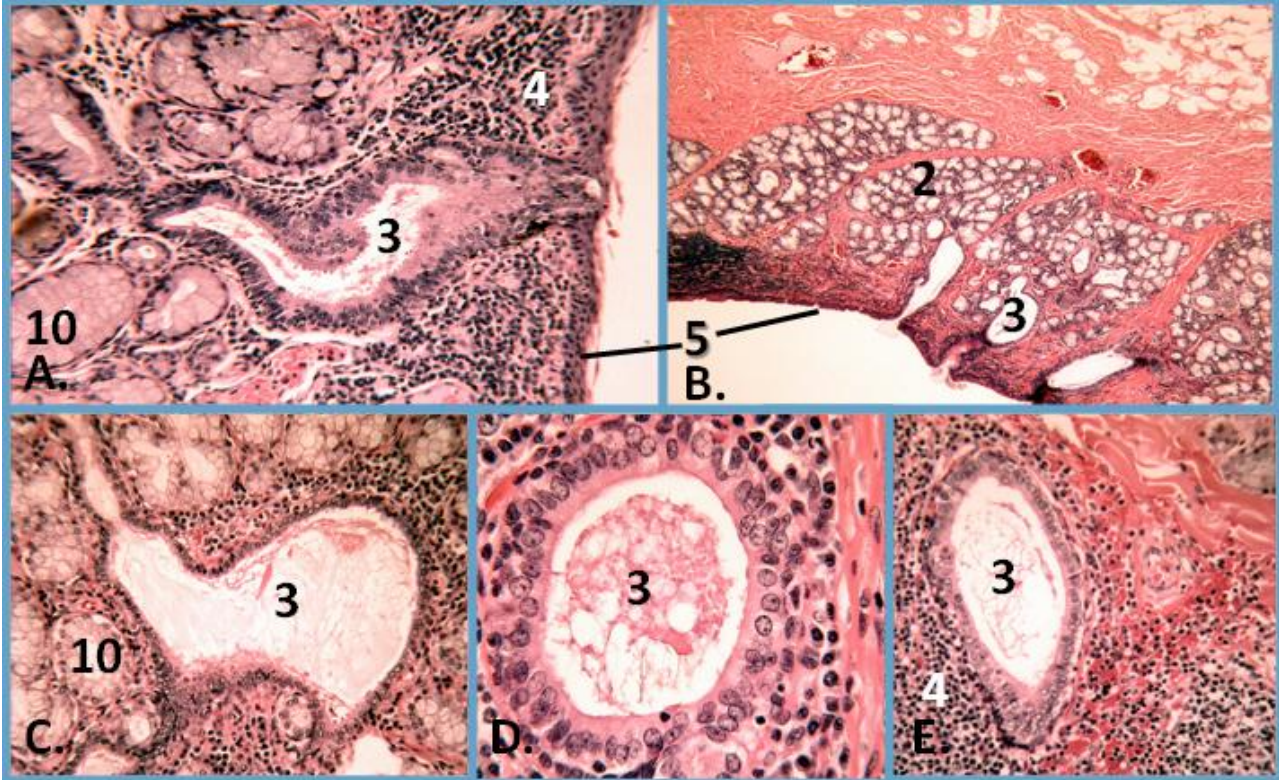


Figure 2-9. Ducts and duct-associated lymphoid tissue (DALY) of the upper eyelid. A. Serpentine duct, H&E x25. B. Ducts originating in the accessory gland of the upper eyelid winding through lymphatic tissue, H&E x10. C. Duct within diffuse lymphoid and glandular tissue, H&E x25. D. Duct and associated columnar epithelium, H&E x40. E. Duct associated with a lymphoid nodule, H&E x25.

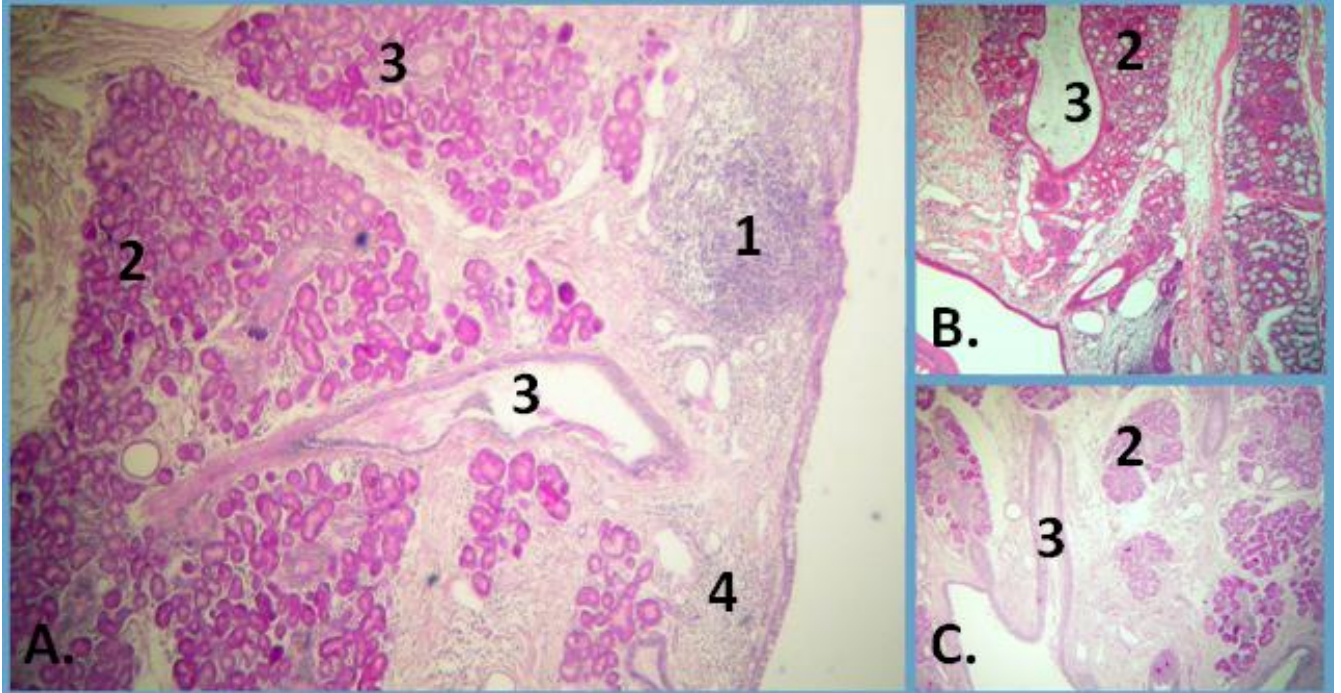


Figure 2-10. Ducts and glands of the upper and third eyelid. A. Third eyelid with nictitating gland, prominent duct, and lymphoid nodule on the palpebral side, PAS x2. B. Ducts and accessory glands of the upper eyelid, PAS x2. C. Duct and accessory glands near the fornix, PAS x2.

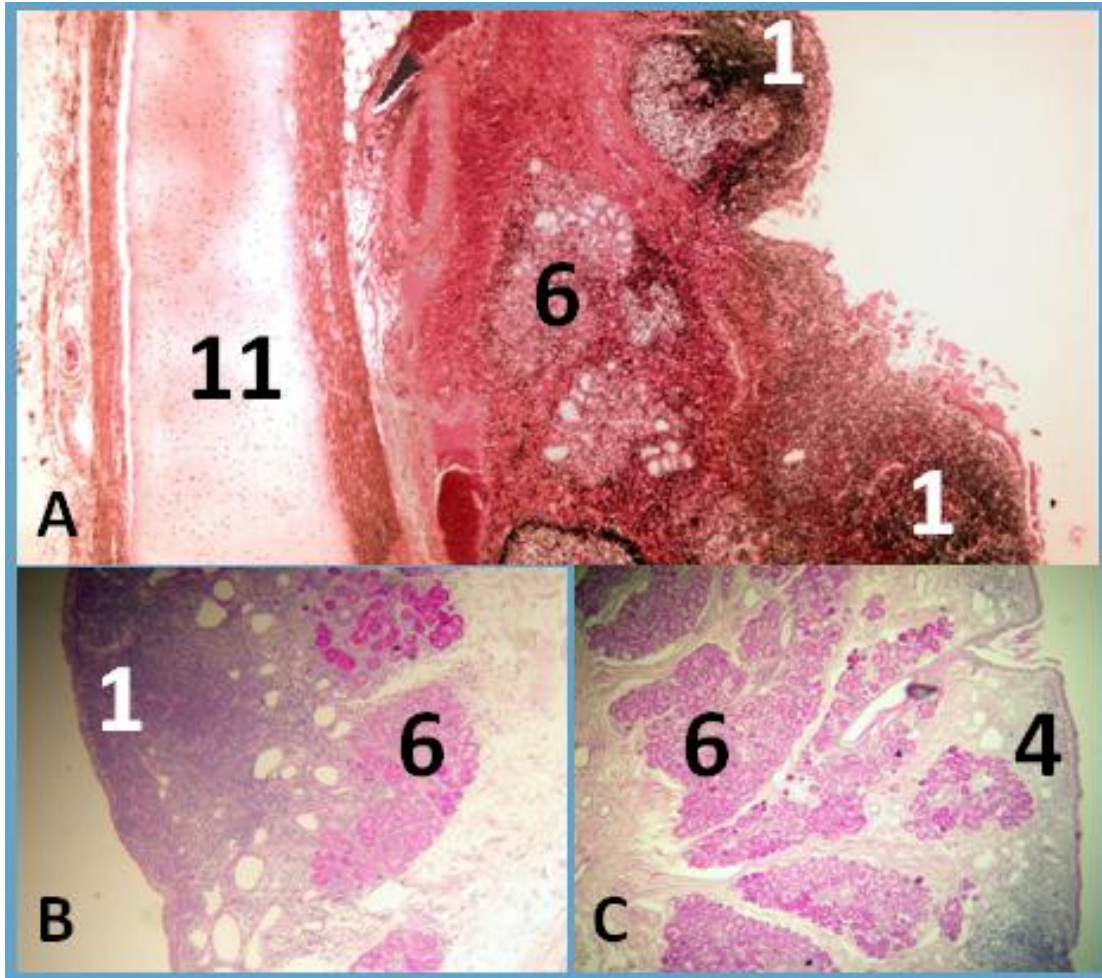


Figure 2-11. Lymphoid tissue of the third eyelid. A. Lymphoid nodules on the bulbar side of the third eyelid, H&E x2. B. Lymphoid nodule on the palpebral side of the third eyelid and nictitating gland, PAS x2. C. Nictitating gland and diffuse lymphoid tissue on the palpebral side of the third eyelid, PAS x2.

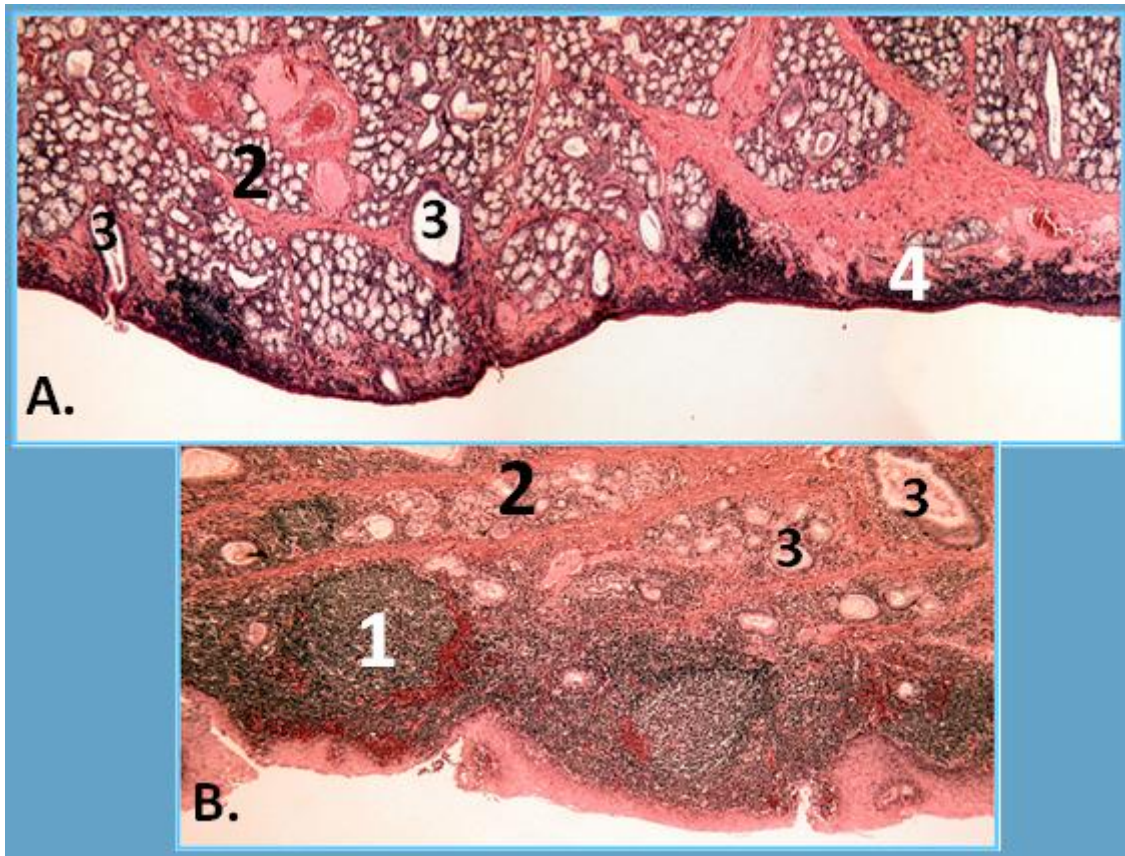


Figure 2-12. Lymphoid tissue from manatees whose cause of death (COD) was acute watercraft related. A. Diffuse lymphoid tissue, H&E x2. B. Nodular lymphoid tissue, H&E x2.



Figure 2-13. Diffuse CALT and accessory glands of a manatee whose COD was cold stress related, H&E x2.

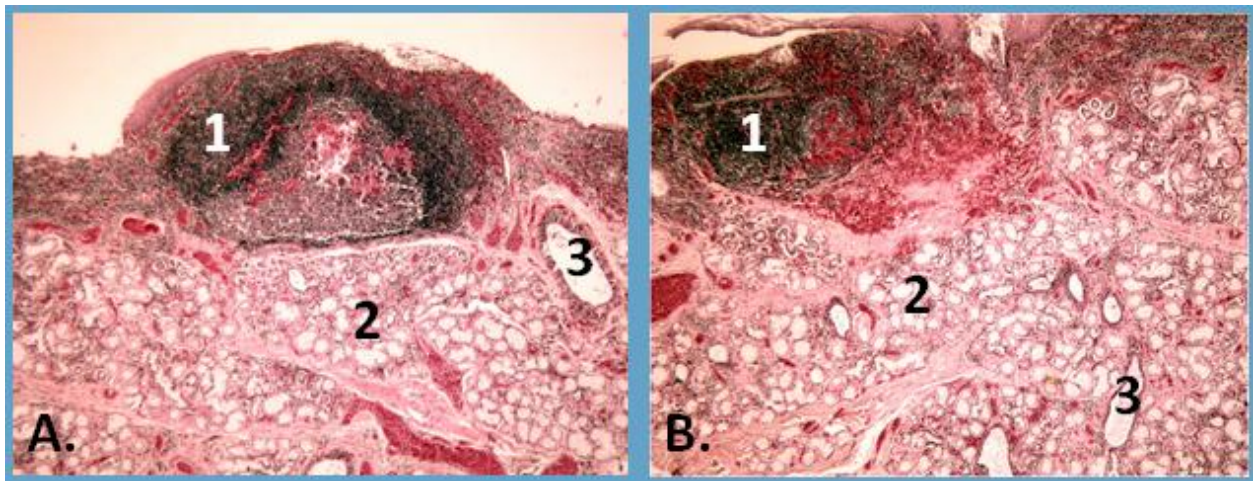


Figure 2-14. A.-B.CALT with lymphoid nodules and hemorrhaging in the upper eyelid of a manatee whose COD was red tide related, H&E x10.

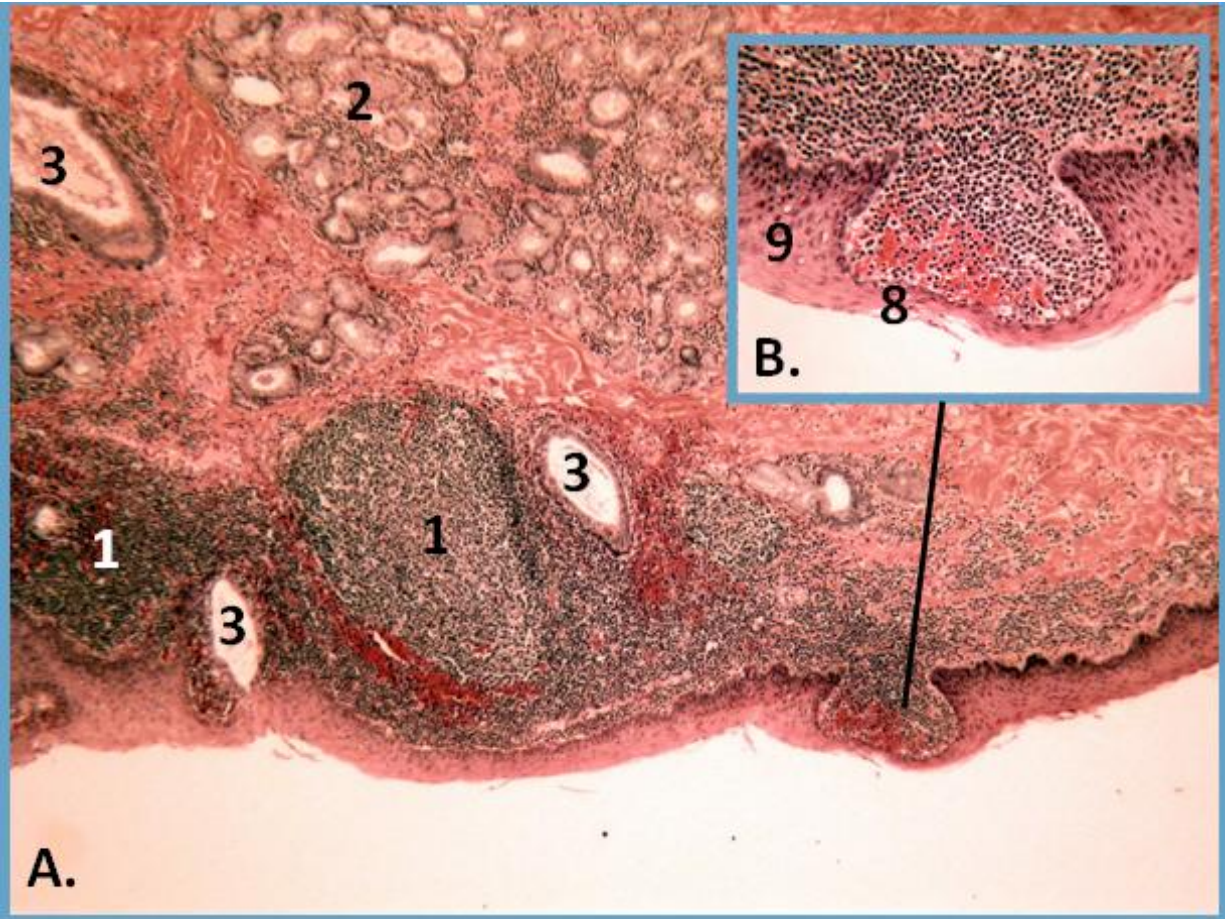


Figure 2-15. Lymphoid nodules. A. CALT with a protruding lymphoid nodule, H&E x2.
B. Protruding lymphoid nodule with potential M-cells, H&E x25.

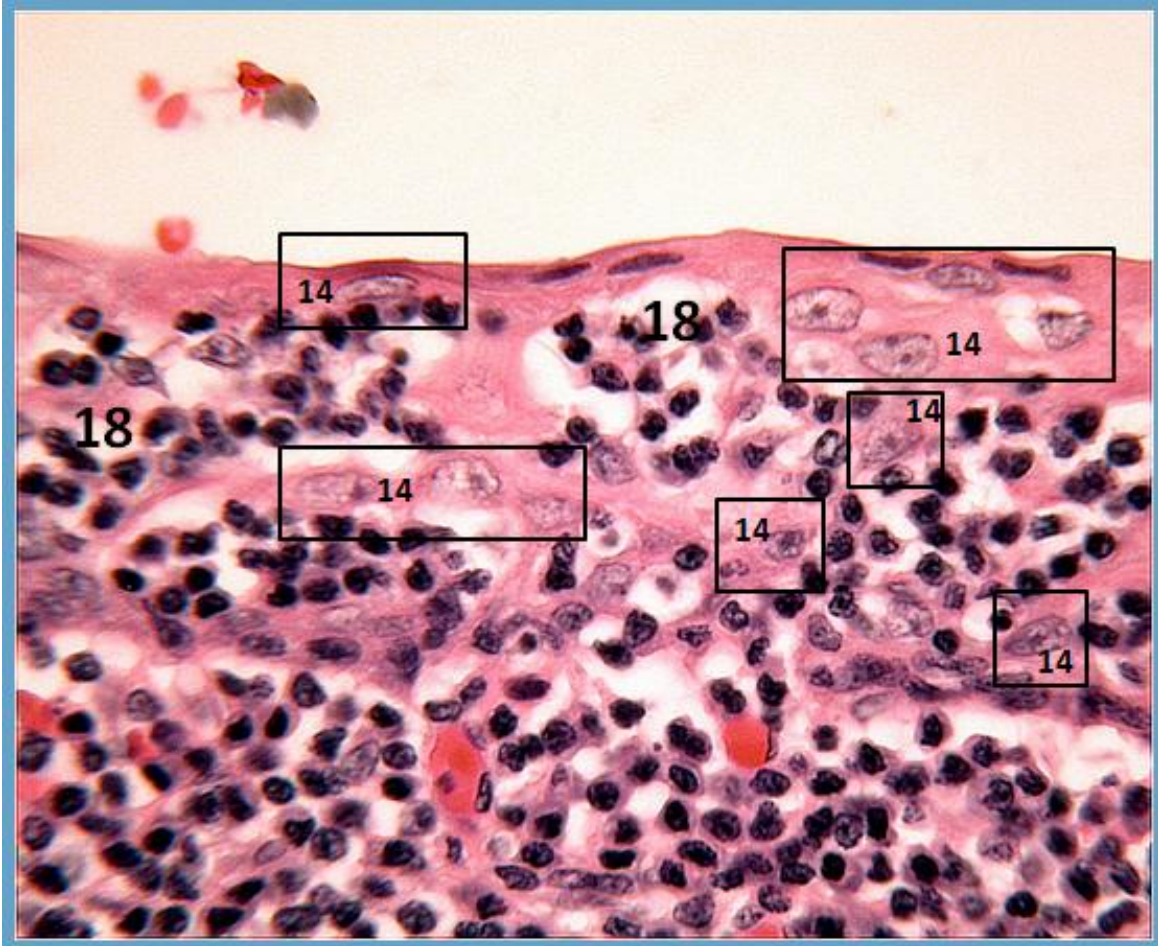


Figure 2-16. Numerous M-cells at the apical surface of a lymphoid nodule in the upper eyelid.

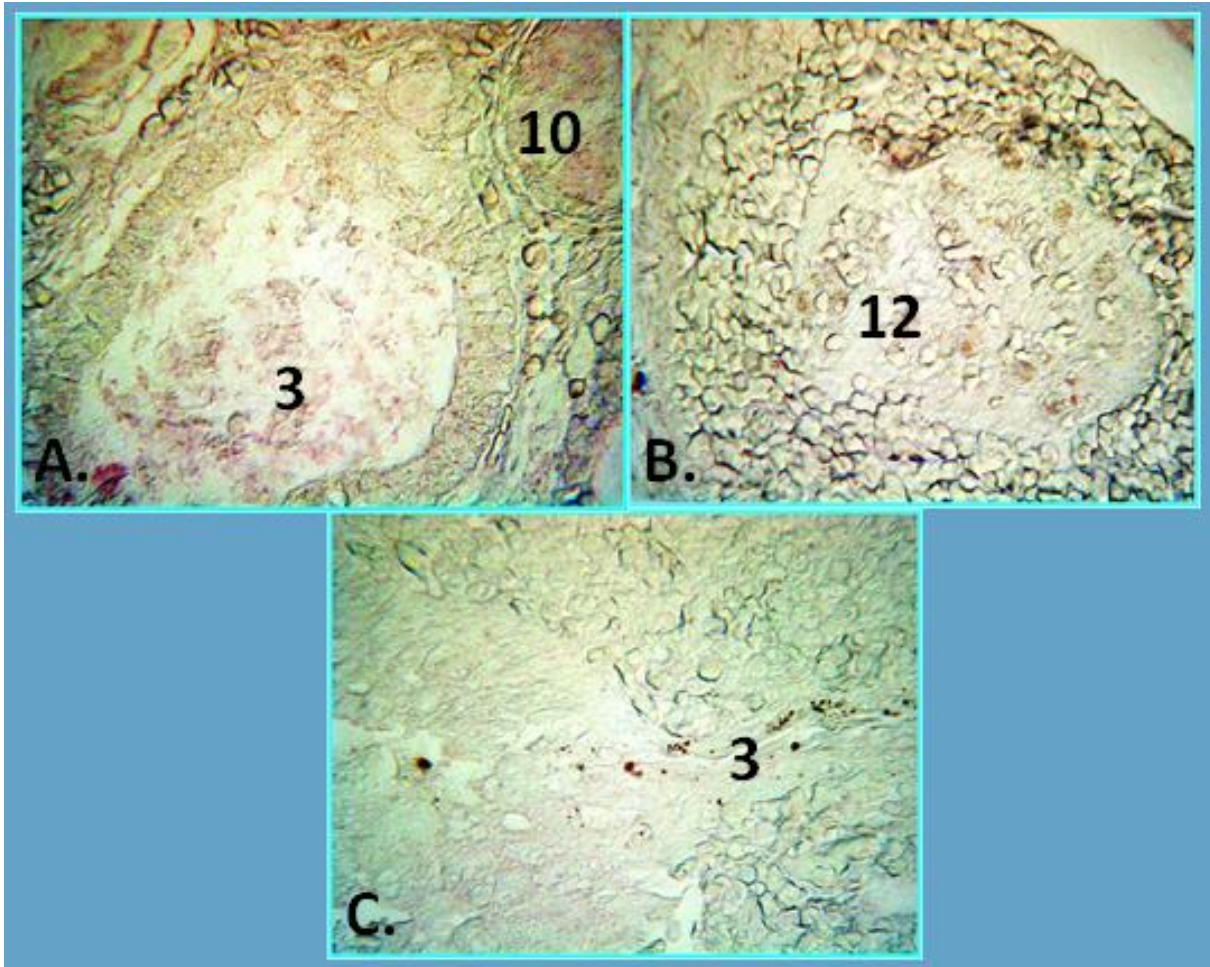


Figure 2-17. Immunohistochemical localization of immunoglobulin G (IgG) in the CALT using the mouse anti-manatee IgG mAb in a red tide COD manatee. A. Moderate reactivity in the goblet like cells and duct mucous in the upper eyelid, x25. B. Moderate reactivity in a lymphoid nodule of the upper eyelid, x25. C. Strong reactivity associated with a duct in the upper eyelid emptying onto the bulbar conjunctiva, x10.

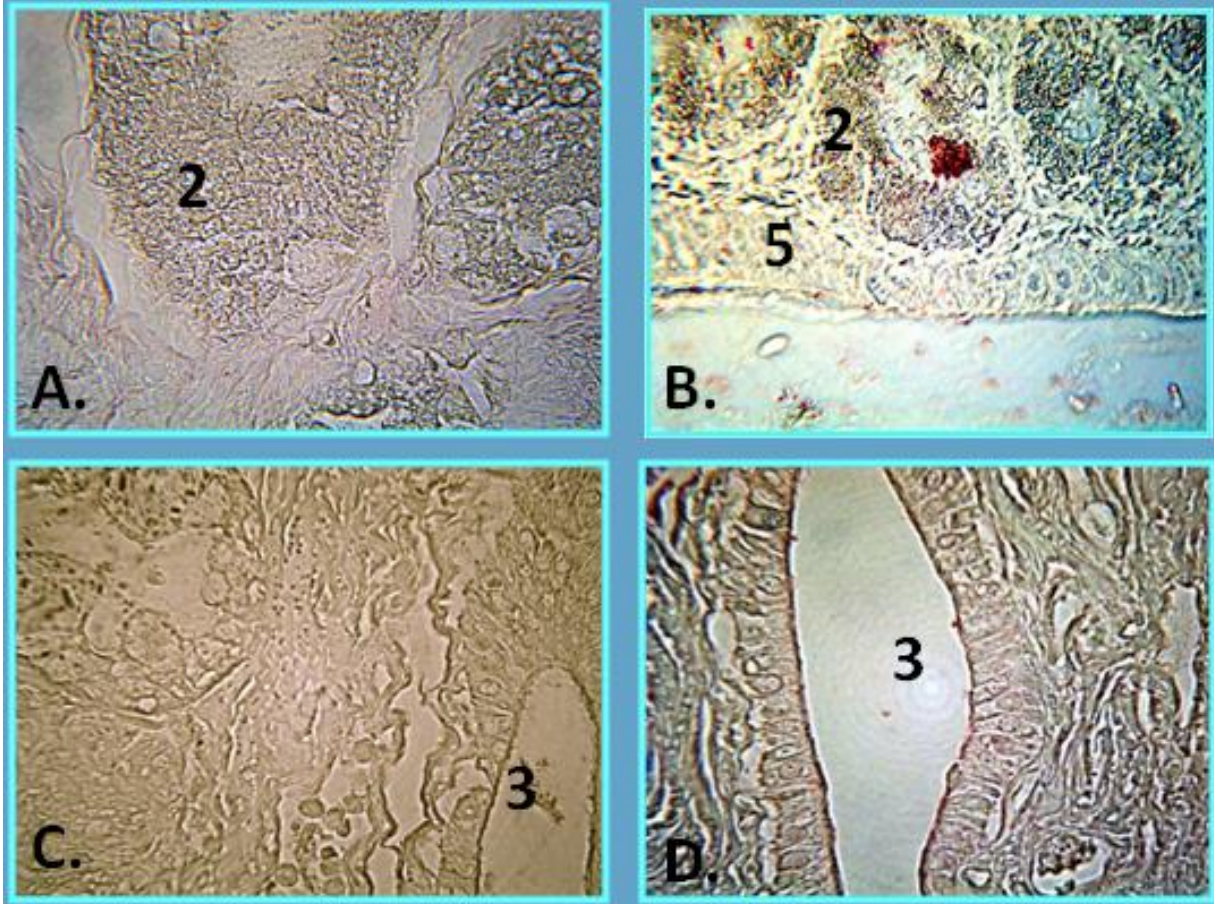


Figure 2-18. Immunohistochemical localization of IgG in manatees with various CODs. A.-B. Variable reactivity in manatees whose COD was acute watercraft related, x10. C.-D. No reactivity in manatees whose COD was cold stress related, x25.

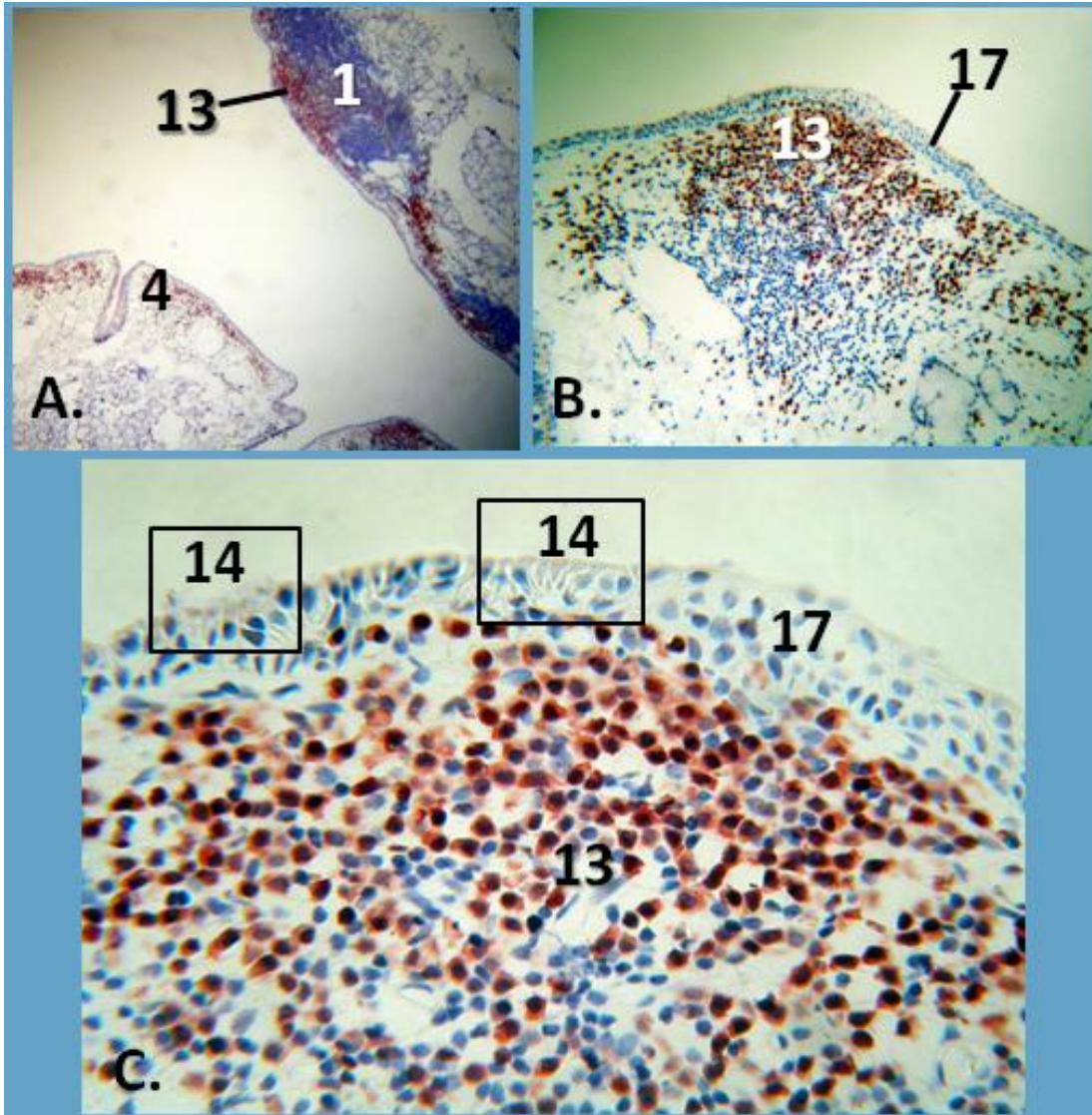


Figure 2-19. Immunohistochemical localization of plasma cells within the CALT using the Mum-1 mAb. A. Strong reactivity throughout the diffuse lymphoid tissue and in the subepithelial domes and germinal centers of lymphoid nodules, x2. B. Lymphoid nodule demonstrating strong presence of plasma cells in the subepithelial dome, x10. C. Apical surface of the lymphoid nodule with areas of potential M-cells, x25.

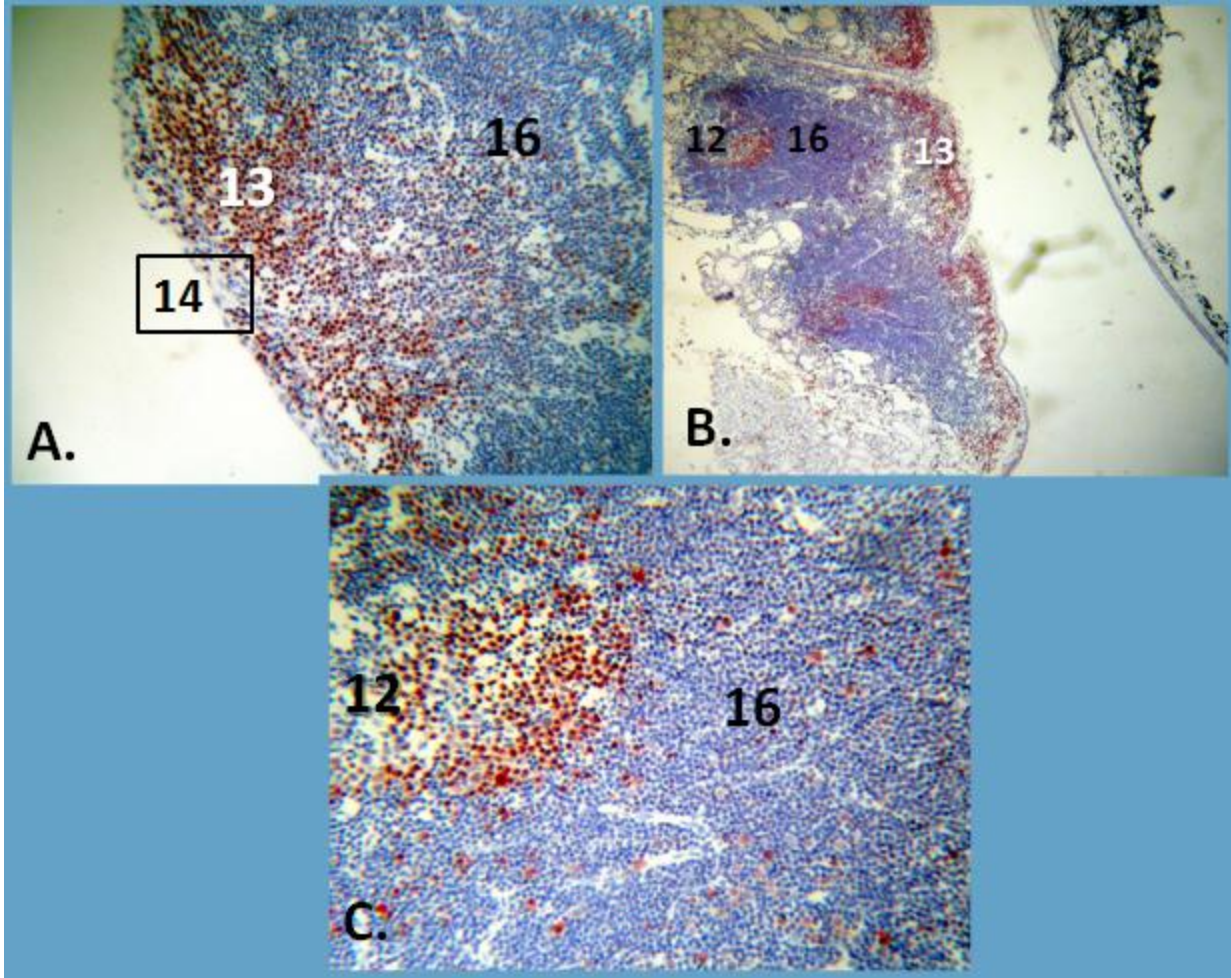


Figure 2-20. Immunohistochemical localization of plasma cells (via Mum-1 mAb) in the third eyelid. A. Strong reactivity on the subepithelial dome with potential M-cell region, x10. B. Bulbar side of the third eyelid with plasma cells concentrated throughout the SED and GC with diffuse distribution in the IFR and corona/mantle zone, x2. C. Germinal center and corona/mantle zone of a lymphoid nodules, x10.

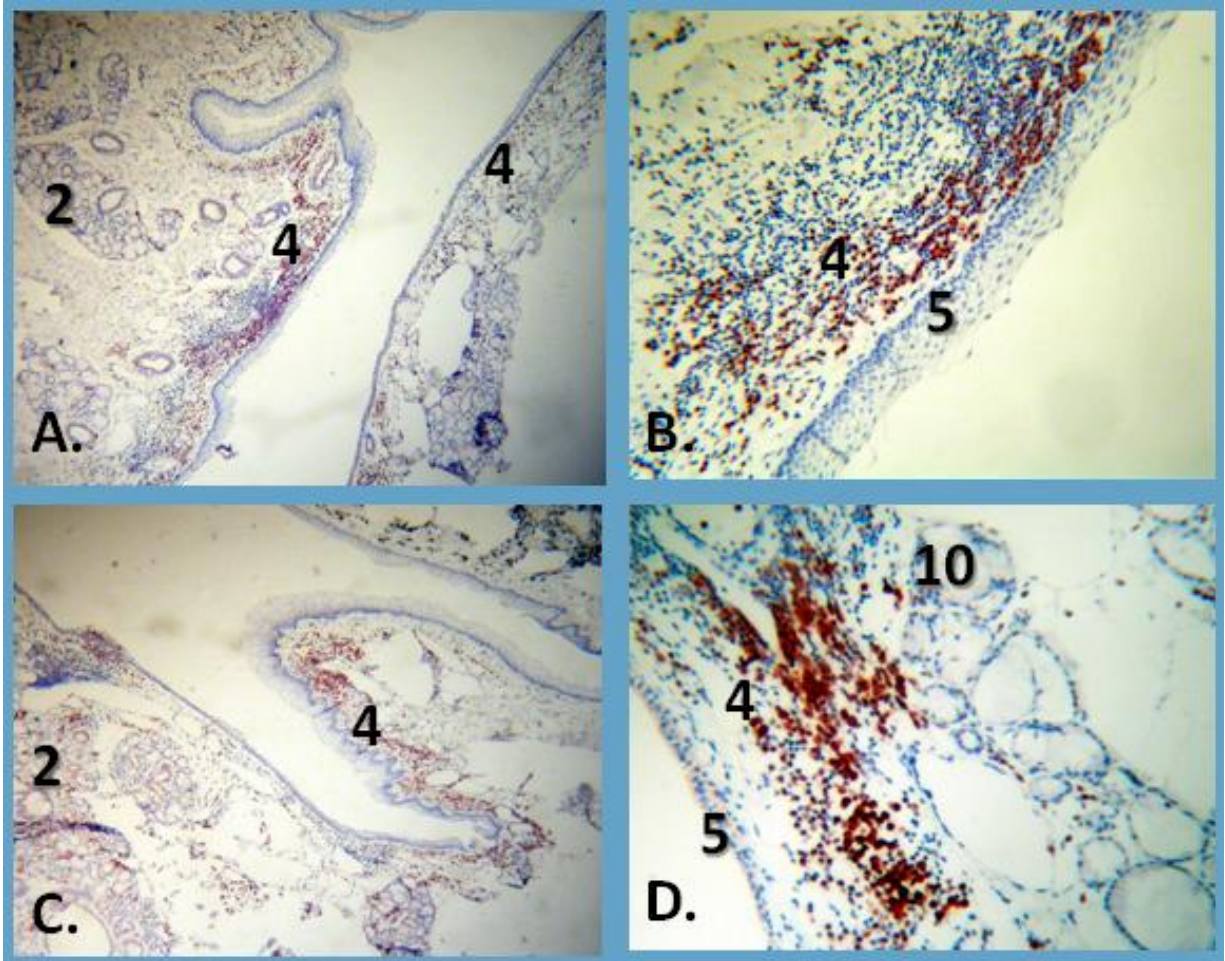


Figure 2-21. Immunohistochemical localization of plasma cells in diffuse lymphoid tissue. A. Upper eyelid and third eyelid, x2. B. Upper eyelid, x10. C. Fornix, x2. D. Third eyelid, x10.

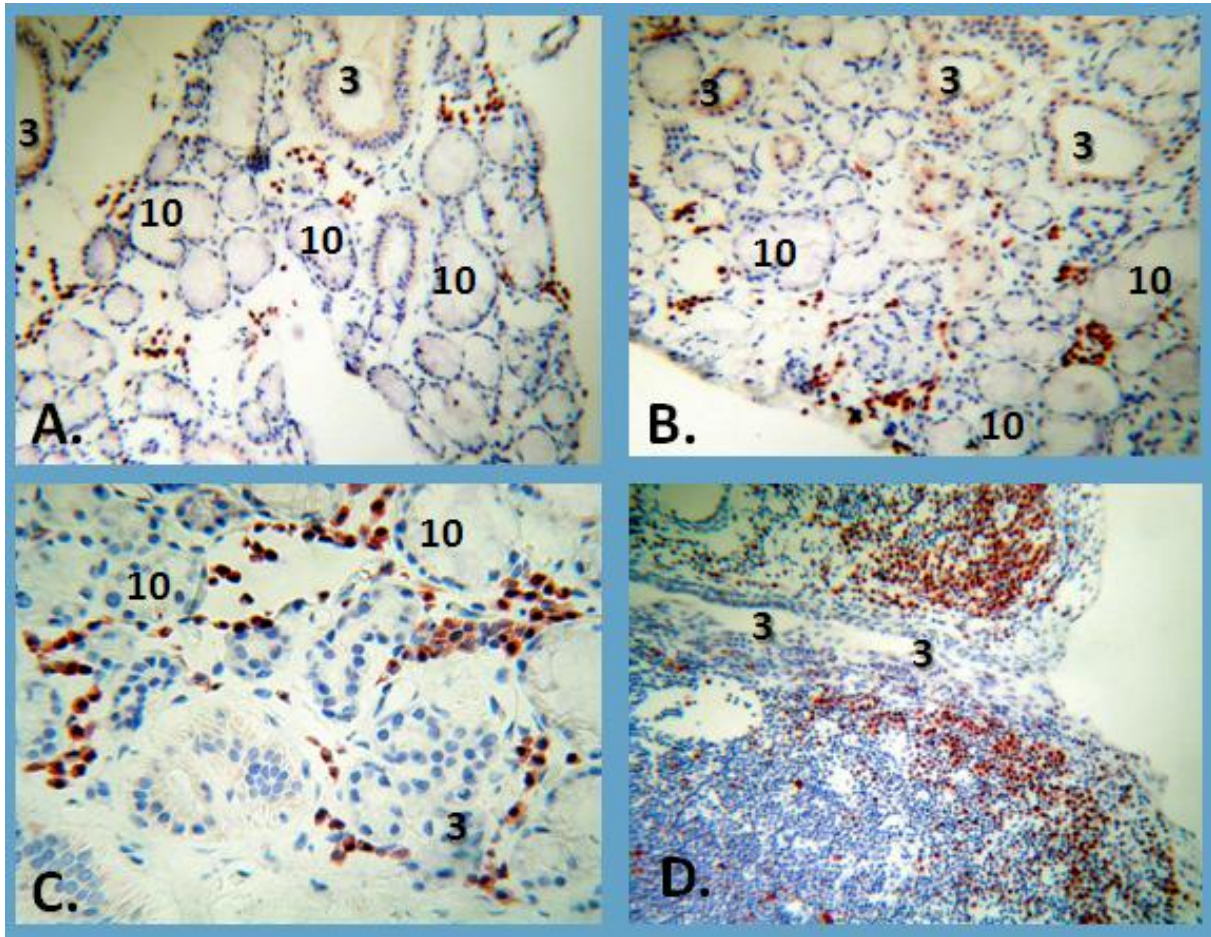


Figure 2-22. Immunohistochemical localization of plasma cells in the accessory glands and ducts. A.-B. Diffuse plasma cell distribution throughout the accessory gland of the upper eyelid and in the duct epithelium, x10. C. Goblet like cells of the accessory gland, x25. D. Diffuse lymphoid tissue associated with a duct in the upper eyelid, x2.

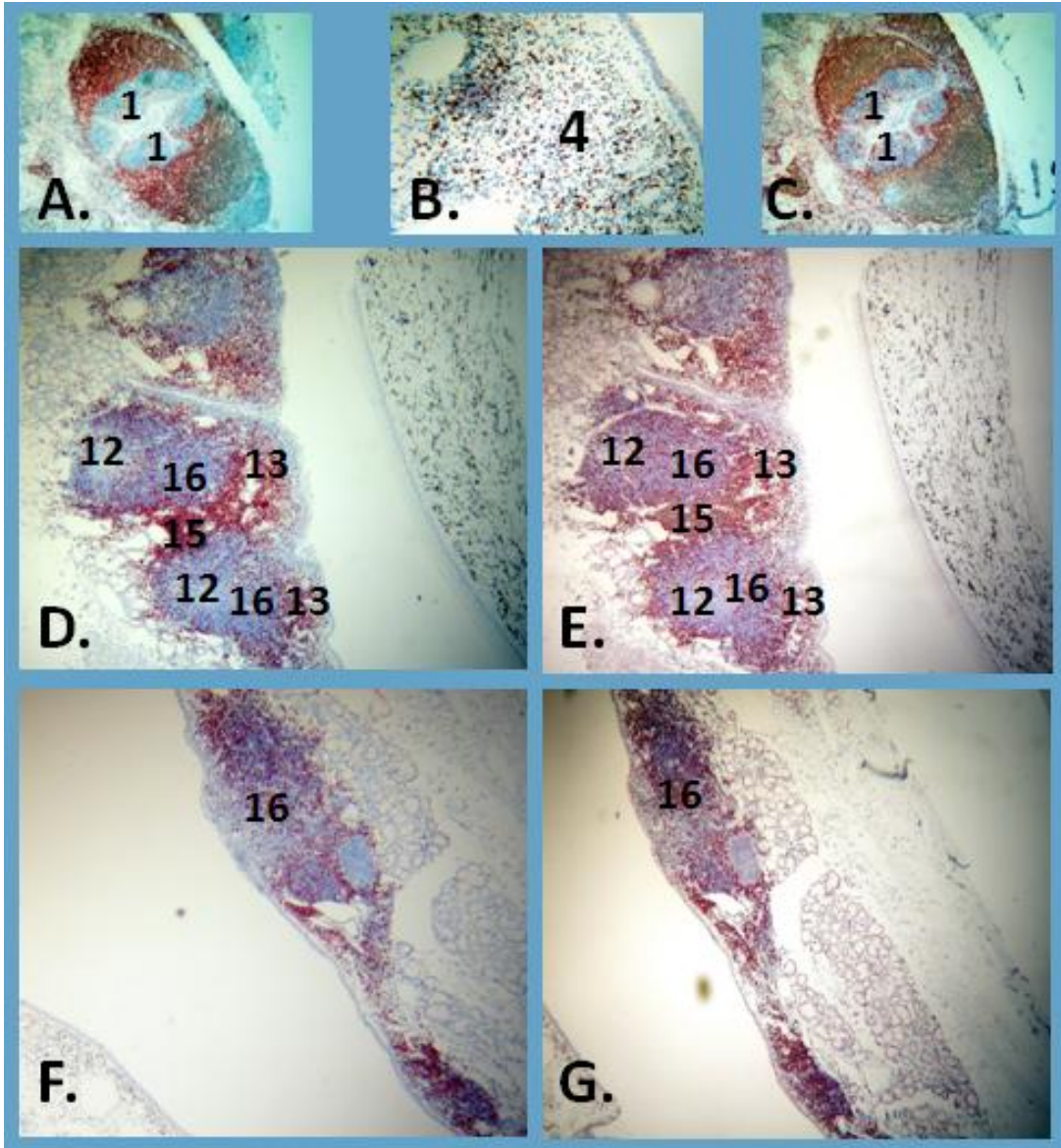


Figure 2-23. Immunohistochemical localization of T cells (via CD3) in the CALT. A.&C. Canine lymphoid tissue positive control for CD3 mAb and pAb respectively, x2. B. Diffuse lymphoid tissue in the upper eyelid, x10. D.-E. Strong reactivity in the SED and IFR with moderate reactivity in the corona/mantle zone and little to no reactivity in the GC (mAb and pAb respectively), x2. F.-G. Strong reactivity in the nodular and diffuse lymphoid tissue with little to no reactivity associated with the glands of the third eyelid (mAb and pAb respectively), x2.

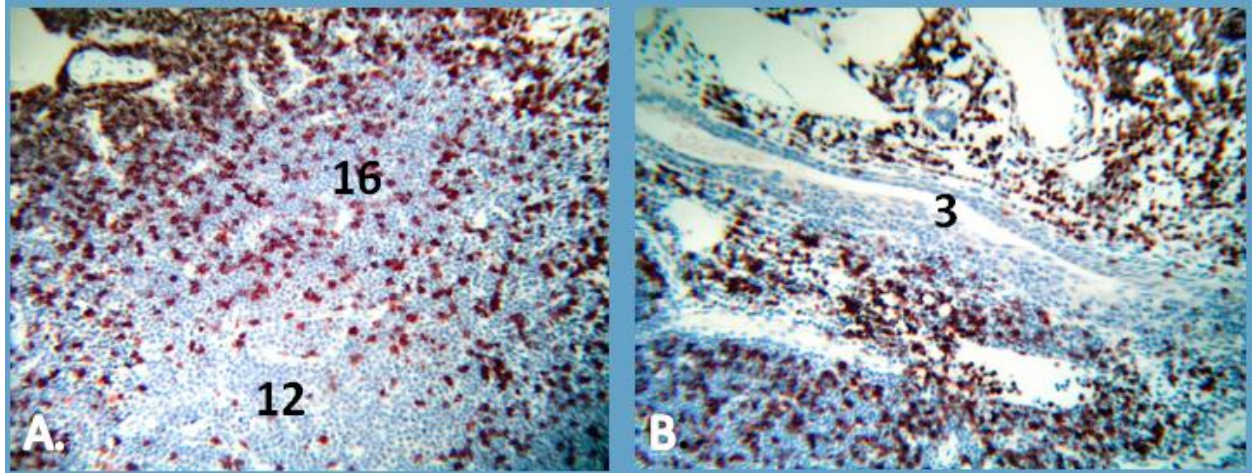


Figure 2-24. Immunohistochemical localization in of T cells (via CD3) in the CALT. A. Diffuse T cells distribution throughout the corona/mantle zone, little to no reactivity in the GC, and strong T cell presence in the SED and IFR in the upper eyelid, x25. B. T cells surrounding a duct in the third eyelid, x10.

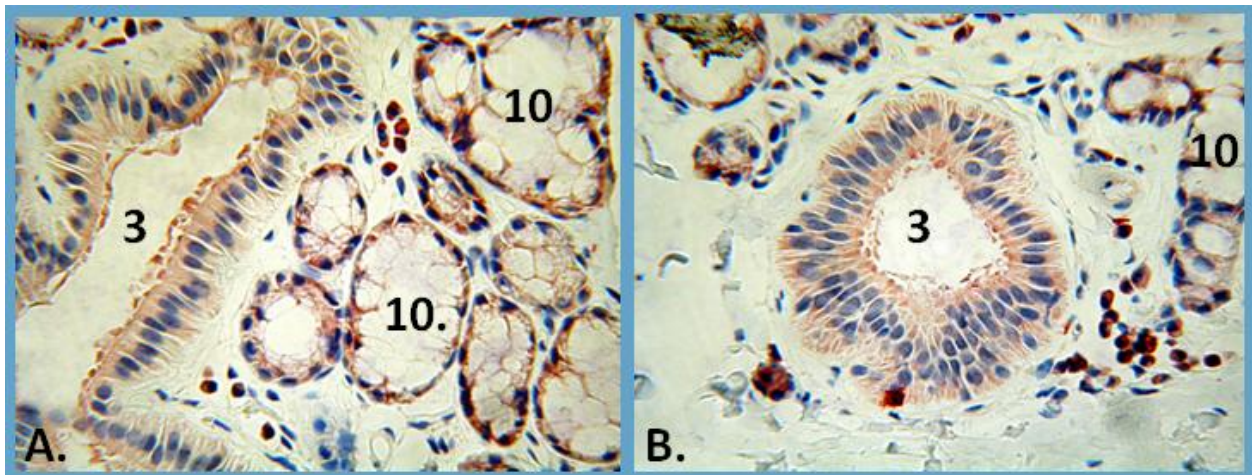


Figure 2-25. A.-B. Immunohistochemical localization of T-cells (via CD3) associated with the goblet like cells and ducts of the upper eyelid, x40.

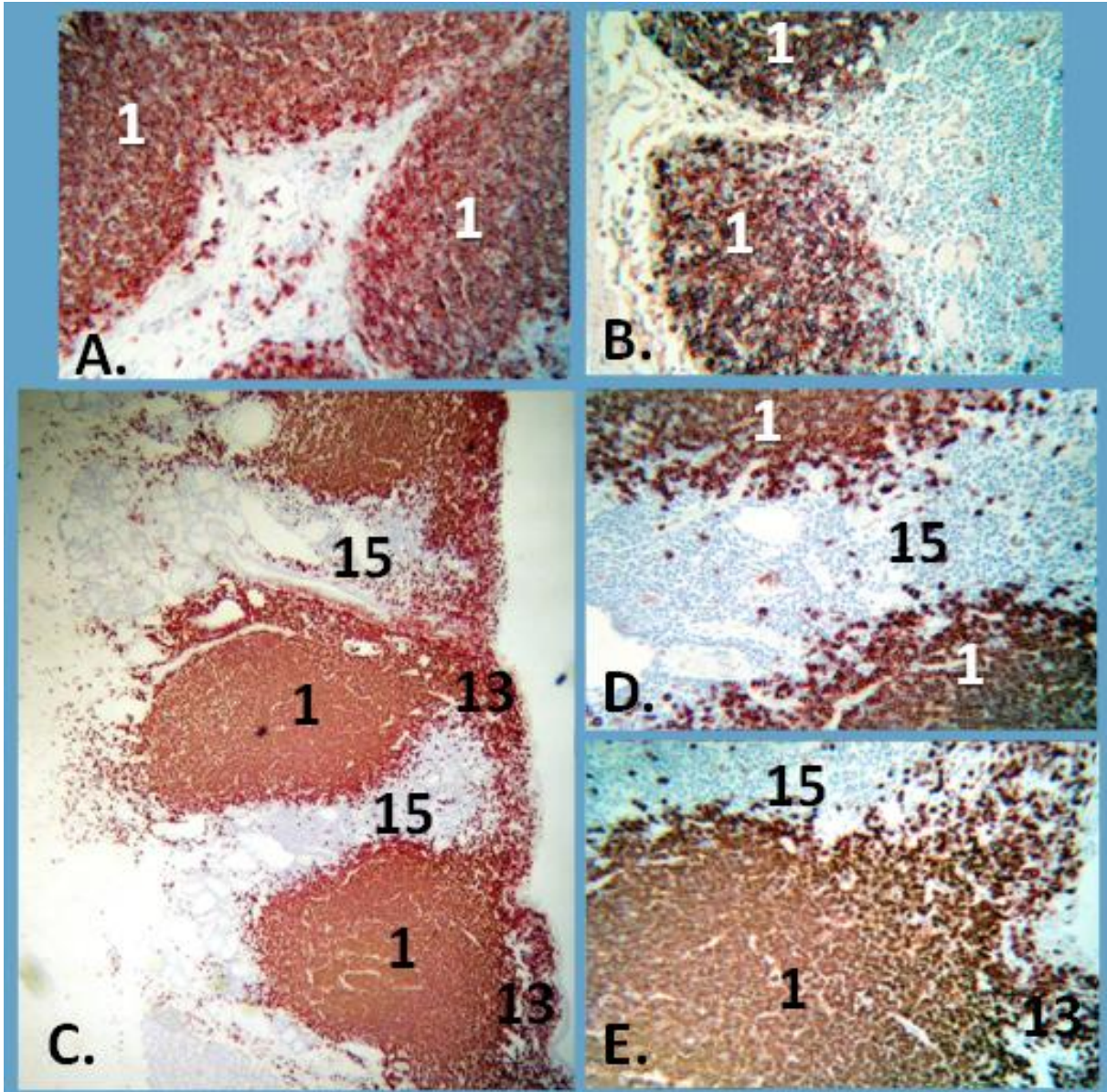


Figure 2-26. Immunohistochemical localization of B cells (via CD20) in the CALT. A.-B. Positive controls using canine lymphoid tissue. C. Strong B cell presence throughout the lymphoid nodules. Little to no reactivity in the IFR, x2. D. Interfollicular region with associated lymphoid nodules, x10. E. Lymphoid nodule, x10.

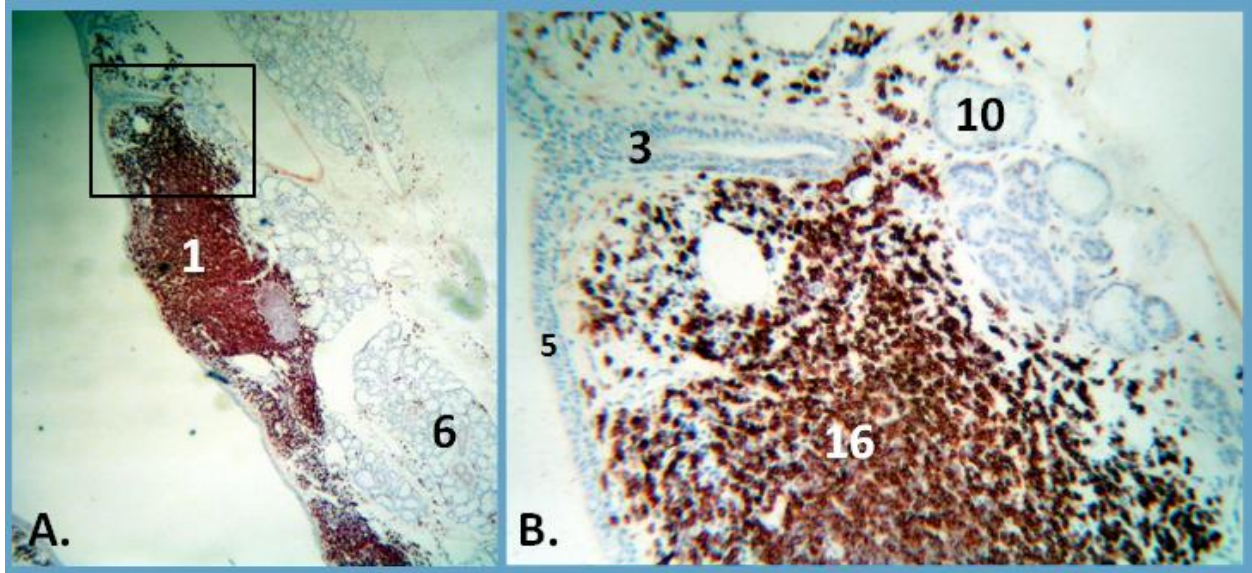


Figure 2-27. A.-B. Immunohistochemical localization of B cells (via CD20) in the third eyelid exhibiting strong reactivity in the lymphoid nodules and diffuse lymphoid tissue with little to no reactivity associated with the nictitating gland, x2 and x25 respectively.

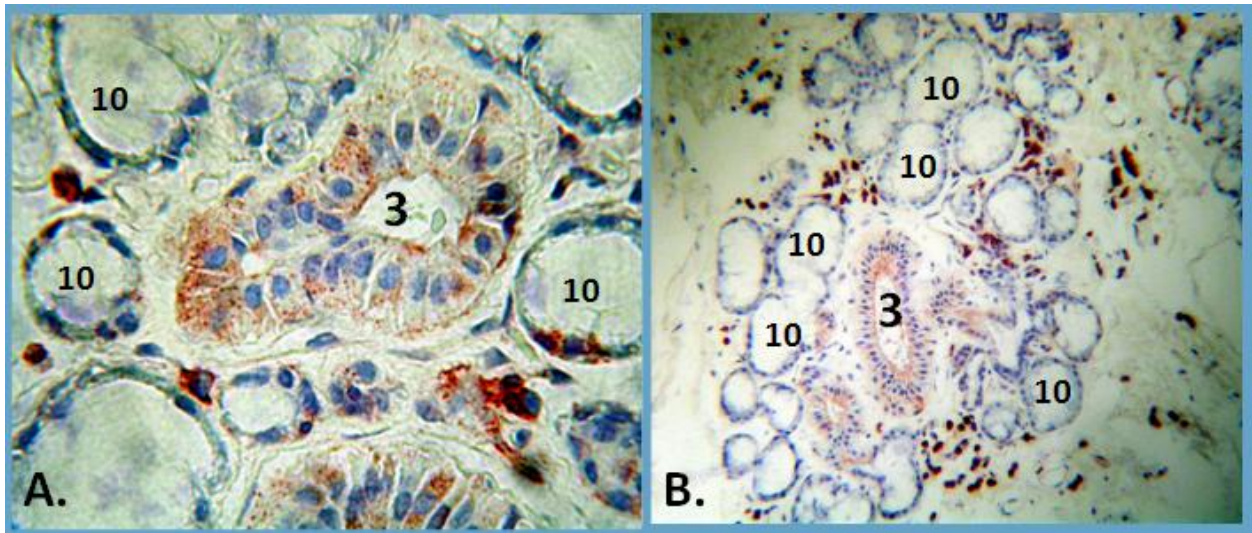


Figure 2-28. Immunohistochemical localization of B cells (via CD20) associated with the accessory gland and ducts of the upper eyelid. A. Duct and goblet-like cells, x40. B. Duct and goblet-like cells, x25.

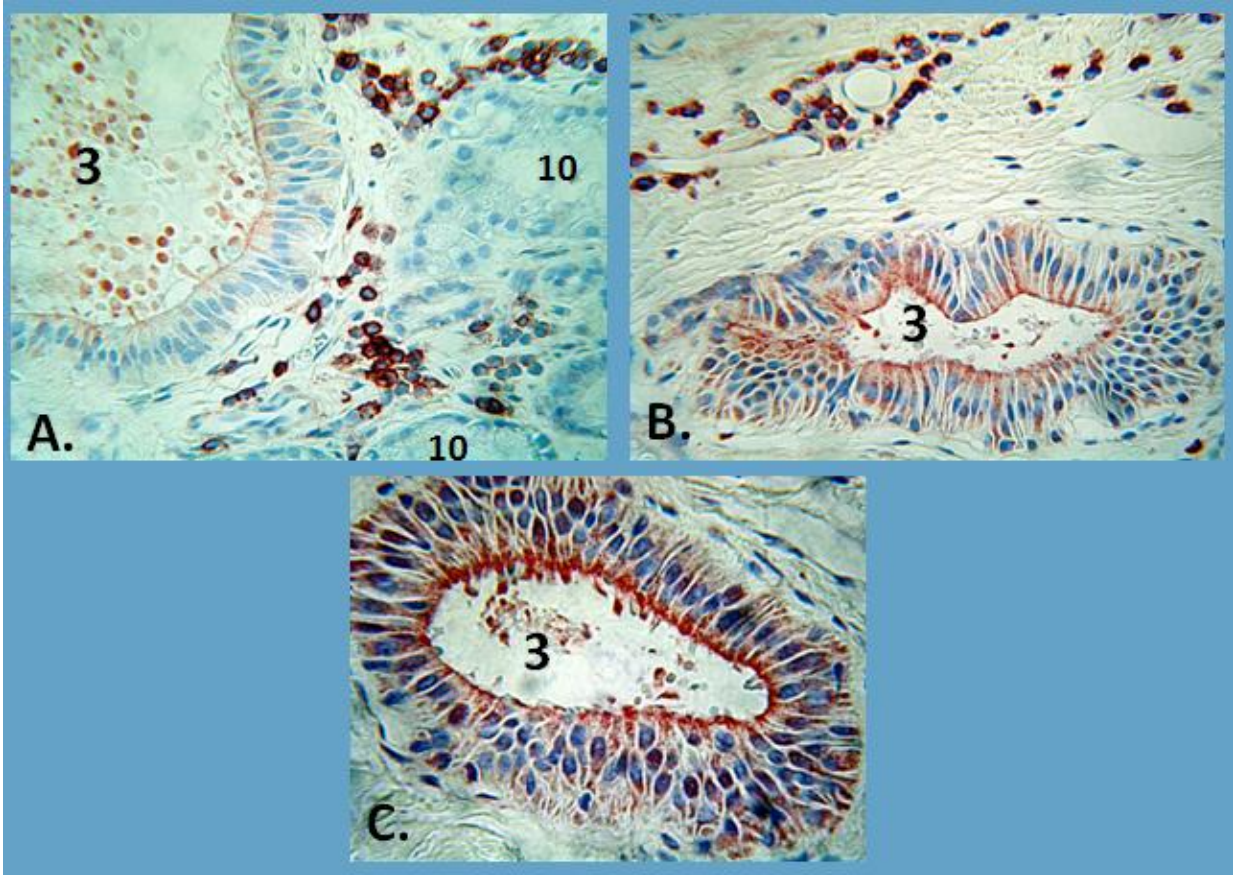


Figure 2-29. Immunohistochemical localization of B cells (via CD20) associated with the ducts of the upper eyelid. A.-C. Ducts within the accessory gland containing mucous secretions, x40.

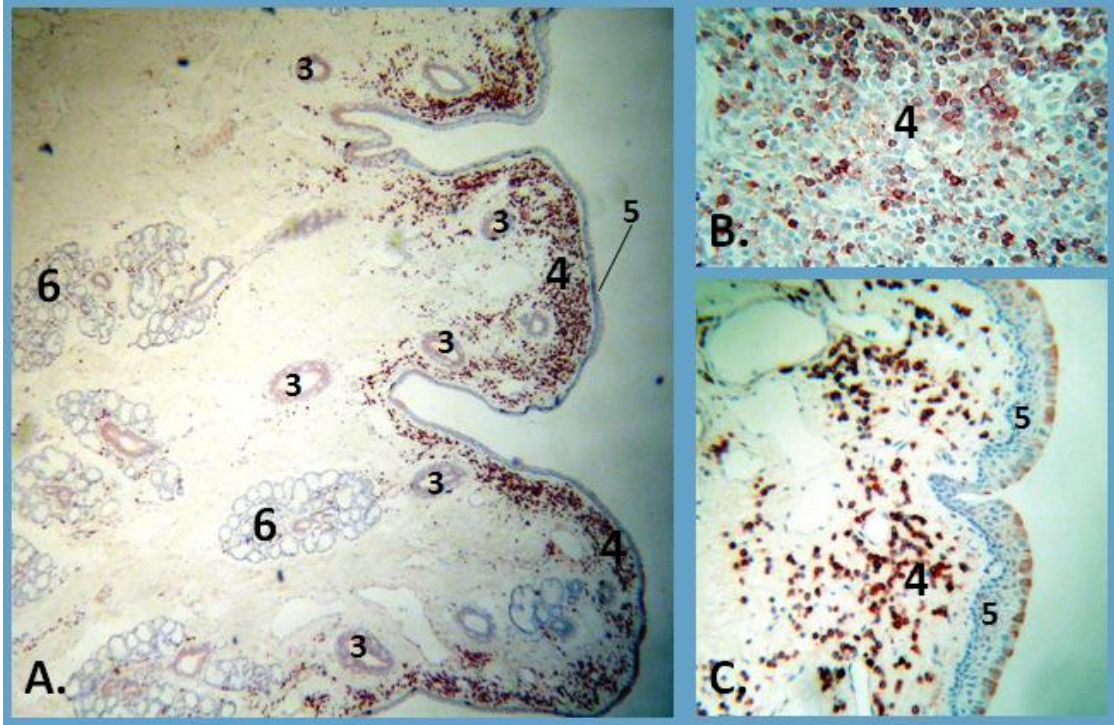


Figure 2-30. Immunohistochemical localization of B cells (via CD20) in diffuse lymphoid tissue. A. Diffuse lymphoid tissue of the upper eyelid, x2. B. Diffuse lymphoid tissue and B cell distribution, x25. C. B cell localization in diffuse lymphoid tissue and conjunctival epithelium, x10.

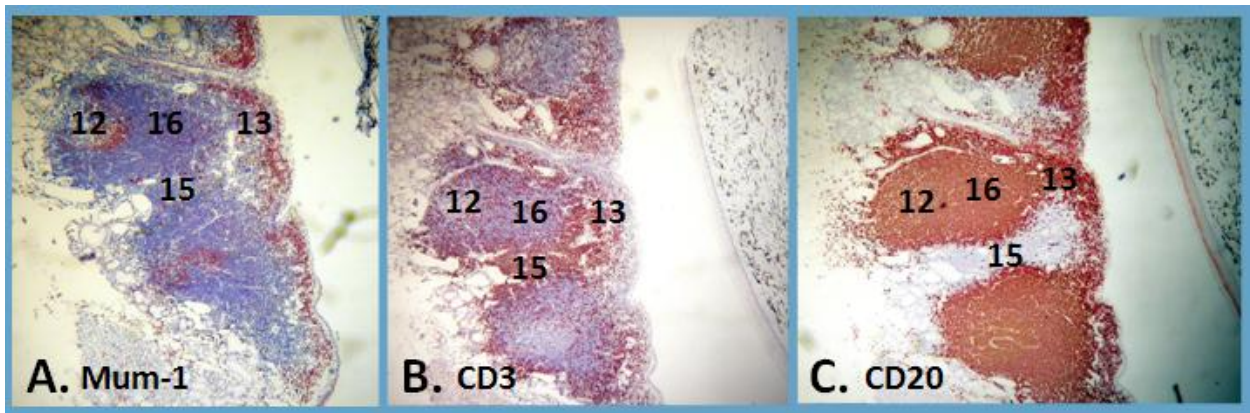


Figure 2-31. Summary of immunohistochemical localization in the CALT A. Plasma cells (Mum-1 mAb), x2. B. T cells (CD3 mAb), x2. C. B cells (CD20 mAb), x2.

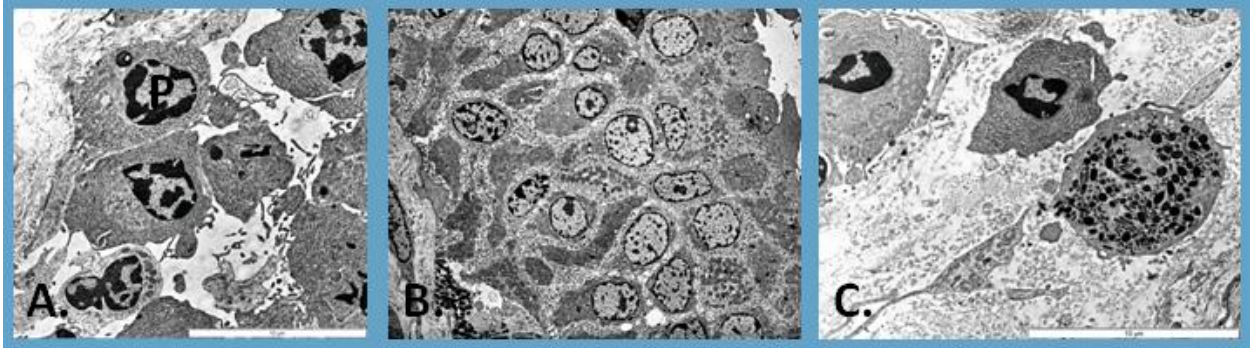


Figure 2-32. CALT within the lower eyelid of an adult male. A. Edge of the follicle contains numerous plasma cells. B. Most of the overlying epithelium is stratified. C. Variety of cells of defense within this region.

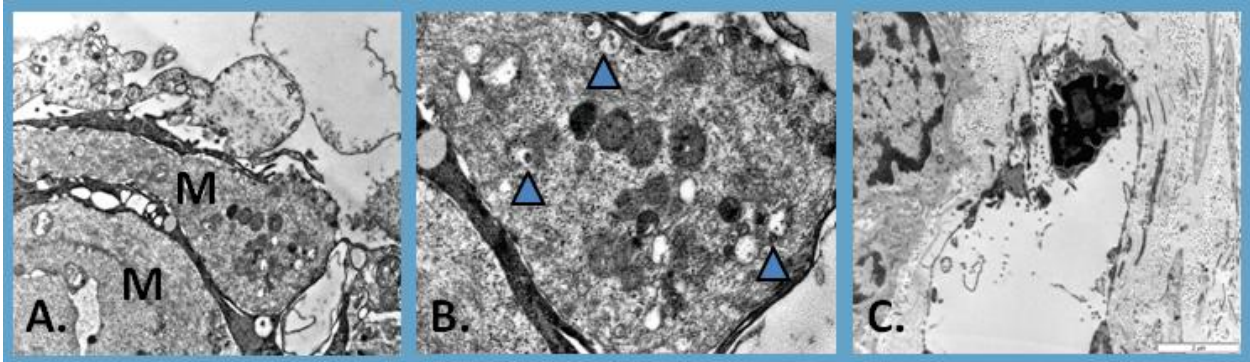


Figure 2-33. A.-B. TEM of epithelial lining and apparent M cells with endocytotic vesicles (solid arrows), x5000 and x12000 respectively. C. Numerous lymphatic vessels occur in this region.

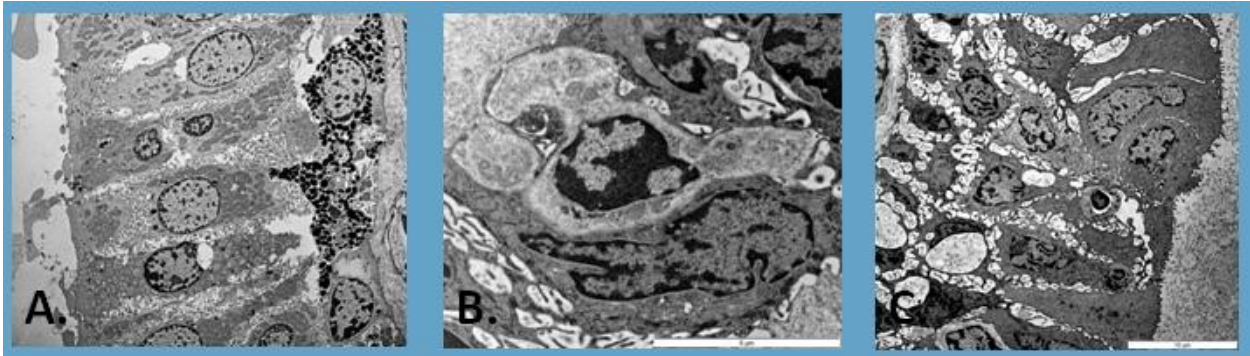


Figure 2-34. Large ducts emptying nearby accessory glands are lined by simple columnar epithelia. A.-C. TEM reveals extensive cellular processes between adjacent cells with varying amounts of intercellular space often occupied with other cells.

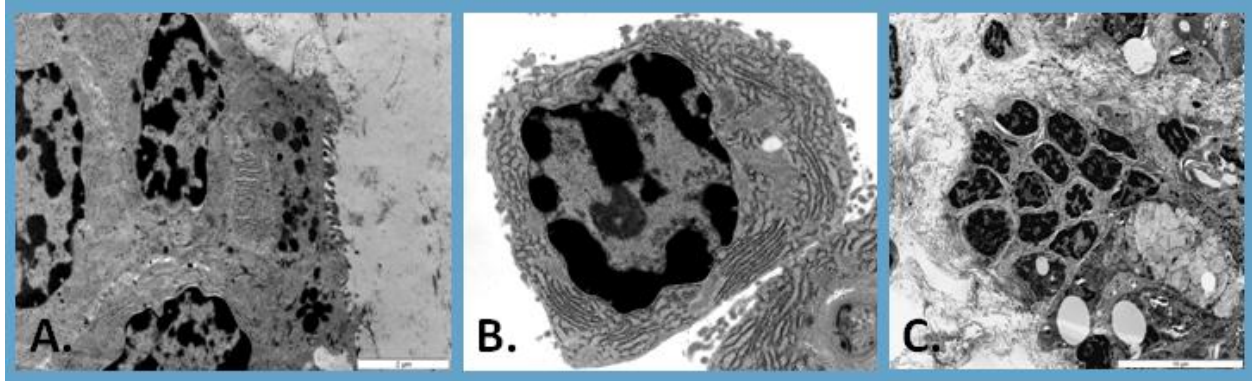


Figure 2-35. CALT associated with the nictitating membrane and gland. A. Lined by pseudostratified columnar epithelium. B. Plasma cell that is diffusely scattered among glandular tissue, x10000. C. Cluster of lymphocytes next to an adenomere, x5000.

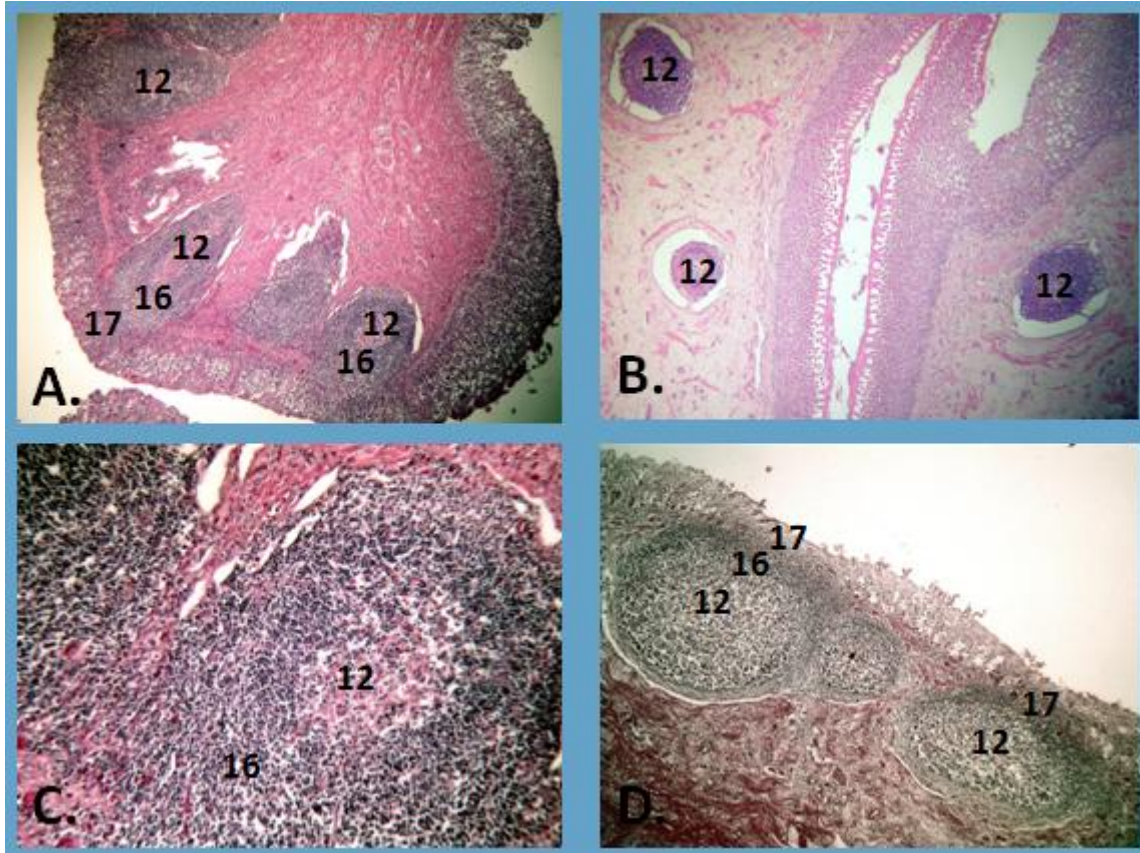


Figure 2-36. Gut-associated lymphoid tissue (GALT). The mucosa and submucosa contain diffuse and nodular lymphatic tissue with germinal centers. A. Peyer's patch in the lamina propria of the small intestine, H&E x2. B. Isolated lymphoid follicles in the large intestine, PAS x2. C.-D. Peyer's patch lymphoid nodules, H&E x10 and x2 respectively.



Figure 2-37. Cross section of the small intestine with an aggregations of lymphoid nodules in the lamina propria and submucosa (Peyer's patch), H&E

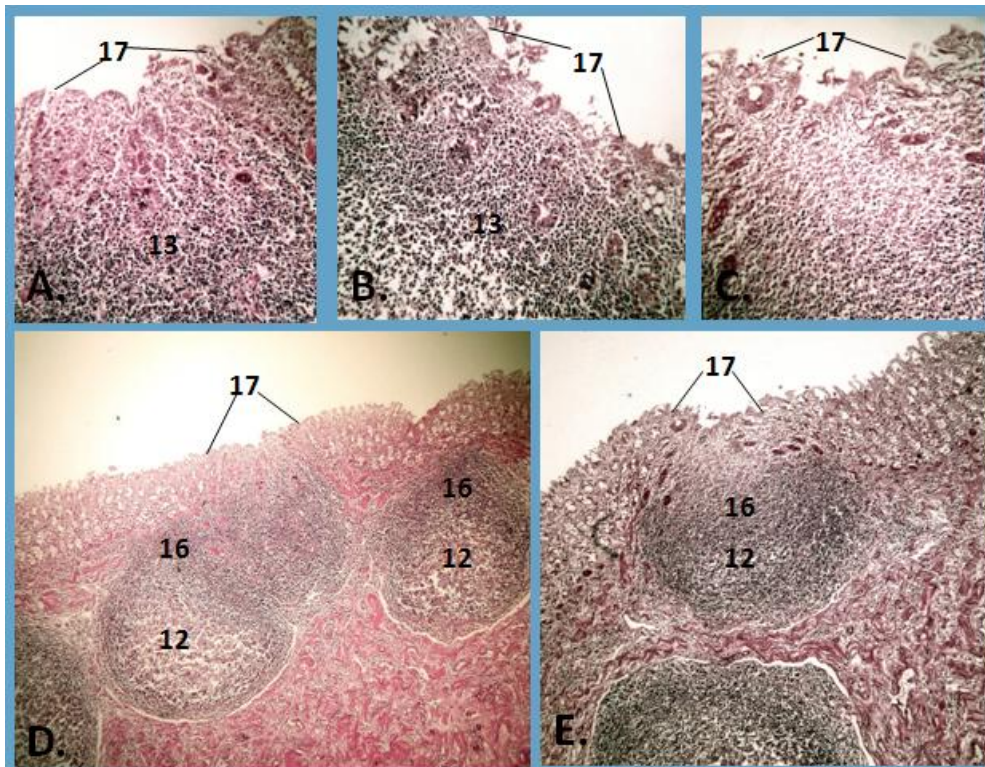


Figure 2-38. Peyer's patch lymphoid nodules. A.-C. Follicle associated epithelium (FAE) and potential M-cell regions, H&E x25. D.-E. Numerous lymphoid nodules with prominent germinal centers, sub epithelial domes, and FAE, H&E x10.

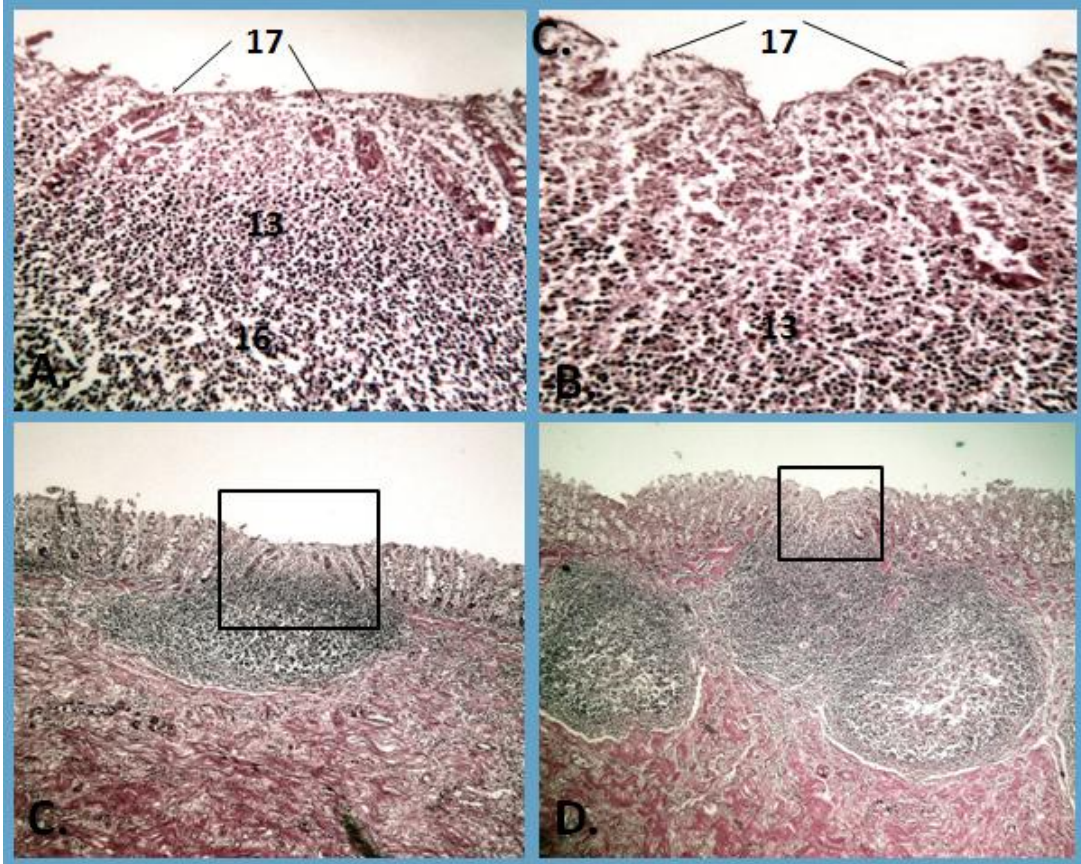


Figure 2-39. A.-D. Follicle associated epithelium which may be associated with M cells in this region, H&E A.-B. x10, C.-D. x2.

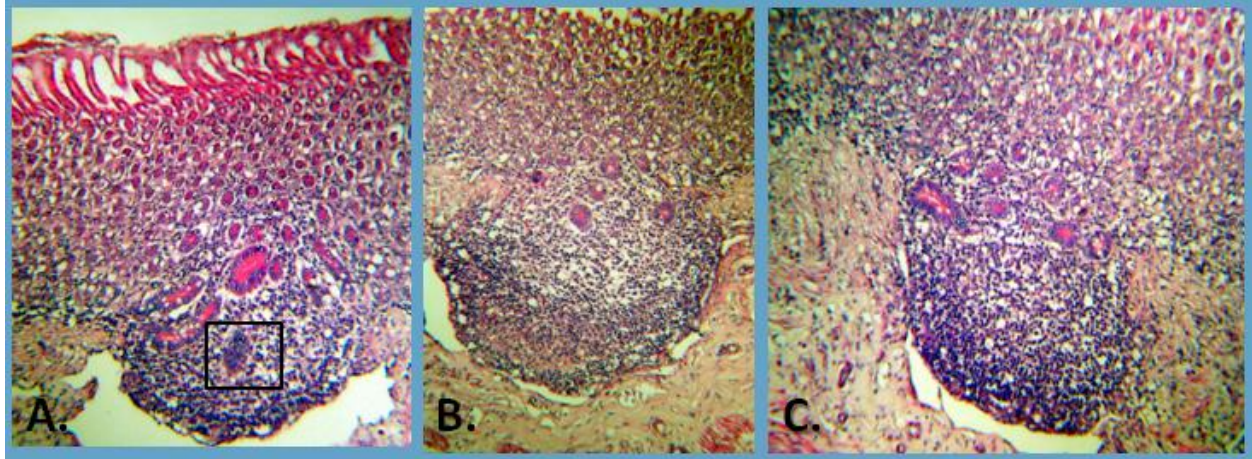


Figure 2-40. A.-C. Potential lymphoglandular complexes and cryptopatch (square) in the colon. Small lymphoid nodules associated with goblet cells, PAS, x2.

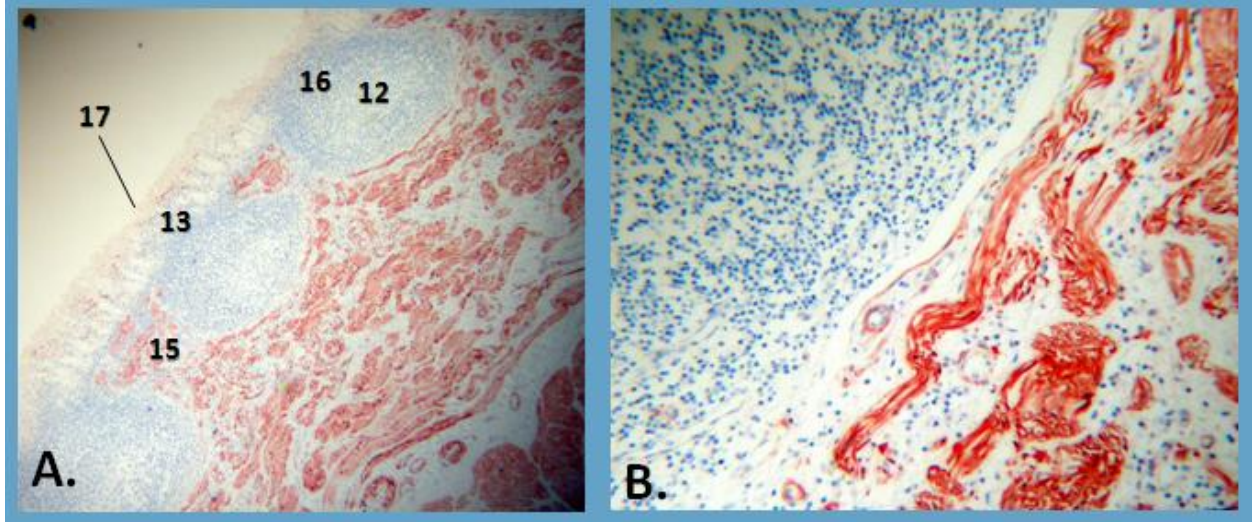


Figure 2-41. A.-B. Immunohistochemical localization of plasma cells (via Mum-1 mAb) in the Peyer's patch. No reactivity in the lymphoid nodules. Potential background staining of the connective tissue in the submucosa. x2 and x25.

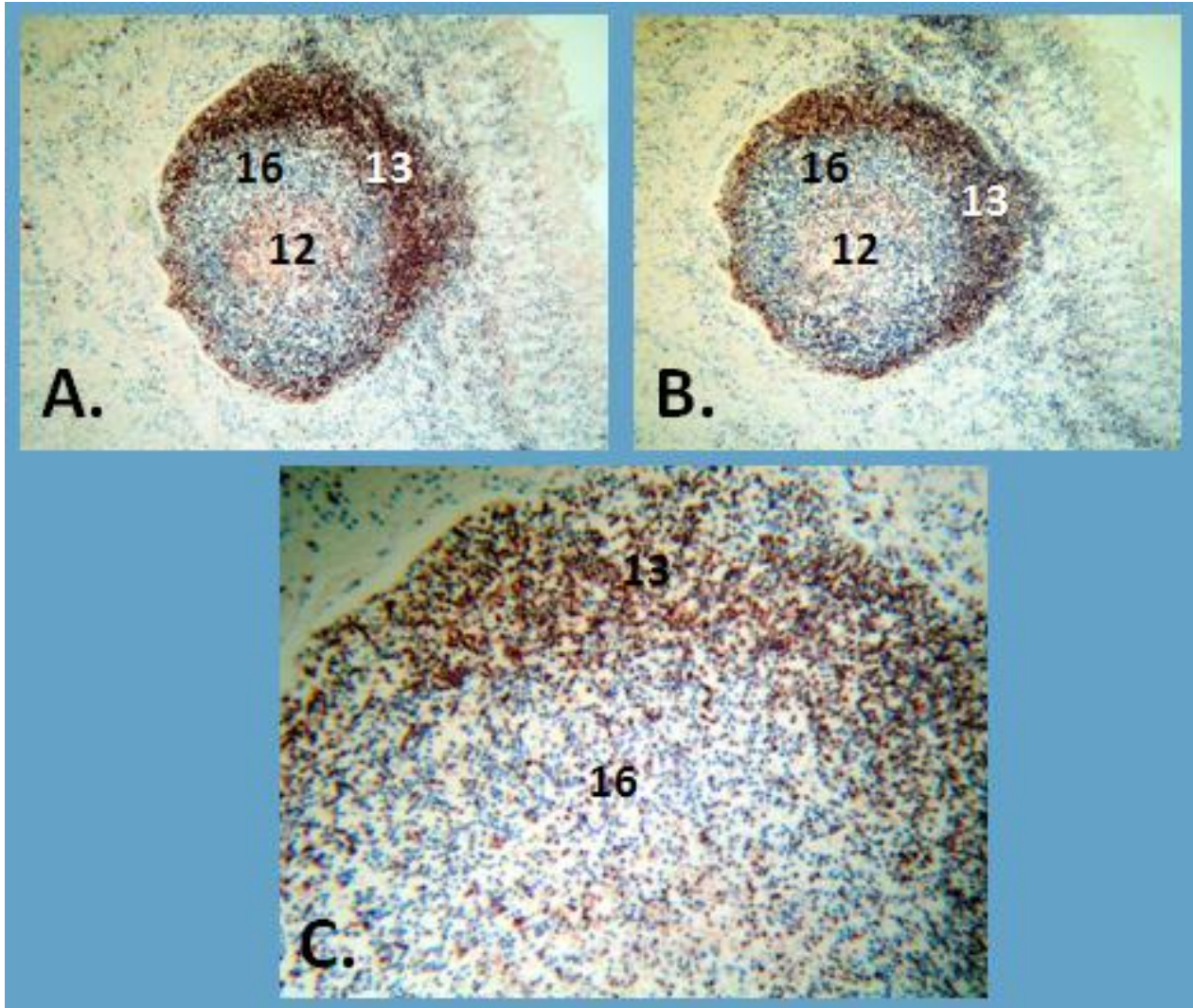


Figure 2-42. Immunohistochemical localization of T cells (via CD3 mAb and pAb) in the Peyer's patch. A.-C. T cell distribution in a lymphoid nodule, concentrated in the subepithelial dome with diffuse reactivity in the germinal center and corona/mantle zone A. and B., mAb and pAb, x2. C. x10.

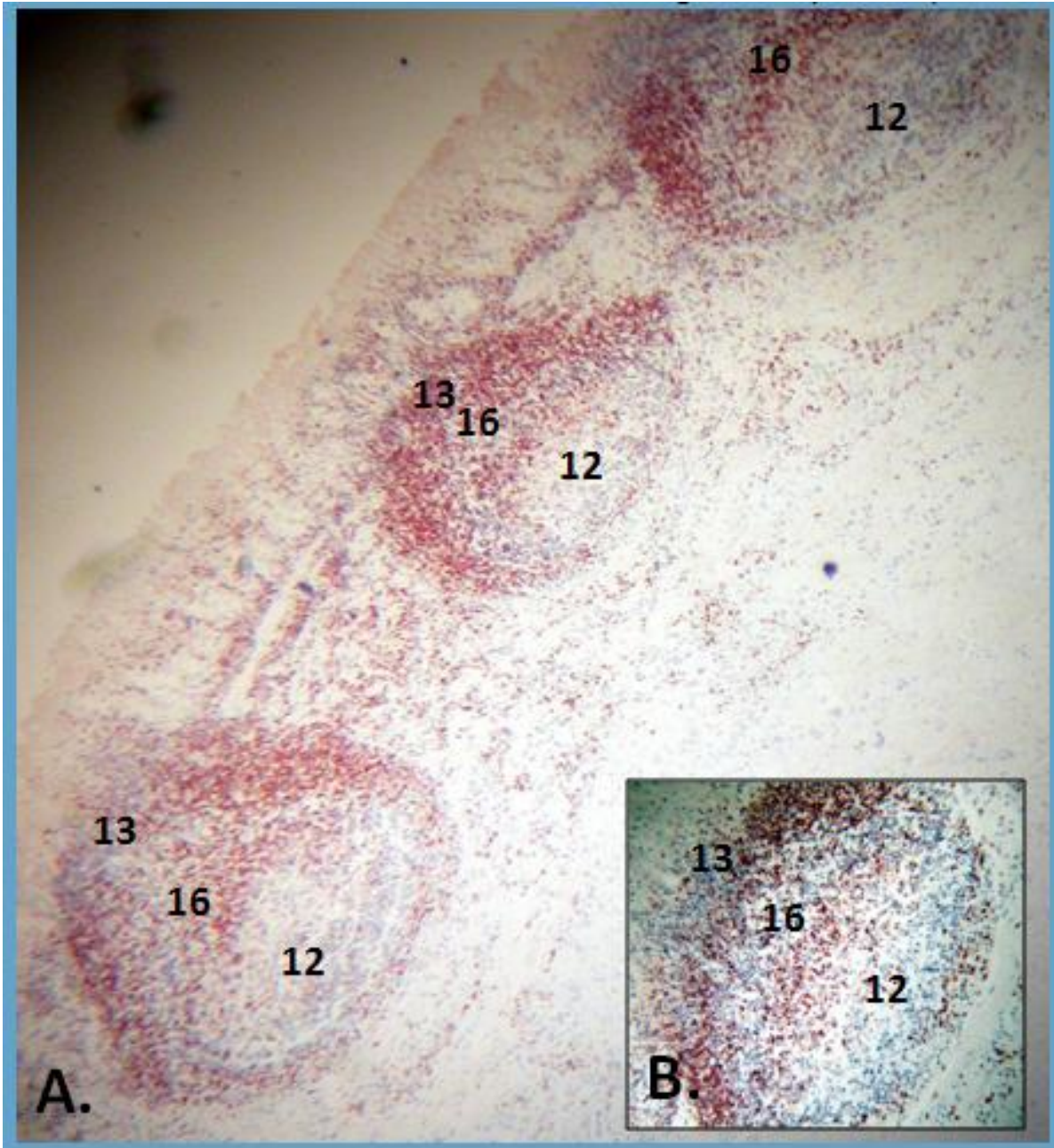


Figure 2-43. Immunohistochemical localization of B cells (via CD20 mAb) in the Peyer's patch. A.-B. Scattered B cell distribution in the diffuse lymphoid tissue, interfollicular regions, and follicle associated epithelium. Little to no reactivity in the germinal centers. Moderate reactivity in the corona/mantle zone. Strong reactivity in subepithelial dome. x2.

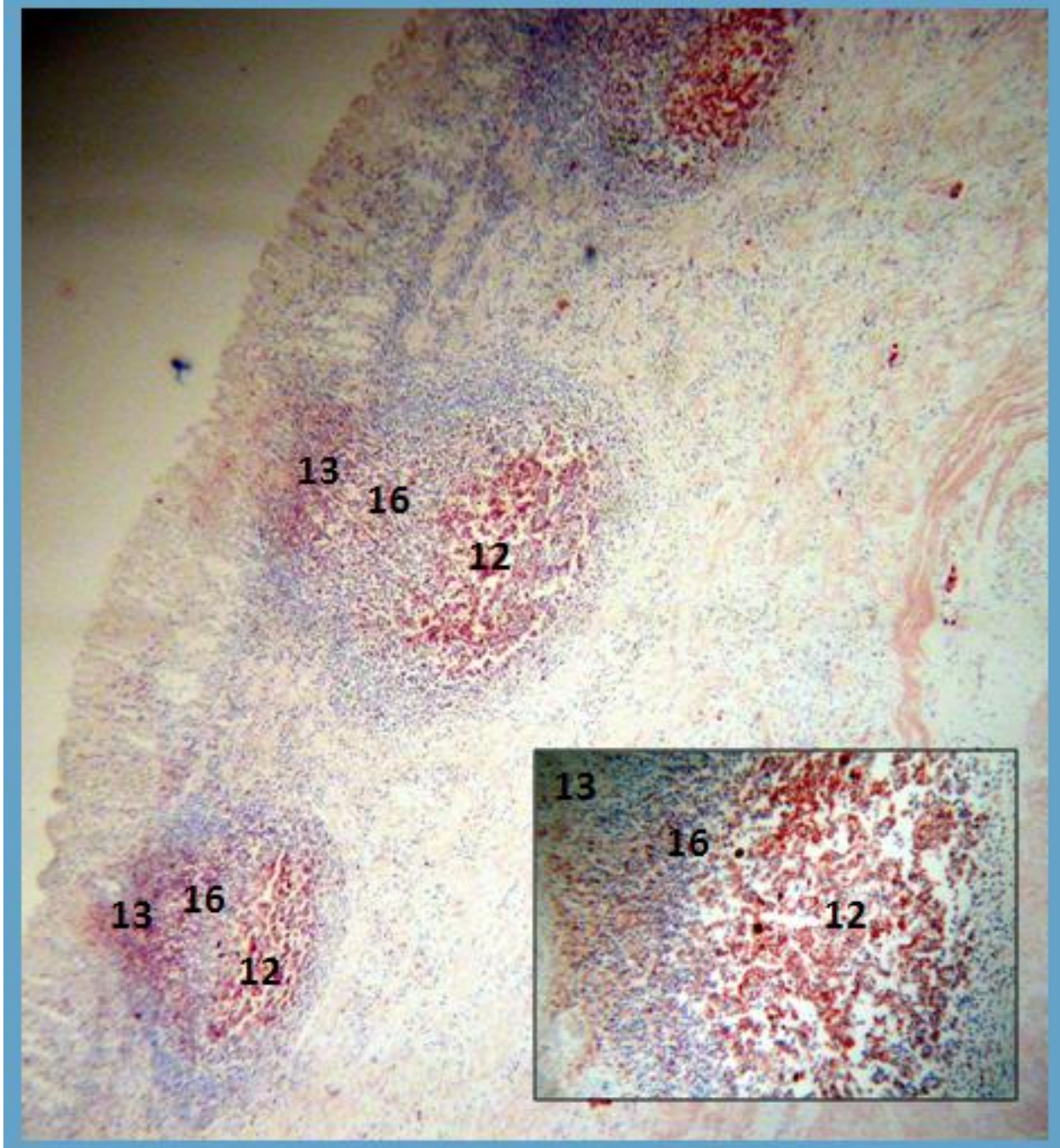


Figure 2-44. Immunohistochemical localization of membrane-bound immunoglobulin in B cells (via CD79 α). Localization was concentrated in the germinal centers and sub epithelial domes with moderate localization in the corona/mantle zone and follicle associated epithelium. The interfollicular regions and diffuse lymphoid tissue exhibited little to no reactivity. x2.

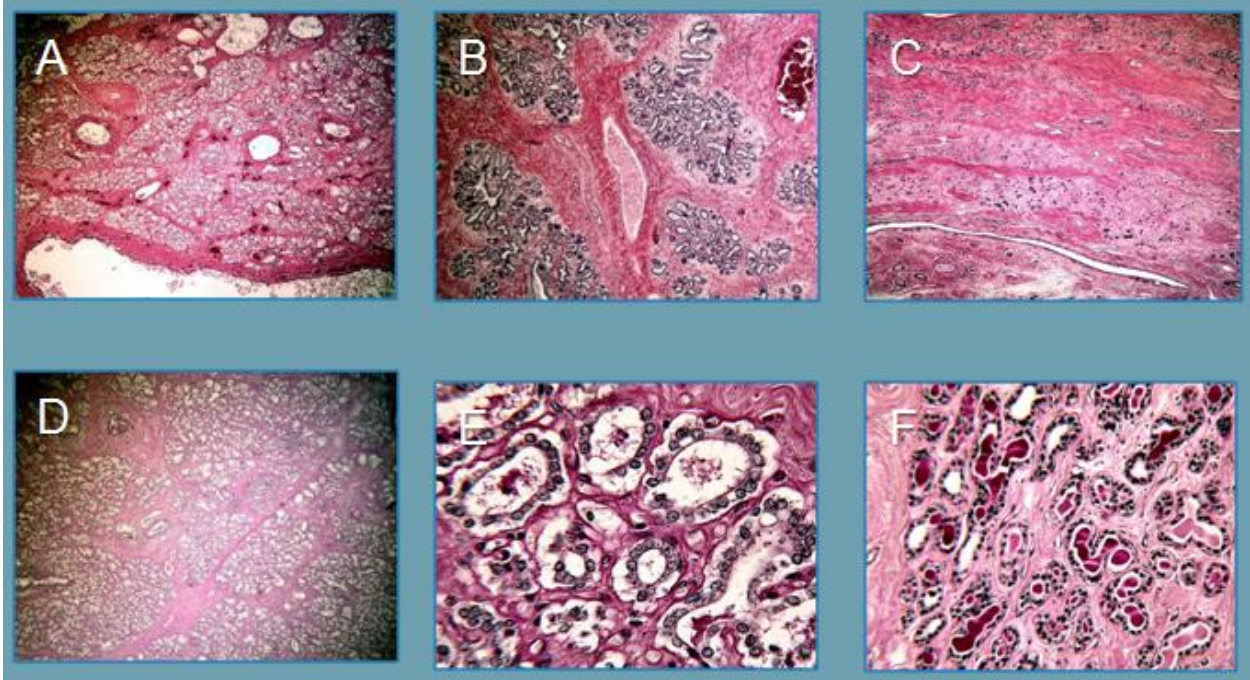


Figure 2-45. The mammary gland of the Florida manatee. A. Lactating manatee, gland overview, H&E x2. B. Enlarging secretory lobules , H&E x2. C. Non-lactating manatee, H&E x2. D. Lactating manatee, gland overview , PAS x2. E. Secretory acini, PAS x25. F. Non-lactating manatee, PAS x25.

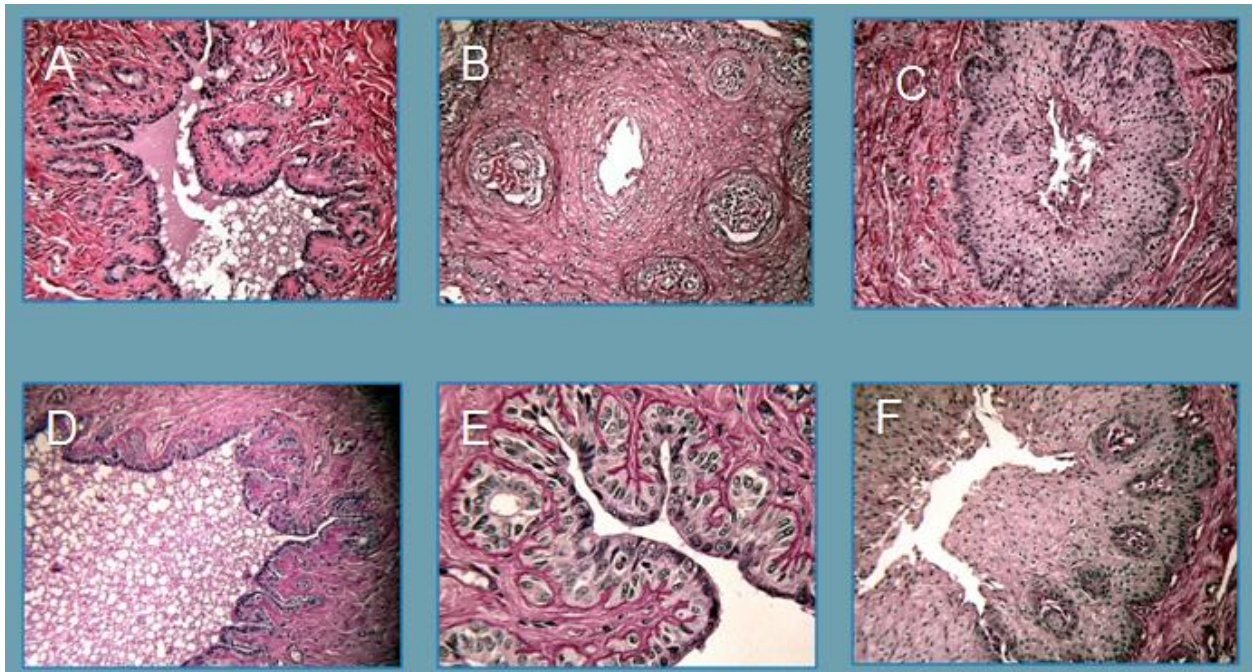


Figure 2-46 The teat of the lactating Florida manatee. A. Large lactiferous duct, H&E x10. B. Lactiferous duct, more proximal, H&E x10. C. Proximal most end of lactiferous duct, H&E x10. D. Distal lactiferous duct, PAS x10. E. Lining of proximal lactiferous duct, PAS x25. F. More proximal lactiferous duct, PAS x10.



Figure 2-47. The progression of lactiferous duct morphology in the teat of a lactating Florida manatee; distal to proximal tip (L to R), H&E x2.

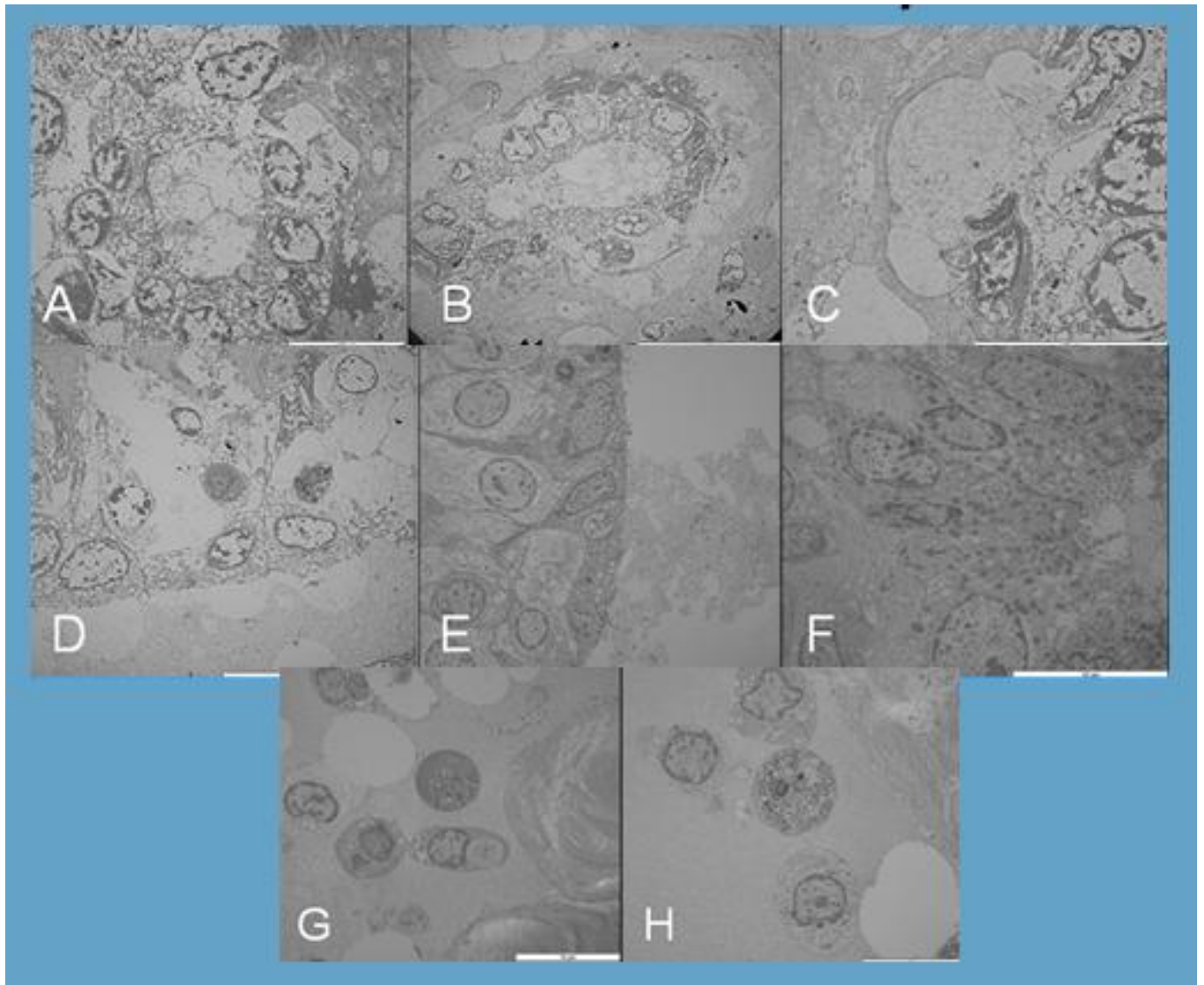


Figure 2-48. Transmission electron microscopy of the mammary gland (A-D) and teat (E-H) in a lactating Florida manatee. A. Acinus with lipid secretion x3000. B. Acinus x2000. C. Secretion of lipid into acinus x5000. D. Duct lining with lymphocyte x2500. E. Duct lining x2500. F. Secretory duct lining x5000. G. Lymph vessel x3000. H. Lymph vessel x3000.

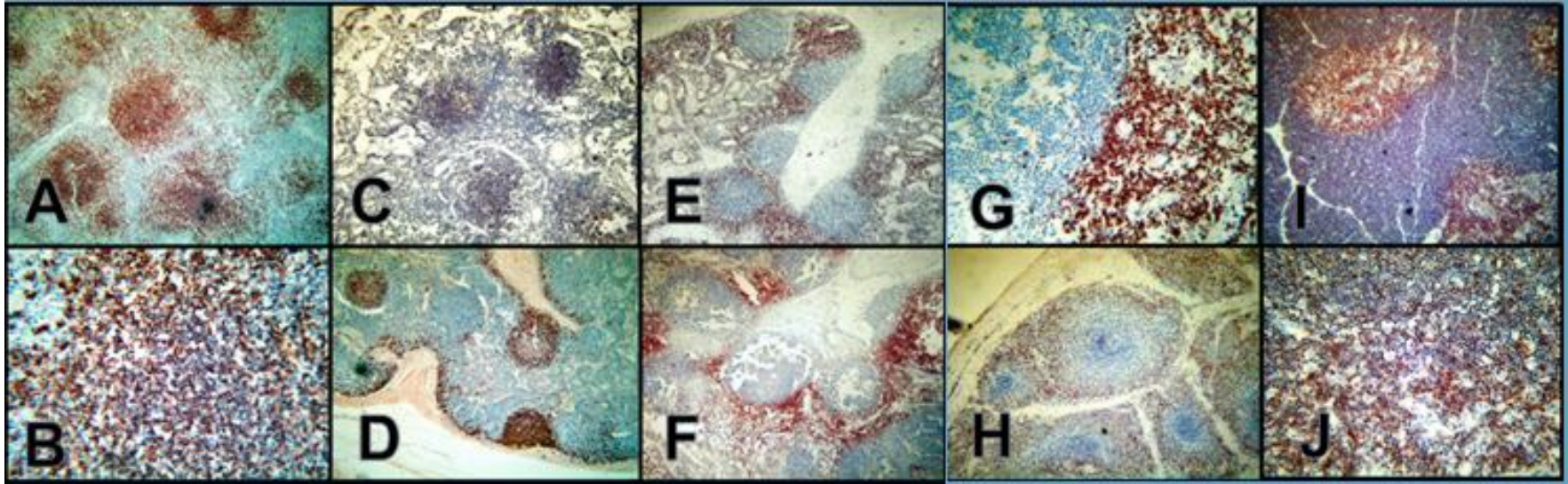


Figure 2-49. The thymus, spleen, and mandibular lymph node of the Florida manatee. A. Spleen, CD20 mAb, x2. B. Spleen, CD20 mAb, x10. C. Mandibular Lymph Node, CD79 α , x2. D. Mandibular Lymph Node, CD20 mAb, x2. E and F. Mandibular Lymph Node, CD3 mAb, x2. G. Mandibular Lymph Node, CD3 mAb, x10. H. Spleen, CD3 mAb, x2. I. Thymus, CD3 mAb, x2. J. Thymus, CD3 mAb, x10.

CHAPTER 3
USE OF BIOLAYER INTERFEROMETRY TO DEFINE BASELINE CIRCULATING AND
SECRETED IMMUNOGLOBULIN G IN WEST INDIAN MANATEE POPULATIONS

Introduction

Immunological data available for sirenians are not extensive. For research, diagnostics, and health monitoring in these species, incorporation of data would allow for more accurate assessments of health and contribute to the data necessary for mitigation of anthropogenic induced stressors. Before further immune related research and diagnostic studies can be pursued, a basic definition of various parameters of the immune system must first be established in order to make accurate correlations to an array of immune related variables. Previous studies have incorporated a UF-developed mouse anti-manatee monoclonal antibody for the detection of immunoglobulin G (IgG) in the development of a competitive ELISA (cELISA) to measure total IgG in blood and tear film. This present study originally sought to expand on this method but the preliminary data generated. However, our initial studies proved incapable of accurately and repeatedly reproducing this assay using a new set of reagents. Thus the aim of this study was redirected to develop a reproducible assay for quantifying total IgG levels in West Indian manatee blood and tear film in order to define baseline reference ranges for circulating and secreted IgG. Primarily involved in secondary immune response, IgG protects the body by binding to an array of pathogens, thus providing protection from viral and bacterial infections. These data will enable establishment of baseline species and population reference ranges that can be incorporated into future sirenian health assessments. “Ongoing health assessments will assist managers in predicting the impacts on local population growth rates due to a more limited carrying capacity of

habitat, with ever increasing anthropogenic threats.” (Robert K. Bonde, personal communication)

Materials and Methods

Study Animals

A set of 293 individual serum/plasma samples from West Indian manatee populations in four countries was analyzed, including Florida manatees (N=166) and Antillean manatees (N=127). Archived tear film was also used for this study (N=56). Archived samples were collected during wild manatee health assessment captures in Florida, Puerto Rico, Belize, and Brazil. As discussed in Chapter 1, manatee health and risk assessment captures are conducted at various times throughout the year and are the result of collaborations among numerous agencies and organizations. Samples collected include feces, urine, tear film, blood, genetic and lesion biopsy, parasites, nasal, oral, and urogenital swabs, and milk when present. Routine sample analysis includes hematological and serum chemistry profiles with additional laboratory tests for immunological, reproductive, and toxicology studies conducted when necessary. As a result of these health assessment captures, a large sample set of tissues has been archived for use in future studies.

Sample Collection and Complete Blood Counts

Blood samples, serum and plasma, were collected from the medial venous plexus of the manatee’s pectoral flipper. Blood collected in EDTA and LiHep Vacutainers, were centrifuged on site, serum/plasma removed, and aliquots stored at -80°C for later analysis. For this study, aliquots averaging 1mL in volume were re-centrifuged prior to analysis. After re-centrifugation, which further clarified a fraction of neat sera, a 30-50 µL aliquot was removed. This ‘micro-aliquot’ was used in this study.

To investigate potential predictors for different IgG levels among Florida manatees, one tube (EDTA Vacutainer) of whole blood was also submitted to the University of Florida-College of Veterinary Medicine's Clinical Pathology department for automated hematological analysis (Harvey et al., 2007) from the Crystal River population (N=83). The 2011 samples from the Belize population (N= 16) were also analyzed. Belize samples were analyzed at the Belize Medical Associates Laboratory.

Tear film samples were collected using Weck-Cel ophthalmic cellulose swabs, placed in pre-weighed 5 mL sample cryovials (combined dry swab and cryovial weight) and stored at -20°C until further analysis. If a pre-sample dry weight was not recorded, the mean weight of weighed sample cryovials was used (Castle et al., 2004).

Immunoglobulins were extracted from swabs using a modified protocol for human tear analysis (Castle et al., 2004; Rohan et al., 2000). Tear film samples were allowed to thaw for 5 minutes at room temperature. Each swab and cryovial was then weighed to determine the volume of sample absorbed. Swabs, with handles cut off, were transferred into a 0.45 µm CA Spin-X centrifuge filter unit (Corning Costar Laboratory Products) and equilibrated in 300 µL of extraction buffer (phosphate-buffered saline, 0.25 M NaCl, and 0.1 mg of aprotinin per mL) for 30 minutes at 4 °C. Units were centrifuged (refrigerated) at 13,000 x g for 20 minutes to allow separation of tear sample from ophthalmic swab. Equilibration and centrifugation steps were repeated, filter unit removed, and combined eluted samples stored at -20°C in the remaining microcentrifuge tube. A dilution factor was calculated for each sample as described in Castle et al., (2004). The dry weight of the swab and cryovials (y) was subtracted from the weight after sample collection (x). This estimated sample weight was then added to

the volume of extraction buffer (0.6 g). The resulting volume was finally divided by the estimate sample volume; $[(x - y) + 0.6g]/(x - y)$.

Florida Sub-Species Populations (Figure 3-1)

Crystal River. Crystal River is a city located on the west coast of Central Florida. It is situated around a spring-fed bay (Kings Bay), keeping the water temperature at a constant 22°C. The group of springs found here is one of the largest found in Florida and home to over 800 Florida manatees. The consistent year round water temperature leads manatees to seek this natural warm water refuge in the cold winter months. Prolonged exposure to water temperatures below 20°C can have detrimental effects on manatee health, a condition known as cold stress syndrome (Bossart et al., 2002; Reep and Bonde, 2006).

For this study, samples collected from annual manatee health assessment captures, which occurred during the winter months, from late October-mid February, typically three times per field season between 2006 and 2011 were included. For this study, blood samples from 83 individuals and paired tear film samples from 27 individuals were included for analysis. Fifty-seven animals were adults, 13 were sub-adults, and 13 were calves. Overall body condition in all but one animal was assessed as 'Good' or 'Excellent'. The remaining animal was assessed as 'Fair'. Of the 83 animals included, 56 were males and 27 were females.

Brevard. Brevard is a county located on the east coast of Florida along the Atlantic Ocean. Brevard is also home to several power plants that serve as artificial warm water refuges for the Florida manatee in the cold winter months. Located along the Indian River Lagoon, the waters around Florida Power & Light (FPL) powerplant have hosted manatee health assessments since 2009. These health assessments, like

those in Crystal River, are conducted 1-2 times per year during the winter months, generally in December and January. For this study, blood from 21 individuals and tear film from 6, were included for analysis.

Alabama. Alabama is a state located to the west of Florida, along the Gulf of Mexico. During the summer months, the Florida manatee range extends north as far as New York, and west as far as Texas. Starting in 2009, manatee health assessments were conducted to assess animals found within Mobile Bay. Most importantly, the samples from individuals collected in 2009 now serve as baselines for manatees potentially exposed to oil from the Deepwater Horizon explosion and oil spill in 2010. Samples from six individuals have been collected in this area, three of which were included in this study. These samples were collected during the month of August 2010.

Lemon Bay. Lemon Bay is located on the West/Southwest coast of Florida, bordering the Gulf of Mexico. The bay expands along Charlotte and Sarasota counties and is designated as an aquatic preserve. From 2005-2007, manatee health assessments were conducted in early summer and late spring. These studies incorporated the health assessment studies with D-tag studies investigating manatee movement. For this study, blood samples from 19 individual manatees were included for analysis.

Everglades. The Everglades are a subtropical wetland system located in south Florida. This area experiences frequent flooding in the wet season and drought in the dry season. Manatee health assessments took place from 2005-2007 and occurred in fall, spring, and summer (June, October, August, and March). For this study, samples from 37 individual manatees were included for analysis.

Miscellaneous. Miscellaneous samples included three animals sampled from Tampa Bay in 2006 and one animal in rehabilitation at Lowry Park Zoo (LPZ) in Tampa, Florida collected in 2008. LPZ is one of only three manatee critical care facilities found in Florida/U.S. The LPZ animal had a chronic water craft injury. Additionally, two archived fetal serum samples were also included for analysis. Analysis of these samples will provide us with preliminary data for passive transfer of immunoglobulins in manatees.

Antillean Sub-Species Populations

Belize. Located in Central America, Belize has an east coast that borders the Caribbean Sea, with Mexico to the north, and Guatemala to the west and south. Belize is home to the second longest barrier reef in the world next to the Great Barrier Reef in Northeast Australia. Antillean manatees inhabit the shallow island waters, marshy coastlines, and abundant lagoons. Since 1997, manatee health assessment captures have been conducted 1-2 times per year, in the late spring and fall months. Capture locations have included the Northern and Southern Lagoons near Gales Point, Placencia Lagoon, and the waters off of Belize City. For this study, blood samples from 83 individuals, collected between 2005 - 2011, were included for analysis. During these 7 years, several manatees were caught for health assessment numerous times. For these animals, mean serum IgG of repeated samples across the years was used for this study, representing one sample per individual manatee. Additionally, paired tear film samples from 15 individuals were also included.

Brazil. Brazil is the largest country in South America and the fifth largest country in the world. Bordered by the Atlantic Ocean on the east, Brazil has an expansive coastline of 7,491 km with numerous archipelagos. It borders 10 of the 12 other South

American countries including Venezuela, Guyana, Suriname, French Guiana, Colombia, Bolivia, Peru, Argentina, Paraguay, and Uruguay. Amazonian manatees are found exclusively in the fresh waters throughout the Amazon and Orinoco River basins while Antillean manatees inhabit riverine and coastal systems. For this study, blood samples from 18 individual Antillean manatees in rehabilitation were included for analysis. These animals are housed at the National Centre for the Conservation of Aquatic Mammals (CMA / ICMBio), which is responsible for the rescue, rehabilitation and release of manatees throughout the northeast coast of Brazil.

Puerto Rico. Puerto Rico is an unincorporated territory of the United States comprised of an archipelago located in the northeastern Caribbean. There are two genetically distinct Antillean manatee populations in Puerto Rico, one along the north coast of the main island and the other along the south coast (Kellogg, 2008). The two populations are separated to the east and west by deep waters with high wave activity. Manatee health assessments were conducted from 2003-2005 in late spring through summer and in the fall (April, May, June, July, and November). Samples from 25 individual manatees were included in this study.

Quantitative Assay Development and Optimization

Bio-Layer Interferometry (BLI) is an optical analytical technique for measuring biomolecular interactions using a novel 'dip and read' approach. As white light travels down the biosensor, the difference in the reflected wavelengths from the internal reference layer and the immobilized protein on the biosensor tip is measured. As binding occurs between the immobilized protein and the sample analyte, the biological layer becomes thicker thereby increasing the wavelength shift (Figure 3-2). Only bound materials create interference, therefore this system is ideal for use with crude samples.

A custom quantitative assay was developed by immobilizing the biotin labeled anti-manatee IgG antibody on a streptavidin biosensor.

Assay Reagents. Purified manatee IgG was used for generating standard curves as well as for positive controls. Three milliliters of manatee IgG was purified from plasma by chromatography using a 5 mL Protein G Sepharose Fast Flow column. The antibody was eluted from the column and collected 1 – 3 mL fractions. The absorbance of each fraction was measured at 280 nm on a spectrophotometer. The fractions with the highest absorbance readings were pooled, concentrated, and followed by another absorbance reading at 280 nm. A 10% Novex NuPage Bis-Tris gel was run to evaluate the purity and molecular weight of the material eluted from the Protein G column. The resulting purified IgG (13.8 mgs) at a concentration of 9.6 mg/mL was used for this study.

Purified mouse anti-manatee IgG mAb (HL 767) was biotinylated using EZ-Link Sulfo-NHS LC Biotin. Six hundred micrograms of manatee antibody (3.15 mg/mL) and biotin were incubated at room temperature for two hours to allow for binding. For BLI, 1-3 moles of biotin per mole of protein are ideal, therefore a target of 2 moles of biotin/protein (2:1 biotin:protein ratio) was used in the biotinylation reaction. Unbound biotin was removed and antibody conjugate desalted using a Thermo Scientific Zeba Desalting Spin column. The biotinylated antibody was then read on a spectrophotometer at 280 nm wavelength and the protein concentration was determined to be 0.86 mg/mL and 1.74 moles biotin / mole protein. The moles of biotin per mole of protein were determined using the Pierce biotin incorporation kit (HABA displacement assay). Two milligrams of an additional stock of antibody (5.9 mg/mL) were also

biotinylated by the same methods resulting in a final concentration of 0.73 mg/mL and 2.9 moles of biotin / protein.

Optimizations. Streptavidin biosensor loading conditions were optimized by serially diluting biotinylated HL 767, from 100 $\mu\text{g/mL}$ to 1.56 $\mu\text{g/mL}$. A 4 step BLI assay was run to determine optimal conditions; baseline (1x Kinetics Buffer (KB) (10x KB in PBS), loading (HL 767), baseline (1xKB), association (10 $\mu\text{g/mL}$ purified manatee IgG). Biocytin (100 $\mu\text{g/mL}$), an analog of biotin, was used to block the biosensors after the antibody had been loaded, to reduce background binding interference encountered when the moles of biotin per protein in one stock or mAb varied from another stock. This allowed for assay standardization. Ultimately, 25 $\mu\text{g/mL}$ was chosen as the optimum loading concentration. The loading curve reached saturation within the recommended time of 10 minutes and the slope of the loading curve was neither too steep nor too shallow.

To determine the optimal serum/tear dilutions, two randomly selected samples, 1 serum, 1 plasma and two randomly selected tear samples with unknown IgG concentrations were used. Tear samples were tested from 1:1 to 1:256 dilutions. Serum samples were tested from 1:50 to 1:3200. Optimal dilutions of 1:250 and 1:500 (both diluted in 1xKB) were determined for serum/plasma samples. The optimal tear film dilution selected was 'undiluted'. Due to the process of tear film processing, the tear sample is already diluted before assay analysis. Calculated dilution factors ranged from 2.61 to 45.12.

In order to maximize sample throughput and minimize expense, it was necessary to develop sensor regeneration conditions. The regeneration step removes the analyte

leaving the ligand (biotinylated HL 767) intact. Seven regeneration reagents were tested: 10 mM glycine pH 3.5, 2.3, 2.5, and 1.7 and 20 mM glycine pH 2.9, 2.5, and 1.7. The 10 mM glycine pH 1.7 reagent worked the best. This reagent stripped off the analyte completely and gave the same result when dipped into a control well containing 20 µg/mL of purified manatee IgG. Due to space constraints on the 96 well sample plate, the number of regeneration cycles was limited to 7. Two wells contained 1xKB (negative control) and two contained 20 µg/mL of purified manatee IgG (positive control).

Standard Curves. Two columns of streptavidin biosensors (16 sensors) loaded with biotinylated anti-manatee IgG mAb (HL 767) were dipped into standards containing a known amount of purified manatee IgG, serially diluted 1:2 from 100 µg/mL for blood analysis and from 2.5 µg/mL for tear film (Figures 3-3 and 3-4). The analysis of these known samples allowed creation of a duplicate standard curve. Standard curves were saved as an Octet QKe file and imported for subsequent analyses. As long as the assay conditions, biosensor lot number, and reagents are the same as those used to generate the standard curve, one duplicate standard curve can be imported/used for multiple assays. This process saved both time and money.

Octet QKe. The mouse anti-manatee IgG monoclonal antibody (HL 767) was incorporated into a biolayer interferometry assay using the Octet QKe system (ForteBio, Inc.). Before loading optimized samples and reagents onto the assay plate, 100 µL/well of 1xKB was placed in one column of a 96-well black polystyrene half-area (sensor plate). This plate was then placed in the sensor tray. Eight streptavidin biosensors were transferred to the sensor tray, allowing sensors to incubate in the 1xKB for 5 min.

at room temperature. This incubation step removes the dried sucrose that covers and protects and the reactive groups (streptavidin) on the sensor tip. In a second 96-well sample plate, the assay reagents and samples were loaded (100 μ L/well). The assay steps are as follows (Figure 3-5).

1. Baseline 1 - 1xKB, 120 seconds (column 1)
 2. Loading - HL 767 at 25 μ g/mL, 300 seconds (column 2)
 3. Blocking - Biocytin at 100 μ g/mL, 120 seconds (column 3)
 4. Baseline 1 – 1xKB, 120 seconds (column 1)
 5. Regeneration – 10 mM Glycine pH 1.7, 5 seconds (column 5)
 6. Baseline 2 – 1xKB, 5 seconds (column 4)
 7. Regeneration – 10 mM Glycine pH 1.7, 5 seconds (column 5)
 8. Baseline 2 – 1xKB, 5 seconds (column 4)
 9. Regeneration – 10 mM Glycine pH 1.7, 5 seconds (column 5)
 10. Baseline 1 - 1xKB, 120 seconds (column 1)
 11. Association 1 – 1:250 and 1:500 serum/plasma dilutions, 300 seconds (columns 6)
 12. Baseline 1 - 1xKB, 120 seconds (column 1)
- Repeat steps 5-10 and 12 for Associations 2-7 (columns 7-12) by appending to steps listed above.
 - Negative Control: Two wells of 1xKB, 100 μ L/well
 - Positive Control: Two wells of 20 μ g/mL purified IgG, 100 μ L/well

Data Analysis and IgG Levels

Total IgG for each unknown sample or control was analyzed using the Octet QKe Data Analysis program by multiplying the sample well concentration (determined from the binding signal of the sample compared to the standard curve) by the dilution factor. Significance was defined as a P-value < 0.05 for all tests. Manatee serum/plasma samples were grouped by subspecies, population, sex, location, age class, and year. Paired and unpaired t-tests were used to observe differences between these groups as well as the relationship between circulating and secreted total IgG. Pearson's correlation was used to investigate the potential CBC predictors of total circulating IgG. Reference ranges were defined as described in Ruiz et al., (2009) for baseline

circulating IgG in bottlenose dolphin, “the mean IgG value \pm (1.645 x standard deviation), representing a 90% confidence interval, or 90% of the normal data points on the distribution curve”.

Results

Circulating IgG Levels (Appendix B)

Florida Sub-Species. For Florida manatees, the mean total circulating IgG was 10.44 mg/mL with standard deviation of 3.66 mg/mL. Manatees from Brevard County were found to have the highest levels of circulating IgG with a mean of 15.16 mg/mL (SD of 4.65 mg/mL). The Lemon Bay population had the lowest mean at 8.3 mg/mL (SD of 3.5mg/mL). Both populations were significantly different from the Crystal River population. There was no significant difference however between the Crystal River population (10.06 mg/mL) and the Everglades (9.67 mg/mL), Tampa Bay (11.03 mg/mL), or Alabama (11.29 mg/mL) populations; $P = 0.4857, 0.5499, \text{ and } 0.4438$ respectively. When populations were divided between winter samples (Brevard and Crystal River) and spring, summer, fall samples (Lemon Bay, Tampa Bay, Everglades, and Alabama) a significant difference of $P=0.0054$ was observed. Similarly, when samples were grouped by East coast (Brevard) and West coast (Crystal River, Tampa Bay, Alabama, and Lemon Bay) populations, a significant difference was observed; mean total IgG 15.16 mg/mL vs. 9.83 mg/mL respectively.

Overall, the IgG levels did not vary greatly between populations, with the exception of the Brevard County population (Figure 3-6 and 3-7). Additionally, there was also no significant difference in mean total IgG between years for any of the populations investigated. Crystal River males and females showed no significant differences with total circulating IgG levels of 9.73 mg/mL and 10.83 mg/mL

respectively, $P=0.0751$ (Figure 3-8). A trend was observed among age class. Using a student's t-test, a significant difference in mean serum IgG was observed between adults and calves; mean values in Adults 10.63 mg/mL, SubAdults 9.61 mg/mL, and Calves 8.24 mg/mL. A reference range for total IgG in the Florida manatee was calculated as 4.42 mg/mL to 16.46 mg/mL (Figure 3-9). Samples ranged from 2.67 mg/mL to 26.5 mg/mL (Figure 3-6). Additionally, using the methods from this study, two samples of fetal Florida manatee sera were also analyzed. A mean of 26.01 mg/mL suggests significant passive placental transfer of antibodies from cow to calf, which has been previously undocumented in this species.

Antillean Sub-Species. (Figure 3-6) Mean total circulating IgG for Antillean manatees was 8.20 mg/mL (S.D.= 3.12 mg/mL) . Antillean manatees from Belize had a mean IgG of 9.68 mg/mL (SD = 5.05 mg/mL). Mean IgG for animals from both the Belize and Puerto Rico populations were significantly higher than the mean value for the Brazil population, 4.16 mg/mL (SD = 1.98 mg/mL). Manatees from Puerto Rico had a mean total IgG of 10.76 mg/mL (SD = 2.33 mg/mL). When Puerto Rico samples were compared between years, a significant variation was observed (Figure 3-10); 2003 = 9.69 mg/mL, 2004=10.5 mg/mL, and 2005 = 12.22 mg/mL. Antillean manatee samples from Belize showed a significant cyclical distribution between 2005 - 2011, peaking in 2009; (mg/mL) 8.13, 7.38, 9.51, 11.36, 16.13, 11.56, and 8.77 (Figure 3-11). There was no significant difference between males and females from the Belize population, $P=0.4384$.

When mean IgG values were compared between Florida and Antillean populations, a significant difference was observed ($P = 0.0103$) when all samples were

included. However, when the significantly low Brazil samples were excluded from analysis, there was no significant difference between sub-species.

Secreted IgG Levels in Tear Film

Secreted IgG levels were highest in Florida manatees from Brevard County at 0.2480 mg/mL (SD = 0.1853 mg/mL). Manatee populations in Crystal River and Belize showed comparable secretory IgG levels of 0.0509 mg/mL (SD = 0.9641 mg/mL) and 0.0475 mg/mL (SD = 0.0432 mg/mL) respectively. Significant variations were observed between individuals. Tear film samples were collected from both the right and left eyes of an individual and overall, there was a weak correlation ($R^2 = 0.2836$) and no significant difference between samples from right eyes versus the left eyes, $P = 0.1427$ (Figure 3-12). When circulating total IgG values were compared to secreted total IgG, no significant correlation was observed, $R^2 = 0.0675$ (Figure 3-13). (Appendix C)

Reference Ranges (Figure 3-9)

Reference ranges were established by species, sub-species, and population. The reference range for mean total circulating IgG in the West Indian manatee was 2.81 mg/mL to 16.2 mg/mL. Circulating IgG reference ranges for Florida manatees was 4.42 mg/mL to 16.46 mg/mL and for Antillean manatees, 1.32 mg/mL to 17.14 mg/mL. These values include all West Indian manatee samples collected and do not take into account outliers, hence the high SD and subsequent wide reference ranges. Within the Florida manatee samples, population reference ranges were as follows; Crystal River 5.57-14.55 mg/mL, Lemon Bay 2.43 - 14.17 mg/mL, Everglades 4.32-15.02 mg/mL, and Brevard 7.51-22.81 mg/mL. Within the Antillean manatee samples, population reference ranges are as follow; Puerto Rico 6.93 - 14.59 mg/mL, Brazil 0.43 - 7.79

mg/mL, and Belize 1.37 -17.99 mg/mL. Reference ranges were not established for the Tampa Bay or Alabama populations due to low sample size (N=3).

Predictors of Total IgG Levels

For the Crystal River population (N=83) and the 2011 samples from the Belize population (N=16), complete blood cell counts were analyzed as well as total protein, total globulin, and SAA values to investigate any potential predictors of total circulating IgG values. In bottlenose dolphins, WBC and high eosinophil counts were observed to be the best predictors of IgG levels when captive managed populations were compared to a free-ranging population. In the West Indian manatee, no such correlations were observed. There were no significant correlations between total IgG values and any of the blood parameters analyzed (Appendix D). For the Belize population, WBC counts had the strongest correlation to total IgG, $R^2 = 0.3533$. For the Crystal River population, total globulin had the strongest correlation to total IgG, $R^2 = 0.3441$. This parameter was not analyzed for the Belize population.

Discussion

Sub-Species and Population Variability

The difference between sub-species was not significant when Brazil samples were omitted from analysis. The Brazil samples were significantly lower than all other West Indian manatee population levels. In other populations, particularly the Belize population, low numbers like those comparable to Brazil population levels were observed, however, the upper limit of the reference range was much higher and therefore the mean value was higher. Therefore, the low total IgG values observed in the Brazil population could be the result of a difference in the number of samples analyzed (Brazil N=18 and Belize N=83) and/or the result of wild Antillean manatees

(Belize) vs. animals in rehabilitation (Brazil). While the wild manatees included in this study were assumed 'healthy' unless otherwise noted, the same cannot be said for the Brazil population animals as they do not represent the wild population of animals found in Brazilian waters. A second possible explanation for low mean total IgG in the Brazil population could be contamination or degradation of samples during transport (freeze/thaw).

In the Florida manatee, the Brevard population had significantly higher circulating and secreted IgG levels compared to the Crystal River population, even though both population samples were collected in the winter months (Figure 3-10). The Crystal River population is a more protected population with natural warm water springs in close proximity to the shallower waters of Kings Bay and the Gulf of Mexico. The Crystal River population consistently has lower incidence of cold stress reported rescues as well. The Brevard population is in an artificial warm water refuge that is often more overcrowded during the cold winter months than Crystal River due to the limited area of warm water effluent available. Most recently, with the closure/re-construction of the FPL powerplant, heaters were installed to warm the waters typically warmed by the powerplant effluent. However, water temperatures only reach approximately 19 °C (below the 20°C critical temperature for cold stress syndrome) and the powerplant waters are much colder than in Kings Bay due to the influx of water from the Atlantic Ocean into the Indian River Lagoon on which the powerplant lies. Higher circulating IgG levels could be reflective of poorer water quality due to the powerplant effluent as well as the large volume of dead and decaying fish in the area that had succumbed to the cold water temperatures. Brevard County consistently has a higher number of cold

stress related rescues conducted each year (FWC-FWRI, 2012a). Similarly, when total circulating IgG in east coast versus west coast populations were compared, the east coast samples were found to be significantly higher. However, the east coast is represented by a single population (Brevard) that was found to have significantly higher levels of total IgG than all other Florida manatee populations. Using Crystal River as the reference for Florida manatee population, no significant difference was found between this population and the Everglades, Tampa Bay, and Alabama populations (Figure 3-6). The Lemon Bay population, however, was considered to be significantly lower than that of Crystal River which could reflect seasonality of sampling. When winter samples were compared to spring, summer, and fall samples, a low, but significant difference was observed. Additionally, while there was no significant difference in mean total circulating IgG between years in the Florida manatee populations, a possible cyclical trend was observed in the Crystal River population and to a lesser extent in the Everglades population (Figures 3-14 and 3-15). To confirm a trend across years however, yearly population sampling would be required. There was a significant difference observed between years for the Belize population. However, this could reflect differences between sampling sites within Belize from one year to another and/or the effects of extreme weather events on manatee health. Samples from 2009 had the highest mean IgG at 16.13 mg/mL (Figure 3-11). The year prior, though after the 2008 sampling, Belize experienced an extreme flood event, particularly at the Gales Point sample site, due to Hurricane Arthur (May 31 - June 1) that was believed to have negatively impacted the surrounding sea grass beds.

Secreted and Circulating IgG Correlations

The mucosal immune system is not only capable of inducing a response reflected in all tissues of the mucosal immune system via the common mucosal immune system (CMIS) pathways, but it is also capable of inducing a systemic response. Tear film collection is virtually non-invasive and should protein levels in both tears and blood show a strong correlation, tear analysis would be a non-invasive approach to measuring health in an animal. In this study, tear film and blood samples were analyzed for 48 individual animals from the Crystal River, Belize, and Brevard populations. Tear samples were collected from both right and left eyes. Eye exams were not conducted and therefore sample collections from both eyes account for potential ocular pathologies that might occur in one eye but not the other. The mean total IgG values of both the right and left eyes was taken and compared to mean blood values. No significant correlation was found between blood and tear total IgG values, however there were general correlations (Figure 3-13). For example, the Brevard population had the highest baseline circulating IgG as well as the highest secreted baseline IgG. However, with a tear film sample size of 6 for this population, more samples are needed for analysis in order for a strong and reliable conclusion to be drawn. There was also no significant difference between samples from the right eye and those from the left, although outliers were observed (Figure 3-12).

Additionally, the methods for tear film processing were based on methods for analysis of protein in human tear film (Castle et al., 2004). Human tear film is much less viscous at 0.44-0.84 cP whereas manatee tear film is the most viscous of any mammal studies to date at 88.0 cP (Brightman et al., 2003; Tiffany, 2001). It was noted in several samples, that mucous appeared to remain on the ophthalmic swab after

processing. Tear film samples collected from humans, are able to be done so in a controlled experimental setting where the degree of contamination and to a certain degree, sample purity, can be controlled. Manatee tear film samples for this study were collected in the field, in sandy, wet, and muddy conditions. Tear film samples were often contaminated by algae on the manatees' skin, sloughed skin, freshwater used to induce breathing during health assessments, sand, and mud. Attempts were made to obtain the 'purest' sample possible by avoiding the eyes when water was used to induce breathing, shielding the eyes during health assessment, wearing latex gloves during sample collection, as well as wiping away tear film that appeared to have particulate matter contained within it to stimulate further tear secretion while the animal was being processed for health assessment studies. A positive control was not used in this study. Repeated samples collected from captive managed animals would allow us to know only assess reproducibility in our methods but would also allow us to have further control of sample quality versus samples collected in health assessment field conditions. For future studies, a positive control will be included and the effects of viscosity of effective tear film processing will be explored.

Outliers

With the reference range for mean total circulating IgG in the West Indian manatee being 2.81 mg/mL to 16.2 mg/mL, 9 samples (1.365 – 2.6675 mg/mL), from the Belize (3), Brazil (5), and Lemon Bay (1) populations, measured below the lower limit of the reference range. Twenty-six samples (16.35 – 26.8 mg/mL) from the Puerto Rico (1), Belize (12), Everglades (2), Brevard (8), and Crystal River (3) populations measured above the upper limit of the reference range. (Appendix B)

Among the individual outliers was a captive orphaned manatee in rehabilitation from the Belize population (mean circulating IgG 1.365 and 1.6915 mg/mL). Twenty eight percent of the Brazil population samples from captive managed manatees in rehabilitation (1.875 – 2.4725 mg/mL) were also below the lower limit of the species reference range. The Belize animal that was brought into rehabilitation as an orphaned calf accounts for the lowest overall total circulating IgG level. In general, blood values for this animal appear within the normal range. Samples from this individual over multiple years were analyzed with consistent results. This could be the result of the so called 'hygiene hypothesis' (Bloomfield et al., 2006). Since the manatee is in a somewhat sterile rehabilitation environment and has been since it was a calf, this animal was not exposed to the potential pathogens typically encountered in Antillean manatee calves that help them to build immunological memory. This could also account for the low IgG levels observed in the Brazil population animals as they often enter rehabilitation as calves. This could be of concern when considering release of this animal and potentially other orphaned calves, should this be a trend. Further analysis of the immune function of this rehab animal is needed to ensure that it is well suited for release.

Additionally, while within the species and sub-species reference ranges, a manatee that was rescued during the course of the Brevard health assessments with a chronic entanglement had a mean total circulating IgG level of 5.76 mg/mL and was the only animal below the Brevard population reference range. This animal was emaciated and lethargic upon rescue. The entanglement had progressed to the point that the pectoral flipper self-amputated upon rescue due to the severe necrosis. This animal

was potentially immune suppressed which may have been reflective of the low level of circulating IgG.

Ten and a half percent of the Belize, 5% of the Everglades, 38% of Brevard, and 3.3% of the Crystal River populations animals were above the upper limit of the species reference range (Appendix B). For these animals, numbers were comparable when compared to population reference ranges: 9.6% Belize, 5% Everglades, 5.4% of Crystal River. For the Brevard population, however, only 4.8% (1 sample) was above the upper limit of the population reference range. One captive manatee in rehabilitation at Lowry Park Zoo with a chronic boat strike injury was also above the upper limit of the species and sub-species reference ranges with a mean circulating IgG of 24.26 mg/mL. This animal had a chronic boat strike injury with severe inflammation and thus a very active immune response in progress which may account for elevated circulating IgG levels. Blood parameters for the 3.3% of Crystal River animals revealed that they were all generally within the normal manatee hematological parameters with only the 21.46 mg/mL animal having an elevated SAA value of >120 µg/mL indicative of an inflammatory response (Harvey et al., 2007; Harr et al., 2011). These animals were also categorized as having excellent body condition as well during health assessments. So while elevated circulating IgG could be reflective of an inflammatory response, more studies are needed to investigate other possible correlations such as age or individual variability.

Passive Transfer

Two samples of fetal manatee sera were included for analysis. Both samples had significantly higher levels of total serum IgG when compared to species, sub-species, and population reference ranges and are consistent with passive transfer of

maternal antibodies from cow to calf across the placenta. Currently, the degree of passive transfer of immunoglobulins is not known for this species. However, in the historically related elephant, failure of passive transfer (FPT) is presumed. FPT can have serious implications for the care and management of orphaned or rejected calves where hand rearing is required. Studies are currently being conducted in the Asian elephant (Chapter 4) and show a significant degree of immunoglobulin transfer across the placenta. The placental morphology of the manatee, similar to that of the elephant, suggests that some degree of passive transfer is possible, though the true extent remains to be defined. To most effectively examine this hypothesis in manatees, samples from pre-suckling manatees as well as colostrum are needed. These samples are difficult to obtain in Florida since captive breeding programs do not exist. Samples are opportunistic and often collected from orphaned animals entering rehabilitation or carcasses, such as the two fetal serum samples used in this study. Collaborative studies with international facilities in which manatee breeding opportunistically occurs are being pursued to further examine this area of manatee immunology and reproduction.

Conclusion and Future Studies

The Octet system provides better accuracy and reproducibility and allows for a more rapid analysis of IgG when compared to an ELISA format. For circulating IgG in the manatee, assay optimization resulted in a calculated inter-plate and intra-plate variability of 8.3% and 2.3% respectively and a standard deviation of 0.54 mg/mL. Reusing the sensors offers additional benefits such as reduced operational cost and increased throughput. Quantification of IgG can be used to define baseline reference ranges for a species or population further aiding in the tools available for assessment of

health in sirenians (Figure 3-9). IgG levels often correlate with disease state, reflect the immunocompetence of an individual, or reflect exposure to environmental pathogens. Additionally, recent research supports the role of marine mammals as sentinel species, with immune function gaining attention as an indicator of aquatic ecosystem health. Using this technology, baseline IgG reference ranges in the West Indian were defined, while variations between sub-species and populations were discussed above.

Future studies in the West Indian manatee would focus on reproductive immunology including immune response throughout gestation, passive transfer of immunoglobulins, and immune development in calves. Similarly, the immune system of manatees in rehabilitation should be investigated, with particular focus on orphaned calves. The data provided by this study give us the tools necessary to pursue these further immune studies. Now that baseline values for IgG have been established, they can be incorporated into the development of additional assays for the further investigation of the immune system and immune response in the manatee.



Figure 3-1. Florida manatee populations and blood sample numbers. Green=Alabama, Pink=Crystal River, Yellow-Lemon Bay, Purple-Everglades, and Orange-Brevard.

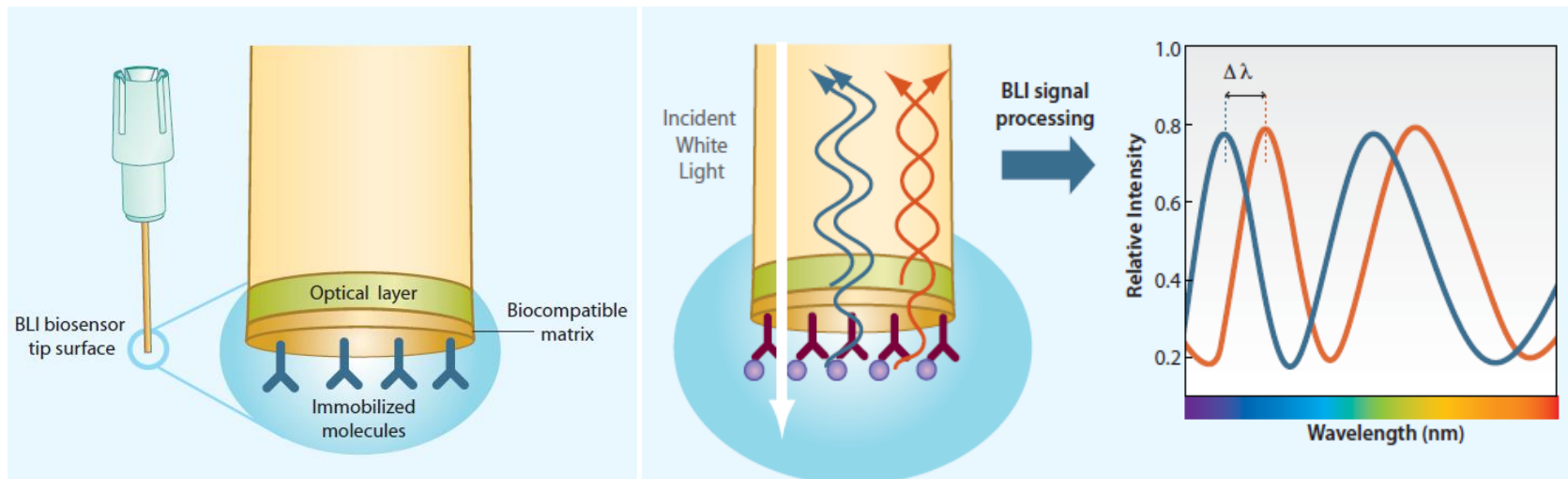


Figure 3-2. Biosensor tip with immobilized protein and the change in bilayer thickness and resulting wavelength shift (Images used with permission from ForteBio, Inc.).

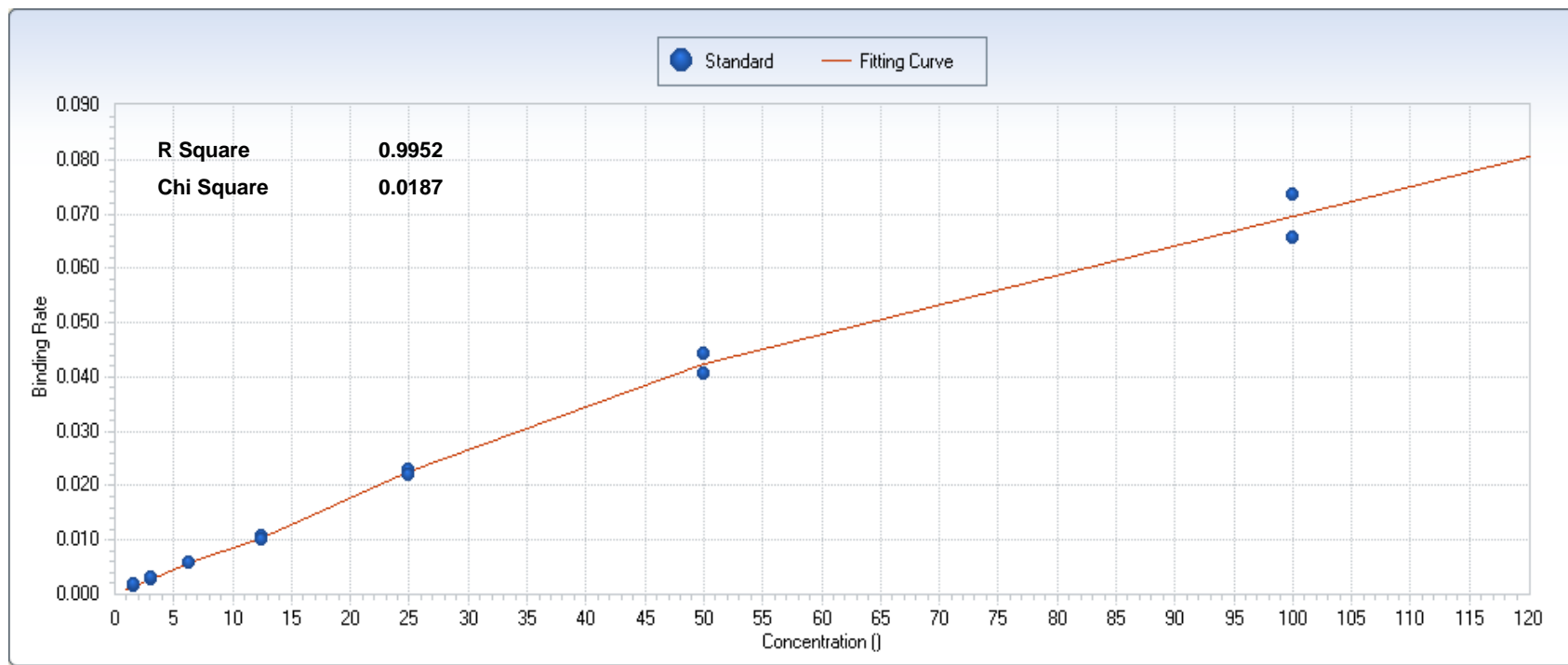


Figure 3-3. Biolayer Interferometry assay duplicate standard curve for quantitative analysis of immunoglobulin G (IgG) in manatee sera. Purified manatee IgG was used for the standards, serially diluted 1:2 from 100 µg/mL.

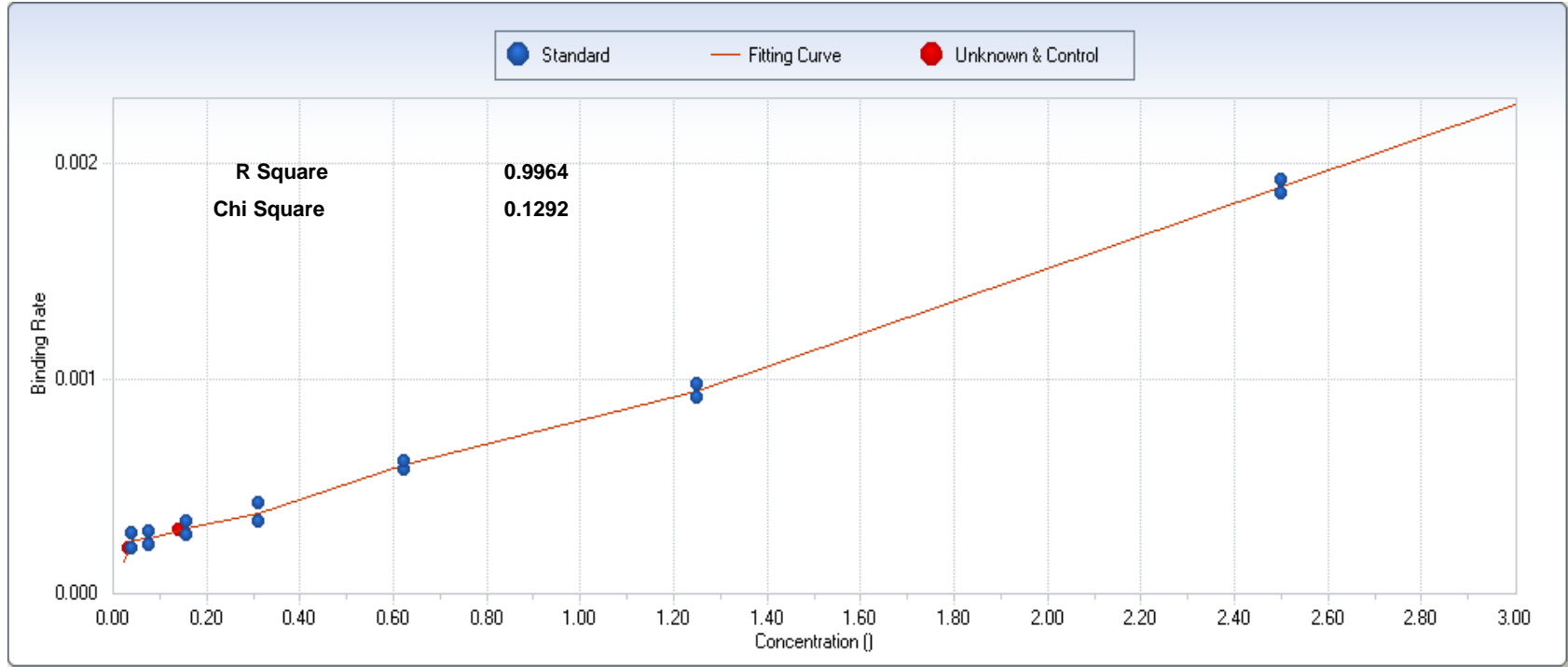


Figure 3-4. Biolayer Interferometry assay duplicate standard curve for quantitative analysis of immunoglobulin G (IgG) in manatee tear film. Purified manatee IgG was used for the standards, serially diluted 1:2 from 2.5 $\mu\text{g}/\text{mL}$.

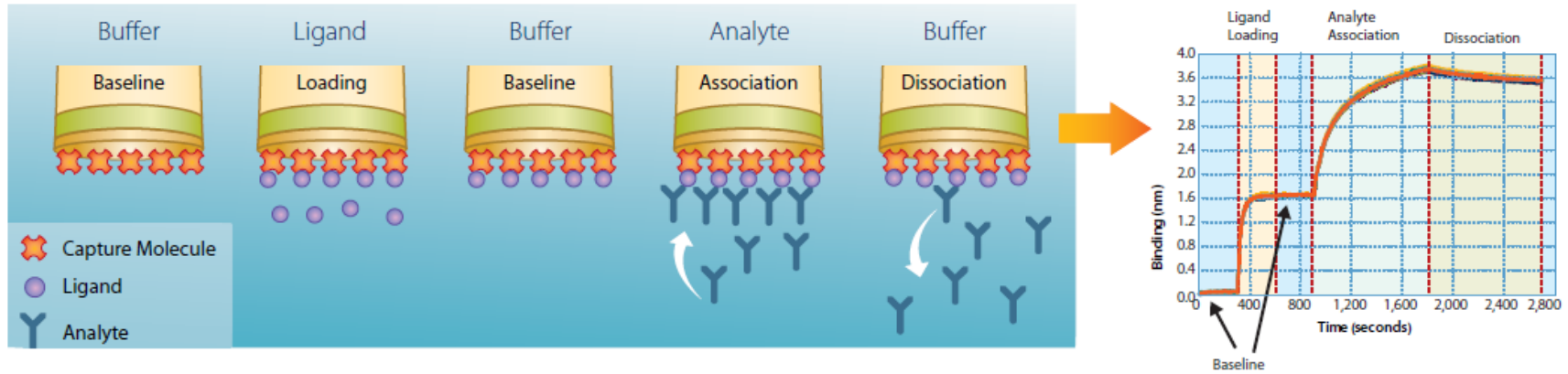


Figure 3-5. Basic Kinetics Assay Steps. Quantitative IgG Assay_Step 1-Baseline1, 1xKB (aka Buffer), Step 2-Load, 25 $\mu\text{g}/\text{mL}$ HL 767 mAb (aka Ligand), Step 3-Blocking, 100 $\mu\text{g}/\text{mL}$ Biocytin, Step 4 Baseline1, 1xKB, Step 5-Regeneration, 10 mM Glycine pH 1.7, Step 6-Baseline2, 1xKB, Step 7-Regeneration, 10 mM Glycine pH 1.7, Step 8-Baseline2, 1xKB, Step 9-Regeneration, 10 mM Glycine pH 1.7, Step 10-Baseline1, 1xKB, Step 11-Association (aka Analyte), serum or tear film dilution, Step 12-Baseline1, 1xKB. (Image used with permission from ForteBio, Inc.)

Total Circulating IgG (mg/mL) Range

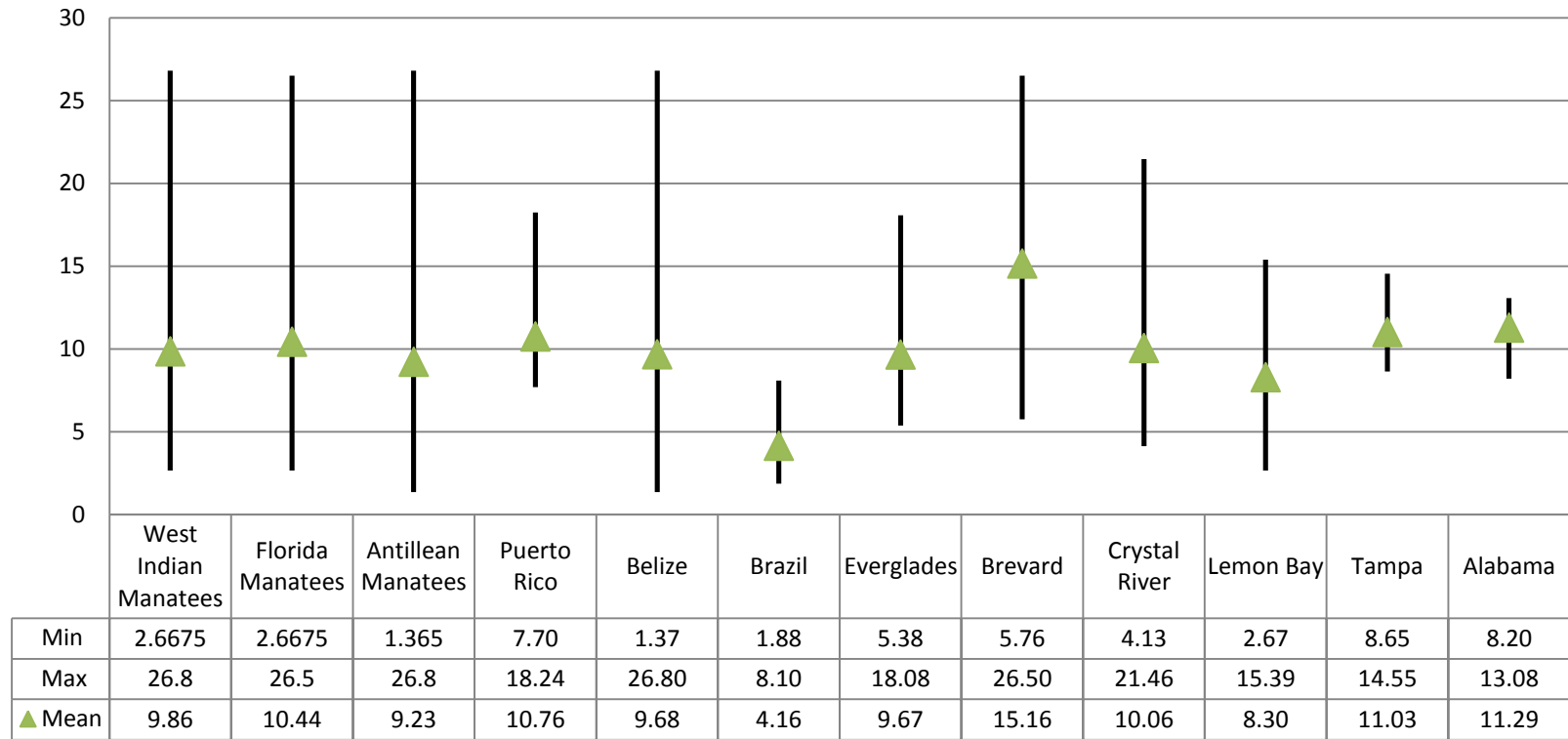


Figure 3-6. Species, sub-species, and population mean, minimum, and maximum total circulating IgG.

Mean IgG vs. Median IgG

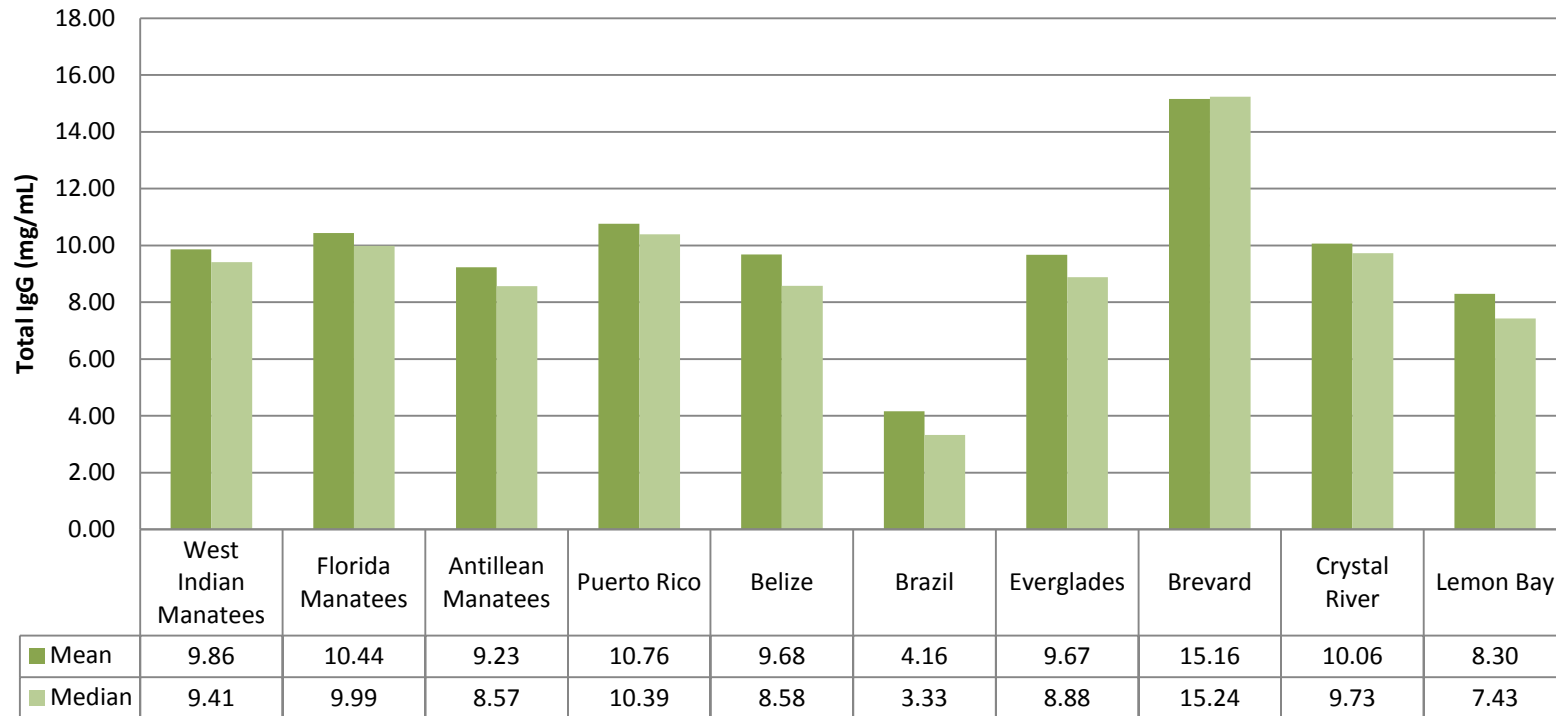


Figure 3-7. Mean circulating IgG versus median circulating IgG in the West Indian manatee.

Total IgG (mg/mL) Males vs. Females

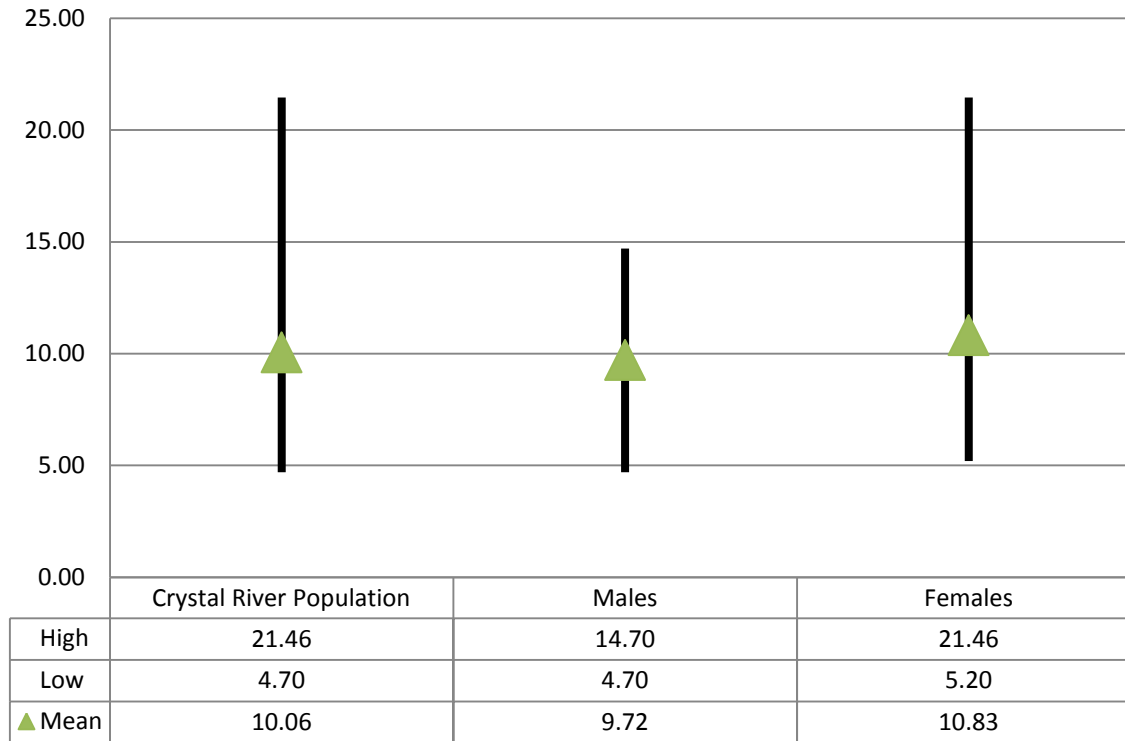


Figure 3-8. Total circulating IgG in males versus females in the Crystal River Florida manatee population. No significant difference was observed, $P=0.0751$.

Total Circulating IgG (mg/mL) Reference Ranges

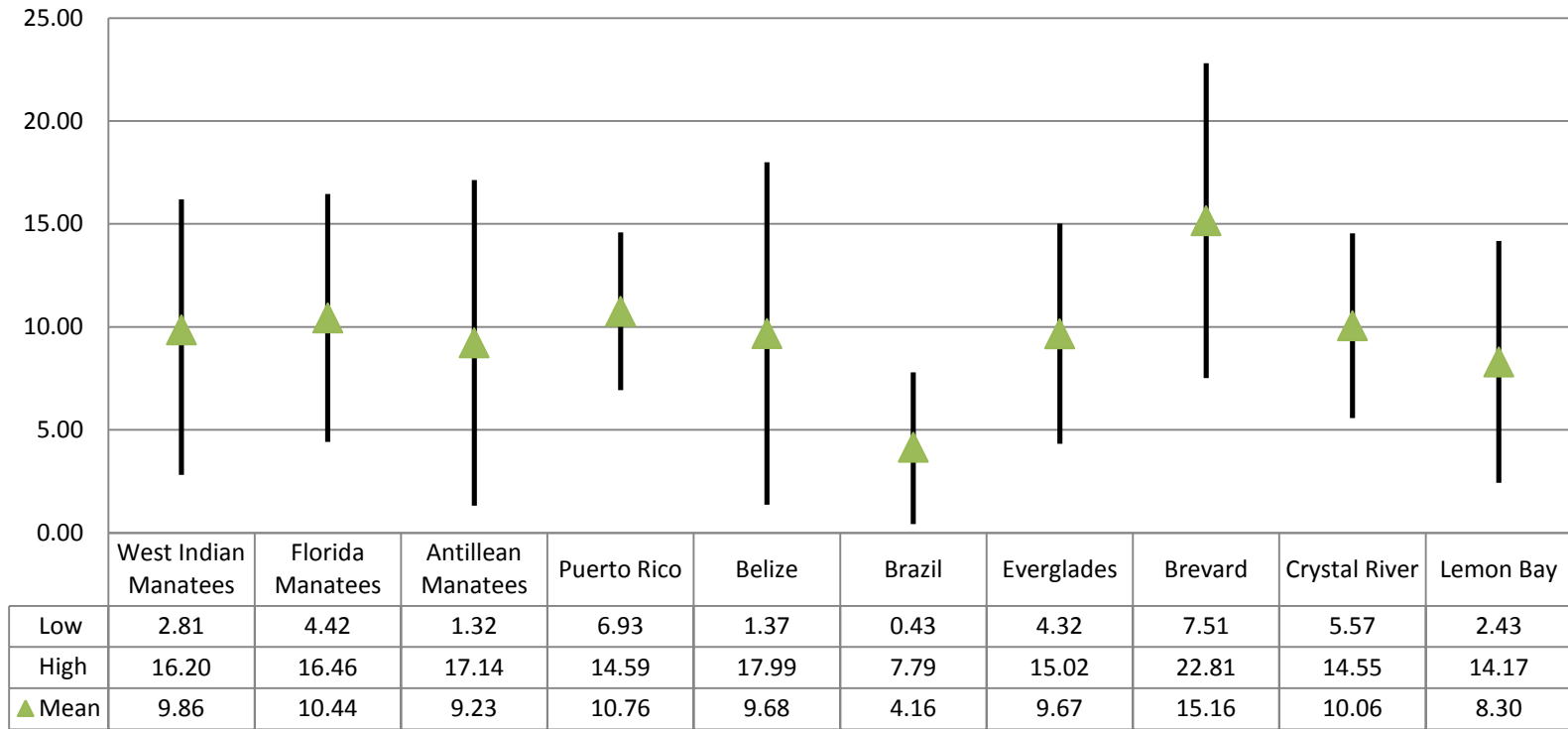


Figure 3-9. Total circulating IgG reference ranges by species, sub-species, and populations.

Total Serum IgG (mg/mL) for Puerto Rico (Years 2003-2005)

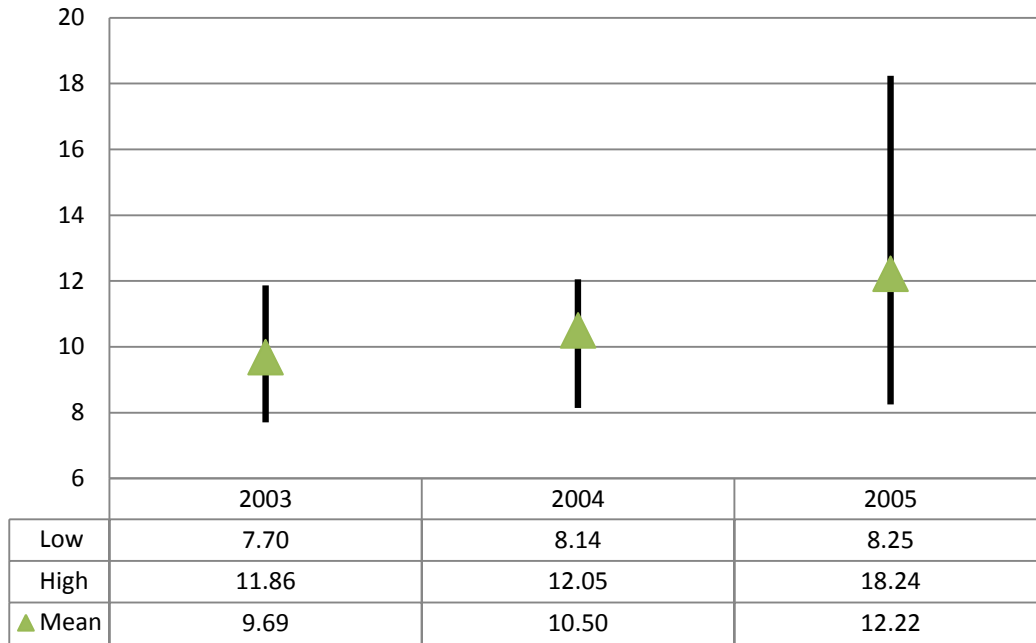


Figure 3-10. Total circulating IgG for the Puerto Rico Antillean manatee population.

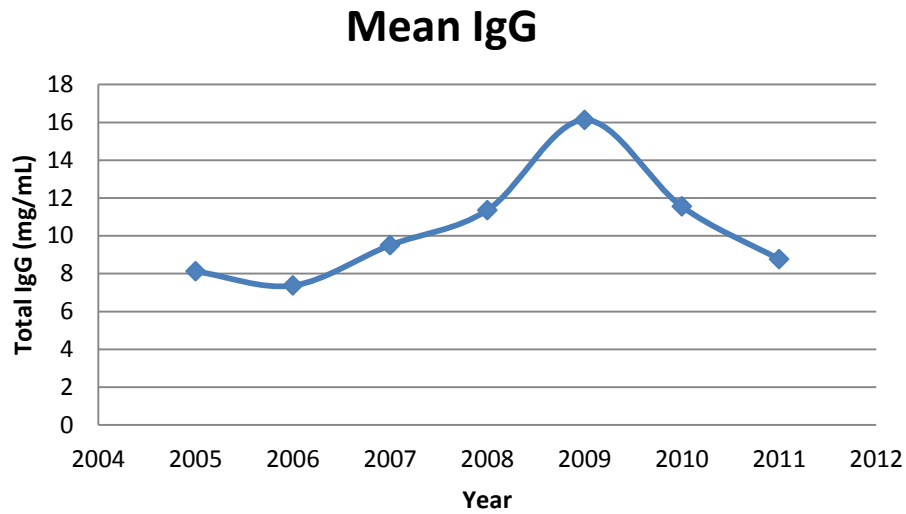


Figure 3-11. Mean circulating total IgG for the Belize Antillean manatee populations. Year 2005 = 8.13 mg/mL (N = 30, SD = 4.50), Year 2006 = 7.38 mg/mL (N = 17, SD = 3.96), Year 2007 = 9.51 mg/mL (N = 24, SD = 4.51), Year 2008 = 11.36 mg/mL (N = 4, SD = 3.14), Year 2009 = 16.13 mg/mL (N = 12, SD = 6.21), Year 2010 = 11.56 mg/mL (N = 11, SD = 6.55), and Year 2011 = 8.77 mg/mL (N = 16, SD = 2.66). This figure includes the repeat total IgG values from individuals sampled in multiple years.

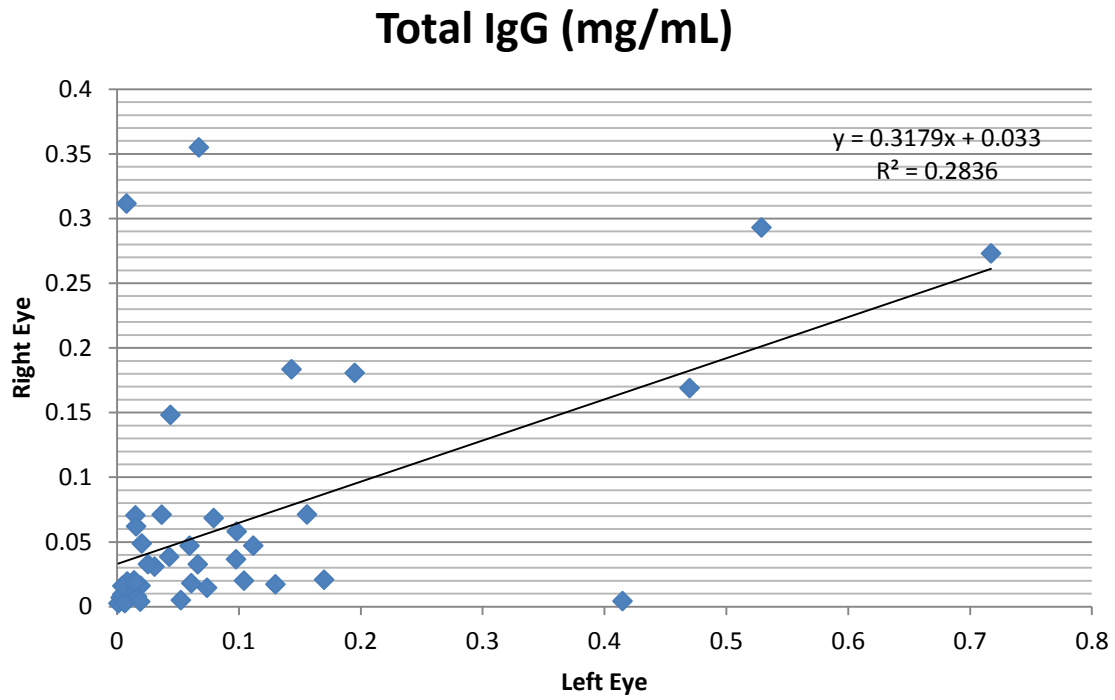


Figure 3-12. Mean total IgG in manatee tear film, right eye samples versus left eye samples.

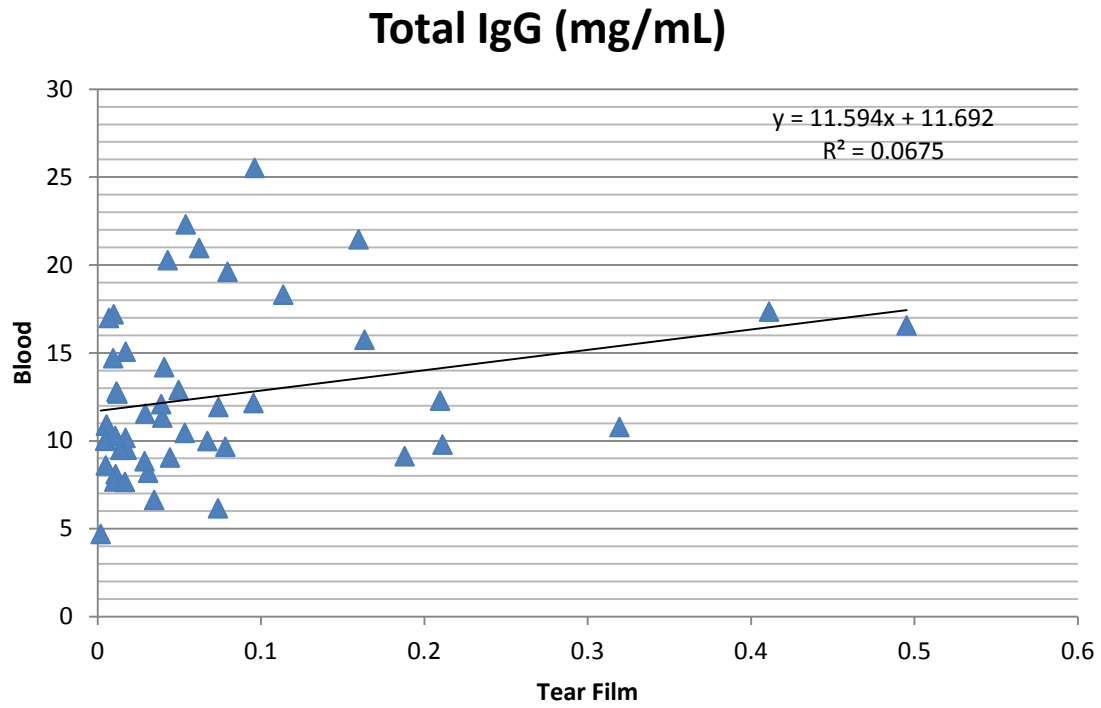


Figure 3-13. Mean total circulating IgG (blood) versus mean total secreted IgG (tear film).

Mean Total IgG-Crystal River

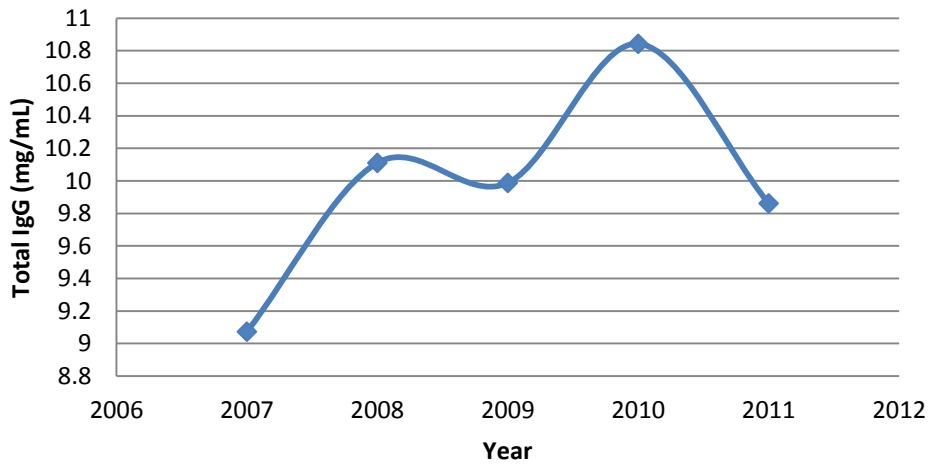


Figure 3-14. Mean circulating total IgG for the Crystal River Florida manatee population across 5 years. Year 2007 = 9.07 mg/mL (N = 12, SD = 1.84) Year 2008 = 10.11 mg/mL (N = 26, SD = 2.62), Year 2009 = 9.99 mg/mL (N = 22, SD = 1.86), Year 2010 = 10.84 mg/mL (N = 19, SD = 4.87), and Year 2011 = 9.86 mg/mL (N = 13, SD = 2.45).

Mean Total IgG-Everglades

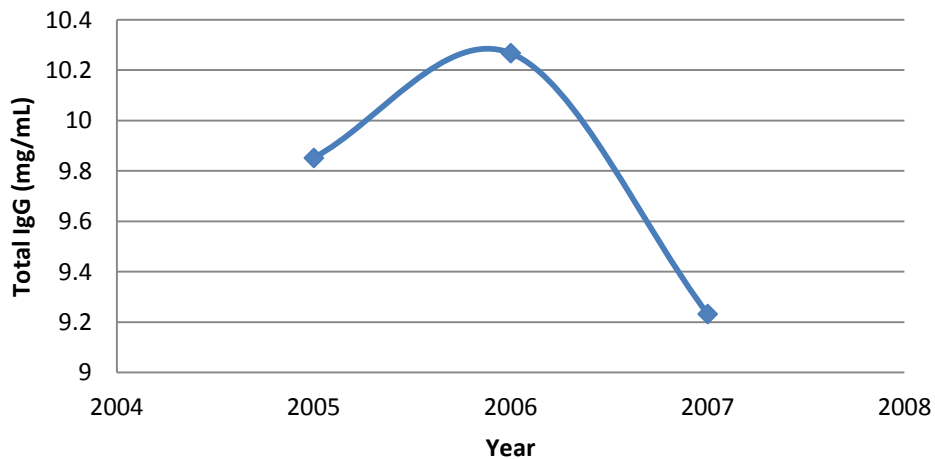


Figure 3-15. Mean circulating total IgG for the Everglades Florida manatee population across years. Year 2005 = 9.85 mg/mL (N = 6, SD = 4.37), Year 2006 = 10.27 mg/mL (N = 12, SD = 3.20), and Year 2007 = 9.23 mg/mL (N = 19, SD = 2.02).

CHAPTER 4 UTILIZATION OF A MONOCLONAL ANTIBODY FOR THE DETECTION OF IMMUNOGLOBULIN G IN THE ASIAN ELEPHANT

Introduction

“There is a paucity of literature on the anatomic and functional aspects of the elephant immune system. Much research is needed” (Lowenstine, 2006). The field of wildlife immunology is relatively new with limited tools available for research and diagnostics such as species specific antibodies. Closely related species can sometimes serve as a substitute when antibodies show cross species reactivity. The elephant, which belongs to the order Proboscidea, has been found to be closely related to the order Sirenia (manatee and dugongs). To date, the evidence for the close phylogenetic relationship of the Sirenia and Proboscidea consists of a combination of similarities across a wide range of characteristics, such as chromosomal painting, mitochondrial rRNA sequences, as well as dental, taxepodial and other skeletal features (Carter et al., 2004; Kellogg et al., 2007; Kleimschmidt et al., 1986; Lavergne et al., 1996; Murata et al., 2003; Nishihara et al., 2005; Pardini et al., 2007; Rasmussen et al., 1990; Samuelson et al., 2007; Seiffert et al., 2007).

In previous studies, several monoclonal and polyclonal antibodies specific for manatee immunoglobulin G (IgG) and IgM have been developed (manuscript in preparation). Primarily involved in secondary immune response, IgG protects the body by binding to an array of pathogens, thus providing protection from viral and bacterial infections. This immune protein is found in all body fluids and is the predominant antibody found in blood and extracellular fluid. While transferred from dam to calf in milk and colostrum, IgG is also the only antibody capable of crossing the placenta thereby providing the fetus with humoral immune protection (Murphy et al., 2008).

These manatee specific IgG antibodies, however, show no cross reactivity with elephant tissues. Therefore, a species specific antibody was developed for the detection of elephant IgG as previously discussed (Chapters 1 and 2).

Compared to other captive megavertebrates, the survival rate for elephant calves, particularly Asian elephants, is very low (Emanuelson and Kinzley, 2002; Gage, 2008). At times, human intervention is required and hand-rearing is considered a difficult task. The Species Survival Plan (SSP) states that it “strongly recommends that calves *not* be hand-reared, but rather encourages managers to reintroduce the calves to the dams if at all possible” (Emanuelson and Kinzley, 2002; Emanuelson, 2006; Gage, 2008). When hand rearing is required, oral immunoglobulin supplementation is a major part of neonatal care protocols (Emanuelson and Kinzley, 2002; Emanuelson, 2006; Weber and Miller, 2012). Elephants are believed to acquire maternal immune protection entirely postnatally via colostrum and milk and as such, orphaned calves are presumed to experience failure of passive transfer (FPT) of immunoglobulins. FPT can contribute to the mortality of hand-reared calves by potentially increasing susceptibility to pathogens such as Elephant Endotheliotropic Herpesvirus (EEHV). Transfer of immunoglobulins can occur passively, across the placenta, and/or actively, through ingestion of colostrum and milk. While it is presumed that there is no passive transfer across the placenta in elephants, it has not been confirmed. IgG is the only immunoglobulin that is prenatally transferred in mammals, such as humans, as it is the only one that can cross the placenta. For elephants, histological investigations of the placenta have led us to suspect that some degree of transfer is possible before birth (Allen et al., 2003; Allen, 2006; Carter et al., 2004). Elephants have an

endotheliochorial placenta, similar to that found in dogs and cats, with the maternal blood vessels ensheathed by cellular trophoblasts. The basement membrane of the maternal endothelial cells is thickened, but trophoblast cells extend narrow processes through the membrane. The fetal side is comprised of deeply indented fetal capillaries, reducing the diffusion distance between maternal and fetal blood. Due to the presumed FPT across the placenta, much of the neonatal elephant care is modeled after the methods of care for foals in which FPT across the placenta has been confirmed. If a hand-reared elephant calf does not receive colostrum, plasma is administered to provide essential immunoglobulins. However, quantitative data for immunoglobulins in elephant plasma is also currently unknown and therefore veterinarians and managers are left to use crude estimations of the exact volume of plasma to be administered in order to provide adequate calf immune protection. Knowing the baseline circulating IgG levels as well as the extent of prenatal transfer of immunoglobulins in elephants can be critical for their management in the event that a calf is orphaned or rejected. This would be of particular importance in evaluating the immune development and assessing disease susceptibility in calves, further aiding in resources available for successful neonatal care and hand rearing in this species. Using the anti-elephant monoclonal antibody (mAb) for the detection of IgG, the aim of this study was to develop a quantitative assay for measuring total IgG in order to establish baseline reference ranges as well as investigate passive transfer of maternal immunoglobulins from dam to calf, a subject which remains undefined in the elephant.

Material and Methods

Study Animals

Archived Asian elephant blood samples were maintained in a -80°C freezer as part of the Tissue Bank at the University of Florida-Zoological Medicine Program. Serum was collected from the auricular veins on the caudal pinnae. Samples represent males and females, as well as a range of age classes including calf, juvenile and adult. Serum samples were centrifuged at 3000g for 5 min. to better clarify the samples. Thirty microliters from the serum samples discussed below, were aliquoted and stored at -20°C until analysis.

Vaccination-Assay Validation. We analyzed pre-vaccination and several post-vaccination samples from 8 elephants vaccinated for rabies (IMRAB 3, killed virus rabies vaccine) and tetanus (tetanus toxoid vaccine). Assay validation included analysis of immunological response (total IgG) to a vaccine antigen in addition to the standard inter- and intra-plate variability tests discussed below. Rabies and tetanus titers (OD 405 nm) were also determined for these samples using a sandwich ELISA format that incorporated the anti-elephant monoclonal antibody (mAb) discussed below, demonstrating the specificity of the mAb in detecting seroconversion (Isaza et al., 2006). Serum samples were collected 8, 15, and 29 days post vaccination while pre-vaccination samples were collected 2-8 months prior. Additionally, 5 elephants that were vaccinated with the tetanus toxoid vaccine only, were also included for analysis. For these animals, only pre- and post-vaccination samples were included. Pre-vaccination samples were collected 5 days before vaccination and post-vaccination samples collected 27 days after vaccination.

Population Baseline. Archived serum samples from 26 Asian elephants were used to determine baseline circulating IgG levels for a captive population. Samples included serum from 9 individuals collected on the 3rd of August, 2010, 15 collected on the 5th of March, 2011, 1 collected on the 4th March, 2011, and 1 collected on the 9th of February, 2011. All 26 elephants were part of the same captive managed unit. Males and females are included in the analysis, though the samples, and captive managed Asian elephants in general, are skewed towards females, therefore differences between sex will not be investigated.

Passive Transfer of Immunoglobulins. For the investigation of passive transfer of immunoglobulins across the placenta in the Asian elephants, 25 blood samples from 7 individual dams and their calves (11 individuals) were included for analysis. Samples from dams were collected 1-13 days before parturition with one sample being collected 2 months after parturition (N=11). Samples were confirmed to be collected from calves pre-suckling (N=5), from calves on the day of birth (suckling unknown) (N=4), and/or at varied times throughout lactation/nursing (N=2). Two samples of cord blood were also included for the analysis of passive transfer of immunoglobulins. Additionally, one focal animal, a tuberculosis (TB) positive dam and her calf were also included for investigation of passive transfer via the analysis of TB antibodies in a pre-suckling calf.

Tuberculosis, Rabies, and Tetanus Assay

Testing for actively shedding TB, is accomplished by obtaining a culture from the animal via a trunk wash, which is often performed routinely due to the intermittent shedding nature of mycobacterial infections. Testing for tuberculosis (both actively shedding and latent) in blood is conducted using either a lateral flow assay format (Chembio STAT-PAK) or a MultiAntigen Print ImmunoAssay (MAPIA). The Chembio

STAT-PAKs include either the PrimaTB STAT-PAK which is used for antibody detection in animals infected with *M.tuberculosis* or *M.bovis*, while the Elephant TB STAT-PAK detects antibodies for *M.tuberculosis*, *M.bovis*, *M. microti*, or *M.pinnipedii*. The MAPIA assesses the presence of antibodies to 10 individual mycobacterial antigens (ESAT-6, 14 kDa, MPT63, 19 kDa, MPT70, MPT64, MPT51, MTC28, Ag85B, 38 kDa, MPT32, and KatG).

Using modified indirect ELISAs, tuberculosis, rabies and tetanus titers were established. In brief, these ELISAs used recombinant tuberculosis antigens ESAT-6 @ 1 µg/mL and CFP-10 @ 2 µg/mL, an IMRAB 3 rabies vaccine antigen at 10 µg/mL, and a tetanus toxoid antigen at 5 µg/mL. Maxi Sorp 96 well, flat bottom, immuno plates were coated with the aforementioned antigens and incubated overnight at 4° C. Plates were washed 4 times with 300 µL per well of PBS/Tween, blocked with 300 µL/well of 1% BSA/PBS for 1 hour at room temperature and then washed. Elephant serum samples were diluted to 1:100 in BSA/PBS for tuberculosis and rabies testing and 1:600 in BSA/PBS for tetanus testing. Plates were sealed and then incubated for 1 hour at room temperature on a nutator, 50 µL/well. Plates were washed again and wells were then incubated for 1 hour with biotinylated HL 2007 at 0.5 µg/mL concentration for rabies and tetanus assays and 1 µg/mL for the tuberculosis assay. The plates were washed again and then given alkaline-phosphatase labeled Streptavidin at 1:2000 in PBS. Plates were incubated for one hour at room temperature on a nutator. Plates were washed a final time and *p*-nitrophenyl phosphate substrate (P-NPP) was added to all wells. Plates were read on a spectrophotometer at 405 nm wavelength after 30 minutes and 1 hour in substrate.

cELISA Development and Validation for Elephant IgG Quantification

Assay Regents. Purified elephant IgG was used for plate coating and standards for the competitive ELISA. Two mLs of Asian elephant serum, diluted 1:10 in PBS, were used for purification by affinity chromatography using a 1 mL Protein A Sepharose Fast Flow column, which was shown to bind elephant IgG. The dilution was passed over the column 24 times with a final rinse of PBS. The bound elephant IgG was eluted from the column using a 0.1M glycine elution buffer, pH 2.8. The eluted fractions were collected and neutralized with 2.0M Tris pH 9 and using a spectrophotometer, absorbance readings were taken at 280 nm wavelength. The eluted fractions with the highest absorbance values were pooled, concentrated using an Amicon Ultra 15 centrifugal filter, buffer exchanged to PBS, and then read again resulting in a yield of 13.5 mgs. For use in cELISA, this was further diluted to 1 mg/mL. To verify purification of the desired sized protein, under reduced conditions, we used a 10% Novex NuPage Bis-Tris gel, including the purified elephant IgG at 1 and 2 μ g per lane, a 1:60 dilution of the IgG depleted flow through, and a 1:15 and 1:45 dilution of elephant serum. Staining with colloidal blue revealed bands at 50 and 19 kDa signifying the IgG heavy chain and light chain for elephant IgG.

Several aliquots of biotinylated mouse anti-elephant IgG mAb (HL 2007) were archived and used in the initial phases of this study. Due to reagent degradation, a new stock of antibody was required. Cloned HL 2007 (7C1-3D9), anti-elephant IgG hybridoma cells were grown in Becton Dickenson Biosciences Cell Mab Medium Quantum Yield and 10% low IgG FBS in a 37°C, 7% CO₂ incubator, and allowed to grow for several days. Cells were then injected into a CeLLine classic 350 flask where they grew concentrated supernatant which was collected at 8, 13, and 19 days. Fresh

culture medium was added to replace the harvested supernatant three times to allow for cell growth, after which, all concentrated supernatant was pooled. Thirty five milliliters of CL 350 concentrated supt was then purified by affinity chromatography using a 5 mL HiTrap Protein G Sepharose column, passing over the column 14 times to bind the mouse anti elephant IgG. The mouse anti-elephant IgG was then eluted, neutralized, pooled, and concentrated like that of the purified elephant IgG described previously. The final antibody yield was 10.81 mgs at 9.24 mg/mL. As with the purified IgG, a Coomassie gel was also run to verify purification of the monoclonal antibody (HL 2007). For this gel, the purified antibody was run at 0.25 mg/mL and the flow through supernatant at 1:10 dilution. Purified HL 2007 was biotinylated using EZ-Link Sulfo-NHS LC Biotin. The elephant antibody and biotin incubated at room temperature for two hours to allow for binding. Unbound biotin was removed and antibody desalted using Thermo Scientific Zeba Desalting Spin column. The biotinylated antibody was read on a spectrophotometer at 280 nm wavelength and the final concentration read. This concentration (1.28 mg/mL) was used for optimization of antibody used for competitive ELISAs.

Reagent Optimization. Optimization of reagent concentrations included coating concentration of purified elephant IgG, anti-elephant IgG mAb concentration, and elephant serum concentrations. Optimization of coating and antibody concentration employed a direct ELISA format. In a Maxi Sorp 96 well, flat bottom, immuno plate, 280 μ L per well of BSA/PBS was added to each well and left to incubate overnight at 4°C to block. The plate was then washed 4 times with 300 μ L per well of PBS/Tween (BioTek ELx405 Select CW, Winooski, Vermont). For coating concentration optimization,

duplicate rows of a Maxi Sorp 96 well, flat bottom, immuno plate were coated with 50 μ L of purified elephant IgG serially diluted in PBS, ranging from 4 – 0.5 μ g/mL (2 - 0.25 μ g/mL final). Across the columns, 50 μ L of 0.688 mg/mL mouse anti-elephant mAb was added in serial dilutions ranging from 40 – 0.3 μ g/mL (20 - 0.156 μ g/mL final). To one column, 100 μ L of BSA/PBS only was added, serving as a negative control. These reagents were left to incubate for 1 hour on a nutator at room temperature and then washed as previously described. To each well, 50 μ L of a 1:2000 dilution of Streptavidin-alkaline phosphatase (Invitrogen) was added and incubated on a nutator for 1 hour at room temperature. After a final wash, 100 μ L/well of P-NPP substrate (4-nitrophenyl phosphate disodium salt hexahydrate) (Sigma) was added to all wells and left to develop for 1 hour. At 30 min and 60 min, absorbance readings were taken on a spectrophotometer (Molecular Devices Spectramax Plus) at 405 nm wavelength. The dilutions were analyzed and an optimal coating concentration of 0.5 μ g/mL of purified elephant IgG was identified and an antibody concentration of 3.0 μ g/mL were selected based on 70% of the maximum OD readings (using the SoftMax Pro software (Molecular Devices, Sunnyvale, CA) in which there was a range of values that were similar.

Standard Curve and Antibody Re-optimization. Serving as positive controls, known elephant IgG concentrations diluted in PBS were used to generate duplicate standard curves for each cELISA plate run. A 96-well polypropylene micro plate (competition plate) was blocked with 280 μ L/well of BSA /PBS blocking buffer (sealed) overnight at 4°C. Each well of a Nunc Maxisorp plate (the ELISA plate) was coated with 0.5 μ g/mL (diluted in PBS) concentrated purified elephant IgG, sealed, and also left to

incubate overnight at 4°C. The following day, the contents of the polypropylene competition plate were flicked out and blotted dry. Duplicate columns of 50 μ L/well of purified elephant IgG were serially diluted in BSA/PBS ranging from 2-0.06 μ g/mL, 8-0.25 μ g/mL, 30-0.9 μ g/mL, and 50-1.4 μ g/mL (1-0.03 μ g/mL, 4-0.125 μ g/mL, 15-0.45 μ g/mL, and 25-0.7 μ g/mL final) with 3 columns of PBS only and 2 rows of BSA/PBS only, serving as negative controls. Fifty microliters of biotinylated HL 2007 was added to each well (minus those with BSA/PBS only) at a concentration of 7 μ g/mL diluted in BSA/PBS (3.5 μ g/mL final), sealed, placed on a nutator and left to incubate for 1 hr at room temperature. The Nunc Maxisorp ELISA plate was washed as described above and 280 μ L of BSA/PBS blocking buffer was added to each well and left to incubate at room temperature for 1 hour. The ELISA plate was then washed again and 50 μ L of each well were transferred from the competition plate to the ELISA plate where it was again sealed and left to incubate on a nutator for 1 hour at room temperature. The competition plate was discarded and the ELISA plate was washed again. The secondary antibody, 50 μ L/well of alkaline phosphatase-labeled Streptavidin (Invitrogen), was then added at a 1:2000 dilution and left to incubate again on the nutator for 1 hour at room temperature. After a final wash, 100 μ L of 1mg/mL *p*-nitrophenyl phosphate substrate (P-NPP) were added to all wells. The P-NPP was made 15 min before use and placed on a nutator for 5 min. At 30 min and 60 min of incubation at room temperature, OD readings were taken at 405 nm wavelength. Using the standard curve equation in the SoftMax Pro software, the OD readings were plotted against the IgG concentrations and a standard curve ranging from 4 to 0.125 μ g/mL was chosen. (Figure 4-1)

Due to suspected degradation of the 0.68 mg/mL stock, a new stock of biotinylated HL 2007 was developed, at 1.28 mg/mL, and used for all subsequent assays. Optimization of this new stock of antibody incorporated the optimized coating concentration and standard curve. Using the competitive ELISA format as previously discussed, coating, incubation, and wash were conducted as above. Once blotted, 50 μ L/well of purified IgG, serially diluted 8 to 0.125 μ g/mL (4 to 0.06 μ g/mL final), and was added to rows A-G of the competition plate. The new stock of biotinylated antibody was serially diluted at 2 to 0.15 μ g/mL (1 to 0.075 μ g/mL final), in duplicate columns, across the competition plate. Row H contained 50 μ L of the serially diluted biotinylated antibody and 50 μ L of BSA/PBS, serving as a positive control. Column 12 contained 50 μ L of the serially diluted purified IgG and 50 μ L of BSA/PBS, serving as a negative control. Samples were left to incubate in the competition plate for 1 hour at 37°C on a nutator. The ELISA plate was washed and 280 μ L BSA/PBS blocking buffer was added to each well. It too, was left to incubate for 1 hour at 37°C. The remaining washes as well as the transfer, addition of the secondary antibody, addition of substrate, and OD readings, were performed as discussed above.

Serum Optimization. Using the optimized competition reaction conditions and the standard curve, three Asian elephant serum samples were selected for optimization of serum dilutions. These samples were randomly selected and IgG levels were unknown. Similar to the protocol described above for standard curve and antibody re-optimization, a 96-well polypropylene micro plate (competition plate) was blocked with 280 μ L/well of BSA /PBS blocking buffer (sealed) overnight at 4°C. Each well of a Nunc Maxisorp plate (the ELISA plate) was coated with the optimized 0.5 μ g/ μ L (diluted in

PBS) purified elephant IgG, sealed, and left to incubate overnight at 4°C, with the exception of well G12 which was coated with 2 µg/mL of biotinylated HL 2007. This well would serve as the positive control for the alkaline phosphatase-labeled Streptavidin (Invitrogen). The following day, the blocking buffer in the polypropylene competition plate was flicked out and blotted dry. For the standard control, duplicate columns (1 & 2) of 50 µL/well of purified elephant IgG were serially diluted in BSA/PBS ranging from 8 to 0.125 µg/mL (final dilutions 4 to 0.06 µg/mL). Column 12 and Row H served as the negative and positive controls respectively (50 µL BSA/PBS + serially diluted serum and 50 µL BSA/PBS + biotinylated HL 2007 respectively). In the remaining wells, 50 µL of elephant serum (in triplicate) from the three animals was serially diluted in BSA/PBS ranging from 1:2000 to 1:128000 (1:4000 to 1:126000 final dilutions). Fifty microliters of 0.6 µg/mL of biotinylated mAb HL 2007 (0.3 µg/mL final dilution) were added to all wells in rows A-G. The serum and antibody plate was sealed and placed on a nutator to incubate for 1 hour at room temperature. Meanwhile, the contents of the ELISA plate were washed out as described above and 280 µL BSA/PBS blocking buffer were added, plate sealed, and left to block for 1 hour at room temperature. After the allotted time, 50 µL from each well of the competition plate were transferred to the ELISA plate. The competition plate was then discarded and the ELISA plate was sealed and placed on the nutator to incubate for 1 hour at room temperature. After an additional wash, 50 µL/well of the secondary antibody, alkaline phosphatase-labeled Streptavidin (Invitrogen), were added at a 1:2000 dilution and left to incubate again on the nutator for 1 hour at room temperature. After a final wash, 100 µL of 1 mg/mL *p*-nitrophenyl phosphate substrate (P-NPP) were added to all wells. As before, the P-NPP was made

15 min before use and placed on a nutator for 5 min at 30 min and 60 min of incubation at room temperature, OD readings were taken at 405 nm wavelength. Using the SoftMax Pro software, we were able to identify which dilutions gave an OD reading that fell within the linear aspect of the standard curve previously discussed. Based on this assessment, optimal serum dilutions of 1:32000 and 1:64000 were chosen.

Inter- and Intra-Plate Variability. A competitive ELISA, as previously described, was used for both intra- and inter-assay validation. The mean results from 3 randomly selected elephant serum samples run at 1:32000 and 1:64000 dilutions and distributed throughout the plate were used for both analyses. For intra-assay validation, the 1:32000 serum dilutions were replicated a total of 12 times per animal and the 1:64000 dilutions replicated 8 times per animal, both at varying locations within the same plate. Inter-plate validations included 6 competitive assays run on three separate days (2/day). The 1:32000 and 1:64000 serum dilutions were replicated 9 times per animal within each assay plate. The mean value of the results was determined along with the standard deviation (SD). The coefficient of variation (CV) both within and between assays, expressed as a percentage, was also calculated by dividing the SD by the mean value.

Octet QKe Quantitative Assay. The biotinylated HL 2007 was incorporated into a biolayer interferometry assay using the Octet QKe system (ForteBio, Inc.). Bio-layer interferometry (BLI) is an optical analytical technique that measures biomolecular interactions using a novel 'dip and read' approach. As white light travels down the biosensor, the difference in the reflected wavelengths from the internal reference layer and the immobilized protein on the biosensor tip are measured (Figure 4-2). As binding

occurs between the immobilized protein and the sample analyte, the biological layer becomes thicker thereby increasing the wavelength shift. Only bound materials create interference, therefore this system is ideal for crude sample use. As described in Chapter 4, a custom quantitative assay was developed by immobilizing biotin-labeled anti-elephant IgG antibody on a streptavidin biosensor (Figure 4-3).

Based on the quantitative IgG protocol for the manatee (Chapter 3), a standard curve was generated for analysis of 7 serum samples from pre-suckling Asian elephant calves (N=5) using the basic kinetics setting on the Octet QKe. Two columns of streptavidin biosensors (16 biosensors total) were loaded into the biosensor tray where they were incubated at room temperature for 15 min in 1x kinetics buffer (KB). In the 96-well sensor plate, one column was loaded with 100 μ L/well of 1xKB (Baseline Step), one column with 100 μ L/well of biotinylated HL 2007 (Loading Step), and 2 columns with 100 μ L of serially diluted purified elephant serum (Association Steps) ranging from 100 to 1.56 μ g/mL with the bottom two wells consisting of 100 μ L 1xKB, serving as a negative control. Using the Octet QKe kinetics program, the assay steps were defined. Column 1 consisted of the 'baseline step' in which the sensors were dipped in for 120 sec to create a baseline reading, column 1. Sensors were then loaded with biotinylated HL 2007 (loading step, column 2) by dipping the sensors into column 2 for 300 sec. A baseline reading was repeated (column 1, 120 sec) before the sensors were finally dipped into the serum dilutions (association step, column 3) for 900 sec. In a second assay, and a second set of biosensors, steps 1-3 were repeated. The association step was dipped into column 4 to create a duplicate standard curve. After the biosensors were assigned to the samples and the plate definitions saved, the experiment was run.

A data analysis session was opened to determine the sample concentrations using the known concentrations. From these data, a reference standard curve was saved for later analysis of samples with unknown IgG values (Figure 4-4).

For analysis of pre-suckling elephant serum samples, eight streptavidin biosensors were incubated in 100 μ L/well of 1x kinetics buffer (KB) for 15 min at room temperature prior to analysis. As described above, 100 μ Ls of 1xKB/well were placed in one column of a 96-well sample plate, with 100 μ L/well of biotinylated HL 2007 at 25 μ g/mL added to a second well, and 100 μ L/well of elephant serum, diluted 1:1000 in 1xKB, added to a third well. The remaining well consisted of a negative control of 1xKB. Using the Octet QKe kinetics program, the assay steps were defined. As above, column 1 consisted of the 'baseline step' in which the sensors were dipped in for 120 sec to create a baseline reading. Sensors were then loaded with biotinylated HL 2007 (loading step) by dipping the sensors into column 2 for 300 sec. A baseline reading was repeated (column 1, 120 sec) before the sensors were finally dipped into the serum dilutions (association step) for 900 sec. The biosensors were assigned to the samples and the plate definitions saved. After the experiment was run, a data analysis session was opened to determine the sample concentration using the reference set of saved standards. Using the data analysis software, the method file was loaded and the association step selected for quantification. The saved standard curve was loaded and the data analyzed.

Data Analysis

Within each assay, the location of the mean result on the standard curve determined whether IgG detection was considered accurate. If the mean result value fell above or below the linear segment of the standard curve, it was considered outside of the accurate detection range and excluded from analysis (Figure 4-1). For assay

standardization, each serum sample was run at 1:32000 and 1:64000 dilutions. When the mean value for both dilutions measured within the accurate detection range, the average was taken. Additionally, if the CV% of the sample results was greater than 10%, the OD values of the triplicate or duplicate samples were investigated and adjustments made to 'mask' an outlier reading from analysis (Figure 4-5). If 'masking' one OD reading continued to exhibit a CV > 10%, the sample was excluded from analysis. A sample in which one of the duplicate or triplicate samples has been 'masked' is noted as an adjusted sample. Student t-tests were used to further analyze differences in total serum IgG values, rabies titers, and tetanus titers between pre- and post-vaccination dates. Biolayer interferometry assays were analyzed as described in Chapter 3 for manatee IgG.

Reference Ranges

Reference ranges will be defined as described in Ruiz et. al., (2009) for baseline circulating IgG in bottlenose dolphin, "the mean IgG value $\pm(1.645 \times \text{standard deviation})$, representing a 90% confidence interval, or 90% of the normal data points on the distribution curve".

Results

cELISA and Population Levels

When the mean result value fell above or below the linear segment of the standard curve, it was considered outside of the accurate detection range and excluded from analysis. Assay plates 29-34 were run for inter-assay variability and assay plate 26 for intra-assay variability. Assay plate 29 was excluded from analysis due to errors in generating the standard curve. The inter- and intra-plate variability was 8.53% and

11.8% respectively. When the plates used to calculate the inter-assay variability analysis were also used to calculate intra-assay variability, the CV = 6.37%.

Centrifugation of the archived serum samples typically resulted in the separation of serum and a lipid-like film. The centrifuged samples exhibited increased accuracy when repeatedly analyzed, whereas the uncentrifuged samples often exhibited higher total IgG values (as much as 18 mg/mL higher) that were highly variable, had CVs > 10%, and resulted in mean results outside the linear segment of the standard curve. A total of 9 assays were run to determine the total circulating IgG levels in a population of 26 captive managed Asian elephants. Each sample was analyzed independently within the assay and in comparison between duplicate samples in replicate assay. The measured total IgG for each animal was determined by averaging the values calculated across 5 repeated assays. Initially, 30 μ L sample aliquots were stored at 4°C (for a maximum of 2 weeks) after initial thaw to reduce protein degradation from repeated freeze thaw cycles. Similar protocols were also employed for the biotinylated HL 2007 mAb. It was found that the serum samples were highly susceptible to fungal growth at this temperature, and that both the serum and biotinylated HL2007 mAb degraded quickly at 4°C. For this reason, the initial 3 population assays were excluded from further analysis and for subsequent assays, multiple aliquots of serum and biotinylated HL 2007 mAb were made and stored at -20°C until analysis to reduce freeze thaw cycles. The mean total IgG for this population of Asian elephants was 14.85 mg/mL (SD=5.31). Sample averages ranged from 7.7 mg/mL at the minimum and 32.14 mg/mL at the maximum (Figure 4-6). As mentioned above, sample values were considered outside of the accurate detection range if the mean value fell above or below

the linear range of the standard curve. The reference range for accurate detection using the 1:32000 serum dilution was 7.16 mg/mL to 15.68 mg/mL and for the 1:64000 serum dilution, 15.94 mg/mL to 36.9 mg/mL. Samples ranging from 11.1 mg/mL to 22.09 mg/mL were within the accurate detection range at both serum dilutions (Figure 5-7). While not yet optimized for elephant serum, Octet QKe analysis verified this trend, revealing values of 13.14 mg/mL and 32.03 mg/mL respectively. These values were also verified through repeated cELISA analysis. A reference range of 6.12 mg/mL to 23.58 mg/mL was calculated.

Vaccine Response

Response to rabies and tetanus vaccines was assessed via measurement of vaccine titers as well as total IgG. For 2 animals, pre-vaccination samples did not meet the criteria for total IgG analysis and were noted. One sample had CVs > 10% and the other exhibited a mean value that was not within the accurate detection range. Using the biotinylated HL 2007 mAb, an antibody response of similar intensity was detected in 7 of the 8 animals vaccinated against rabies and tetanus concurrently, while 1 animal appeared unreactive (Figures 4-8 and 4-9). Total IgG values varied among individuals and were significant for only two of the eight animals (Figure 4-10). Similarly, only 1 of the 5 animals vaccinated against tetanus only exhibited a significant difference between pre-and post-vaccination total IgG levels (Figure 4-11).

Passive Transfer of Immunoglobulins

The calf samples analyzed in this study support the hypothesis that immunoglobulins are passively transferred from dam to calf across the placenta in Asian elephants. All pre-suckling samples resulted in total IgG measurements ≥ 22 mg/mL (Appendix E and Table 4-1). All cord blood samples analyzed measured > 18 mg/mL.

In addition to repeated testing via cELISA, the Octet QKe system was used to run biolayer interferometry (BLI) assays to validate the presence of IgG in pre-suckling Asian elephant serum samples. This assay was not optimized for elephants and therefore IgG levels were not necessarily expected to match those observed in the cELISA. Immunoglobulin G levels measured via BLI assay were comparable to those measured in the cELISA with total IgG levels > 22 mg/mL (SD = 2.054), confirming the presence of IgG in these pre-suckling samples.

Furthermore, the calf of a tuberculosis (TB) positive dam exhibited high TB antibodies in the pre-suckling serum sample. Seroconversion was detected in this dam at 7 years old, just one year before her first pregnancy. She remained positive throughout gestation and her first calf (not included in this focal study) had measurable TB antibodies from birth. Treatment was not administered at this time partially due to culture negative results and partially to the reproductive state of the dam (1st gestation, lactation, 2nd gestation). At 11 years old, this dam gave birth to a second calf. In the pre-suckling serum sample, high levels of TB antibodies were detectable. The dam became culture positive for TB at 13 years old and remained positive throughout lactation. At 14 years old, treatment began which continued for 2 years. The dam remained STAT-PAK reactive and MAPIA positive for TB both during and after treatment. At four years old, the calf was also STAT-PAK reactive and MAPIA positive for TB. However, at 5 years old and with no history of treatment for tuberculosis, the calf tested negative via MAPIA (Appendix E).

Discussion

Species specific antibodies are an invaluable tool for research and diagnostic studies, particularly when commercially and/or related species antibodies are either not

available or show little to no cross reactivity. The availability of species specific reagents, such as monoclonal antibodies, has facilitated the development of various assays for the detection and quantification of immunoglobulins in the elephant. In this study, we were able to demonstrate the use of a mouse anti-elephant monoclonal antibody (HL 2007 mAb) in sandwich ELISAs, the development of a cELISA, and in biolayer interferometry (BLI) assays. With these assays, we are able to measure tuberculosis, tetanus, and rabies titers (via sandwich ELISA) as well as quantify total IgG in Asian elephant serum (via cELISA and BLI). Furthermore, these quantitative assays have allowed us to investigate population baseline IgG levels and passive transfer of IgG across the placenta.

Incorporation of biotinylated HL 2007 mAb in rabies and tetanus assays demonstrated the use of this species specific antibody in detecting seroconversion. In terrestrial mammals and also in an aquatic mammal (bottlenose dolphin), antibody response after initial antigen exposure is typically undetectable for several days following antigen challenge with levels peaking at 10-14 days post exposure (Tizard, 2000; Murphy et al., 2006). While humoral response to the vaccine antigens in this study was comparable among 7 of 8 animals, individual response to antigenic challenge in general and/or to a specific vaccine antigen varied (Figures 4-8 and 4-9). One animal appeared to have little to no response to either the rabies or tetanus vaccine antigen. For reactive animals, rabies titers showed a marked increase between the first and second post vaccination sampling dates, approaching peak levels around 15 days post vaccination before plateauing or gradually declining. Similarly, this marked increase was also observed in tetanus titers, however, titers for 3 animals continued to peak after

15 days. While total IgG varied among these individuals, 6 animal samples showed little to no gradual increase post vaccination with 2 animals exhibiting significant, though low, post vaccination total IgG response (Figure 4-10).

Pre-vaccination samples were collected 2-8 months prior to vaccination against rabies and tetanus. These animal samples were collected opportunistically and consequently, may not accurately reflect immediate pre-vaccination values. However, due to the little to no measurable change in levels, across all assays, between the pre-vaccination sample and the 1st post-vaccination samples, we feel confident that the pre-vaccination sample values are within 'normal' values for the individual. To confirm this, samples collected at the same time point immediately prior to vaccination would be ideal. Pre- and post-vaccination samples from animals vaccinated against tetanus only exhibited total IgG values similar to those animals vaccinated against rabies and tetanus (Figures 4-10 and 4-11). Pre-vaccination samples were collected just 5 days before vaccination and post-vaccination samples collected 27 days after.

Pre-vaccination samples collected for both animal sets discussed above, fell within the reference range established based on a captive managed population of 26 Asian elephants. Samples were measured irrespective of sex or age due to small samples size, opportunistic sampling, and preponderance of female Asian elephants in captive managed settings. While the 1:32000 dilution proved more accurate for animals with total IgG values between 7.16 and 15.68 mg/mL and the 1:64000 dilution for animals with total IgG values between 15.94 mg/mL and 36.9 mg/mL, there was a degree of overlap (Figure 4-7). Samples with total IgG values ranging from 11.1mg/mL to 22.09 mg/mL, were often within the accurate detection range for both dilutions. The

calculated population mean fell within this range, as well as in the uppermost range for the 1:32000 dilution and just below the lower limit of accurate detection for the 1:64000. These data combined with the population reference range calculated in this study (6.12 mg/mL to 23.58 mg/mL) lead us to conclude that multiple dilutions are needed to avoid over or underestimation of total IgG values in elephants. This study provides a total IgG reference range for a single captive managed population of Asian elephants, thus providing preliminary data for further immunological studies in this species. For future applications, sample size would be increased in order to investigate variability among populations, sex, and age. This would provide the most accurate determination of reference ranges for total IgG in Asian elephants. The observed baseline IgG levels of a single captive managed population are likely a conservative estimate.

Baseline parameters of immune function in a species are essential for immunological research and diagnostics as well as for contributing to our knowledge of elephant biology. Compared to other captive megavertebrates, the survival rate for elephant calves, particularly Asian elephants, is very low (Emanuelson and Kinzley, 2002; Emanuelson, 2006). Mammalian neonates are highly vulnerable to infectious disease at birth largely due to their less active and less developed immune systems. Generally, longer gestational periods are correlated with an increase in neonatal response to a broad range of antigens, however, the order in which the neonate develops the ability to respond to a particular antigen is species specific and remains to be defined for elephants (Tizard, 2000). Maternal antibodies, transferred across the placenta and/or through colostrum and milk, provide the calf with humoral immune protection while the calf's immune system further develops resulting in antibody

production. There is a significant inverse correlation between the level of immunoglobulin absorption in a calf and neonatal mortality.

Transfer of immunity from dam to calf varies among species and placental structure. There are three main types of placentation (Tizard, 2000). Hemochorial placentas, such as those found in human and non-human primates, allow for placental transfer of IgG. Epitheliochorial placentas, such as those found in ruminants, horses, and dolphins, do not allow for placental transfer of IgG due to the increased number of maternal and fetal tissue layers retained (Mossman, 1987). Endotheliochorial placentas, such as those found in cats, dogs, seals, and manatees, do allow for some transfer for IgG across the placenta, though specific IgG levels vary among species (Tizard, 2000). Elephants have an endotheliochorial placenta, with the maternal blood vessels ensheathed by cellular trophoblasts (Allen et al., 2003; Allen, 2006). The basement membrane of the maternal endothelial cells is thickened, but trophoblast cells extend narrow processes through the membrane. The fetal side is comprised of deeply indented fetal capillaries, reducing the diffusion distance between maternal and fetal blood. However, elephants have thus far been considered to experience failure of passive transfer of immunoglobulins across the placenta though it had never been confirmed (Emanuelson and Kinzley, 2002; Emanuelson, 2006; Weber and Miller, 2012).

This study hypothesized that, based on the placental morphology of elephants, IgG is passively transferred from dam to calf across the placenta. Transfer of immunoglobulin from dam to calf can occur passively, across the placenta, and/or actively, through ingestion of colostrum of milk. A failure of passive transfer (FPT) of

immunoglobulins is generally defined as a failure to achieve a given level of serum immunoglobulins. Whether a calf acquires these immunoglobulins via transplacental transfer or via ingestion, maternal antibodies are essential for providing immune protection in neonates. After birth, it is typical for maternal antibodies to be catabolized and consequently for calf serum IgG levels to decline. During this period, where a large percentage of maternal antibodies have been catabolized and the calf immune system is beginning to produce antibodies, a calf can experience a period of increased susceptibility due to a lack of adequate immune protection. In horses, this occurs approximately 8 weeks after birth, with the calf only beginning to produce antibodies around 5 weeks old (Tizard, 2000).

Total IgG serum levels are approximately 10-15 mg/mL in horses, 17 - 20 mg/mL in sheep, and 17 - 27 mg/mL in cattle (Tizard, 2000). FPT is diagnosed when serum measures < 8 mg/mL in calves and lambs and < 2mg/mL in foals with preferred serum levels of 16 and 8 mg/mL respectively. Partial failure of passive transfer is diagnosed if serum values fall within these parameters. However, approximately 75% of foals with total IgG levels between 2 - 4 mg/mL, remain healthy with no treatment (Tizard, 2000).

Using archived samples collected opportunistically from dams and both pre- and post-suckling calves, this study confirmed placental transfer of immunoglobulins in the Asian elephant. With a population mean of 14.85 mg/mL total IgG, all pre-suckling serum samples measured well above the mean at levels > 23 mg/mL (N=5) (Table 4-1 and Appendix E). While the Octet QKe system has not yet been optimized for elephant samples, BLI assays were able to confirm the presence of IgG in pre-suckling samples (all pre-suckle samples > 22 mg/mL) using the previously optimized quantitative IgG

assay conditions for the historically related manatee (Appendix E). Both cord serum samples analyzed also measured greater than the population mean with a cord blood mean being 22.65 mg/mL. All dam serum IgG samples measured within the population reference range, though they varied between individuals and seemingly among pregnancies (Appendix E).

Further evidence of transplacental transfer of immunoglobulins in elephants comes from the analysis of one focal tuberculosis (TB) positive dam and her calf. Throughout gestation, this dam remained culture negative for TB, though seroconversion had been confirmed in 2002 and continued throughout the gestational period of the dam's first calf, which, while not included in this study, tested positive for TB antibodies at birth. This dam's second calf, born in 2006, also tested positive for TB antibodies in pre-suckling serum samples, though at levels much higher than those of the dam. The dam eventually became culture positive in 2007 and treatment was started. Though treatment has now ended, this dam remains MAPIA positive and STAT-PAK reactive for TB (Appendix E). Due to the high TB titers at birth, this second calf was monitored closely and in 2010 was MAPIA positive and STAT-PAK negative. This calf was never culture positive and therefore, was never treated for TB infection. As of 2011, the calf was MAPIA negative and STAT-PAK unreactive. These data implies that the TB antibodies measured in the calf were maternally derived since they appeared in pre-suckle serum samples and the calf never exhibited clinical signs of TB infection. This naturally acquired passive immunity in the calf appears to have lasted nearly 5 years without the need for vaccination and/or booster.

Failure of passive transfer is also influenced by the quality and quantity of immunoglobulins produced, failure of timely colostrum ingestion, and/or inadequate absorption in the intestinal epithelium. Placental complications or deformities could also influence the passive transfer of immunoglobulins from dam to calf before birth. While high levels of transplacentally transferred IgG were measured in elephant calf serum in this study, these data do not suggest that colostrum and/or milk are not important in neonatal protection and development. Transplacentally transferred IgG does not induce local protection. Secretory antibodies incapable of crossing the placenta, are present at high concentrations in mammalian secretions such as milk and are important for protection of mucosal surfaces such as the gastrointestinal tract of neonates.

Currently, due to the presumed FPT across the placenta, much of the neonatal elephant care is modeled after the methods of care for foals. If a hand-reared elephant calf does not receive colostrum, plasma is administered to provide essential immunoglobulins; orally within the first 12 – 24 hours post partum, intravenously thereafter. However, until this study, quantitative data for immunoglobulins in elephant serum/plasma were unknown. Veterinarians and managers used crude estimations of the exact volume of plasma to be administered in order to provide adequate calf immune protection. The quantitative ELISA and BLI assay developed in this study can both be used to measure the total IgG levels in elephant calf serum as well as more accurately administer plasma IgG should it still be deemed necessary. These study data suggest that under 'normal' reproductive conditions, elephant calves receive adequate transfer of IgG before birth and that colostrum/milk ingestion may be more

important for providing local immune protection than for priming systemic immunoglobulins.

The data presented in this study serves as a foundation for future immunological studies in elephants, particularly as they relate to reproductive immunology and immune development. This study used archived and opportunistically collected samples for analysis. Ideal future studies will include serial serum samples from a dam throughout gestation and lactation, serial milk and colostrum samples, and serial serum samples from a calf throughout nursing and weaning. These samples would allow us to investigate a variety of research questions related to elephant immunology and development that would provide critical data for neonatal care and management, particularly in the event that a calf is orphaned or rejected. These data would also prove valuable in assessing disease susceptibility in calves, further aiding in resources available for successful neonatal care and hand rearing in this species.

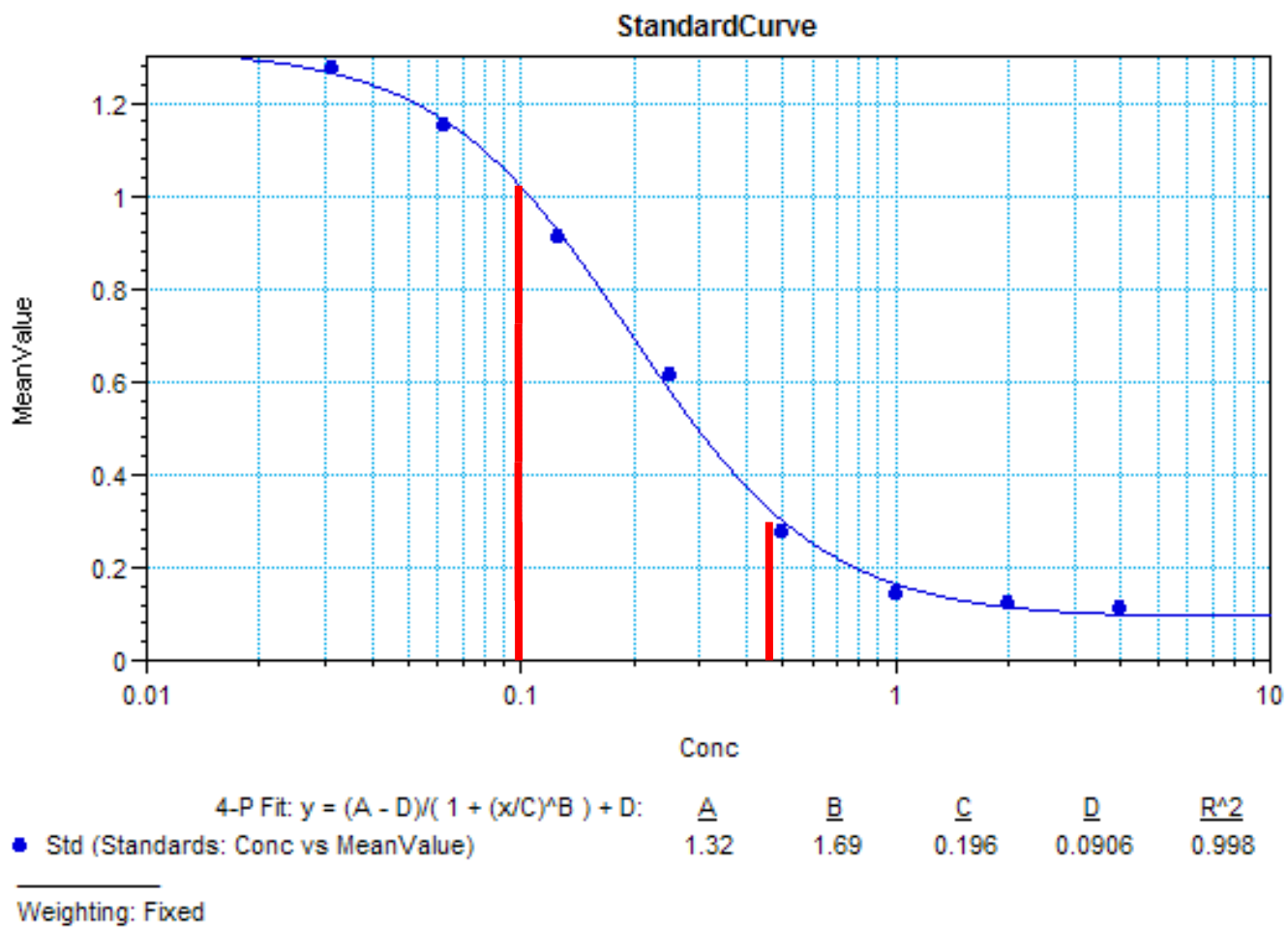


Figure 4-1. Standard curve of the competitive ELISA for quantification of elephant IgG in serum, 4 µg/mL – 0.03 µg/mL. Mean value accurate detection range on the linear segment of the standard curve = mean values between 1.000 and 0.390.

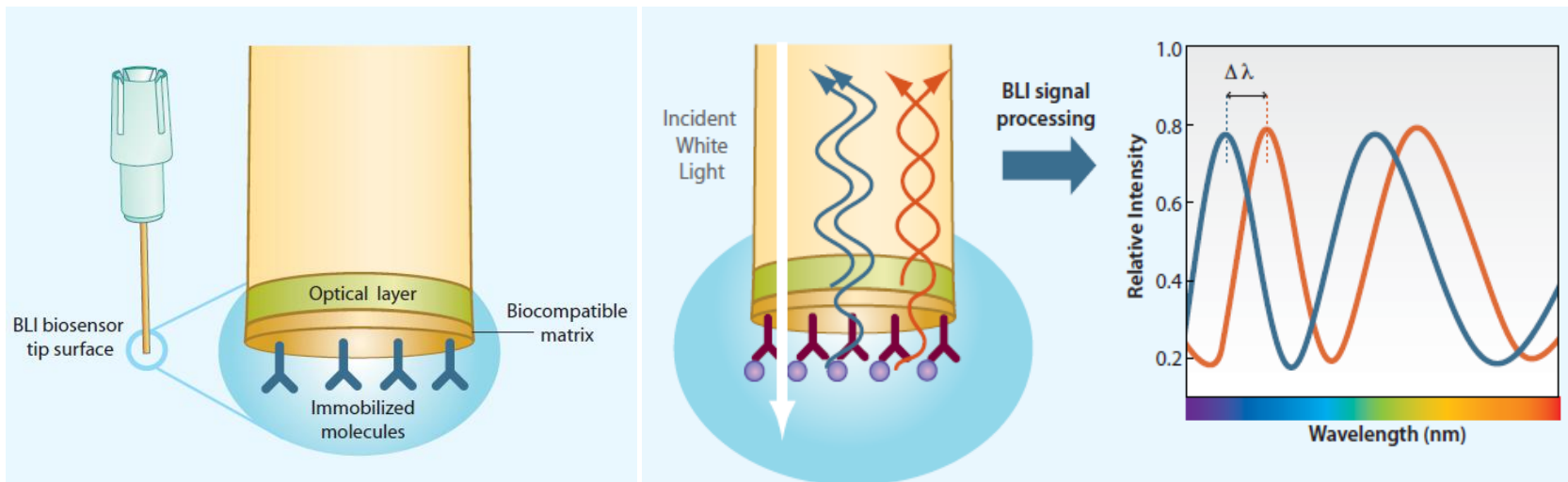


Figure 4-2. Biosensor tip with immobilized protein and the change in bilayer thickness and resulting wavelength shift. (Images used with permission from ForteBio, Inc.)

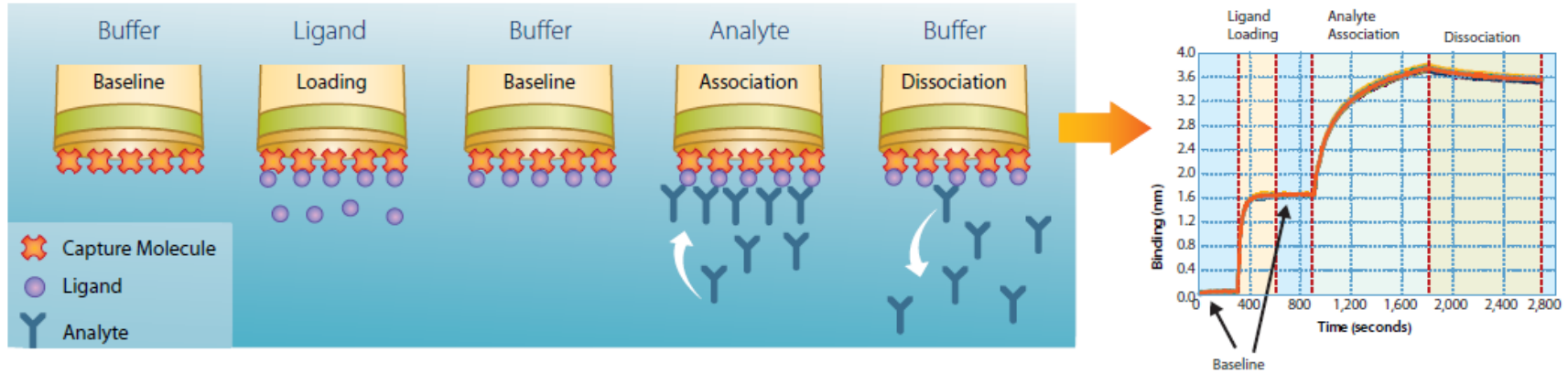


Figure 4-3. Basic Kinetics Assay Steps. Quantitative IgG Assay_Step 1-Baseline1, Step 2-Load, Step 3-Baseline1, Step 4-Regeneration, Step 5-Baseline2, Step 6-Regeneration, Step 7-Baseline2, Step 8-Regeneration, Step 9-Baseline1, Step 10-Association, Step 11-Baseline1. (Image used with permission from ForteBio, Inc.)

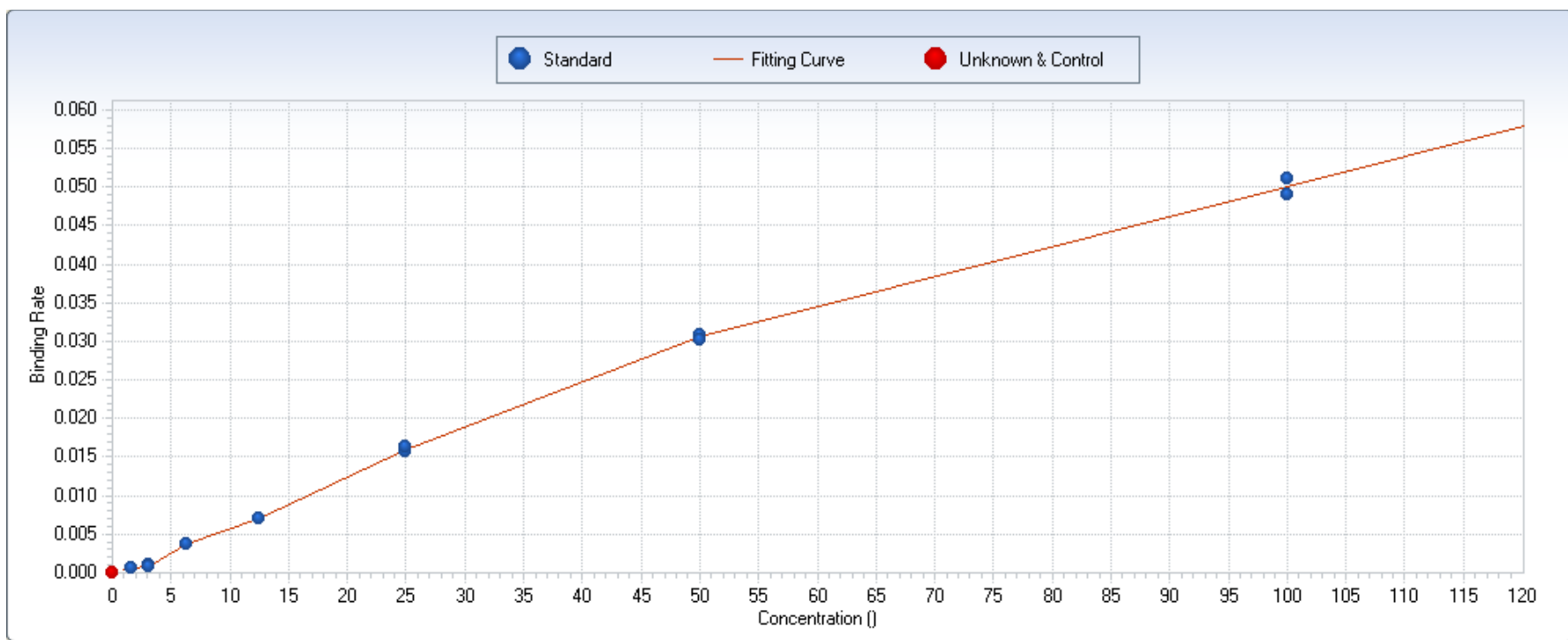


Figure 4-4. Duplicate standard curve for the Octet QKe quantitative elephant biolayer interferometry assay, 100 $\mu\text{g}/\text{mL}$ to 0.156 $\mu\text{g}/\text{mL}$. $R^2 = 0.9993$. $X^2 = 0.0085$.

Plate01														
	1	2	3	4	5	6	7	8	9	10	11	12		
A	0.121	0.109	0.261	0.265	0.364	0.218	0.229	0.217	0.164	0.186	0.187		Endpoint	
B	0.116	0.112	0.578	0.522	0.578	0.527	0.511	0.492	0.361	0.384	0.377		Lm1 405	
C	0.133	0.134	0.195	0.193	0.186	0.213	0.224	0.221	0.193	0.197	0.202		Automix: Off Calibrate: On	
D	0.257	0.226	0.523	0.479	0.458	0.445	0.521	0.525	0.496	0.458	0.498		Pasted Data	
E	0.470	0.466	0.169	0.165	0.152	0.155	0.166	0.156	0.230	0.233	0.234			
F	0.650	0.743	0.257	0.282	0.371	0.338	0.270	0.300	0.453	0.487	0.542			
G	0.988	1.001	1.272	1.262	1.194	1.170	1.239	1.054	1.179	1.174	1.291			
H	1.261	1.106	1.125	1.222	1.238	1.140	1.246	1.244	1.208	1.272	1.353			

Wavelength Combination: !Lm1
Mean Temperature: 21.4
Data Type: Absorbance
Data pasted (5:27 PM 3/8/2012)

Figure 4-5. OD results (405nm) for quantitative elephant IgG cELISA. Samples with hash marks represent 'masked' samples.

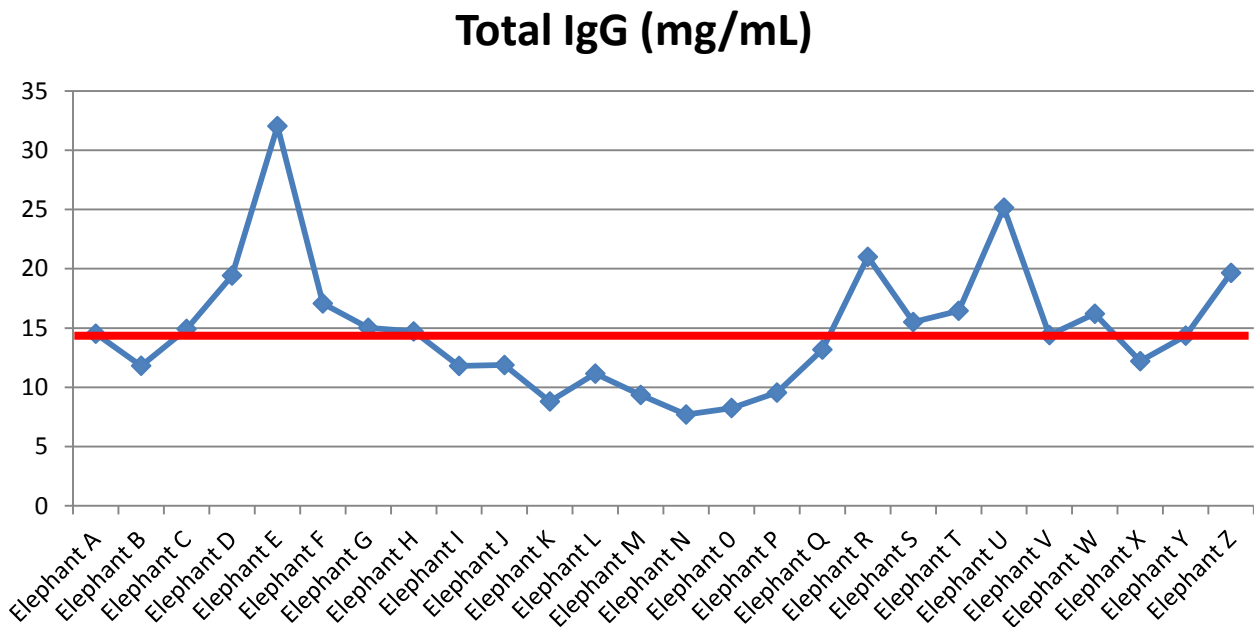


Figure 4-6. Total IgG values for captive manage population of Asian elephants (N=26). Mean serum IgG = 14.85 mg/mL (SD = 5.31).

Total IgG Accurate Detection Range

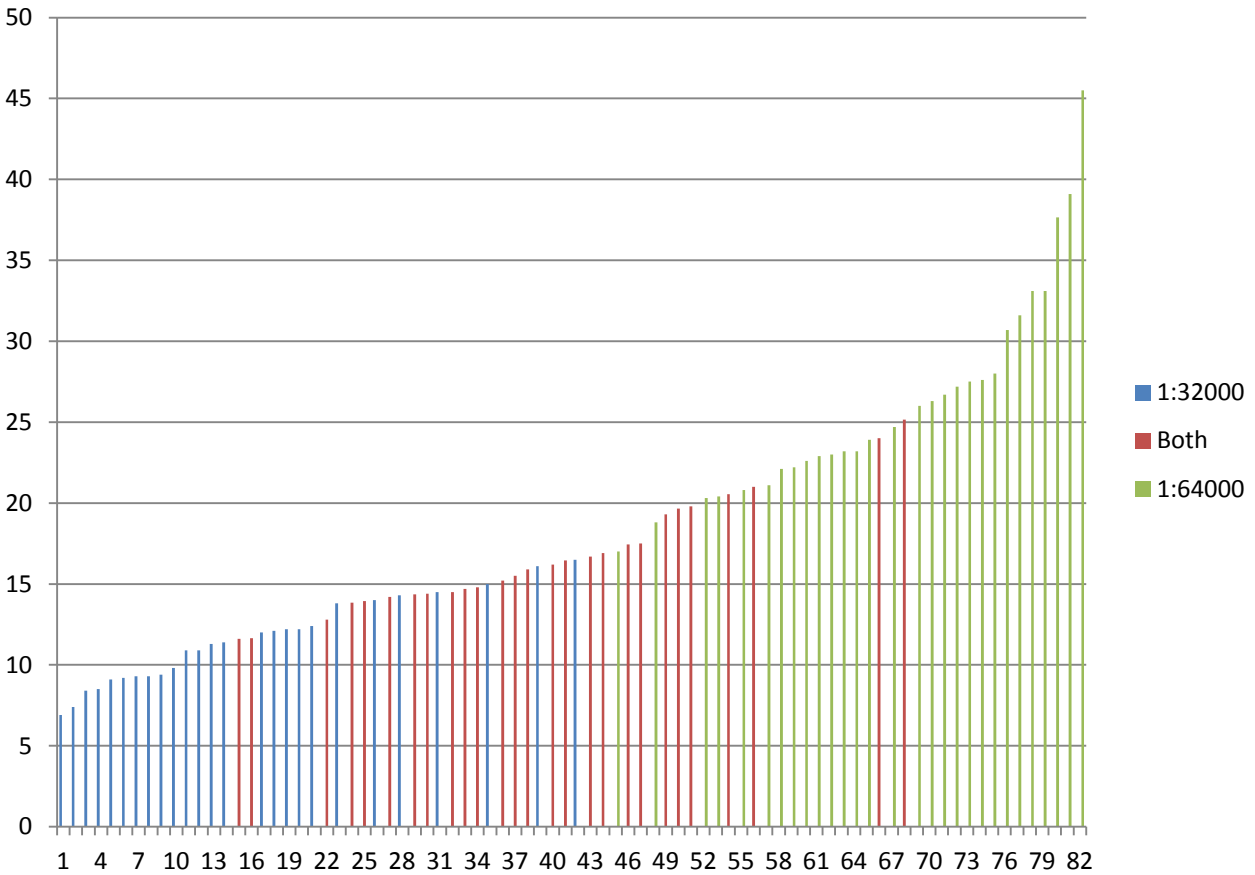


Figure 4-7. Distribution of total IgG values for 82 serum samples (N=26). The reference range for accurate detection using the 1:32000 serum dilution was 7.16 mg/mL to 15.68 mg/mL (blue bars) and for the 1:64000 serum dilution, 15.94 mg/mL to 36.9 mg/mL (green bars). Samples ranging from 11.1 mg/mL to 22.09 mg/mL were within the accurate detection range at both serum dilutions (red bars). Y axis = total IgG (mg/ml). X axis = Sample number.

Rabies Titers Pre- and Post-Vaccination

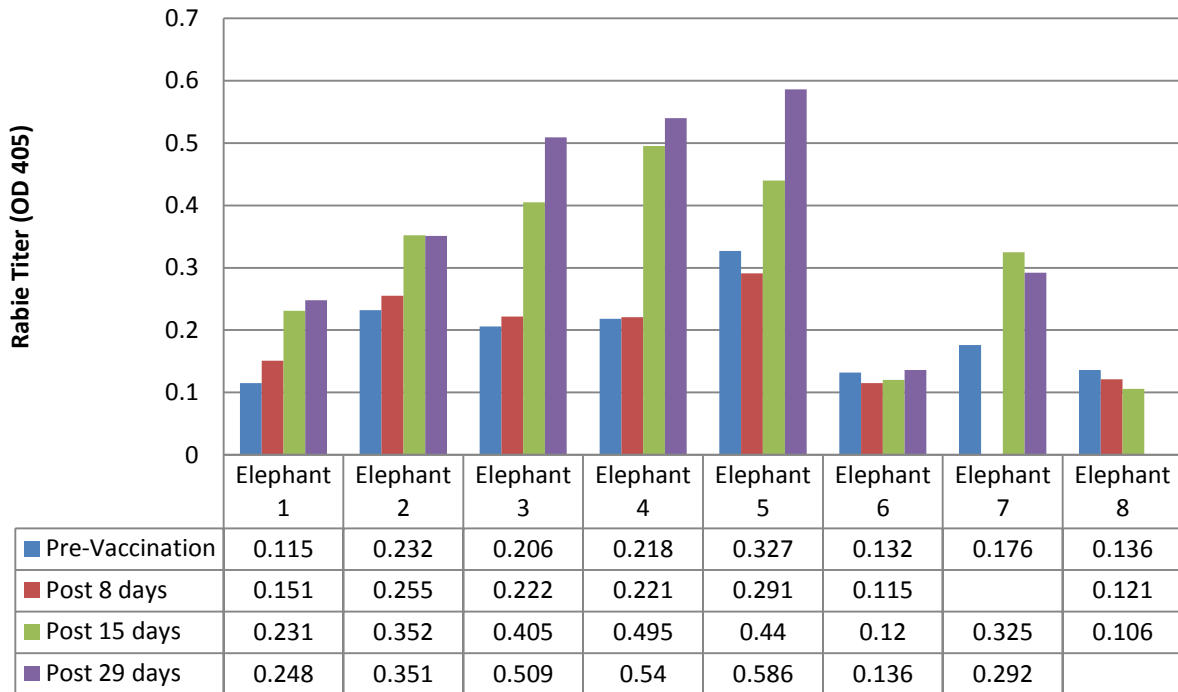


Figure 4-8. Rabies titers for 8 Asian elephants. Blue = pre-vaccination, red = 8 days post-vaccination, green = 15 days post-vaccination, purple = 29 days post-vaccination. For elephant 6 and 8, this was their first vaccination.

Tetanus Titers Pre- and Post-Vaccination

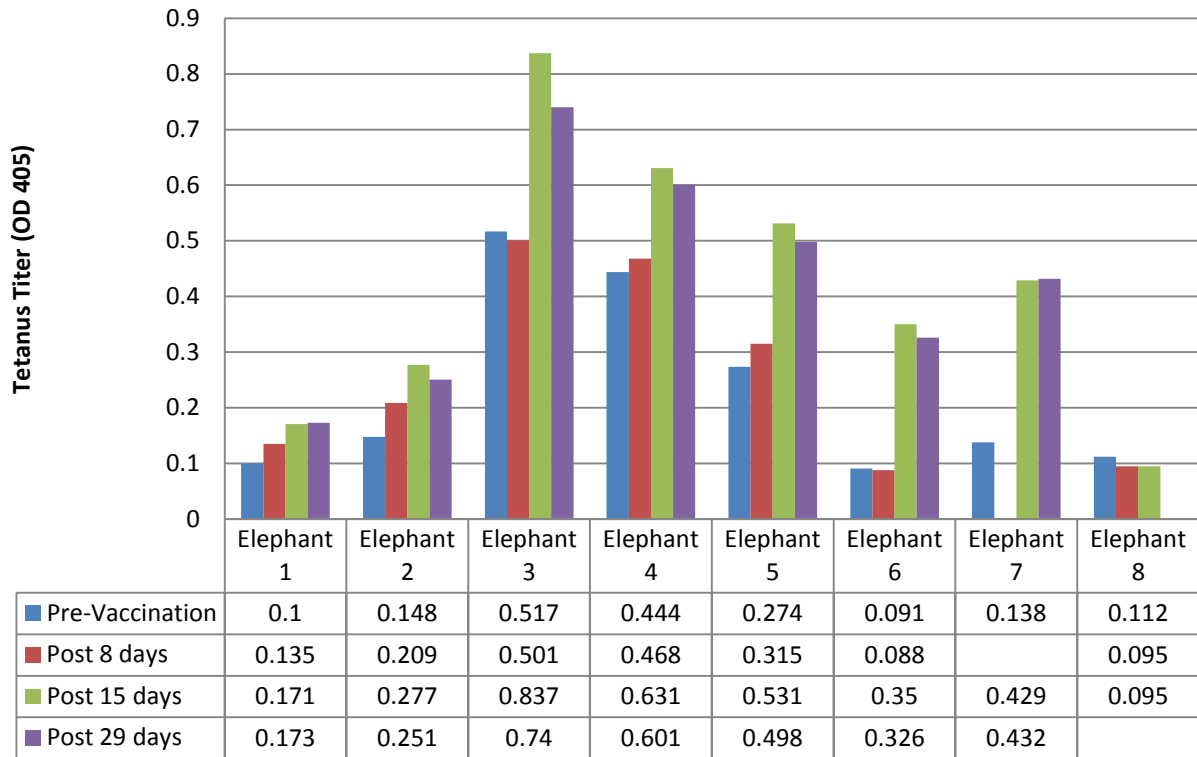


Figure 4-9. Tetanus titers for 8 Asian elephants. Blue = pre-vaccination, red = 8 days post-vaccination, green = 15 days post-vaccination, purple = 29 days post-vaccination.

Total Serum IgG Pre- and Post-Vaccination (Rabies and Tetanus)

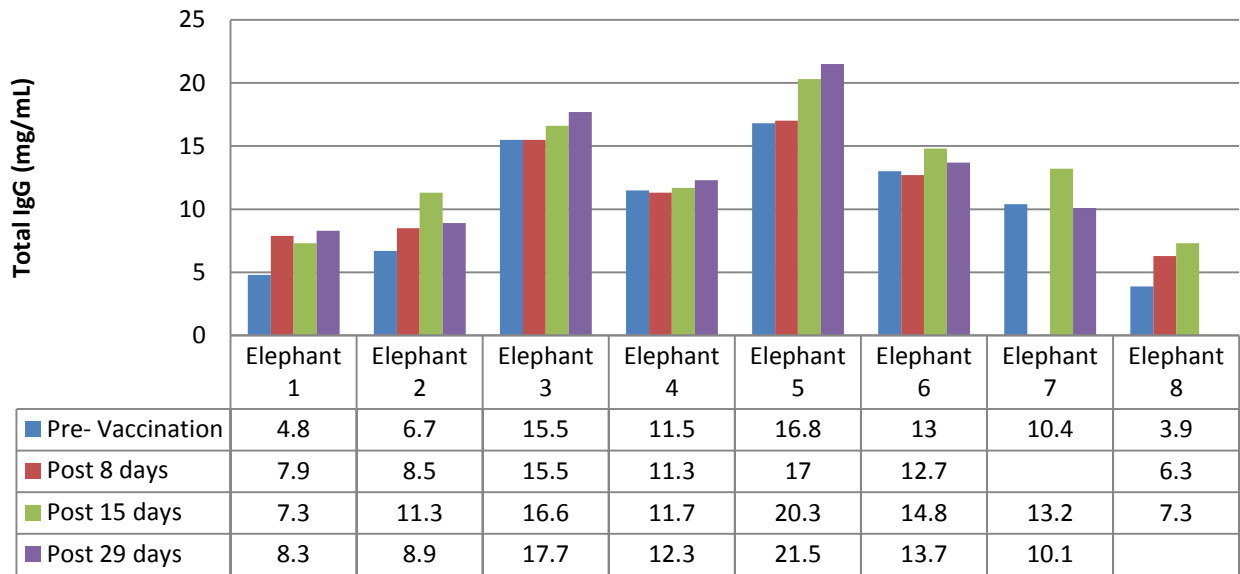


Figure 4-10. Total serum IgG levels for 8 Asian elephants vaccinated concurrently against rabies and tetanus. Blue = pre-vaccination, red = 8 days post-vaccination, green = 15 days post-vaccination, purple = 29 days post-vaccination.

Total Serum IgG Pre- and Post-Tetanus Vaccination

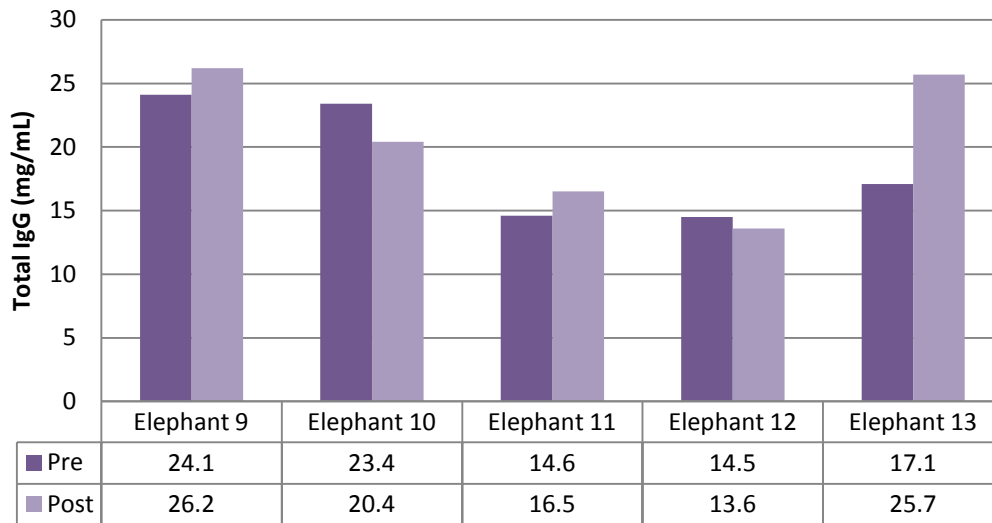


Figure 4-11. Total serum IgG levels for 5 Asian elephants vaccinated against tetanus only.

Table 4-1. A comparison of total serum IgG (mg/mL) values for pre-suckling Asian elephant calves and IgG range for a captive Asian elephant population using two quantitative assay formats.

	Calf 1-2	Calf 1-3	Calf 3-1	Calf 5	Calf 7-2	Population Range
cELISA	27.95	33.40	22.55	33.60	22.00	7.7 - 32.14
Octet QKe	27.10	22.10	21.70	26.90	23.30	13.14 - 32.03

CHAPTER 5 CONCLUSIONS AND FUTURE DIRECTIONS

There are few studies that been conducted regarding the immune system of the manatee and elephants resulting in insufficient immunological data available for research diagnostics, and health monitoring in these species (Bossart et al., 1998, 2002; Guo, et al., 2011; Kelly et al., 1998; Lowenstine, 2006; Sweat et al., 2005; Walsh et al., 2004). Incorporation of these data would allow for more accurate assessments of health as well as mitigation of immune effectors. By incorporating cross-reactive antibody identification, various cellular and morphological histochemical techniques, and the development of quantitative assays for measuring immunoglobulins, this study was able to provide baseline immunological data for the West Indian manatee and Asian elephant, thereby furthering the tools available future immune related studies in these species.

This study focused on various aspects of the humoral immune response and mucosa associated lymphoid tissues in paenungulata. Previous studies by University of Florida researchers had resulted in the development of several species specific monoclonal antibodies that were used in this study (mouse anti-manatee IgG mAb and mouse anti-elephant IgG mAb) (manuscripts in preparation). In this study, we aimed to add to the available reagents, via IgA and/or S-IgA identification, purification, and monoclonal antibody development, particularly to aid in further investigations of the mucosal immune system. Immunoglobulin A (IgA) is found in two main forms, the monomeric form found in serum and the dimeric secretory form (S-IgA) found on mucosal surfaces. S-IgA contains two monomeric IgA molecules bound by a J-Chain and wrapped in a cleaved polymeric immunoglobulin receptor (pIgR) called the

secretory component (SC). Circulating IgA levels are generally quite low, with high levels indicative of a disease state (Ogra et al., 1999). Contrary to IgA, S-IgA is found exclusively in mucosal secretions covering mucosal surfaces such as the gastrointestinal, reproductive, and respiratory tracts, unless disease alters this balance. S-IgA coats mucosal surfaces and prevents binding of pathogens. Cleveland et al. (1991) presented a new form of secretory component found in amniotic fluid of humans suggesting that this may be an early expression of the mucosal immune system in a developing fetus. Generally at birth, in mammals that exhibit passive transfer of antibodies (such as humans), IgG is the sole immunoglobulin present as it is the only one that can cross the placenta (Murphy et al., 2006). Buening et al. (1978) measured the levels of SC, IgA, and IgG in both healthy and combined immunodeficient foals and found that all were positive for the presence of SC at birth, which would support the findings of Cleveland et al. (1991). The presence of SC at birth has been documented in several other species with subsequent presence of S-IgA becoming evident approximately two weeks after birth (Araujo and Giugliano, 2001). Even in the case of IgG passive transfer in humans, breast-feeding has been shown to protect infants from intestinal infections. Similarly, van Elk et al. (2007) reported on a 3-day-old dolphin that lacked maternally acquired immunity and died as a result of *Escherichia coli* septicemia. Free SC and lactoferrin were found to inhibit adhesion of enteropathogenic *Escherichia coli* (Araujo and Giugliano, 2001). In addition to passive transfer, S-IgA levels in saliva have been found to correlate to the presence of HPV infection (Gonçalves et al., 2006). Women positive for either oral or genital HPV were found to have lower levels of S-IgA

possibly suggesting a predisposition to contracting the disease due to lack of sufficient mucosal protection.

To date, several attempts have been made by UF researchers, both past and present, to identify and purify IgA and/or S-IgA in the manatee and elephant including those discussed below conducted in this study (unpublished data). No prior published studies have been conducted on manatee immunoglobulin; however the two studies that have investigated elephant immunoglobulin found no evidence of IgA (Guo et al., 2011; Kelley et al., 1998). A previous UF study employed a Jacalin agarose IgA purification method, investigating IgA in manatee serum (unpublished data). This method is commonly used for other mammalian species, but proved unsuitable for manatee IgA (Kahamaru et al., 1982; O'Daly and Cebra, 1990; Parr et al., 1995; Shearer et al., 1997). Since IgA is found in low concentrations in serum, we hypothesized that using milk for identification and purification might prove to be more successful.

The first of our studies aimed to identify and purify secretory immunoglobulin A (S-IgA) from the milk of the Florida manatee and Asian elephant using adaptations from methods previously described for other species (German et al., 1998; Hemsley et al., 2000; Sen et al., 1976; Burns et al., 1982). These methods include screening of commercially available antibodies by ELISA and Western blot, affinity column chromatography to isolate the target protein, Western Blot to screen eluted sample, and liquid chromatography tandem mass spectrometry (LC-M/S M/S) to identify the protein of interest.

Archived milk samples from the Florida manatee and the Asian elephant were used for this study. Milk samples from the manatees were pooled and centrifuged at 10,000 x g (30 min, room temperature). The centrifuged milk separated into 3 layers: a pelleted fraction of aggregated proteins; a clarified fraction containing soluble proteins; and an upper lipid layer. Both the aggregated protein layer and lipid layer were refrozen should they be needed for later analysis. The clarified fraction was removed and stored at -20°C until required for further purification. Whey was prepared from the clarified fraction by isoelectric precipitation of the caseins at pH 4.6 and centrifugation at 10,000 x g (30 min, 4°C). The whey fraction was dialyzed against 0.02 M phosphate-buffered saline pH 7.2 (PBS) and concentrated by 60% saturated ammonium sulphate precipitation. Following centrifugation (10,000 x g, 30 min, 4°C) the pellet, if present, was resuspended in a small volume of PBS and dialyzed against this buffer. (Centrifugation methods from Doolin, et al., 2001)

The whey fractions were run on a 10% Novex Bis-Tris/MOPS NuPAGE gel and a 4 to 12 % Bis-Tris/MES NuPAGE gel and stained to evaluate band size and intensity. The samples were reduced and denatured. Sixteen bands were chosen for protein identification based on published molecular weights for target immunoglobulin proteins (Figures 5-1 and 5-2). The target bands were then subjected to liquid chromatography tandem mass spectrometry (LC-MS/MS) and compared to available protein sequence databases for protein identification. The aim of the gel LC-MS/MS was to identify S-IgA protein sequences. Should homologous sequences have been identified from other species and commercial antibodies against S-IgA from these other species have been available, these antibodies would have been tested for cross reactivity with manatee

and elephant S-IgA. If cross reactivity was confirmed, these antibodies would then have been used to prepare an affinity column for purification of S-IgA from manatee and elephant milk. Protein identification of the 16 selected bands revealed that albumin, serum albumin precursor, and keratins were the predominant proteins in the samples (Figures 5-3 and 5-4). Both manatee and elephant milk samples matched with partial sequences of 23 species. Immunoglobulin proteins were found in the majority of the targeted bands, however whole sequences and strong matches were limited presumably due to the low percentage of the target proteins in the samples. One possible explanation for the low quantity could be attributed to the later stage of lactation at which the milk was collected. For this study, stage of lactation was unknown for our archived manatee milk samples and elephant milk samples were collected at the latter stages of lactation (~1 year). Early milk and/or colostrum is preferred as S-IgA levels are higher at this time. The lack of strong matches in the database could also imply a unique sequence in manatee and elephant proteins that does not match current database sequences.

In a second study we also used the defatted and decaseinated milk samples and then passed them over a CaptureSelect[®] affinity column (GE Healthcare and BAC) which had proved useful in capturing dolphin IgA (unpublished data). The bound immunoglobulin was then eluted from the column. Both the proteins liberated from the matrix and a portion of the eluted sample were screened by SDS-PAGE to look for bands representing the target proteins. Again, no bands in the IgA molecular weight range were identified. While the manatee genome is not yet available, we conducted a preliminary BLAST search using nucleotide sequences for IgM, pIgR, SC, J-chain, IgA,

and S-IgA in a variety of mammalian species against the African elephant genome. This search revealed data supporting the presence of IgM, pIgR, SC, and J-chain within the African elephant genome, but no evidence of IgA or S-IgA. Preliminary investigation of other Afrotherian genomes also revealed no evidence of IgA. These data, combined with the limited literature available on elephant immunoglobulins leads us to suspect that Afrotheria, including manatees and elephants, lack IgA and S-IgA, though more studies must be conducted to confirm this hypothesis.

Selective IgA deficiency (SIgAD) has been observed in humans and while some people are asymptomatic, others experience recurrent infections centered on mucosal surfaces including respiratory tract infections, sinus infections, diarrhea, conjunctivitis, asthma, and allergies (Hammarström et al., 2000; Ogra et al., 1999). In the manatee, elephant, and potentially other Afrotherians, the current data do not support IgA deficiency, which occurs in 1:400 – 1:700 individuals of human descent, but rather an evolutionary adaptation or divergence. To confirm this hypothesis, future studies will focus on IgM and in particular, IgM in secretions and IgM secreting plasma cells in the GALT. We will also continue investigations of classical IgA associated proteins: the J-chain, secretory component (SC), and polymeric immunoglobulin receptor (pIgR) and their distribution within MALT tissues as discussed above. SC and J-chain are also associated with S-IgM. IgM has been observed to compensate functionally in individuals with selective IgA deficiency (Ogra et al., 1999). IgA and IgM will also be further investigated in serum and secretions. In humans with SIgAD, no significant difference is generally observed in serum IgM levels though IgA levels are low or absent (Ogra et al., 1999). At mucosal surfaces and in secretions however, IgM levels may be

elevated to compensate for lack of IgA and S-IgA. Currently, most diagnostic tests for SIgAD focus on identifying deficiencies such as a deficient antibody response to pneumococcal immunization (specific polysaccharide antibody deficiency [SPAD]) or measuring levels of IgG2 and IgG4 which have been observed at reduced or absent levels concomitant with SIgAD in some individuals (Hammarström et al., 2000).

Alternatively, individual examination and diagnosis can also include a review of family history, as SIgAD has been identified as a possible inherited autoimmune disease, and/or documented recurrent mucosal related infections (Ogra et al., 1999). None of these methods for diagnosis however, would apply to manatees and elephants, as our data suggest that their lack of IgA is not a deficiency but rather a consequence of evolution. Additionally, some methods such as measuring response to a particular vaccine are not feasible due to the endangered status of the species in this study.

In order to investigate these proteins in serum/secretions and/or immune tissues, species specific monoclonal antibodies are desirable due to their specificity. For commercially available antibodies however, the specificity of mAbs may prove to be a disadvantage when screening manatee tissues therefore pAbs should also be included. As we had discussed in Chapter 2, not all commercially available antibodies are capable of cross reacting with manatee and/or elephant tissues. While the potential exists for more conserved proteins such as secretory component to cross react and those from closely related species are preferred, species specific antibodies are most desirable. Monoclonal antibodies could be developed for IgM (in the elephant), SC, pIgR, and/or J-chain by several methods. The first method would employ the African elephant genome and soon to be completed Florida manatee genome. As previously

mentioned, a preliminary BLAST search of the African elephant genome revealed data to support the presence of IgM, pIgR, SC, and J-chain, but not IgA or S-IgA, a trend that was also observed in preliminary investigation of other Afrotherian genomes. Using this nucleotide sequence BLAST search using our target protein sequences identified in GenBank against the manatee and elephant genomes we can identify similar sequences. With these BLAST results, the conserved homologous regions would be used to make degenerate primers to be used in PCR. The PCR product of our amplified target protein DNA would then be inserted into an expression vector and cloned. The resulting antigen could be used for the production of monoclonal antibodies that may cross react in multiple species exhibiting these conserved regions rather than be species specific.

Additionally, the African elephant and Florida manatee genomes can also be used to investigate IgG subclass specificity of the existing IgG mAbs as well as potential other IgG subclasses suggested in previous studies (Kelly et al., 1998). In SIgAD humans, concomitant deficiency in IgG2 and IgG4 has been observed and while deficiency is not suspected in manatees and elephants, these species may lack comparable subtypes reflecting an adaptation/compensation to lack of IgA rather than a linked deficiency. Identification of the IgG subclass specificity for the anti-manatee and anti-elephant monoclonal antibodies used in this study would allow us to most accurately assess IgG in these species. IgG1 is the predominant subclass observed in mammalian species. The antibodies used in this study may be specific for a shared trait among subclasses that allows us to truly measure total IgG or it could be specific for a subclass which is much less represented in serum/plasma making the total IgG values

observed in this study underestimated. Based on the manatee and elephant IgG calculated reference ranges, we suspect that the mAbs used were specific for IgG1 or a shared trait as total IgG levels were comparable to those of other mammalian species, though this remains to be confirmed.

As previously discussed, a pAb for the detection of manatee IgM has already been developed (manuscript in preparation). Due to the large molecular size of IgM, size-exclusion chromatography could allow us to purify IgM in elephant serum, providing us with a purified antigen for monoclonal antibody development. Two additional methods could be employed to provide further evidence for lack of IgA, though both rely on existing antibodies that cross react with manatee and elephant. Assuming a commercially available cross reactive antibody for J-chain and/or secretory component can be identified, this could be coupled to an affinity column in which a secretion such as milk would be passed over thereby binding all immunoglobulins that possess these proteins (IgM and S-IgA). Ideally, colostrum or milk collected within the first 2 weeks post partum from clinically healthy animals would be most preferable as IgA levels would be at their highest if present (Ogra et al., 1999). Serum would not be effective for this method as serum IgA is monomeric containing no J-chain and secretory immunoglobulins (with SC) are not found in serum. The bound proteins would then be eluted from the column and the eluted material subjected to SDS-PAGE to verify purification and identify proteins by size. To separate IgM from any S-IgA in the samples, size-exclusion chromatography would be employed using the remaining eluted material. Once again, a gel would be run to verify purification. If purification of a single protein (IgM or S-IgA) is verified, the corresponding elution or flow through could then

be used as the purified antigen for monoclonal antibody development. If the purification is not achieved due to the presence of multiple proteins in the sample within that size range, a Coomassie-stained SDS-PAGE gel could again be run to identify the target proteins with the corresponding bands being excised for liquid chromatography tandem mass spectrometry (LC-MS/MS). LC-MS/MS would allow us to identify peptide sequences that could then be used for peptide synthesis. A synthetic peptide for the target protein could then be used as a recombinant antigen for monoclonal antibody development. Identification of peptides however, is limited to the degree of homology between the target protein sequence and those of other species in the existing databases. The purity of the initial sample is also essential to identify the protein of interest which is why the use of crude milk, or other secretion, is not ideal. Future studies would then include quantitative analysis of IgM in serum as well as tear, milk, and fecal secretions via the cELISA or BLI assays discussed in previous chapters to further define the role of IgM in IgA lacking species.

IgM B cells are found within the GALT, expressing activation induced cytidine deaminase (AID) and α -germline transcripts prior to undergoing isotype switch recombination and somatic hypermutation into IgA secreting plasma cells. Preferential switching of B cells from IgM to IgA has been shown to be induced by secretion of IL-6 and high levels of retinal dehydrogenase expression by dendritic cells in the Peyer's patch (Golby and Spencer, 2002; Fagarasan, 2008). Retinal dehydrogenases are required for the generation of retinoic acid (RA) which is responsible for upregulation with the T and B cell gut homing molecules $\alpha 4\beta 7$ integrin and CCR9. Immunoglobulin A expresses high levels of CCR9 and CCR10, receptors for chemokines TECK/CCL25 on

the epithelium of the small intestine and MEC/CCL28 on the epithelium of the large intestine, which explains the preferential homing of IgA plasmablasts, but not IgM, to the lamina propria (Nilssen et al., 1992). If elephants and manatees lack IgA, IgM could have adapted to express these chemokine receptors for homing to gastrointestinal inductive sites. If this is an evolutionary adaptation however, IgM may have evolved to express similar, though distinct chemokine receptors from those used by IgA. Co-staining of GALT or other MALT tissues from clinically healthy adult animals with a species specific IgM monoclonal antibody (which already exists for the manatee) and antibodies for gut or mucosal homing molecules could also allow us to identify which antibody type is preferentially homing to mucosal tissues. In a species lacking IgA, this should be IgM. Additionally, co-localization of secretory component, pIgR, and/or J-chain with IgM in tissues will also provide us with further data to support the compensatory role of IgM in the tissues of IgA lacking species. With these data, we could pursue further immunological studies to characterize (cellularly and morphologically) 'normal' mucosal immune tissues in healthy adult individuals that would then serve as a reference for investigating the effects of age/development, disease, reproductive state, anthropogenic and naturally occurring stressors, and so on; thereby adding to the tools available for conservation and management of these species.

Our collaboration with the University of California, Davis-School of Veterinary Medicine for the flow cytometry and a portion of the immunohistochemistry conducted in this study revealed several additional antibodies that cross react with manatee immune tissues. The antibodies for an uncharacterized pan-leukocyte marker (equine), gamma-

delta T cells (bovine) and the MHC class II antigen (bovine) exhibited cross reactivity via flow cytometry. These antibodies have reported to bind only native proteins and therefore would likely not bind in formalin-fixed manatee tissue sections. We therefore will collect lymph nodes, spleen, and thymus samples from a fresh dead adult manatee from the Florida Fish and Wildlife Conservation Commission's Marine Mammal Pathobiology Laboratory to snap freeze thereby allowing us to preserve these native proteins. With these samples, we will immunohistochemically characterize the cross reactive antibodies identified. Application of the above-mentioned antibodies will allow us to expand on the phenotypic identification of leukocyte subpopulations in manatees.

Thus far, all identified cross reactive antibodies have shown patterns of binding consistent with those found in variety of other species which include several marine mammals (Cesta, 2006; Ogra et al., 1999). Development of manatee specific antibodies as discussed above would be most useful for future studies. As previously mentioned, these studies will focus on IgM and its role in mucosal associated lymphoid tissues. Immunohistochemically, for this study, GALT samples focused on tissue sections around the lymphoid nodules of the Peyer's patches and isolated lymphoid follicles. Future studies will be expanded to include the lamina propria allowing us to further investigate GALT effector sites. Furthermore, the potential lymphoglandular complexes and cryptopatches identified in this study will be further investigated. These immune tissues were observed in several H&E and/or PAS stained samples. Additional samples of paraffin embedded GALT from fresh dead adult manatees will be serially sectioned for immunohistochemical investigation. Cryptopatches are characterized immunohistochemically via the presence of T cell clusters whereas lymphoglandular

complexes are distinguished from Peyer's patches predominantly by their location in the colon and reduced size, number of follicles, and smaller germinal centers.

In manatee CALT, morphological changes were observed and appeared to be reflective of cause of death. This study could be expanded not only to include a greater number of samples for more accurate analysis, but to also investigate the potential correlation with CALT and water quality/composition. For example, investigating the effects of various water systems for captive managed manatees; closed water system systems that use chlorine vs. ozone. The effects of salinity could also be investigated; i.e. the St. Johns River population of manatees who are predominantly in fresh water vs. Indian River Lagoon manatees who inhabit salt and brackish water systems. Additionally, we would like to investigate the differences between manatee species and sub-species and potential correlations with habitat and water quality.

The CALT in the manatee appears to have been somewhat concomitantly reinvented with the nasolacrimal system (Samuelson et al., manuscript in preparation). The CALT of the Florida manatee appears to be the most developed of any mammal studied to date, having a lymphoid layer that is especially prominent along the superficial conjunctiva of the upper eyelid and both the bulbar and palpebral conjunctiva of the nictitating membrane. Immunohistochemistry revealed what appears to be overlapping inductive and effector sites not classically observed in mucosal immune tissue. Investigation of elephant and hyrax CALT could confirm this hypothesis. This could also be a specialized adaptation to an aquatic environment and/or the sphincter like eye closure that results in a more even distribution of foreign matter vs. accumulation as seen in terrestrial species. Therefore, we plan to investigate the CALT

in a variety of other marine mammals. While both morphologically and cellularly, these CALT follicles are comparable to the Peyer's patches of the gastrointestinal tract, areas of lymphatic aggregates, similar to cryptopatches in the gastrointestinal tract, were observed though further investigation is needed.

In this study, we also investigated immunoglobulin G (IgG) in tear film and blood of two paenungulata species. Using a newly developed quantitative cELISA for measuring IgG in the Asian elephant and a newly developed biolayer interferometry assay for measuring IgG in the West Indian manatee, we were able to define baseline circulating IgG reference ranges as well as investigate passive transfer of immunoglobulins in these species. The Octet system provided better accuracy and reproducibility and allowed for a more rapid analysis of IgG when compared to the ELISA format. For circulating IgG in the manatee, assay optimization resulted in a calculated inter-plate and intra-plate variability of 8.3% and 2.3% respectively. For the elephant cELISA, the inter- and intra-plate variability was 8.53% and 11.8% respectively. Reusing the sensors offers additional benefits such as reduced operational cost and increased throughput. While the biolayer interferometry assay was not optimized for elephants in this study, we would like to employ this method for future studies due to the increased accuracy, reduced cost, and increased throughput.

The mean total IgG for the captive managed population of Asian elephants in this study was 14.85 mg/mL (SD=5.31) with a calculated reference range of 6.12 mg/mL to 23.58 mg/mL. For West Indian manatees, the mean total circulating IgG was 9.86 mg/mL with standard deviation of 4.3 mg/mL. The reference range for mean total circulating IgG in the West Indian manatee was 2.81 mg/mL to 16.2 mg/mL. These

values were comparable to those observed in most other mammalian species (Table 5-1). However, only one captive managed population of Asian elephants was included in this study (N=26). The observed baseline IgG levels of a single captive managed population are likely a conservative estimate. For future studies, we would like to include numerous elephant populations, both captive managed and wild to most accurately define baseline circulating IgG.

In the bottlenose dolphin, white blood cell counts (WBC) and eosinophils counts were the best predictors of total IgG levels and it was hypothesized that these data were reflective of parasite load (Ruiz et al., 2009). In the current study, a fitted linear regression model was used to examine the relationship between multiple hematological parameters and total circulating IgG in the manatee. No significant correlation was found between any of the values examined though WBC in the Antillean manatee and total globulin in the Florida manatee did exhibit a weak correlation. Further statistical analysis of these parameters is needed to further explore potential relationships. Additionally, the majority of animals included in this study were deemed to have 'excellent' and 'good' body condition during health assessments and blood values were generally within the normal range for health manatees (Harvey et al., 2007). To further investigate potential predictors of total IgG levels, I propose using samples from manatees in rehabilitation or clinically 'unhealthy' adult animals. The variations in hematological and total IgG values observed in this study were from a single time point and could reflect natural fluctuations within the individual. Inclusion of manatees in rehabilitation would allow for serial sampling and would also allow for investigation of trends as there may be a delay in response between fluctuations in certain

hematological parameters versus total IgG levels. Serial samples from the same individual would also allow us to investigate individual humoral immune response to injury, disease, and/or treatment. Hematological parameters were not investigated in the elephant and could elucidate potential predictors of total circulating IgG. Calves would not be included for this analysis as immune development is largely unknown.

Future studies in the West Indian manatee and Asian elephant would also focus on immune development and reproductive immunology. The result from 2 fetal manatee serum samples in this study suggest passive transfer of immunoglobulins across the placenta. We plan to use serum samples from pre-suckling manatee calves as well as colostrum/milk samples to further define passive transfer. Due to the shared placental morphology and other similarities that group the manatee and elephant in paenungulata, we feel confident that the fetal serum samples used in this study, do in fact indicate passive transfer of immunoglobulins as we demonstrated in the Asian elephant.

Compared to other captive megavertebrates, the survival rate for elephant calves, particularly Asian elephants, is very low. At times, human intervention is required and hand-rearing is considered a difficult task. The Species Survival Plan (SSP) stated that it “strongly recommends that calves *not* be hand-reared, but rather encourages managers to reintroduce the calves to the dams if at all possible”. When caring for elephant calves, much is modeled after the methods of care for foals in which failure of passive transfer of immunoglobulins has been confirmed. Currently, if a hand-reared elephant calf does not receive colostrum, plasma is administered to provide essential immunoglobulins. This study confirms passive transfer of immunoglobulins

and provides a method to measure IgG levels. Because failure of passive transfer can still occur due to premature birth, malformations of the placenta, or other reproductive complications, therapeutic administration of IgG may still be required. The data in this study suggest variability among individual IgG levels. By quantitatively measuring total IgG levels in the elephant from which the plasma will be collected for administration to the calf, veterinarians and managers can more accurately determine the amount of IgG administered. Further studies are still needed however, to determine what levels need to be administered as well as the mechanisms of immunoglobulin uptake in the calf to determine the most effective strategies for neonatal care and management. Mammalian neonates are highly vulnerable to infectious disease at birth largely due to their less active and less developed immune systems. Knowing the extent and mechanisms on immune development in these species will allow for identification of critical periods such as when maternal antibodies in the calf have been almost entirely catabolized and the calf's production of immunoglobulins is not yet fully functional.

This study provides the first report of passive transfer of immunoglobulins in the elephant and manatee. The effects of maternal antibodies in the development of the neonatal immune system have yet to be investigated. In elephants, of particular concern is the transmission of diseases such as the highly fatal EEHV. Whether the virus is transmitted from dam to calf via prenatal transfer of blood, postnatal transfer of milk, or via contact during early development at which calves are most vulnerable remains unknown. By measuring immunoglobulins in calves and cows/dams we can better assess the correlation between maternally transferred antibodies and those

produced by the calves, allowing for a more accurate assessment of any potential maternally transferred diseases and/or passive immunization.

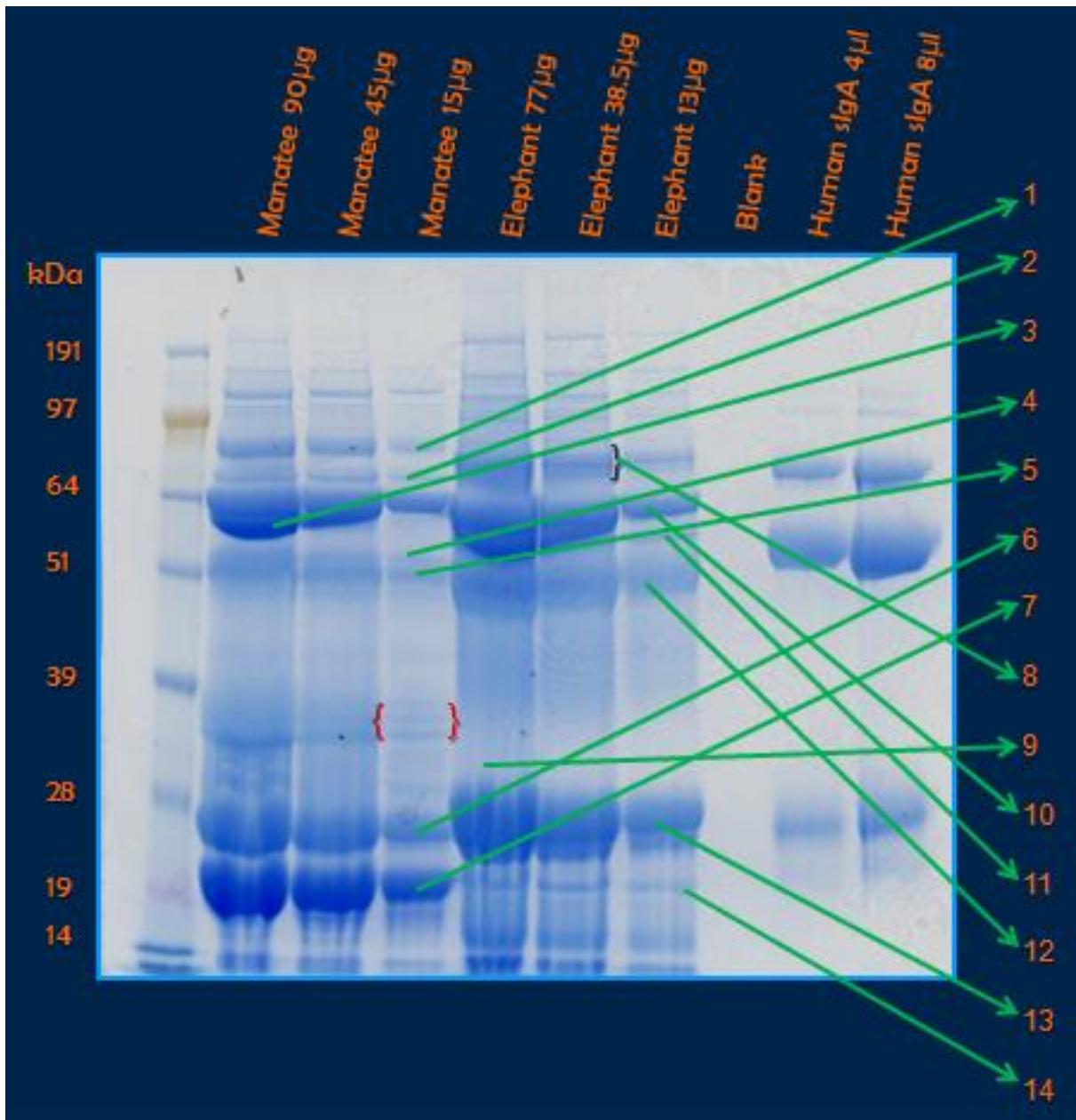


Figure 5-1. Simple Blue stained gel of milk proteins. Defatted and decaseinated elephant and manatee milk proteins were analyzed in a 10% Novex Bis-Tris/MOPS NuPAGE gel which was ideal for visualizing the majority of the remaining target proteins bands. This gel also showed bands at the molecular weight for caseins in the manatee (red). Secretory Component: Bands 1,2,8. IgA Heavy Chain: 3,10,11. IgG Heavy Chain: 4,5,12. Light Chain: 6,7,9,13,14.

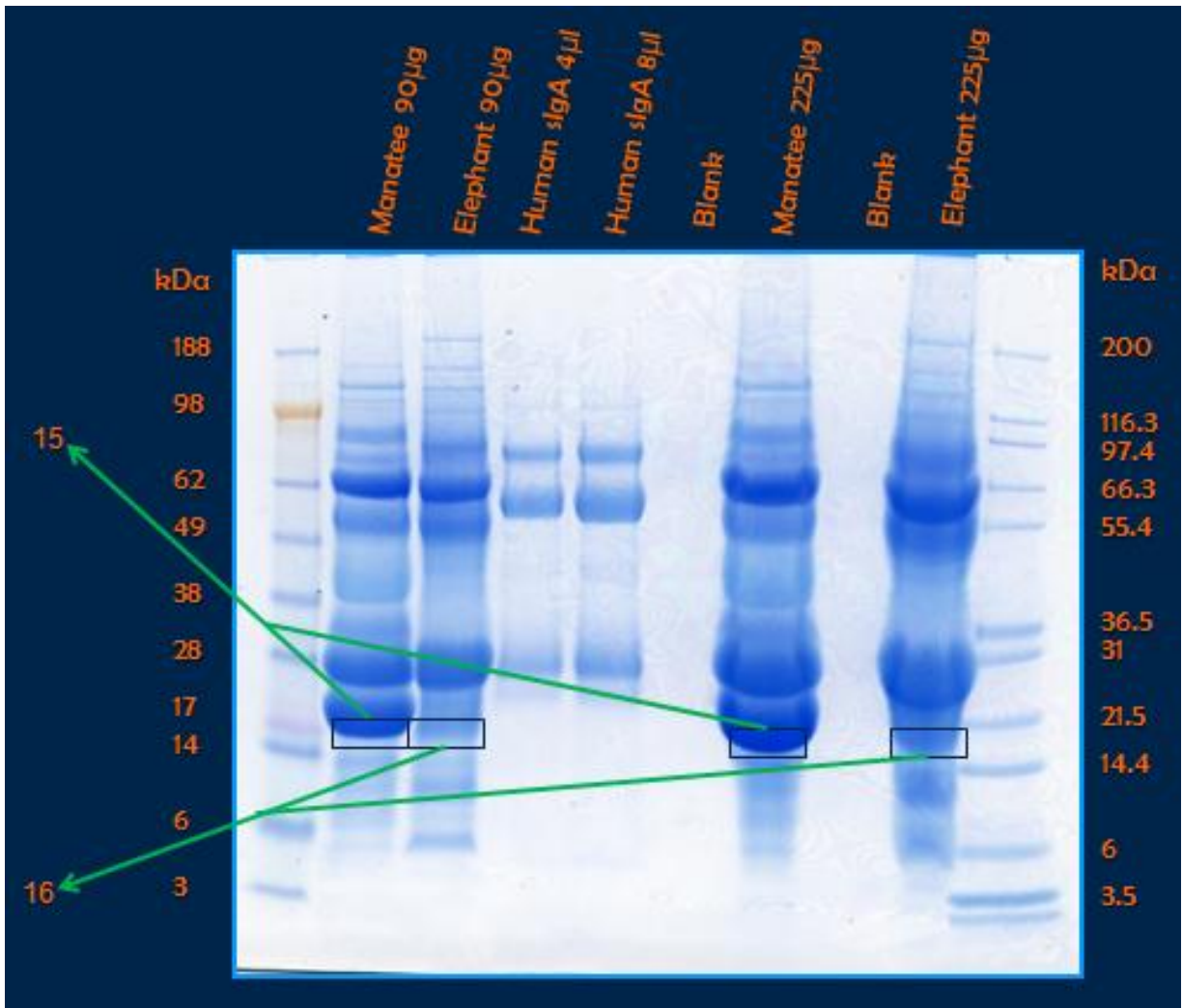


Figure 5-2. Simple Blue stained gel for J-chain. Defatted and decaseinated elephant and manatee milk proteins were analyzed in a 4 to 12 % Bis-Tris/MES NuPAGE gel which proved better at separating small molecular weight proteins bands. Bands 15 and 16 correspond to J-chain molecular weight.

Band 1- Secretory Component (12)	Band 2- Secretory Component (17)	Band 3- IgA or IgG Heavy Chain (7)
keratin 25D isoform 4 +	keratin 1 +	butyrophilin +
keratin 1 +	CD36 antigen +	albumin +
albumin, bovine +	lactoferrin +	hemopexin +
keratin 2 +	Ig heavy chain variable region -	Ig heavy chain variable region -
gelsolin a +	polymeric immunoglobulin receptor -	serum albumin precursor -
keratin , type 1 cytoskeletal 14 +	lactotransferrin [Homo sapiens] -	
Band 7- Light Chain (7)	Band 8- Secretory Component (24)	Band 9- Light Chain (19)
keratin 1 +	Serum albumin precursor +	keratin 25D isoform 4 +
keratin 25D isoform 4 +	keratin 25D isoform 4 +	serum albumin precursor +
serum albumin precursor -	lactoferrin +	lactoferrin -
beta-lactoglobulin -	Transferrin +	Ig heavy chain variable region -
alpha-2-macroglobulin -	lactotransferrin -	lactalbumin, alpha -
	poly-Ig receptor -	Immunoglobulin lambda -
Band 12- IgG Heavy Chain (25)	Band 13- Light Chain (9)	Band 14- Light Chain (11)
keratin 25D isoform 4 +	keratin 25D isoform 4 +	keratin 1 +
serum albumin precursor +	inhib. of kappa lt. polyp. gene enhancer in B-cells +	keratin 25D isoform 4 +
Ig heavy chain variable region -	serum albumin precursor -	Keratin, type I cytoskeletal 14 +
IgM heavy chain variable region -	(V-J). Ig heavy chain V-region -	inhib. of kappa lt. polyp. gene enhancer in B-cells +
IgG-3 heavy chain constant region -	Ig kappa chain variable region -	serum albumin precursor -
Ig heavy chain variable region -	MHC class I antigen alpha 1 subunit -	Alpha-lactalbumin A -

Figure 5-3. Protein identification in manatee milk. Gel LC-M/S M/S was efficient in identifying the proteins of highest concentration in each band, but proved less useful in detecting low concentration or highly variable proteins such as many of the target immunoglobulin proteins. This table identifies the target protein for each band and the total number of proteins identified through protein sequence database matching. For each band, the strongest matches (+) as well as those related to the target protein or of special interest (-) are listed.

Band 4- IgG Heavy Chain (13)	Band 5- IgG Heavy Chain (16)	Band 6- Light Chain (16)
keratin 1 +	keratin 25D isoform 4 +	keratin 1 +
keratin 25D isoform 4 +	Ig heavy chain variable region -	serum albumin precursor - (V-J). Ig heavy chain V-region -
serum albumin precursor -	IgG-5 heavy chain constant region -	Ig kappa chain V-II region MIL -
IgG 5-heavy chain constant region -	IgG heavy chain B -	Ig kappa light chain -
IgG heavy chain B -	IgG-4 chain C region -	Ig V kappa light-chain -
IgG-4 chain C region -	Ig heavy chain V-D-J-region -	
Band 10- IgA Heavy Chain (10)	Band 11- IgA Heavy Chain (16)	
serum albumin precursor +	serum albumin precursor +	
Keratin, type I +	keratin 1 +	
leukocyte Ig-like receptor -	inhibitor of kappa lt. polyp. gene enhancer in B-cells -	
serpin peptidase inhibitor -	Ig heavy chain -	
inhibitor of kappa lt. polyp. gene enhancer in B-cells -	Ig heavy chain constant region of IgA membrane form -	
preproalbumin -	alpha-2-macroglobulin isoform 3 -	
Band 15-J-chain (14)	Band 16- J-Chain (20)	
keratin 1 +	keratin 25D isoform 4 +	
beta-lactoglobulin -	keratin 1 +	
alpha-2-macroglobulin -	inhib. of kappa lt. polyp. gene enhancer in B-cells +	
albumin -	Alpha-lactalbumin A -	
Hemoglobin subunit beta (Beta-globin) -	IgAV-D-J-heavy chain -	
Fibrinogen alpha chain precursor -	Ig lambda light chain VLJ region -	

Figure 5-4. Protein identification in manatee milk. Gel LC-M/S M/S was efficient in identifying the proteins of highest concentration in each band, but proved less useful in detecting low concentration or highly variable proteins such as many of the target immunoglobulin proteins. This table identifies the target protein for each band and the total number of proteins identified through protein sequence database matching. For each band, the strongest matches (+) as well as those related to the target protein or of special interest (-) are listed.

Table 5-1. Mean concentration (mg/mL) and range IgG in mammalian species. Methods for measuring IgG varies between studies and species. *Bottlenose dolphin values are likely underestimates due to standardization of quantitative methods for analysis.

Species	Mean IgG (mg/mL)	IgG Range (mean +/- SD)
West Indian Manatee	9.86	5.56 - 14.16
Asian Elephant	14.85	9.54 - 20.16
Northern Fur Seal (3-4 year old bulls) (Cavagnolo and Vedros, 1979)	18.06	10.93 - 29.18
Northern Fur Seal (Pregnant females) (Cavagnolo and Vedros, 1979)	19.36	11.05 - 27.94
Bottlenose Dolphin (managed collection, closed pool system) (Ruiz et al., 2009)*	5.78	4.22 - 7.34
Bottlenose Dolphin (managed collection, open bay netted enclosures) (Ruiz et al., 2009)*	6.24	5.24 - 7.24
Bottlenose Dolphin (free-ranging) (Ruiz et al., 2009)*	9.06	7.89 - 10.23
Killer Whale (Taylor et al., 2002)	26.65	16.85 - 36.45
Southern Elephant Seal (Ferreira et al., 2005)	15.9	9.4 - 22.4
Sea Otter (Taylor et al., 2002)	32.76	21.18 - 44.34
Horse (Tizard, 2000)	N/A	10.0 - 15.0
Cattle (Tizard, 2000)	N/A	17.0 - 27.0
Sheep (Tizard, 2000)	N/A	17.0 - 20.0
Pig (Tizard, 2000)	N/A	17.0 - 29.0
Dog (Tizard, 2000)	N/A	10.0 - 20.0
Human (Tizard, 2000)	N/A	8.0 - 16.0

APPENDIX A
TISSUE PROCESSING AND STAINING PROTOCOLS

**TRANSMISSION ELECTRON MICROSCOPY PROCESSING SCHEDULE
MANUAL**

Working phosphate buffer, 3 changes.....	15 minutes each
Osmium tetroxide, 1.0% phosphate buffered	1 hour
Distilled water, 4 changes.....	15 minutes each
Uranyl acetate, 1% aqueous	1 hour
50% ethyl alcohol	15 minutes
75% ethyl alcohol	15 minutes
95% ethyl alcohol	15 minutes
100% (absolute) ethyl alcohol, 4 changes.....	15 minutes each
Equal parts 100% ethyl alcohol and propylene oxide	15 minutes
Propylene oxide, 4 changes	15 minutes each
Equal parts propylene oxide and epoxy resin.....	1 hour
Epoxy resin, 3 changes	1 hour each
Epoxy resin	2 hours
Embed	

**PARAFFIN EMBEDDED TISSUE PROCESSING SCHEDULE
AUTO**

80% alcohol.....	1 hour
95% alcohol, 3 changes.....	1 hour each
100% alcohol, 3 changes.....	1 hour each
Xylene, 3 changes.....	1 hour each
Paraffin, 3 changes.....	1 hour each
Paraffin, under vacuum.....	1 hour
Embed.	

Masson's Trichrome (modified)

Deparaffinize and hydrate to water		
Bouin's solution.....	1 change	60 minutes
(In oven at 56°C)		
Running tap water.....	change until	yellow disappears
Weigert's iron hematoxylin.....	1 change	20 minutes
Tap water rinse		
Biebrich's Scarlet-Acid fuschin.....	1 change	1 minute
Rinse in water		
5% phosphotungstic acid.....	1 change	4 minutes
Light green solution.....	1 change	2 minutes

Rinse in water		
0.5% glacial acetic acid water.....	1 change	2 minutes
Distilled water rinse		
95% ethanol.....	2 changes	2 minutes
100% ethanol.....	2 changes	2 minutes
Xylene.....	3 changes	2 minutes
Mount with Fisher Scientific Mounting Media		

H&E

Deparaffinize and hydrate to water		
Harris' hematoxylin.....	1 change	6–9 minutes
Tap water rinse.....	1 change	10 minutes
Acid alcohol differentiation		
Tap water rinse.....	1 change	5 minutes
Ammonia water rinse		
Running tap water.....	1 change	10 minutes
Dip in 95% alcohol.....	1 change	30 seconds
Eosin.....	1 change	30-120 seconds
95% ethanol.....	2 changes	2 minutes
100% ethanol.....	2 changes	2 minutes
Xylene.....	3 changes	5 minutes
Mount with Fisher Scientific Mounting Media		

PAS

Deparaffinize and hydrate to water		
0.5% Periodic Acid.....	1 change	5 minutes
Running tap water.....	1 change	5 minutes
Schiff Reagent.....	1 change	15 minutes
Running tap water.....	1 change	10 minutes
Harris Hematoxylin.....	1 change	3 minutes
Running tap water.....	1 change	5 minutes
Differentiate in:		
1 % acid alcohol.....	1 change	1 dip
Tap water rinse		
Blue in ammonia water		
Running tap water	1 change	
95% ethanol.....	2 changes	
100% ethanol.....	2 changes	
Xylene.....	3 changes	

Immunohistochemistry

- Place tissue sections on Fisher superfrost positively charged slides
- Incubated at 56°C overnight
- Washed in a series of 3 xylene bathes, dehydrated through a graded series of 100% alcohol (3 times, 2 minutes each) and 95% alcohol (2 times, 2 minutes each), followed by rehydration in tap water for 10 minutes.
- Incubate slides for 20 minutes in 3% hydrogen peroxide
- Wash twice in PBS for 5 minutes each
- Incubate sections in 1.5% blocking serum in PBS for one hour prior to incubation with primary antibody
- The primary antibody will incubate for 30 minutes at room temperature or overnight at 4°C
- Wash with three changes of PBS for 5 minutes
- Incubate biotinylated secondary antibody for 30 minutes
- Wash tissue in three changes of PBS for 5 minutes each
- AB enzyme reagent (avidin and biotinylated HRP) will be added to the tissues and incubate for 30 minutes
- Wash tissue three times, 5 minutes each
- Add substrate solution to slides until the desired level of staining occurs
- Wash with several changes of deionized water
- Place coverslips on the slides using a glycerol gelatin mounting media and
- Examined slides microscopically

APPENDIX B
WEST INDIAN MANATEE CIRCULATING IMMUNOGLOBULIN G

Total Circulating IgG (mg/mL) in West Indian Manatees
Yellow = Above or below the species reference range (2.81 mg/mL to 16.2 mg/mL)
Mean, SD, and Median in Bold

Puerto Rico	Belize	Brazil	Everglades	Brevard	Crystal River	Lemon Bay	Tampa	Alabama
7.7	1.365	1.875	5.375	5.7625	4.1325	2.6675	8.65	8.2
8.1375	1.6915	2.16625	5.625	10.4625	4.265	2.9475	9.875	12.6
8.25	2.335	2.2675	5.6875	10.5725	4.7025	4.0975	14.55	13.075
8.5375	2.9575	2.3825	6.025	10.7875	5.2	5.3		
8.5875	3.2175	2.4725	6.175	11.3875	6.25	6.3875		
8.6375	3.5313	2.8825	6.1875	12.15	6.5125	7.075		
9.0375	3.535	3.02	6.4	12.2875	6.6375	7.1125		
9.1125	3.6675	3.1975	6.525	13.5625	6.7125	7.125		
9.425	4.225	3.21	7.275	13.575	6.8375	7.225		
9.45	4.3775	3.445	7.3125	14.25	6.875	7.425		
9.725	4.49	3.88	7.525	15.2375	7.0375	7.7375		
10.0875	4.5	4.1175	7.5375	15.725	7.2	7.975		
10.2375	4.925	4.915	7.6625	15.875	7.425	9.7625		
10.5375	4.995	6.5875	7.7	16.5625	7.6625	10.5125		
11.2125	5.26875	6.6375	7.75	16.7625	7.6875	11		
11.3125	5.375	6.7	8.05	17.35	7.75	11.2		
11.4625	5.6625	6.975	8.5	17.5125	8.0375	11.5		
11.6875	5.825	8.1	8.725	18.3125	8.1125	15.2625		
11.8	6.1375		8.875	21.4375	8.2875	15.3875		
11.8625	6.1625		9.4125	22.3125	8.2875			

Puerto Rico	Belize	Brazil	Everglades	Brevard	Crystal River	Lemon Bay	Tampa	Alabama
12.05	6.175		9.625	26.5	8.5125			
12.075	6.3125		9.775		8.575			
12.1625	6.6875		10.675		8.6			
14.0625	6.8625		10.7125		8.625			
14.25	6.9		11.15		8.7375			
18.2375	7.0875		11.25		8.8375			
	7.2125		11.35		8.85			
	7.225		11.45		8.8875			
	7.275		11.675		8.9795			
	7.3875		12.3375		9.025			
	7.45		12.8125		9.0875			
	7.4875		12.8125		9.125			
	7.525		13.875		9.225			
	7.6875		14.075		9.275			
	7.7375		14.2125		9.325			
	7.825		17.5625		9.425			
	7.97		18.075		9.45			
	8.0875				9.4875			
	8.125				9.5			
	8.325				9.5			
	8.3625				9.5125			
	8.3875				9.6625			
	8.4375				9.7875			
	8.45				9.975			
	8.5375				9.9875			
	8.55				10			
	8.6				10.0375			
	8.6125				10.05			
	8.7375				10.3875			
	9.05				10.425			
	9.15				10.45			

Puerto Rico	Belize	Brazil	Everglades	Brevard	Crystal River	Lemon Bay	Tampa	Alabama
	9.77				10.5125			
	9.775				10.6375			
	9.833				10.75			
	9.9				10.8875			
	9.95				11.175			
	10.425				11.225			
	10.4375				11.325			
	10.45				11.55			
	10.7375				11.6625			
	10.875				11.725			
	11.35				11.8875			
	11.4625				11.925			
	11.8				11.95			
	12.25				11.9625			
	12.3125				11.9975			
	13.319				12.05			
	15.069				12.0875			
	15.175				12.275			
	15.49				12.2875			
	15.9				12.6875			
	16.525				12.7125			
	17.066				12.7625			
	18.55				12.8			
	18.5875				12.8875			
	19.125				13.3125			
	19.3				13.425			
	19.6125				14.1875			
	20.075				14.5			
	20.275				14.7			
	20.9625				16.35			
	24.52				16.9875			

	26.8				21.4625			
Puerto Rico	Belize	Brazil	Everglades	Brevard	Crystal River	Lemon Bay	Tampa	Alabama
10.76	9.68	4.16	9.67	15.16	10.06	8.30	11.03	11.29
2.33	5.08	1.98	3.25	4.65	2.73	3.57	3.11	2.69
10.39	8.58	3.33	8.88	15.24	9.73	7.43	9.88	12.60

Top to bottom: mean, SD, median for each population.

APPENDIX C
WEST INDIAN MANATEE BLOOD AND TEAR IGG VALUES (MG/ML)

Animal	Tear Average	Blood Average
1	0.005494779	10.91875
2	0.010979102	8.1
3	0.009809735	17.2
4	0.030893855	8.1875
5	0.0171594	15.06875
6	0.017799077	9.5
7	0.09605925	25.525
8	0.07367779	6.1625
9	0.04285945	20.275
10	0.05332825	10.45
11	0.0795031	19.6125
12	0.062167075	20.9625
13	0.163372	15.75
14	0.044265258	9.05
15	0.005057425	10.8625
16	0.0539038	22.3125
17	0.095403848	12.15
18	0.411005	17.35
19	0.4951976	16.5625
20	0.1136028	18.3125
21	0.319439	10.7875
22	0.001873191	4.7025
23	0.0495546	12.8875
24	0.0739365	11.925
25	0.005006485	10.05
26	0.013896816	9.4875

Animal ID	Tear Average	Blood Average
27	0.0287263	8.8375
28	0.0170578	10.1625
29	0.209599655	12.2875
30	0.02912555	11.55
31	0.1879005	9.125
32	0.0671615	9.9875
33	0.006920691	16.9875
34	0.01074765	10.275
35	0.211109	9.7875
36	0.0781745	9.6625
37	0.159726637	21.4625
38	0.039567175	11.325
39	0.00949554	14.7
40	0.004961365	8.6
41	0.01216475	12.6875
42	0.01020327	7.6875
43	0.0345828	6.6375
44	0.04073955	14.1875
45	0.004605512	10
46	0.01669275	7.6625
47	0.011491548	12.8
48	0.038895	12.0875

APPENDIX D
MANATEE IGG LEVELS AND COMPLETE BLOOD COUNTS

Crystal River Manatee IgG Levels and Select CBC Values

Animal ID	Total IgG (mg/mL)	Sex (1=male, 2=female)	Age Class	Eosinophils / uL	WBC, corr. K/uL	Total Protein g/dL	Total Globulin g/dL	SAA ug/mL
1	8.1125	1	Adult	460	6.6	7	3.27	24
2	12.275	2	Adult	420	5.3	8.3	4.54	<10
3	8.7375	1	Subadult	710	6.2	7.2	4.06	49
4	6.8375	1	Adult	270	5.3	7.3	4.09	>120
5	10.75	1	Adult	290	3.7	7.8	4.53	<10
6	11.175	1	Adult	370	3.7	7.7	4.29	15
7	9.225	1	Subadult	390	6.5	7.6	4.02	12
8	7.2	2	Adult	350	4.7	7.1	4.75	<10
9	6.7125	2	Calf	60	12	8	3.88	84
10	10.8875	2	Calf		10.4	7.6	4.05	64
11	9.0875	2	Calf		10.5	7.9	4	42
12	7.425	1	Subadult	340	6.2	7.3	3.59	<10
13	10.45	1	Adult	460	3.8	7.5	3.6	<10
14	6.5125	1	Calf	360	6.5	8	4.2	37
15	8.2875	1	Subadult	520	4.6	7.1	3.8	<10
16	11.725	1	Adult	170	4.1	8.1	4.17	11
17	8.5125	1	Adult	530	4.9	7.3	3.59	>120
18	8.9795	1	Adult	760	8	6.9	3.62	28
19	12.4375	2	Adult-	320	4.9	7.8	4.11	<10
20	11.6625	2	Adult	340	7.6	8.1	3.93	<10
21	4.7025	1	Calf	100	5.1	7.6	3.75	77
22	12.8875	1	Adult	250	5.5	8.4	4.88	<10
23	11.925	1	Adult	370	3.9	8.5	4.75	<10
24	10.05	1	Adult	110	4.3	8.3	4.24	39
25	8.8875	1	Adult	110	3.8	7.1	3.66	11

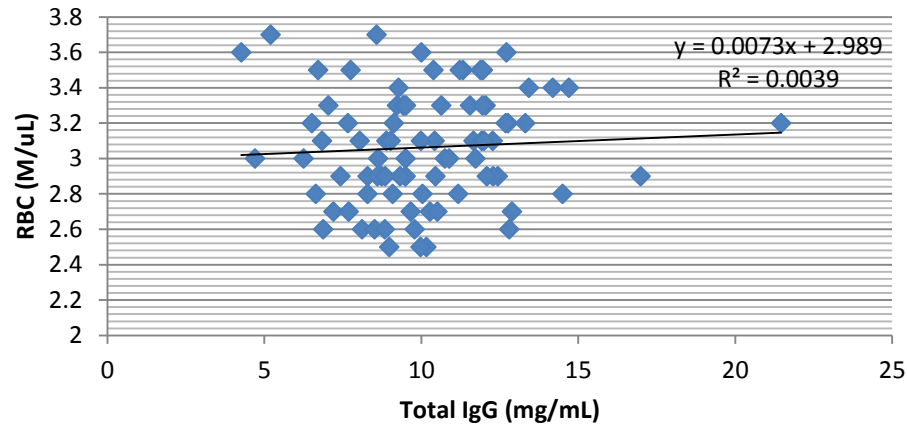
Animal ID	Total IgG (mg/mL)	Sex (1=male, 2=female)	Age Class	Eosinophils / uL	WBC, corr. K/uL	Total Protein g/dL	Total Globulin g/dL	SAA ug/mL
26	13.425	2	Adult	450	7.5	7.6	4	69
27	10.0375	1	Adult	240	4.8	7.1	4	15
28	16.35	1	Adult	660	4.4	7.3	4.11	28
29	8.2875	2	Adult	380	7.5	6.5	3.5	78
30	8.625	1	Adult	310	3.9	7.7	3.77	15
31	13.3125	1	Adult	230	4.7	8.4	4.58	10
32	5.2	2	Calf	530	13.3	7.6	4.14	95
33	6.25	1	Adult	380	6.3	6.1	3.1	41
34	10.425	1	Adult	340	4.8	7.8	4.34	11
35	9.025	1	Adult	480	6.8	7.1	3.35	94
36	9.5	2	Adult	320	4.5	6.6	3.45	60
37	9.425	1	Adult	210	4.2	7.4	3.26	18
38	9.5	2	Adult	430	7.1	6.5	3.78	74
39	9.45	1	Subadult	400	6.6	7.4	4.33	102
40	10.6375	2	Calf	490	12.2	7.6	4.16	<10
41	8.0375	1	Adult	450	4.5	6.4	3.49	25
42	10.3875	2	Subadult	280	7	7.9	4.14	29
43	9.4875	1	Calf	470	7.8	6.7	4.17	99
44	8.8375	2	Calf	260	8.7	8	4.48	26
45	10.1625	2	Adult	560	6.2	7.5	4.27	70
46	12.2875	1	Adult	370	4.7	7.7	4.17	68
47	11.55	1	Adult	140	4.6	7.5	4.22	32
48	9.125	2	Subadult	530	10.6	7.5	4.31	57
49	9.9875	2	Adult	330	5.5	7.6	4.05	<10
50	16.9875	2	Adult	220	2.8	8.2	4.2	<10
51	10.275	1	Adult	1070	5.3	7.2	3.54	<10
52	9.7875	1	Adult	660	6.6	7.3	4.05	<10
53	9.6625	1	Subadult	760	5.8	7.1	3.8	66
54	21.4625	2	Adult	70	7.3	8.6	5.77	>120
55	11.325	1	Subadult	880	6.3	7.6	4.48	89

Animal ID	Total IgG (mg/mL)	Sex (1=male, 2=female)	Age Class	Eosinophils / uL	WBC, corr. K/uL	Total Protein g/dL	Total Globulin g/dL	SAA ug/mL
56	14.7	1	Adult	420	4.7	8	4.7	40
57	8.6	1	Subadult	230	5.8	7.3	4.3	53
58	12.6875	2	Subadult	480	9.5	7.7	3.93	48
59	6.875	2	Adult	220	3.6	7.8	N/A	<10
60	4.265	1	Calf		8.8	6.9	N/A	85
61	14.5	2	Calf	490	5.4	8	N/A	34
62	11.9975	1	Subadult	540	6	8.2	N/A	>120
63	8.575	1	Calf	310	5.1	8.6	N/A	>120
64	9.975	2	Adult	590	3.9	8.3	N/A	23
65	11.225	1	Adult	510	5.1	7.9	N/A	84
66	12.7125	1	Adult	320	5.3	8.4	N/A	25
67	11.8875	1	Adult	270	4.4	7.7	N/A	71
68	11.9625	2	Adult	280	4	8.6	N/A	24
69	12.05	1	Adult	660	6	8.3	N/A	28
70	9.325	2	Adult	880	4.7	7.6	N/A	102
71	7.75	1	Calf	590	6.5	7.8	N/A	>120
72	7.6875	1	Subadult	310	6.2	7.2	N/A	N/A
73	6.6375	1	Adult	330	5.6	7.4	N/A	N/A
74	14.1875	1	Adult	290	7.2	8.7	N/A	N/A
75	10	1	Subadult	130	4.4	8.4	N/A	N/A
76	7.6625	1	Adult	230	7.8	7.7	N/A	N/A
77	12.8	1	Adult	420	3.8	8.6	N/A	N/A
78	12.0875	2	Adult	140	7.1	9	N/A	N/A
79	9.5125	1	Adult	150	4.8	8.6	N/A	N/A
80	8.85	1	Adult	230	5.9	8	N/A	N/A
81	7.0375	1	Adult	190	4.8	7.8	N/A	N/A
82	9.275	1	Adult	730	6.1	7.3	N/A	N/A
83	11.95	2	Adult	280	7.1	7.9	N/A	N/A

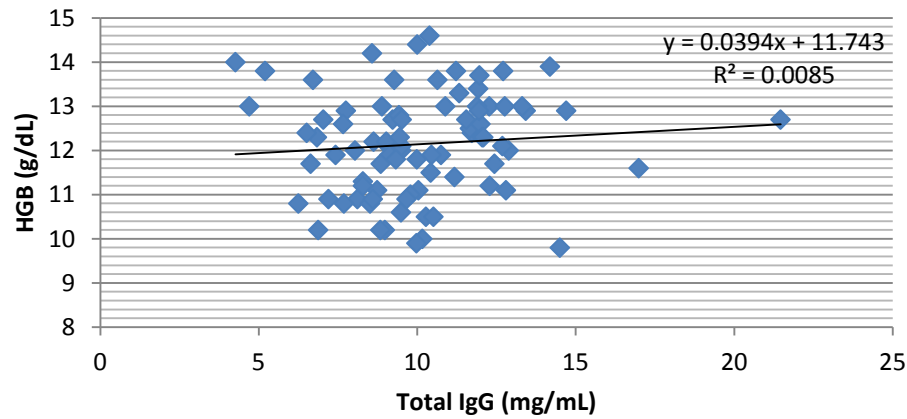
Potential Predictors of Total IgG in the West Indian Manatee

Crystal River Population

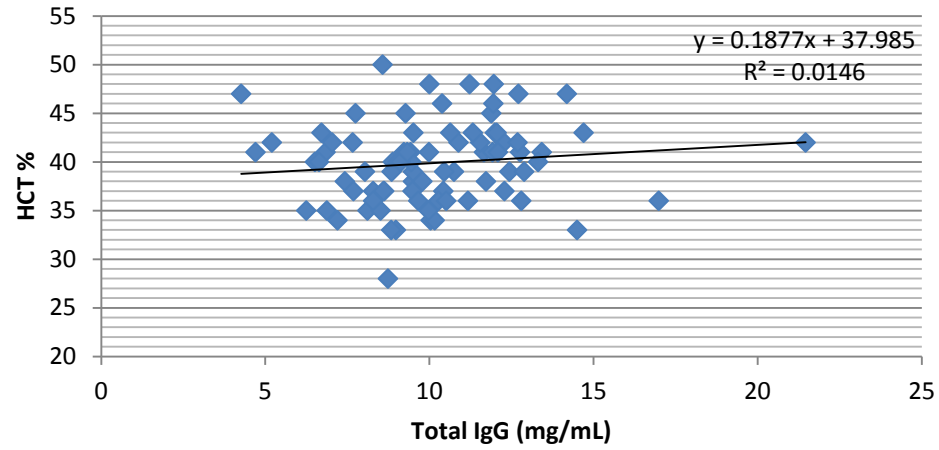
RBC vs. Total IgG



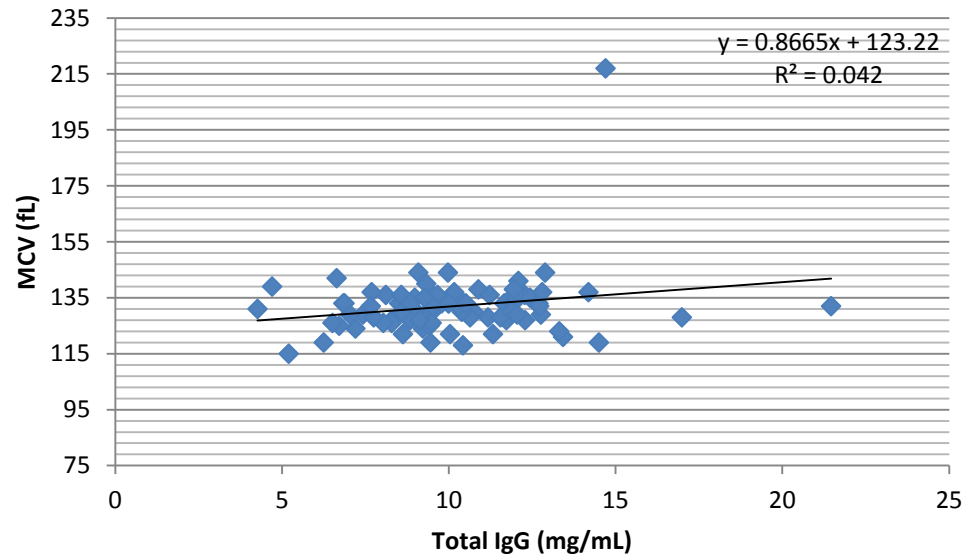
HGB vs. Total IgG



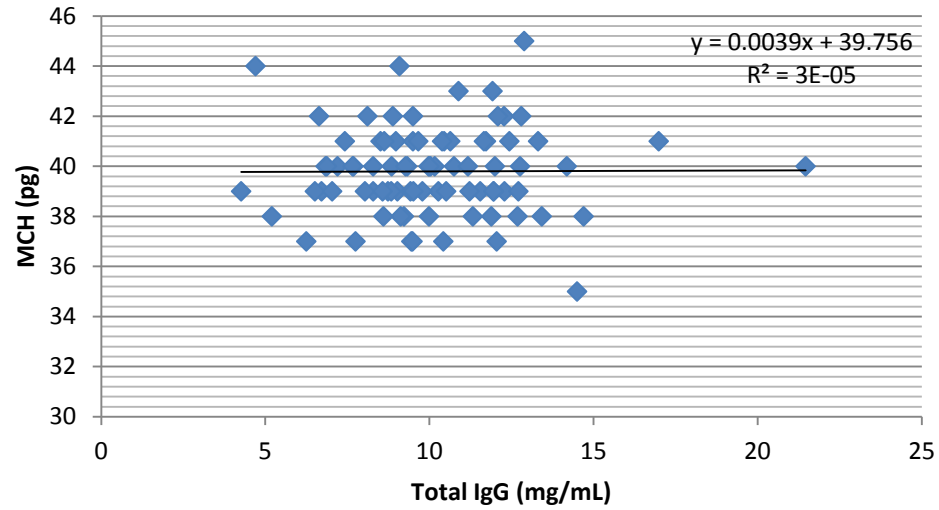
HCT vs. Total IgG



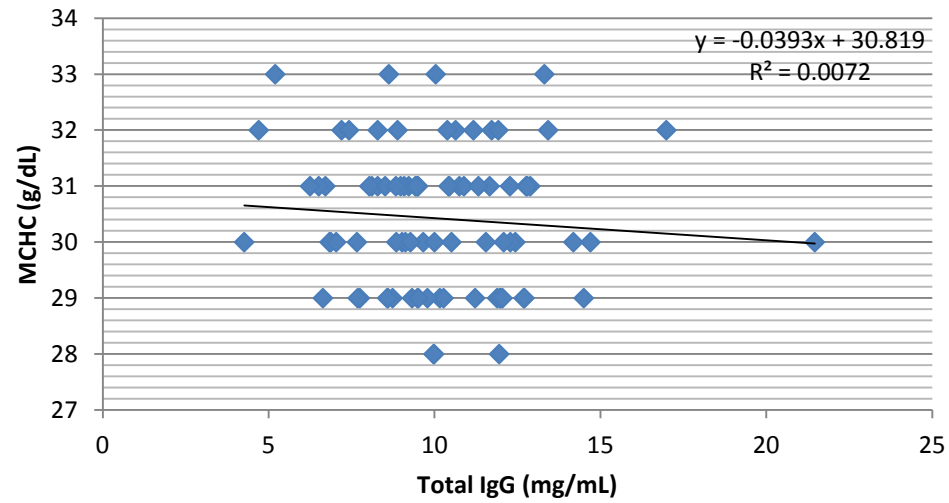
MCV vs. Total IgG



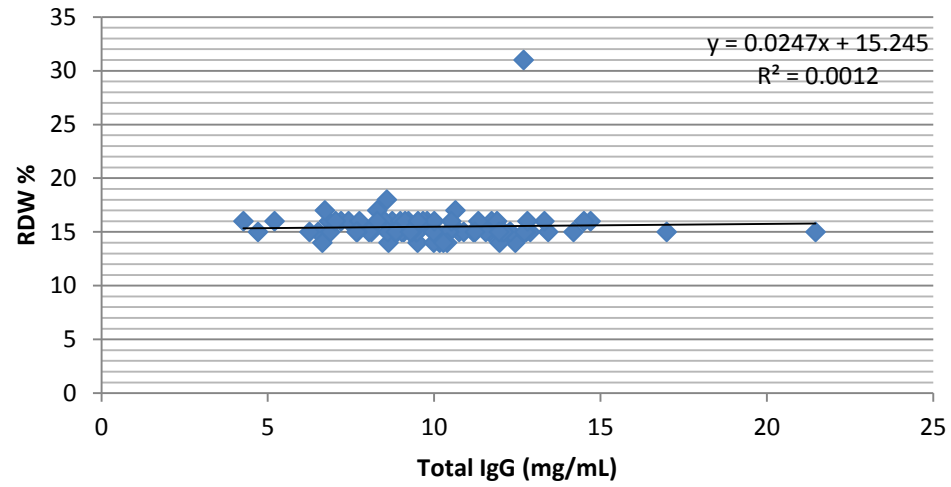
MCH vs. Total IgG



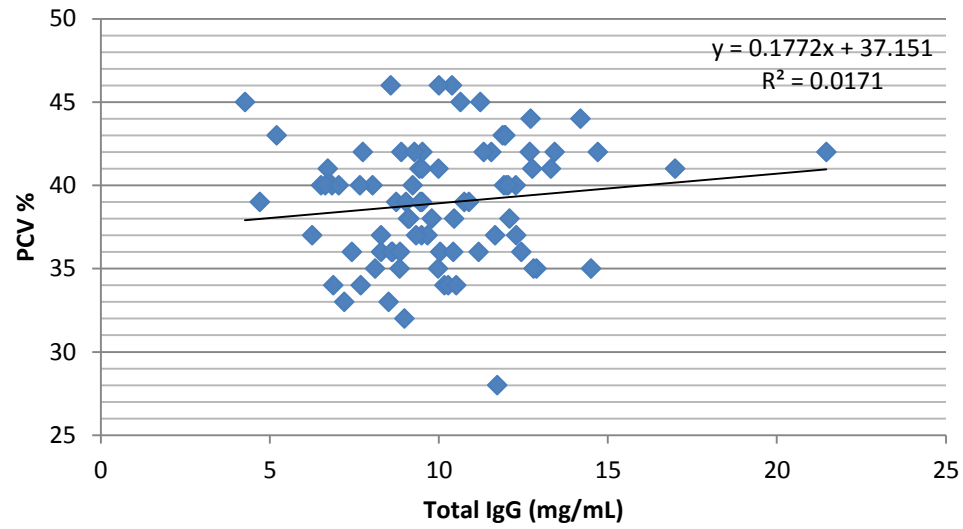
MCHC vs. Total IgG



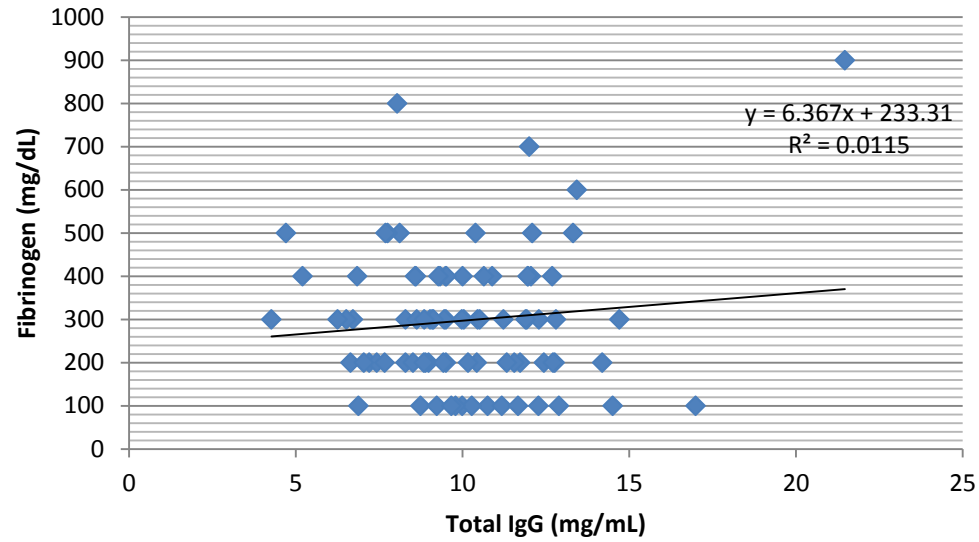
RDW vs. Total IgG



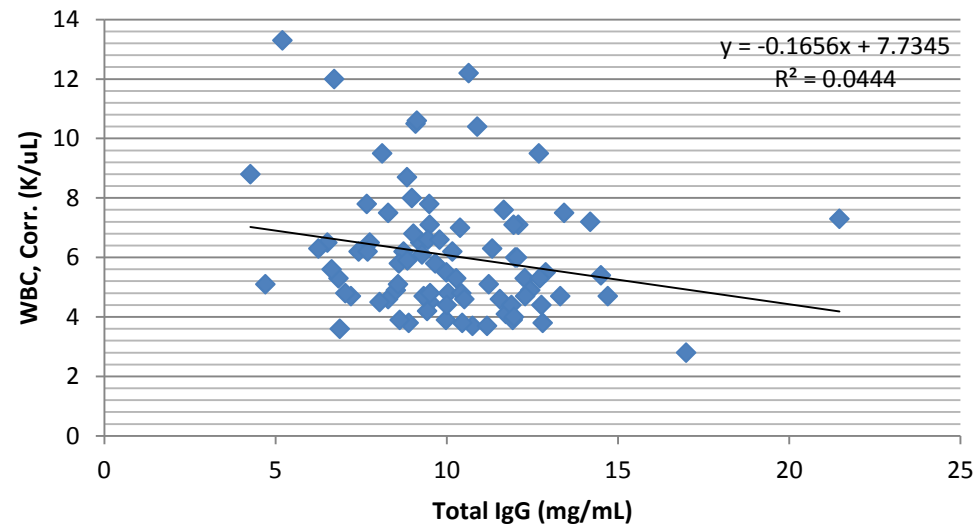
PCV vs. Total IgG



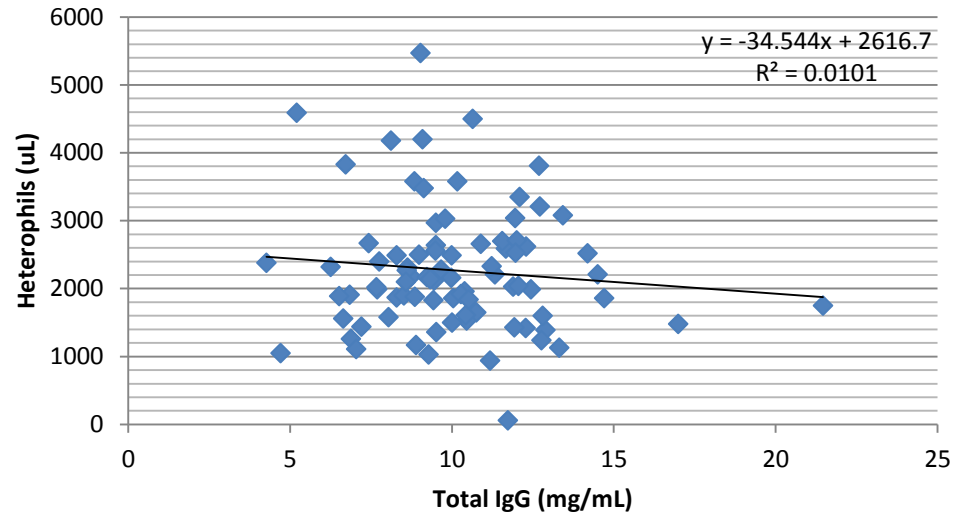
Fibrinogen vs Total IgG



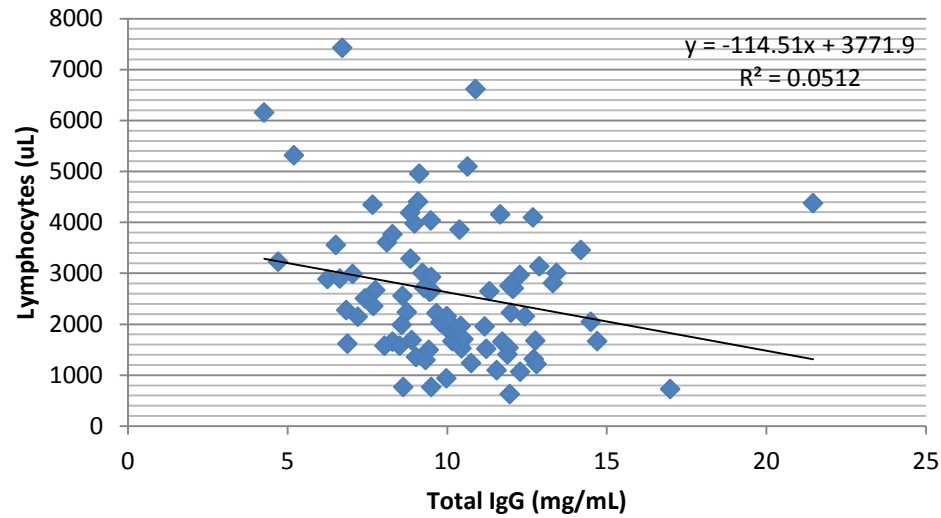
WBC, Corr. vs Total IgG



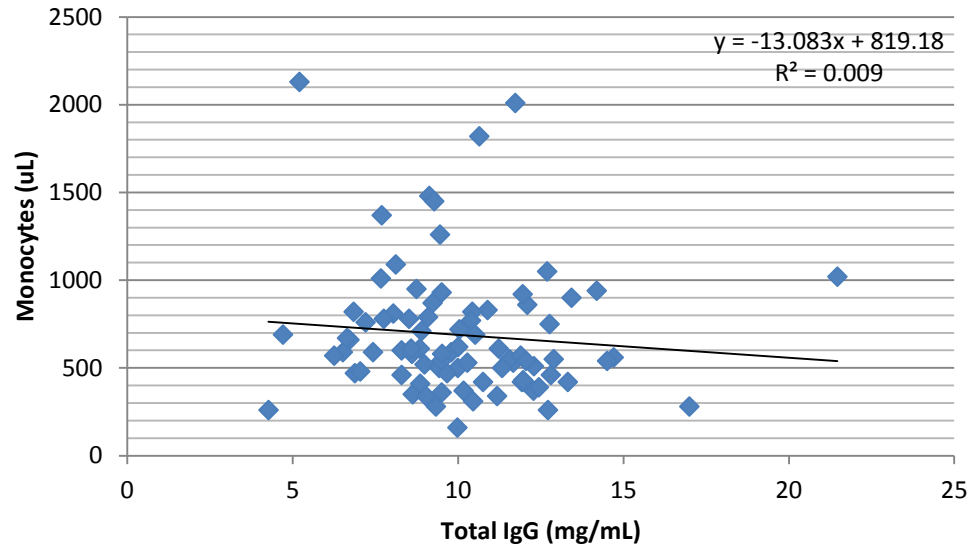
Heterophils vs. Total IgG



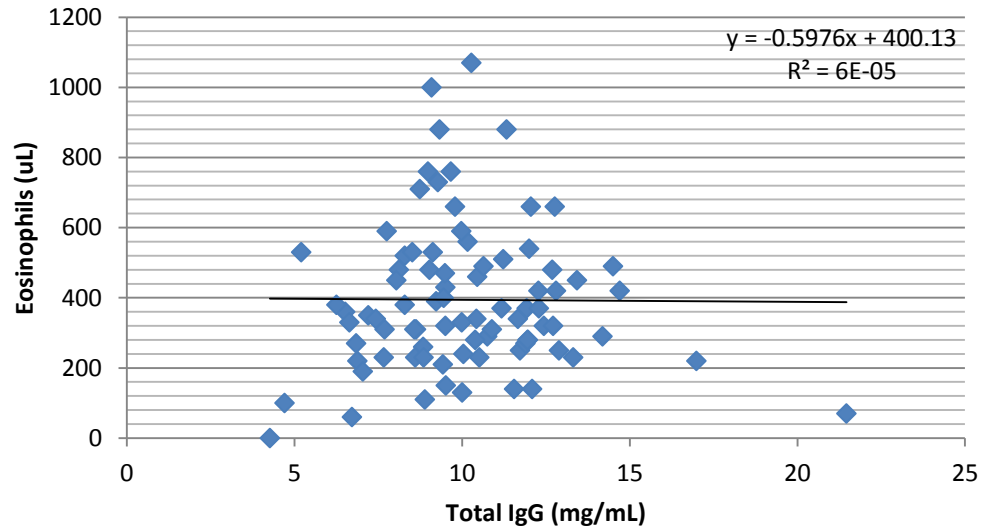
Lymphocytes vs. Total IgG



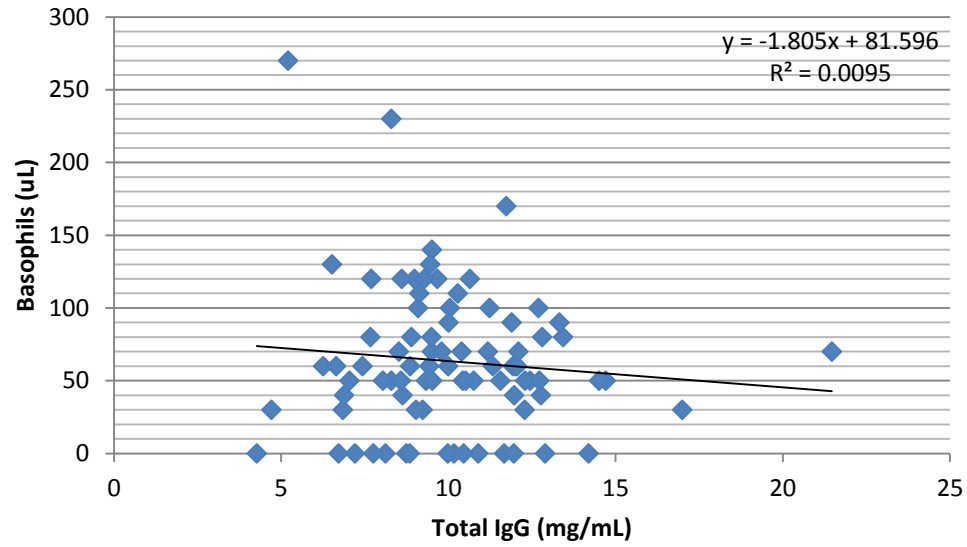
Monocytes vs. Total IgG



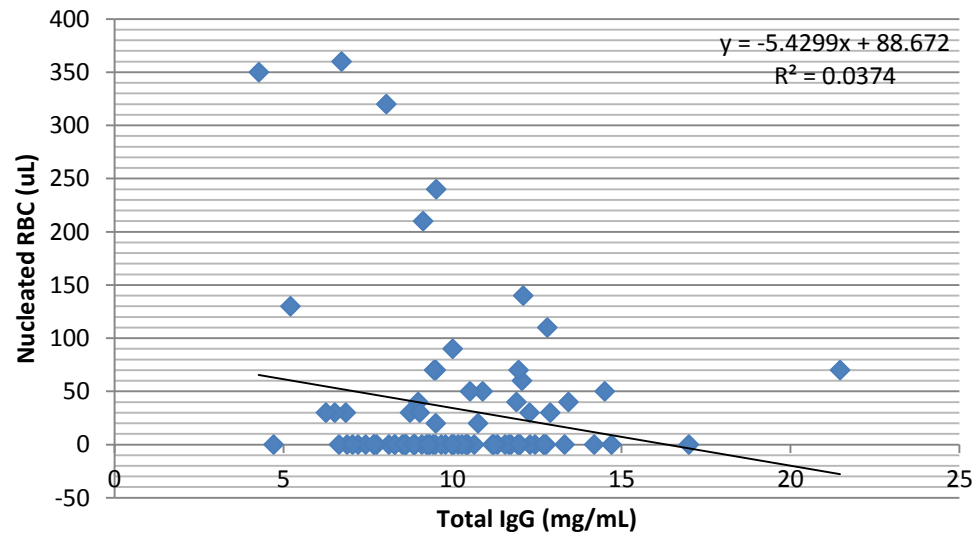
Eosinophils vs. Total IgG



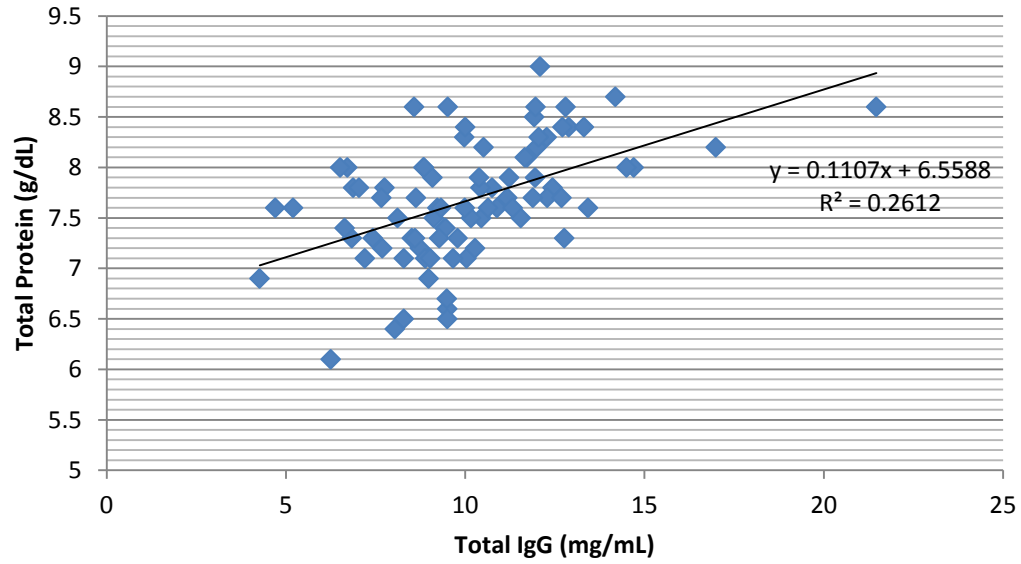
Basophils vs. Total IgG



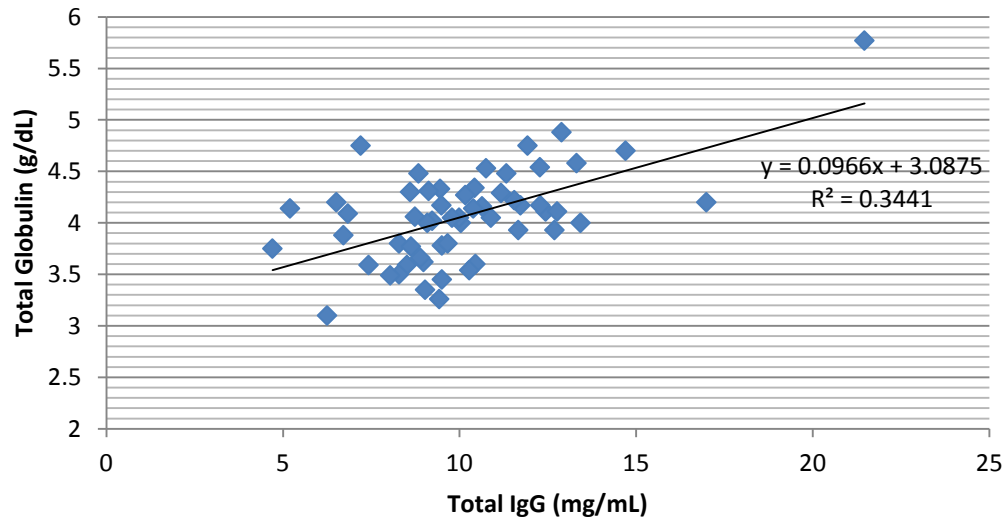
Nucleated RBC vs. Total IgG



Total Protein vs. Total IgG

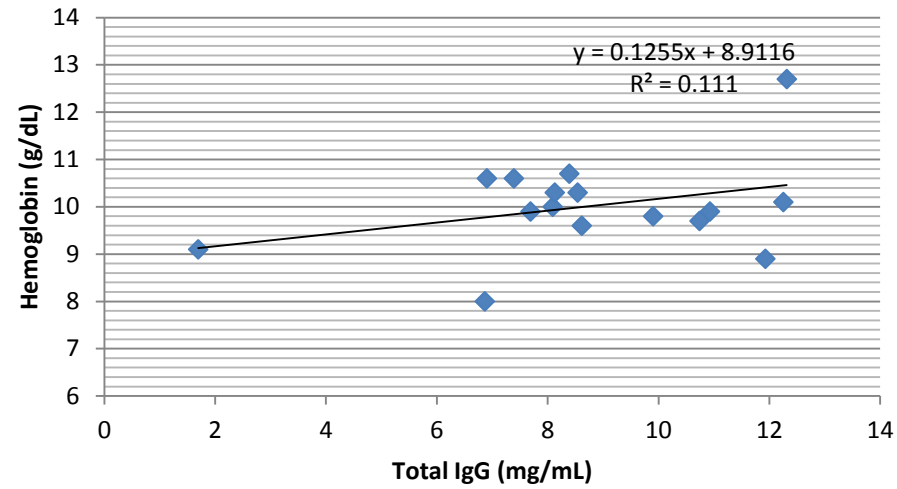


Total Globulin vs. Total IgG

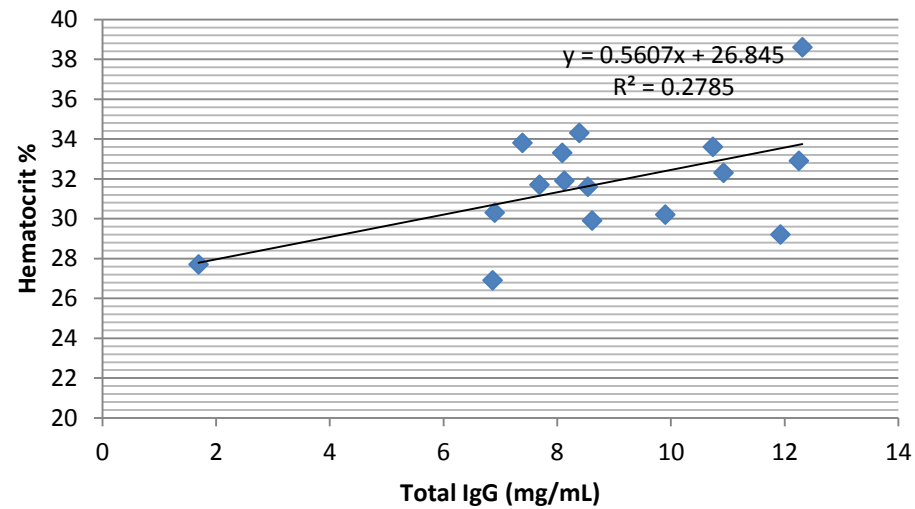


Belize Population

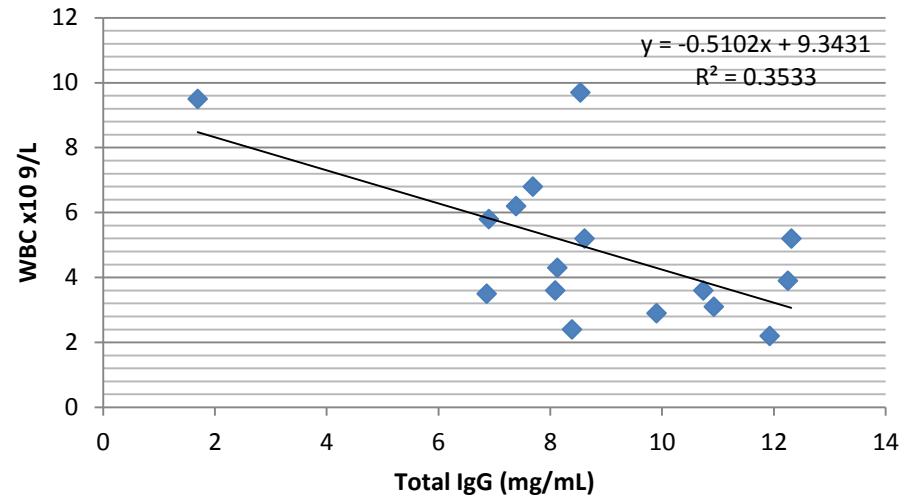
Hemoglobin vs. Total IgG



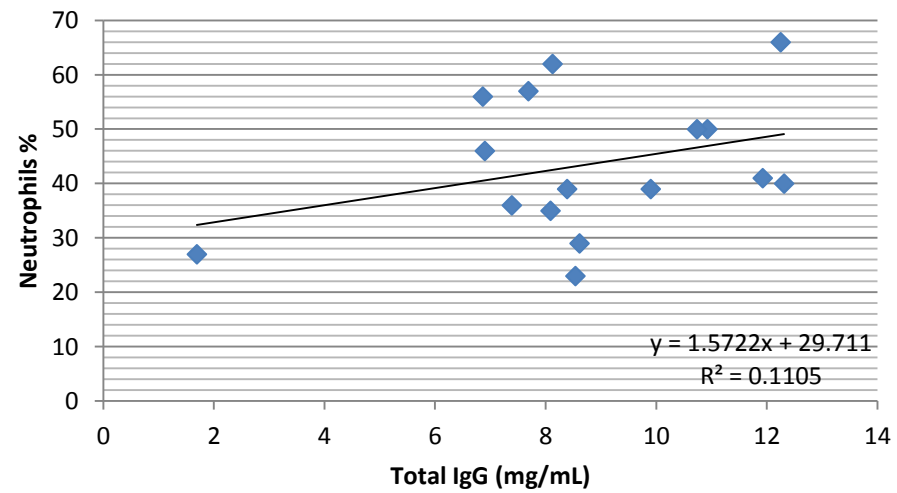
Hematocrit vs. Total IgG



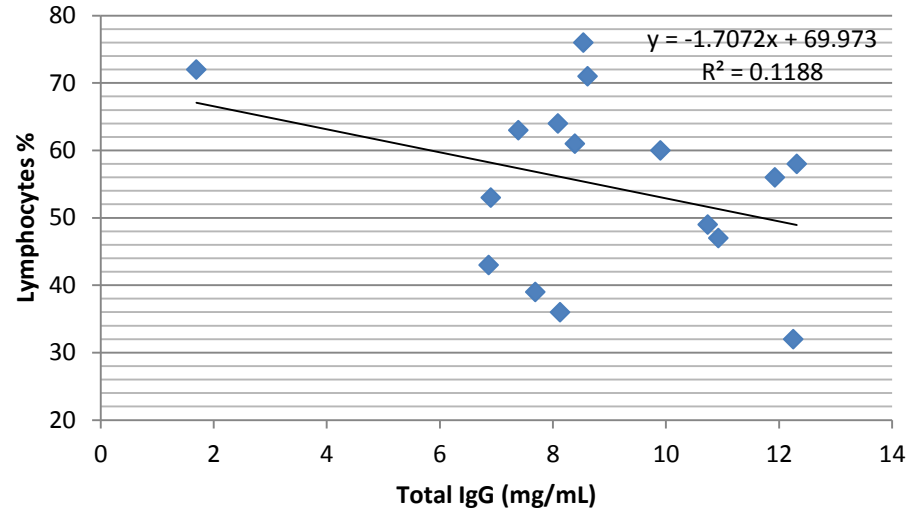
WBC vs. Total IgG



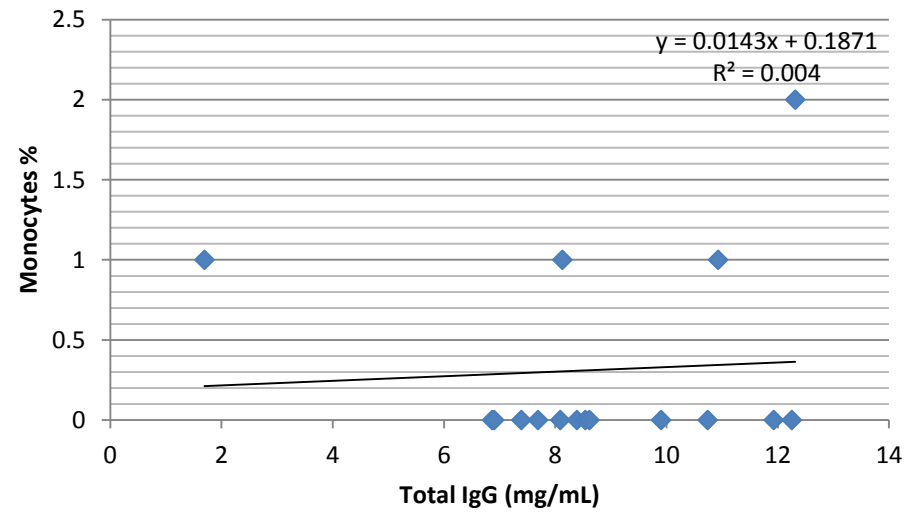
Neutrophils vs. Total IgG



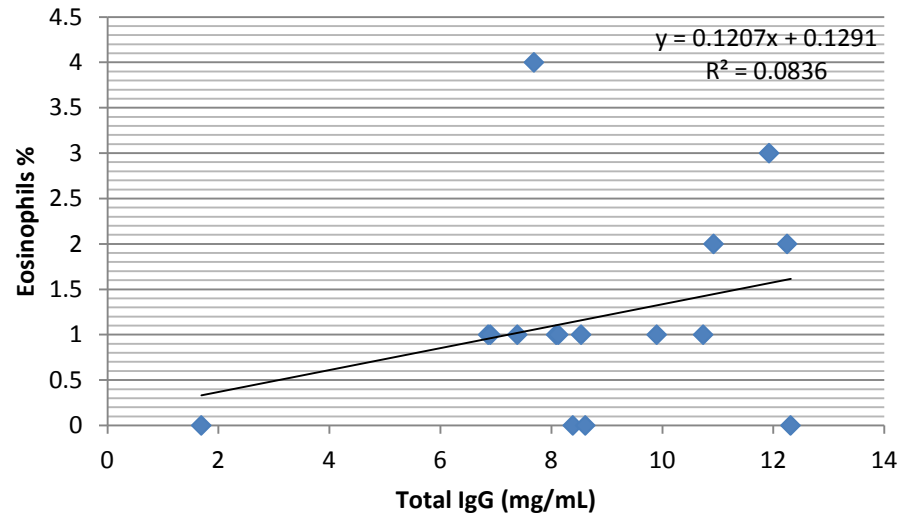
Lymphocytes vs. Total IgG



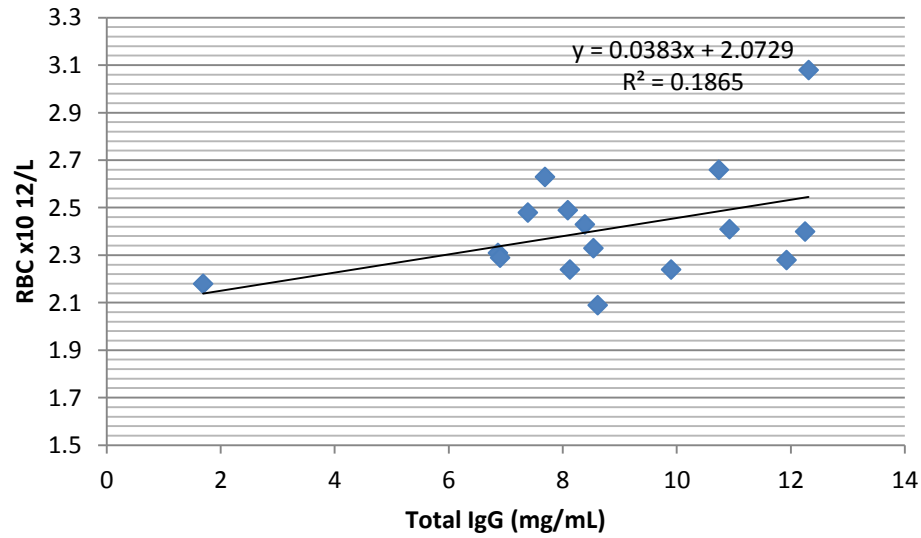
Monocytes vs. Total IgG



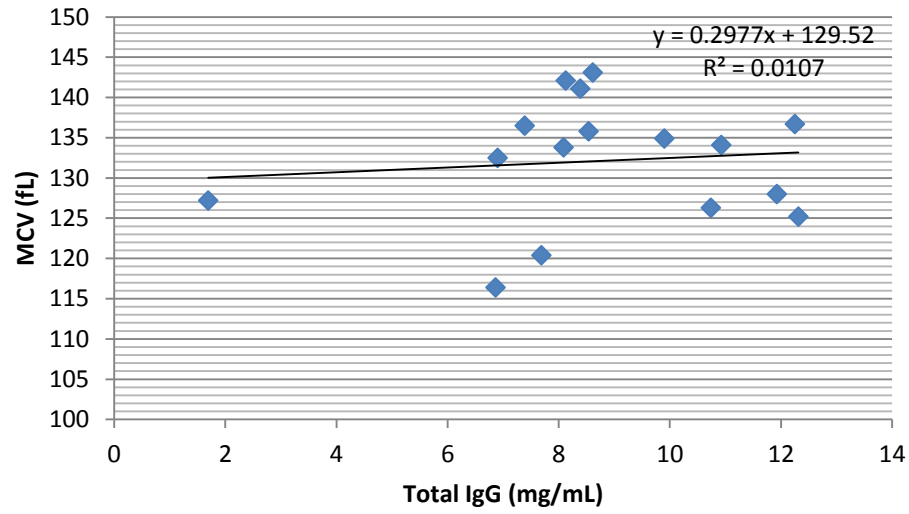
Eosinophils vs. Total IgG



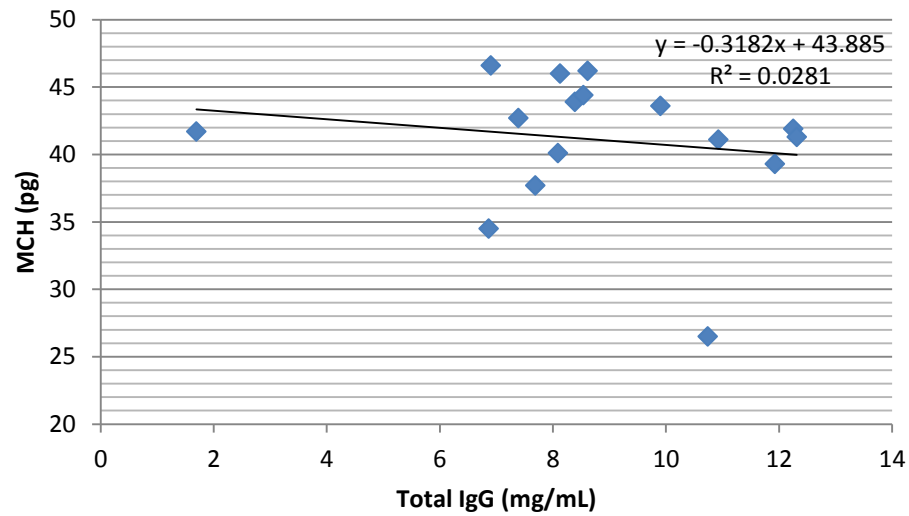
RBC vs. Total IgG



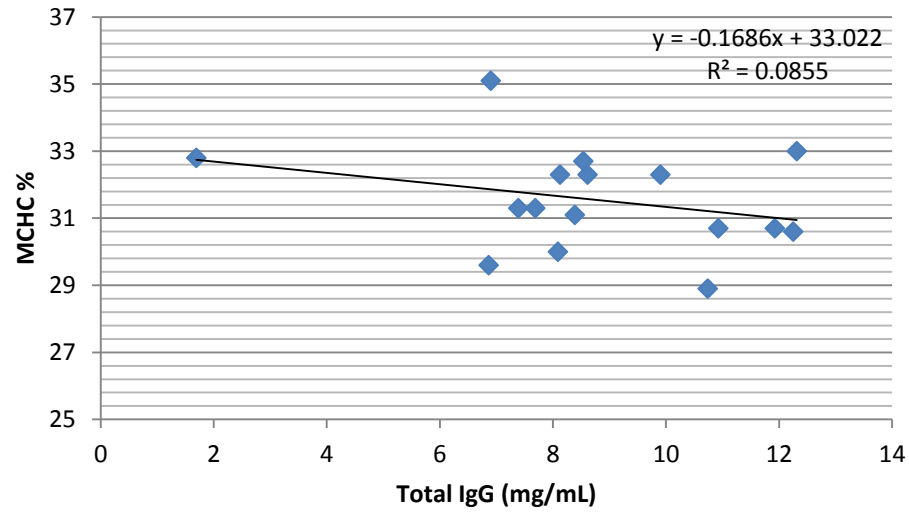
MCV vs. Total IgG



MCH vs. Total IgG



MCHC vs. Total IgG



APPENDIX E
ELEPHANT IGG LEVELS-PASSIVE TRANSFER OF IMMUNOGLOBULINS

Paired dam and calf passive transfer of immunoglobulin samples. Green = confirmed pre-suckling calf serum samples, Yellow = potential pre-suckling calf serum samples collected on calf date of birth (DOB), and Pink = Post-suckling calf serum samples.

Animal/Sample ID (sample date)	Total IgG (mg/mL)	DOB
Dam 1 (3/4/02)	19.8	
Calf 1-1 (3/5/02)	26.7	3/5/2002
Dam 1 (5/30/05)	13.3	
Calf 1-2(6/1/05)	27.95	6/1/2005
Dam1 (4/2/10)	22.15	
Cord 1 (4/3/10)	19.05	
Calf 1-3 (4/3/10)	33.4	4/3/2010
Dam 2 (1/17/09)	19.8	
Calf 2 (1/29/09)	19.75	1/19/2009
Calf 2 (12/22/09)	7.55	
Dam 3 (12/5/03)	12.3	
Calf 3-1 (12/5/03)	22.55	12/5/2003
Dam 3 (6/5/06)	9.7	
Calf 3-2 (4/6/06)	31.2	4/6/2006
Dam 4 (5/20/02)	11.2	
Calf 4 (5/21/02)	27.4	5/21/2002
Dam 5 (4/20/05)	15.1	
Calf 5 (4/21/05)	33.6	4/21/2005
Dam 6 (8/14/99)	20.1	
Calf 6 (8/18/99)	29	8/16/1999
Dam 7 (1/27/05)	12.3	
Calf 7-1 (1/29/02)	37.7	1/29/2002
Damn 7 (1/8/08)	21.8	
Cord 7 (11/9/09)	26.25	
Calf 7-2 (11/9/08)	22	11/9/2009

Tuberculosis (TB) positive Asian elephant dam and calf focal study timeline demonstrating passive transfer of immunoglobulins across the placenta via presence of TB antibodies in pre-suckling Asian elephant calves.

Dam	Calf 1	Calf 2	Date
Birth			1995
Pregnancy	Gestation		2002-2003
TB Seroconverted (during pregnancy)	Birth (TB antibody positive)		2003
Pregnancy		Gestation	2005-2006
		Birth (TB antibody positive)	2006
TB Culture positive			2007
TB Culture positive			2008
TB Treatment Started			2009
MAPIA positive/ STAT PAK reactive		MAPIA positive/ STAT PAK reactive	2010
Treatment Ended		MAPIA negative/ STAT PAK nonreactive	2011
MAPIA positive/ STAT PAK reactive			2011

LIST OF REFERENCES

- Ackerman, B.B., Wright, S.D., Bonde, R.K., Odell, D.K., Banowetz, D.J., 1995. Trends and patterns in manatee mortality in Florida, 1974-1991. In: O'Shea, T.J., Ackerman, B.B., Percival, H.F. (Eds.), Population Biology of the Florida Manatee (*Trichechus manatus latirostris*). National Biological Service, Information Technology Report 1. pp. 223-298.
- Akpek, E.K., Gottsch, A.D., 2003. Immune defense at the ocular surface. *Eye*. 17, 949-956.
- Allen, W. R., 2006. Ovulation, pregnancy, placentation, and husbandry in the African elephant (*Loxodonta africana*). *Phil. Trans. R. Soc.* 361, 821-834.
- Allen, W., Mathias, S., Wooding, F., van Aarde, R., 2003. Placentation in the African elephant (*Loxodonta africana*): II, Morphological changes in the uterus and placenta throughout gestation. *Placenta*. 24, 598-617.
- Araújo, A., Giugliano, L., 2001. Lactoferrin and free secretory component of human milk inhibit the adhesion of enteropathogenic *Escherichia coli* to HeLa cells. *BMC Microbiology*. 1, 25.
- Bachteler, D., Gehnhardt, G., 1999. Active touch performance in the Antillean manatee: evidence for a functional differentiation of facial tactile hairs. *Zoology*. 102 (1), 61-69.
- Bauer, G.B., Colbert, D.E., Fellner, W., Gaspard, J.C., and Littlefield, B., 2003. Underwater visual acuity of two Florida manatees (*Trichechus manatus latirostris*). *International Journal of Comparative Psychology*. 16 (2), 130-142.
- Baugh, T.M., Valade, J.A., Zoodsma, B.J., 1989. Manatee use of *Spartina alterniflora* in Cumberland Sound. *Marine Mammal Science*. 5 (1), 88-90.
- Beck, C., Langtrimm, C., 2002. Application of the Manatee Photo-identification Database for Population Research. Poster presented at the Manatee Population Ecology and Management Workshop, Gainesville, FL.
- Beck, C.A., Reid, J.P., 1995. An automated photo-identification catalog for studies of the life history of the Florida manatee. In: O'Shea, T.J., Ackerman, B.B., and Percival, H.F. (Eds.), Population Biology of the Florida Manatee (*Trichechus manatus latirostris*). National Biological Service, Information Technology Report 1. pp. 120-134.
- Best, 1981. Foods and feeding habits of wild and captive Sirenia. *Mammal Review*. 11(1), 3-29.

- Best, R.C., 1984. The aquatic mammals and reptiles of the Amazon. In: Sioli, H. (Ed.), The Amazon. Limnology and Landscape Ecology of a Mighty Tropical River and its Basin, Netherlands.
- Bloomfield, S.F., Stanwell-Smith, R., Crevel, RWR, Pickup, J., 2006. Too clean, or not too clean: the Hygiene Hypothesis and home hygiene. Clin Exp Allergy. 36 (4), 402-525.
- Bonde, R.K., Aguirre, A.A., Powell, J., 2004. Manatees as sentinels of marine ecosystem health: are they the 200-pound canaries? EcoHealth. 1, 255-262.
- Bossart, G.D., Baden, D.G., Ewing, R.Y., Roberts, B., Wright, S., 1998. Brevetoxicosis in manatees (*Trichechus manatus latirostris*) from the 1996 epizootic: Gross, histologic, and immunohistochemical features. Toxicology Pathology. 26, 276-282.
- Bossart, G.D., 2001. Manatees. In: Dierhauf and Gullord (Eds.), CRC Handbook of Marine Mammal Medicine. Second Edition. CRC Press, London, pp. 939-960.
- Bossart, G.D., Meisner, R., Rommel, S., Ghim, S., Jenson, A.B., 2002. Pathological features of the Florida manatee cold stress syndrome. Aquatic Animals. 29, 9-17.
- Bossart, G., 2006 Marine mammals as sentinel species for oceans and human health, Oceanography. 19, 134-137.
- Brandtzaeg, P., Kiyono, H., Russell, M., 2008. Terminology: nomenclature of mucosa-associated lymphoid tissue. Mucosal Immunology. 1, 31-37.
- Brandtzaeg, P., 2009. Mucosal immunity: induction, dissemination, and effector functions. Scandinavian Journal of Immunology. 70, 505-515.
- Brightman, A.H., Gerds, S. Campbell, T.W., Fedde, M.R., 2003. A study of viscosity of marine mammal tears. Vet Ophthalmol. 6, 359-363.
- Buergelt, C., Bonde, R., 1983. Toxoplasmic meningoencephalitis in a West Indian manatee. Journal of the American Veterinary Medical Association. 183, 1294-1296.
- Bullock, T.H., O'Shea, T.J., McClune, M.C., 1982. Auditory evoked potentials in the West Indian manatee (Sirenia: *Trichechus manatus*). Comparative Biochemistry and Physiology. 85A (1), 139-142.
- Burns, C., Ebersole, J., Allansmith, M., 1982. Immunoglobulin A antibody levels in human tears, saliva, and serum. Infection and Immunology. 6, 1019-1022.
- Carbonare, C., Carbonare, S., Carneiro-Sampaio, M., 2005. Secretory immunoglobulin A obtained from pooled human colostrums and milk for oral passive immunization. Pediatr. Allergy Immunol. 16, 574-581.

- Carter, A., Enders, A., Kunzle, H., Odour-Okelo, A., Vogel, P., 2004. Placentation in species of phylogenetic importance: the Afrotheria. *Animal Reproduction Science*. 82-83, 35-48.
- Carter, A., Miglino, M., Ambrosio, C., Santos, T., Rosas, F., d’Affonseca Neto, J., Lazzarini, S., Carvalho, A., da Silva, V., 2008. Placentation in the Amazonian manatee (*Trichechus inunguis*). *Reproduction, Fertility, and Development*. 20, 537-545.
- Castle, P.E., Rodriguez, A., Bowman, F.P., Herrero, R., Schiffmna, M., Bratti, M.C., Morera, L.A., Schust, D., Crowley-Nowick, P., Hildesheim, A., 2004. Comparison of ophthalmic sponges for measurements of immune markers from cervical secretions. *Clinical and Diagnostic Laboratory Immunology*. 11 (2), 399-405.
- Cesta, M.F., 2006. Normal structure, function, and histology of mucosa-associated lymphoid tissue. *Toxicologic Pathology*. 34, 599-608.
- Choudhury, A., Lahiri Choudhury, D.K., Desai, A., Duckworth, J.W., Easa, P.S., Johnsingh, A.J.T., Fernando, P., Hedges, S., Gunawardena, M., Kurt, F., Karanth, U., Lister, A., Menon, V., Riddle, H., Rübél, A., Wikramanayake, E., 2008. *Elephas maximus*. In: IUCN 2011. IUCN Red List of Threatened Species. Version 2011.2. <www.iucnredlist.org>. Downloaded on 1 February 2012.
- Cleveland, M., Bakos, M., Pyron, D., Rajaraman, S., Goldblum, R., 1991. Characterization of secretory component in amniotic fluid. *The Journal of Immunology*. 147 (1), 181-186.
- Clifton, K.B., Yan, J., Mecholsky, J.J., Reep, R.L., 2008. Material properties of manatee rib bone. *Journal of Zoology*. 274, 150-159.
- Cooper, R., Connell, R., Wellings, S., 1964. Placenta of the Indian elephant. *Science, New Series*. 146, 410-412.
- Dawes, C.J., Lawrence, J.M., 1980. Seasonal changes in the proximate constituents of the seagrasses *Thalassia testudinum*, *Halodule wrightii*, and *Syringodium filiforme*. *Aquatic Botany*. 8 (4), 371-380.
- Dawes, C.J., Lawrence, J.M., 1983. Proximate composition and caloric content of seagrasses. *Marine Technology Society Journal*. 17 (2), 53-58.
- Deutsch, C.J., Reid, J.P., Bonde, R.K., Easton, D.E., Kochman, H.I., O’Shea, T.J., 2003. Seasonal movements, migratory behavior, and site fidelity of West Indian manatees along the Atlantic Coast of the United States. *Wildlife Monographs*. 1-77.
- Deutsch, C.J., Self-Sullivan, C., Mignucci-Giannoni, A., 2008. *Trichechus manatus*. In: IUCN 2011. IUCN Red List of Threatened Species. Version 2011.2. <www.iucnredlist.org>. Downloaded on 1 February 2012.

- Domning, D.P., 1981. Sea cows and sea grasses. *Paleobiology*. 7, 417-420.
- Domning, D.P., 1982. Evolution of manatees - A speculative history. *Journal of Paleontology*. 59, 599-619.
- Domning, D.P., 1983. Marching teeth of the manatee: Its special adaptation to an abrasive diet has enabled this aquatic mammal to outdo the dugong. *Natural History*. 92, 8-11.
- Domning, D.P., Hayek, L.C., 1986. Interspecific and intraspecific morphological variation in manatees (Sirenia: *Trichechus*). *Marine Mammal Science*. 2, 87-144.
- Domning, D.P., 2001. The earliest known fully quadrupedal sirenian. *Nature*. 143, 625-627.
- Domning, D.P., 2005. Fossil Sirenia of the West Atlantic and Caribbean region. VII. Pleistocene *Trichechus manatus* Linnaeus, 1758. *Journal of Vertebrate Paleontology*. 25, 685-701.
- Doolin, E., Midwinter, R., Buddle, B., 2001. Purification of secretory immunoglobulin A from milk of the brushtail possum (*Trichosurus vulpecula*). *New Zealand Veterinary Journal*. 49, 181-186.
- Emanuelson, K., Kinzley, C., 2002. Elephants. In: *Hand-Rearing Wild and Domestic Mammals*. Blackwell, Gage (Ed.). Ames, Iowa. pp. 221-228.
- Emanuelson, K., 2006. Neonatal care and hand rearing. In: Fowler, M. and Mikota, S.K. (Eds.), *Biology, Medicine, and Surgery of Elephants*. Blackwell, Ames, Iowa, pp. 233-242.
- Enders, A., Carter, A., 2004. What can comparative studies of placental structure tell us?-A Review. *Placenta*. 25 (18), 3-9.
- Etheridge, K., Rathbun, G.B., Powell, J.A., Kochman, H.I., 1985. Consumption of aquatic plants by the West Indian manatee. *Journal of Aquatic Plant Management*. 23, 21-25.
- Fagarasan, S., 2008. Evolution, development, mechanism, and function of IgA in the gut. *Curr Opin Immunol*. 20 (2), 170-177.
- Ferreire, A., Martinez, P., Colares, E., Robaldo, R., Berne, M., Miranda Filho, K., Bianchini, A., 2005. Serum immunoglobulin G concentration in the southern elephant seal, *Mirounga leonina* (Linnaeus, 1758), from elephant island (Antarctica): sexual and adrenal steroid hormones effects. *Veterinary Immunology and Immunopathobiology*. 106, 239-245.

- Flewelling, L.J., Naar, J.P., Abbott, J.P., Baden, D.G., Barros, N.B., Bossart, G.D., Bottein, M.D., Hammond, D.G., Haubold, E.M., Heil, C.A., Henry, M.S., Jacocks, H.M., Leighfield, T.A., Pierce, R.H., Pitchford, T.D., Rommel, S.A., Scott, P.S., Steidinger, K.A., Truby, E.W., VanDolah, F.M., Landsberg, J.H., 2005. Red tides and marine mammal mortalities. *Nature*. 435, 755–756.
- Florida Fish and Wildlife Conservation Commission-Fish and Wildlife Research Institute (FWC-FWRI) (2012a) Manatee Mortality Statistics. Accessed 1 February 2012. Available from <http://myfwc.com/research>
- Florida Fish and Wildlife Conservation Commission-Fish and Wildlife Research Institute (FWC-FWRI) (2012b) Manatee Synoptic Surveys. Accessed 1 February 2012. Available from <http://myfwc.com/research>
- Gage, L., 2003. Neonatal elephant mortality. In: Fowler, M. and Miller, M. (Eds.), *Fowler and Miller's Zoo and Wild Animal Medicine*. Saunders Elsevier, Missouri, pp. 365-368.
- German, A., Hall, E., Day, M., 1998. Measurement of IgG, IgM, and IgA concentrations in canine serum, saliva, tears, and bile. *Veterinary Immunology and Immunopathology*. 64, 107-121.
- Gerstein, E.R., Gerstein, L., Forsythe, S.E., Blue, J.E., 1999. The underwater audiogram of the West Indian manatee (*Trichechus manatus latirostris*). *Journal of the Acoustical Society of America*. 105 (6), 3575-3583.
- Giuliano, E.A., Moore, C.P., Philips, T.E., 2002. Morphological evidence of M cells in healthy canine conjunctiva-associated lymphoid tissue. *Graefe's Arch Clin Exp Ophthalmol*. 240, 220-226.
- Golby, S.J.C., Spencer, J., 2002. Where do IgA plasma cells in the gut come from? *Gut*. 51 (2), 150-151.
- Gonçalves, A., Giraldo, P., Barros-Mazon, S., Gondo, M., Amaral, R., Jacyntho, C., 2006. Secretory immunoglobulin A in saliva of women with oral and genital HPV infection. *European Journal of Obstetrics & Gynecology and Reproductive Biology*. 124, 227-231.
- Griebel, U., Schmid, A., 1996. Color vision in the manatee (*Trichechus manatus*). *Vision Research*. 36 (17), 2747-2757.
- Gudmundsson, O., Sullivan, D., Bloch, K., Allansmith, M., 1985. The ocular secretory system of the rat. *Exp Eye Res*. 40, 231-238.
- Guo, Y., Bao, Y., Wang, H., Hu, X., Zhao, Z., Li, N., Zhao, Y., 2011. A preliminary analysis of the immunoglobulin genes in the African elephant (*Loxodonta africana*). *PLoS ONE*. 6 (2), 1-14.

- Gupta, A., Sarin, G., 1983. Serum and tear immunoglobulin levels in acute adenovirus conjunctivitis. *British Journal of Ophthalmology*. 67, 195-198
- Hammarström, L., Vorechovsky, I., Webster, D., 2000. Selective IgA deficiency (SIgAD) and common variable immunodeficiency (CVID). *Clin Exp Immunol*. 120 (2), 225-231.
- Hanson, L., Ahlsted, S., Andersson, B., Carlsson, B., Cole, M., Cruz, J., Dahlgren, U., Ericsson, T., Jalil, F., Khan, S., Mellander, L., Schneerson, R., Svanborg Eden, C., Soderstrom, T., Wadsworth, C., 1983. *Mucosal Immunity*. 1,1-21.
- Harper, J., Samuelson, D., Reep, R., 2005. Corneal vascularization in the Florida manatee (*Trichechus manatus latirostris*) and three-dimensional reconstruction of vessels. *Veterinary Ophthalmology*. 8, 89-99.
- Harr, K., Harvey, J., Bonde, R., Murphy, D., Lowe, M., Menchaca, M., Haubold, E., Francis-Floyd, R., 2006. Comparison of methods used to diagnose generalized inflammatory disease in manatees (*Trichechus manatus latirostris*). *J Zoo Wildlife Med*. 37, 151-159.
- Harvey, J.W., Harr, K.E., Murphy, D., Walsh, M.T., Chittick, E.J., Bonde, R.K., Pate, M.G., Deutsch, C.J., Edwards, H.H., Haubold, E.M., 2007. Clinical biochemistry in healthy manatees (*Trichechus manatus latirostris*). *J Zoo Wildlife Med*. 38, 269-279.
- Hedges, S., 2006. Conservation. In: Fowler, M. and Mikota, S.K. (Eds.), *Biology, Medicine, and Surgery of Elephants*. Blackwell, Ames, Iowa, pp. 475-489.
- Hemsley, S., Cole, N., Canfield, P., Willcox, M., 2000. Protein microanalysis of animal tears. *Research in Veterinary Science*. 68, 207-209.
- IBAMA, 2001. Plano de Ação de Mamíferos Aquáticos do Brasil. Versão II. Ministério do Meio Ambiente, Instituto Brasileiro do Meio Ambiente e dos Recursos Naturais Renováveis, Brasília.
- Isaza, R., Davis, R., Moore, S., Briggs, D., 2006. Results of vaccination of Asian elephants (*Elephas maximus*) with monovalent inactivated rabies vaccine. *AJVR*. 67, 1934-1936.
- Kageyama, M., Nakatsuka, K., Yamaguchi, T., Owen, R., Shimada, T., 2006. Ocular defense mechanisms with special reference to the demonstration and functional morphology of the conjunctiva-associated lymphoid tissue in Japanese monkeys. *Arch Histol Cytol*. 69, 311-322
- Kanamaru, Y., Kuzuya, Y., Tanahashi, T., 1982. Purification of secretory IgA from bovine Colostrum. *Agric Biol Chem*. 46, 1531-1537.

- Kawashima, M., Nakanishi, M., Kuwamura, M., Takeya, M., Yamate, J., 2004. Immunohistochemical Detection of macrophages in the short-finned pilot whale (*Globicephala macrorhynchus*) and risso's dolphin (*Grampus griseus*). *J. Comp. Path.* 130, 32-40.
- Kellogg, M., Burkett, S., Dennis, T., Stone, G., Gray, B., McGuire, P., Zori, R., Stanyon, R., 2007. Chromosome painting in the manatee supports Afrotheria and Paenungulata. *BMC Evolutionary Biology.* 7, 6-13.
- Kellogg, M.E., 2008 Sirenian conservation genetics and Florida manatee (*Trichechus manatus latirostris*) Cytogenetics. PhD Dissertation, University of Florida, Gainesville, Florida. pp.1-144.
- Kelly, P., Carter, S., Azwai, S., Cadman, H., 1998. Isolation and characterization of immunoglobulin g and IgG subclasses of the African elephant (*Loxodonta Africana*). *Comp. Immun. Microbiol. & Infect. Dis.* 21, 65-73.
- King, D., Aldridge, B., Kennedy-Stoskopf, S., Stott, J., 2006: Immunology. In: Dierauf and Gulland (Eds.), *CRC Handbook of Marine Mammal Medicine, Second Edition.* CRC Press, London, pp. 237-252.
- Kleinschmidt, T., Czelusniak, J., Goodman, M., Braunitzer, G., 1986. Paenungulata: A comparison of the hemoglobin sequences from elephant, hyrax, and manatee. *Mol Biol Evol.* 3, 427-435.
- Knop, E., Knop, N., Claus, P., 2008. Local production of secretory IgA in the eye-associated lymphoid tissue (EALT) of the normal human ocular tissue. *IOVS.* 49, 2322-2329.
- Knop, N., Knop, E., 2005a. Ultrastructural anatomy of CALT follicles in the rabbit reveals characteristics of M-cells, germinal centers and high endothelial venules. *J. Anat.* 207, 409-426.
- Knop, E., Knop, N., 2005b. The role of eye-associated lymphoid tissue in corneal immune protection. *J. Anat.* 206, 271-285.
- Knop, N., Knop, E., 2000. Conjunctiva-associated lymphoid tissue In the human eye. *Investigative Ophthalmology & Visual Science.* 41, 1270-1279.
- Koelsch, J.K., 2001. Reproduction in female manatees observed in Sarasota Bay, Florida. *Marine Mammal Science.* 17 (2), 331-341.
- Komohara, Y., Hirahara, J., Horikawa, T., Kawamura, K., Kiyota, E., Sakashita, N., Araki, N., Takeya, M., 2006. AM-3K, an anti-macrophage antibody, recognizes CD163, a molecule associated with anti-inflammatory macrophage phenotype. *J. Histochem. Cytochem.* 54, 763-771.

- Kurimoto, T., Ikeda, A., Tanaka, K., 1982. Purification and identification of horse serum IgA. *Jpn. J. Vet. Sci.* 44, 661-668.
- Langer, P., 2009. Differences in the composition of colostrums and milk in eutherians reflect differences in immunoglobulin transfer. *Journal of Mammalogy.* 90, 332-339.
- Lanyon, J.M., 2003. Distribution and abundance of dugongs in Moreton Bay, Queensland, Australia. *Wildlife Research.* 30, 397-409.
- Larkin, I.V., 2000. Reproductive endocrinology of the Florida manatee (*Trichechus manatus latirostris*): Estrous cycles, seasonal patterns and behavior. PhD diss. University of Florida.
- Larkin, I.L.V, Gasson, V., Reep, R.L., 2007. Observations on Digesta Passage Rates in the Florida manatee (*Trichechus manatus latirostris*). *Zoo Biology.* 26, 503-515.
- Lavergne, A., Douzery, E., Stichler, T., Catzeflis, F.M., Springer, M.S., 1996. Interordinal mammalian relationships: evidence for paenungulate monophyly is provided by complete mitochondrial 12S rRNA sequences. *Mol Phylogenet Evol.* 6, 245-58.
- Lima, R.P., 1997. Peixe-Boi Marinho (*Trichechus manatus*): Distribuição, status de conservação e aspectos tradicionais ao longo do litoral nordeste do Brasil Master's Thesis, Universidade Federal de Pernambuco, Brazil.
- Lowenstine, L., 2006. Endocrine and Immune Systems. In: Fowler, M. and Mikota, M. (Eds.), *Biology, Medicine, and Surgery of Elephants.* Blackwell Publishing, Iowa, pp. 309-315.
- Luna, F.O., 2001. Distribuição, Status de Conservação e Aspectos Tradicionais do peixe-boi marinho (*Trichechus manatus manatus*) no litoral norte do Brasil Master's Thesis, Universidade Federal de Pernambuco, Brazil.
- Marshall, C.D., Huth, G.D., Edmonds, V.M., Halin, D.L., Reep, R.L., 1998. Prehensile use of the perioral bristles during feeding and associated behaviors of the Florida manatee (*Trichechus manatus latirostris*). *Marine Mammal Science.* 14 (2), 274-289.
- Mossman, H.W., 1937. Comparative morphogenesis of the fetal membranes and accessory uterine structures. *Carnegie Inst. Washington Publ.* 479. *Contrib. Embryol.* 26, 129-246.
- Murata, Y., Nikaido, M., Sasaki, T., Cao, Y., Fukumoto, Y., Hasegawa, M., Okada, N., 2003. Afrotherian phylogeny as inferred from complete mitochondrial genomes. *Molecular Phylogenetics and Evolution.* 28, 253-260.

- Murphy, K., Travers, P., Walport, M., (Eds.) 2008. The Mucosal Immune System. In: Janeway's Immunology. Seventh Edition. Garland Science. pp.459-495.
- Niezrecki, C., Phillips, R., Meyer, M., Beusse, D.O., 2003. Acoustic detection of manatee vocalizations. *Journal of the Acoustical Society of America*. 114 (3), 1640-1647.
- Nilssen, D.E., Brandtzaeg, P., Frøland, S.S., Fausa, O., 1992. Subclass composition and J-chain expression of the 'compensatory' gastrointestinal IgG cell population in selective IgA deficiency. *Clin Exp Immunol*. 87 (2), 237-245.
- Nishihara, H., Satta, Y., Nikaido, M., Thewissen, J., Stanhope, M., Okada, N., 2005. A retroposon analysis of Afrotherian phylogeny. *Mol Biol Evol*. 22, 1823-1833.
- Nollens, H., Green, L., Duke, D., Walsh, M.T., Chittick, B., Gearhart, S., Klein, P.A., Jacobson, E.R., 2007. Development and validation of monoclonal and polyclonal antibodies for the detection of immunoglobulin G of bottlenose dolphin (*Tursiops truncatus*). *J Vet Diagn Invest*. 19, 465-470.
- O'Daly, J., Cebra, J., 1971. Rabbit secretory IgA. *The Journal of Immunology*. 107, 436-448.
- Ogra, P.L., Mestecky, J., Lamm, M.E., Strober, W., Bienenstock, J., McGhee, J.R., 1999. *Mucosal Immunology*. London, UK: Academic Press.
- O'Shea, T.J., Beck, C.A, Bonde, R.K., Kochman, H.I., Odell, D.K., 1985. An analysis of manatee mortality patterns in Florida, 1976-1981. *Journal of Wildlife Management* 49 (1), 1-11.
- Owen, R., 1855. On the Fossil Skull of a Mammal (*Prorastomus Sirenoides*, Owen), from the Island of Jamaica. *Quarterly Journal of the Geological Society*. 11, 541-543.
- Pardini, A., O'Brien, P., Fu, B., Bonde, R., Elder, F., Ferguson-Smith, M., Yang, F., Robinson, T., 2007. Chromosome painting among Proboscidea, Hyracoidea and Sirenia: support for Paenungulata (Afrotheria, Mammalia) but not Tethytheria. *Proc. R. Soc. B*. 274, 1333-1340.
- Parr, E., Bozzola, J., Parr, M., 1995. Purification and measurement of secretory IgA in mouse milk. *Journal of Immunological Methods*. 180, 147-157.
- Powell, J.A., 2002. *Manatees: Natural History and Conservation*. Voyageur Press, Stillwater, Minnesota.
- Rainey, W.E., Lowenstein, J.M., Sarich, V.M., Magor, D.M., 1984. Sirenian molecular systematics including the extinct Steller's sea cow (*Hydrodamalis gigas*). *Naturwissenschaften*. 71, 586-588.

- Rasmussen, D., Gagnon, M., Simons, E., 1990. Tereopdy in the carpus and tarsus of oligocene liohyracidea (Mammalis Hyracoidea) and the phyletic position of hyraxes. *Proc. Natl. Acad. Sci.* 87, 4688-4691.
- Rathbun, G.B., Reid, J.P., Bonde, R.K., Powell, J.A., 1995. Reproduction in free-ranging West Indian manatees (*Trichechus manatus*). In: O'Shea, T.J., B.B. Ackerman and H.F. Percival, (Eds.), *Population Biology of the Florida Manatee (Trichechus manatus latirostris)*. National Biological Service, Information Technology Report 1. pp. 135-156.
- Reep, R., Bonde, B., 2006. *The Florida Manatee*. University Press of Florida.
- Reep, R.L., Marshall, C.D., Stoll, M.L., 2002. Tactile hairs on the postcranial body in Florida manatees: A mammalian lateral line? *Brain, Behavior and Evolution.* 59, 141-154.
- Reid, J.P., Rathbun, G.B., Wilcox, J.R., 1991. Distribution patterns of individually identifiable West Indian manatees (*Trichechus manatus*) in Florida. *Marine Mammal Science.* 7, 180-190.
- Reynolds III, J.E., Odell, D.K., 1991. *Manatees and Dugongs Facts on File, Inc.*, New York, NY, USA.
- Rommel, S.A., Reynolds III, J.E., 2000. Diaphragm structure and function in the Florida manatee (*Trichechus manatus latirostris*). *Anatomical Record.* 259 (1), 41-51
- Rommel, S., Haubold, E., Costidis, A., Bossart, G., Meisner, R., 2002. Comparative Distribution of Lymph Nodes in Marine Mammals. *Proceedings for the Florida Marine Mammal Health Conference, 2002, Gainesville, Florida.*
- Rohan, L.C., Edwards, R.E., Kelly, L.A., Coleneelo, K.A., Bowman, F.P., Crowley-Nowick, P.A., 2000. Optimization of the weck-cel collection method for quantification of cytokines in mucosal secretions. *Clinical and Diagnostic Laboratory Immunology.* 7, 45-48.
- Ruiz, C., Nollens, H., Venn-Watson, S., Green, L., Wells, R., Walsh, M., Nolan, B., McBain, J., Jacobson, E., 2009. Baseline circulating immunoglobulin G levels in managed collection and free-ranging bottlenose dolphins (*Tursiops truncatus*). *Dev. and Comp. Imm.* 33, 449-455.
- Sakimoto, T., Shoji, J., Inada, N., Saito, K., Iwasaki, Y., Sawa, M., 2002. Histological study of conjunctiva-associated lymphoid tissue in mouse. *Jpn J Ophthalmol.* 46, 364-369.
- Samuelson, D.A., Reppas, G., Lewis, P., Valle, C., Isaza, R. The loss of the classic nasolacrimal system in the Florida manatee and other selected paenungulate species. *Proceedings for the International Association of Aquatic Animal Medicine Conference, 2007, Orlando, Florida.*

- Savage, R.J.G., Domning, D.P., Thewissen, J.G.M., 1994. Fossil Sirenia of the West Atlantic and Caribbean region. V. The most primitive known sirenian, *Prorastomus sirenoides* Owen, 1855. *Journal of Vertebrate Paleontology*. 14, 427-449.
- Scheffer, V., 1972. The weight of the Steller sea cow. *Journal of Mammalogy*. 53, 912–914.
- Schlegel, T., Brehm, H., Amselgruber, M., 2003. IgA and secretory component (SC) in the third eyelid of domestic animals: a comparative study. *Veterinary Ophthalmology*. 6, 157-161.
- Seiffert, E., 2007. A new estimate of Afrotherian phylogeny based on simultaneous analysis of genomic, morphological, and fossil evidence. *BMC Evolutionary Biology*. 7, 224-236.
- Sen, D., Sarin, G., Mani, K., Saha, K., 1976. Immunoglobulins in tears of normal Indian people. *Brit. J. Ophthal.* 60, 302-304.
- Shearer, M., Corbitt, S., Stanley, J., White, G., Chodosh, J., Chanh, T., Kennedy, R., 1997. Purification and characterization of secretory IgA from baboon colostrums. *Journal of Immunological Methods*. 204, 67-75.
- Shoshani, J., 2006. Taxonomy, classification, history, and evolution of elephants. In: Fowler, M. and Miller, M. (Eds.), *Fowler and Miller's Zoo and Wild Animal Medicine*. Saunders Elsevier, Missouri, pp. 3-14.
- Stejneger, L., 1887. How the great northern sea-cow (*Rytina*) became exterminated. *American Naturalist*. 21, 1047-1054.
- Sweat, J.M., Johnson, C.M., Marikar, Y., Gibbs, E.P., 2005. Characterization of surface interleukin-2 receptor expression on gated populations of peripheral blood mononuclear cells from manatees, *Trichechus manatus latirostris*. *Veterinary Immunology and Immunopathology*. 108, 269-281.
- Taylor, B.C., Brotheridge, R.M., Jessup, D.A., Stott, J.L., 2002. Measurement of serum immunoglobulin concentration in killer whales and sea otters by radial immunodiffusion. *Vet Immunol Immunopathol*. 89(3–4), 187–95.
- Tiffany, J.M., 1991., The viscosity of human tears. *Int Ophthalmol*. 15, 371-373.
- Tizard, I.R., 2000. *Veterinary Immunology: An Introduction*, Sixth Edition. W.B. Saunders Company, Pennsylvania.
- Van de Perre, P., 2003. Transfer of antibody via mother's milk. *Vaccine*. 21, 3374-3376.

- Van Elk, C., van der Bildt, B., Martina, B., Osterhaus, A., Kuiken, T., 2007. Escherichia coli septicemia associated with lack of maternally acquired immunity in a bottlenose dolphin calf. *Vet Pathol.* 44, 88-92.
- Walsh, C.J., Luer, C.A., Noyes, D.R., 2004. Effects of environmental stressors on lymphocyte proliferation in Florida manatees, *Trichechus manatus latirostris*. *Veterinary Immunology and Immunopathology.* 103, 247-256.
- Weber, M.A., Miller, M.A., 2012. Elephant neonatal and pediatric medicine. In: Miller, R.E. and Fowler, M.E. (Eds.), *Fowler's Zoo and Wild Animal Medicine: Current Therapy.* Saunders Elsevier, Missouri, pp. 531-536.
- Wheeler, T., Hodgkinson, A., Prosser, C., Davis, S., 2007. Immune components of colostrums and milk-A historical perspective. *J. Mammary Gland Biol. Neoplasia.* 12, 237-247.
- White, J. R., Francis-Floyd, R., 1990. Manatee Biology and Medicine. In: Diareuf, L. A. and Gulland, F. (Eds), *CRC Handbook of Marine Mammal Medicine.* CRC Press, London, pp. 601-620.
- Wooding, F., Stewart, F., Mathias, S., Allen, W., 2005. Placentation in the African elephant, *Loxodonta africanus*: III, Ultrastructural and functional features of the placenta. *Placenta.* 26, 449-470.
- Zierhut, M., Forrester, J.V., 2000. *Mucosal Immunology and Ocular Disease.* Lisse, The Netherlands: ÆOLUS.

BIOGRAPHICAL SKETCH

Jennifer L. McGee was born in Buffalo, NY, in 1981. She became a NY State licensed wildlife rehabilitator at the age of 16. Jennifer graduated from Buffalo Academy of the Sacred Heart in 1999 and continued to be actively involved in wildlife rehabilitation, research, education outreach, and animal training. She earned her B.Sc. in psychology/biology from Long Island University-Southampton College in 2002, focusing on marine mammal cognition and animal behavior. Jennifer earned her M.Sc. in marine mammal science from the University of Wales-Bangor in 2005. Her thesis research focused on Amazon River dolphin acoustics.

Jennifer has been involved in numerous international aquatic animal research projects in Brazil, Belize, Cuba, the United Kingdom, Germany, Australia, the Kingdom of Tonga, Niue, and Fiji. In 2007, she was accepted as a graduate student in the Aquatic Animal Health Program at the University of Florida's College of Veterinary Medicine. She received her Ph.D. in veterinary medical sciences from the University of Florida-College of Veterinary Medicine in the spring of 2012.